Neural Plasticity

Rehabilitation Induced Neural Plasticity after Acquired Brain Injury

Lead Guest Editor: Andrea Turolla
Guest Editors: Annalena Venneri, Dario Farina, Annachiara Cagnin, and Vincent C. Cheung

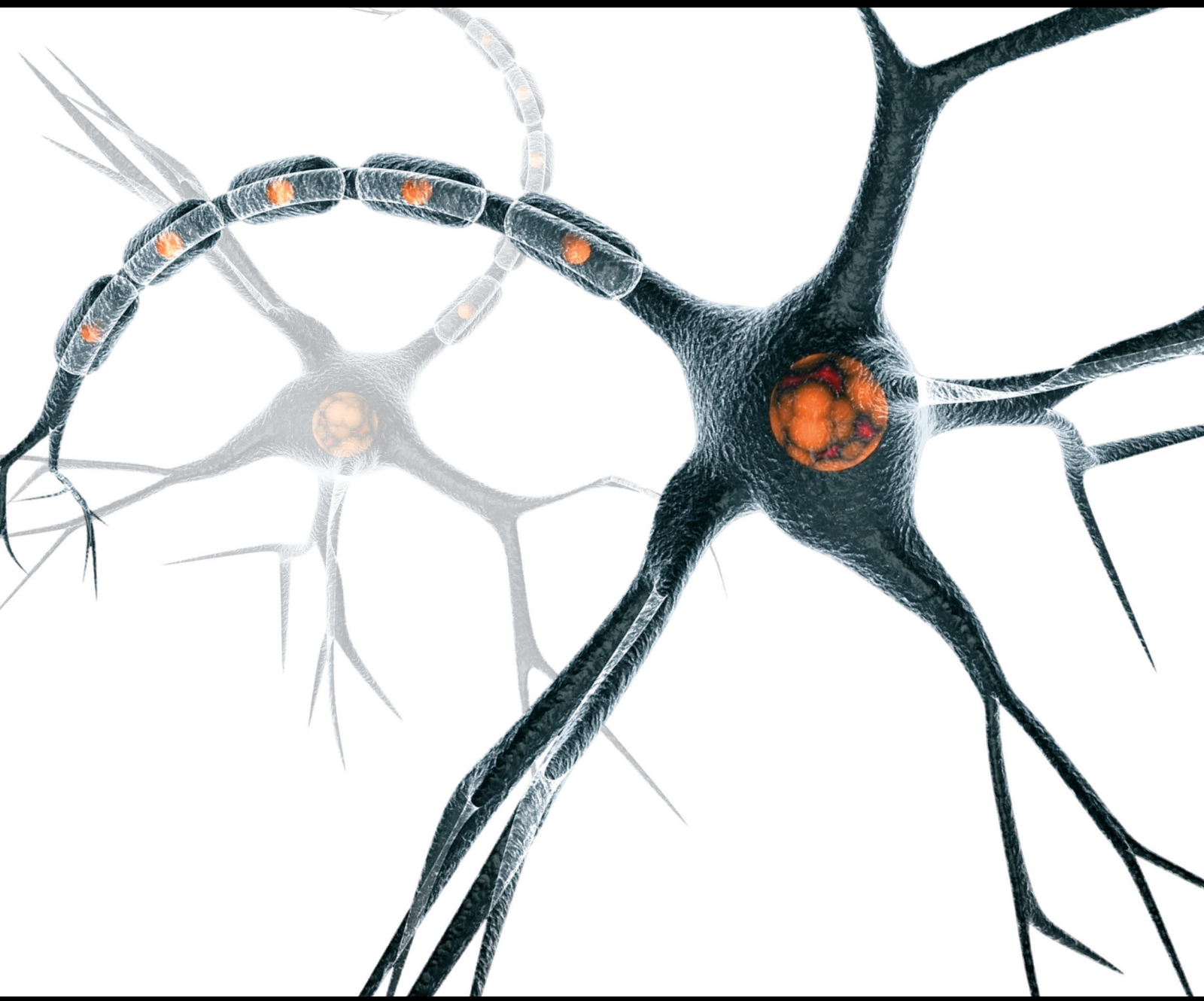

Rehabilitation Induced Neural Plasticity after Acquired Brain Injury

Neural Plasticity

Rehabilitation Induced Neural Plasticity after Acquired Brain Injury

Lead Guest Editor: Andrea Turolla
Guest Editors: Annalena Venneri, Dario Farina, Annachiara Cagnin, and Vincent C. Cheung

Editorial Board

Contents

Rehabilitation Induced Neural Plasticity after Acquired Brain Injury
Andrea Turolla, Annalena Venneri, Dario Farina, Annachiara Cagnin, and Vincent C. K. Cheung
Editorial (3 pages), Article ID 6565418, Volume 2018 (2018)

Quantification of Upper Limb Motor Recovery and EEG Power Changes after Robot-Assisted Bilateral Arm Training in Chronic Stroke Patients: A Prospective Pilot Study
Marialuisa Gandolfi, Emanuela Formaggio, Christian Geroin, Silvia Francesca Storti, Ilaria Boscolo Galazzo, Marta Bortolami, Leopold Saltuari, Alessandro Picelli, Andreas Waldner, Paolo Manganotti, and Nicola Smania
Research Article (15 pages), Article ID 8105480, Volume 2018 (2018)

Motor Improvement of Skilled Forelimb Use Induced by Treatment with Growth Hormone and Rehabilitation Is Dependent on the Onset of the Treatment after Cortical Ablation
Margarita Heredia, Jesús Palomero, Antonio de la Fuente, José María Criado, Javier Yajeya, Jesús Devesa, Pablo Devesa, José Luis Vicente-Villardón, and Adelaida S. Riolobos
Research Article (15 pages), Article ID 6125901, Volume 2018 (2018)

Acoustic Trauma Changes the Parvalbumin-Positive Neurons in Rat Auditory Cortex
Congli Liu, Tao Xu, Xiaopeng Liu, Yina Huang, Haitao Wang, Bin Luo, and Jingwu Sun
Research Article (7 pages), Article ID 9828070, Volume 2018 (2018)

Bilateral Transcranial Direct Current Stimulation Reshapes Resting-State Brain Networks: A Magnetoencephalography Assessment
Giovanni Pellegrino, Matteo Maran, Cristina Turco, Luca Weis, Giovanni Di Pino, Francesco Piccione, and Giorgio Arcara
Research Article (10 pages), Article ID 2782804, Volume 2018 (2018)

Low-Frequency Repetitive Transcranial Magnetic Stimulation for Stroke-Induced Upper Limb Motor Deficit: A Meta-Analysis
Lan Zhang, Guoqiang Xing, Shiquan Shuai, Zhiwei Guo, Huaping Chen, Morgan A. McClure, Xiaojuan Chen, and Qiwen Mu
Review Article (12 pages), Article ID 2758097, Volume 2017 (2018)

Transcutaneous Vagus Nerve Stimulation Combined with Robotic Rehabilitation Improves Upper Limb Function after Stroke
Fioravante Capone, Sandra Miccinilli, Giovanni Pellegrino, Loredana Zollo, Davide Simonetti, Federica Bressi, Lucia Florio, Federico Ranieri, Emma Falato, Alessandro Di Santo, Alessio Pepe, Eugenio Guglielmelli, Silvia Sterzi, and Vincenzo Di Lazzaro
Research Article (6 pages), Article ID 7876507, Volume 2017 (2018)

Interhemispheric Pathways Are Important for Motor Outcome in Individuals with Chronic and Severe Upper Limb Impairment Post Stroke
Kathryn S. Hayward, Jason L. Neva, Cameron S. Mang, Sue Peters, Katie P. Wadden, Jennifer K. Ferris, and Lara A. Boyd
Research Article (12 pages), Article ID 4281532, Volume 2017 (2018)

For Better or Worse: The Effect of Prismatic Adaptation on Auditory Neglect
Isabel Tissieres, Mona Elamly, Stephanie Clarke, and Sonia Crottaz-Herbette
Research Article (11 pages), Article ID 8721240, Volume 2017 (2018)

White Matter Hyperintensity Load Modulates Brain Morphometry and Brain Connectivity in Healthy Adults: A Neuroplastic Mechanism?
Matteo De Marco, Riccardo Manca, Micaela Mitolo, and Annalena Venneri
Research Article (10 pages), Article ID 4050536, Volume 2017 (2018)

Anodal Transcranial Direct Current Stimulation Provokes Neuroplasticity in Repetitive Mild Traumatic Brain Injury in Rats
Ho Jeong Kim and Soo Jeong Han
Research Article (7 pages), Article ID 1372946, Volume 2017 (2018)

Understanding the Mechanisms of Recovery and/or Compensation following Injury
Michael J. Hylin, Abigail L. Kerr, and Ryan Holden
Review Article (12 pages), Article ID 7125057, Volume 2017 (2018)

Assessed and Emerging Biomarkers in Stroke and Training-Mediated Stroke Recovery: State of the Art
Marialuisa Gandolfi, Nicola Smania, Antonio Vella, Alessandro Picelli, and Salvatore Chirumbolo
Review Article (15 pages), Article ID 1389475, Volume 2017 (2018)

Hindawi
Neural Plasticity
Volume 2018, Article ID 6565418, 3 pages
https://doi.org/10.1155/2018/6565418

Editorial

Rehabilitation Induced Neural Plasticity after Acquired Brain Injury

Andrea Turolla,[1] **Annalena Venneri**,[2] **Dario Farina**,[3] **Annachiara Cagnin**,[4] **and Vincent C. K. Cheung**[5,6]

[1]*Laboratory of Neurorehabilitation Technologies, IRCCS San Camillo Hospital Foundation, Venice, Italy*
[2]*Department of Neuroscience, University of Sheffield, Sheffield, UK*
[3]*Faculty of Engineering, Department of Bioengineering, Imperial College London, London, UK*
[4]*Department of Neuroscience, University of Padova, Padua, Italy*
[5]*School of Biomedical Sciences and KIZ-CUHK Joint Laboratory of Bioresources and Molecular Research of Common Diseases, The Chinese University of Hong Kong, Shatin NT, Hong Kong*
[6]*Gerald Choa Neuroscience Centre, Brain and Mind Institute and Department of Biomedical Engineering, The Chinese University of Hong Kong, Shatin NT, Hong Kong*

Correspondence should be addressed to Andrea Turolla; andrea.turolla@ospedalesancamillo.net

Received 3 April 2018; Accepted 3 April 2018; Published 10 May 2018

Motor skill learning refers to the process of optimizing sequences of action for accomplishing specific tasks [1]. Several mechanisms—genetic, neuroanatomical, and neurophysiological—are involved in this process, and they are mostly poorly understood. It has been suggested that the development of sequences of skilled movement involves the strengthening of the spatiotemporal relations between specific neuronal networks while weakening others. This process may occur via changes in connectivity between sets of corticospinal neurons following changes in synaptic efficacy [2]. The spatial and temporal organisation of synaptic weights is known as the "connectivity map", whose existence has been postulated to be the biological substrate for functional behaviours. Some principles governing the organisation of connectivity maps in functional systems include the following: (1) the representation of any individual skill is highly distributed across different cortical regions (fractured somatotopy); (2) adjacent cortical areas are densely interconnected via white matter bundles (interconnectivity); and (3) the more demanding the skill, the larger the proportion of the map is involved in the skill's representation (area equals dexterity).

In recent years, new fundamental properties related to plasticity of connectivity maps have been revealed. Starting from evidence in the motor system [3, 4], it has been widely accepted that, following brain structural damage, both connectivity maps and behavioural skills can at least be partially restored through intense practice and rehabilitation [5]. These findings strengthen the idea that motor maps reflect a level of synaptic connectivity within the cortex that is required for the performance of skills. At the biological level, this idea was further confirmed by experiments on rats in which cholinergic inputs to the motor cortex were removed before skill training, thus preventing learning-dependent motor cortical map reorganization, with consequent impairment of motor learning [6]. On these grounds, skill training might induce plastic changes in synaptic efficacy within the motor cortex, with consequent changes in map topography. At the behavioural level, the most important parameter of task-oriented practice to induce brain plasticity is the intensity of training, defined as the amount of repetition executed for specific tasks. To induce an effective brain reorganisation, a certain threshold of training (i.e., minimum number of repetitions) needs to be reached. This effect is known as

experience-dependent neuroplasticity. In animal models, it was estimated that between 1000 and 10,000 repetitions of the same task (trials) are needed before a permanent change at the synaptic level can be observed [7].

In animal experiments, it has been observed that behavioural motor learning is mediated by promotion of long-term potentiation (LTP) and by inhibition of long-term depression (LTD). None of these two mechanisms occurs with passive repetition without learning. The number of synapses and connections increases during the early stages of training [7], and in experimental settings, this phenomenon can be manipulated by injection of inhibitors of protein synthesis into the cortex, thus promoting or inhibiting skill learning [8]. Conversely, providing training sessions without learning might have detrimental effects such as a decrease in the number of synapses, weakened postsynaptic responses, and impairments in behavioural skills.

The possibility to induce functional reorganisation of cortical circuitries following lesions of the central nervous system through experience-dependent neuroplasticity has provided new perspectives in rehabilitation medicine, whose ultimate goal is to restore functions essential to independence in daily activities. *Neural Plasticity* sets out to publish a special issue devoted to the topic of *Rehabilitation Induced Neural Plasticity after Acquired Brain Injury*. The result is a collection of twelve outstanding articles submitted by investigators from 10 countries across Asia, Europe, North America, and Australia.

Current theories on the mechanisms underpinning recovery or compensation after brain injury have been outstandingly reviewed by M. J. Hylin et al. from the United States. Both human and animal models were considered to define how true recovery may be distinguished from compensation in the clinic. In this regard, the concepts of neuroanatomical effects of brain lesions, behavioural effects of recovery and compensation, brain functional reserve, and the impact of the timing and intensity of rehabilitation on neural plasticity were explored.

Two other reviews further provide a comprehensive background on rehabilitation-induced neural plasticity. M. Gandolfi et al. from Italy summarised the current available evidence on biomarkers mediating training-dependent recovery after stroke. Five groups of biomarkers were recognised as crucial for recovery: myokines, neurotrophic factors, neuropeptides, growth factors (GF) and GF-like molecules, and cytokines. On the other hand, more aiming at clinical translational research, L. Zhang et al. from China and the United States conducted a meta-analysis of the effects of low-frequency repetitive transcranial magnetic stimulation (LF-rTMS) on recovery of upper limb motor function and neuromodulation of cortical plasticity, after stroke. Overall, 22 studies were pooled for a total of 619 participants enrolled. Results indicated that stimulating the contralesional hemisphere with 1 Hz frequency has short-term efficacy on finger flexibility and activity dexterity. The above effects were also detectable as neurophysiological phenomena at the levels of resting-state motor threshold and motor-evoked potential. These authors concluded that LF-rTMS should be suggested as an add-on treatment to improve upper limb motor function in stroke survivors.

In addition to the aforementioned reviews and meta-analyses, three papers investigate specific mechanisms of rehabilitation-induced neural plasticity in rat models. M. Heredia et al. from Spain explored whether administering growth hormone (GH) followed by rehabilitation after severe injury of the motor cortex could have positive short- and/or long-term effects on the recovery of the affected upper limb. Results indicated that coupling GH with motor rehabilitation has positive effects when applied either immediately after or long after injury (i.e., 35 days postinjury). In contrast, GH administration alone resulted in improved nestin and actin reexpression, but without significant changes at the behavioural level. H. J. Kim et al. explored the use of anodal transcranial direct current stimulation (tDCS) to promote recovery of motor and somatosensory functions after repetitive mild traumatic brain injury (rmTBI). For both motor-evoked potential (MEP) and somatosensory-evoked potential (SEP), amplitude and latency were larger in the tDCS group but shorter in the sham-tDCS group. These results suggest that anodal tDCS might be a useful tool for promoting transient motor recovery by increasing synchronization of cortical firing, even in human survivors soon after concussions. C. Liu et al. from China explored the effect of acoustic trauma on the central and peripheral nervous systems. Changes in parvalbumin-containing neurons (PV neurons) were investigated in rats exposed to a one-hour noise stimulation. Results indicated that PV neurons were more apparent in the cortex of the noise-exposed group, suggesting the presence of a compensatory mechanism that maintains a stable state of the brain.

Four original clinical trials offer new evidence on the neuroplastic effects conferred by established rehabilitation modalities (i.e., prismatic adaptation, tDCS, and robotics) for stroke survivors. I. Tissieres et al. from Switzerland tested whether rightward prismatic adaptation (R-PA) might reduce visuospatial neglect symptoms. Results in stroke survivors with unilateral spatial neglect showed that in the half of tested subjects, extinction of dichotic listening in the left ear was alleviated by R-PA. Interestingly, the brain lesions of the nonresponders all involved the right dorsal attentional system and posterior temporal cortex. These authors concluded that shifting in hemispheric dominance within the ventral attentional system might be an appropriate model for interpreting these behavioural results. G. Pellegrino et al. from Italy tested, using magnetoencephalography (MEG), whether neural plasticity is induced by bilateral tDCS in the sensorimotor areas. They conducted a double-blind randomized controlled trial where tDCS was compared with sham-tDCS. Results indicated that tDCS reduced left frontal alpha, beta, and gamma power while global connectivity in delta, alpha, beta, and gamma frequencies increased. M. Gandolfi et al. from Italy and Austria quantified the neural electroencephalography (EEG) correlates of robot-aided bilateral arm training (BAT) for the recovery of upper limb function after stroke. Results indicated that providing robot-aided BAT induced complex shifting of desynchronization across hemispheres

in a task specific manner. Specifically, alpha and beta desynchronization that were bilateral in the sensorimotor areas before training became, after training, ipsilesional to the stroke-affected hemisphere for passive movements of the affected hand and contralesional during active movements of the affected hand. These authors concluded that robot-aided BAT might be helpful to promote differentiation of EEG patterns after stroke. F. Capone et al. from Italy designed a proof-of-concept study to explore the effect of combining robotic rehabilitation with noninvasive vagus nerve stimulation (VNF) for the recovery of upper limb motor function after stroke. The study was a double-blind, semi-randomised, and sham-controlled trial involving 14 patients with diverse presentations. Their results demonstrate that this innovative modality was safe and that patients receiving robotics with VNS gained better motor functions after treatment than patients treated by sham VNS.

Finally, two longitudinal studies investigate neuroimaging biomarkers for ageing subjects and stroke survivors. M. De Marco et al. from the UK and Italy, by studying the effect of small white matter lesions accumulated in the ageing brain, suggested that even in the absence of overt disease, the brain responds with a compensatory (neuroplastic) response to the accumulation of white matter damage over time, thus leading to increases in regional grey matter density and modifications in functional connectivity. K. S. Hayward et al. from Canada and Australia explored whether structural brain biomarkers (e.g., functions of the corticospinal tract, transcallosal inhibition, and their own fractional anisotropy) can predict severity of motor impairment after stroke. Cluster analysis indicated that functionality and structure of the corpus callosum can predict which patients have chronic and severe motor impairment of upper limb motor function.

Overall, this collection of papers argues convincingly that for the rehabilitation field, now is the time to forge even more pipelines going from basic neuroscientific results to novel, effective interventions for patients [9]. Our knowledge in the neural plasticity induced by rehabilitation in people with acquired brain injuries has reached the critical point that demands any proposal of innovative approach to be founded on both hard scientific rationale and robust clinical evidence of effectiveness. More importantly, we believe that a more solid understanding of the neuroscientific basis underpinning the effectiveness of some promising existing interventions should not only allow their further improvement but also promote their appropriate use in current clinical practice and delivery of rehabilitation services. Hopefully, this publication and other recent studies will encourage more clinicians, rehabilitation engineers, and neuroscientists to work together to further dissect the neural mechanisms underscoring functional recovery after acquired brain injuries and translate these findings into novel therapies.

Acknowledgments

This project has been supported by the following grant to Andrea Turolla: "Modularity for sensory motor control: implications of muscles synergies in motor recovery after stroke" (Grant no. GR-2011-02348942), Ministero della Salute.

Andrea Turolla
Annalena Venneri
Dario Farina
Annachiara Cagnin
Vincent C. K. Cheung

References

[1] M. -H. Monfils, E. J. Plautz, and J. A. Kleim, "In search of the motor engram: motor map plasticity as a mechanism for encoding motor experience," *The Neuroscientist*, vol. 11, no. 5, pp. 471–483, 2005.

[2] G. Hess and J. P. Donoghue, "Long-term potentiation of horizontal connections provides a mechanism to reorganize cortical motor maps," *Journal of Neurophysiology*, vol. 71, no. 6, pp. 2543–2547, 1994.

[3] R. J. Nudo, "Neural bases of recovery after brain injury," *Journal of Communication Disorders*, vol. 44, no. 5, pp. 515–520, 2011.

[4] R. J. Nudo, B. M. Wise, F. SiFuentes, and G. W. Milliken, "Neural substrates for the effects of rehabilitative training on motor recovery after ischemic infarct," *Science*, vol. 272, no. 5269, pp. 1791–1794, 1996.

[5] J. A. Kleim, R. Bruneau, P. VandenBerg, E. MacDonald, R. Mulrooney, and D. Pocock, "Motor cortex stimulation enhances motor recovery and reduces peri-infarct dysfunction following ischemic insult," *Neurological Research*, vol. 25, no. 8, pp. 789–793, 2003.

[6] J. M. Conner, A. Culberson, C. Packowski, A. A. Chiba, and M. H. Tuszynski, "Lesions of the basal forebrain cholinergic system impair task acquisition and abolish cortical plasticity associated with motor skill learning," *Neuron*, vol. 38, no. 5, pp. 819–829, 2003.

[7] J. A. Kleim and T. A. Jones, "Principles of experience-dependent neural plasticity: implications for rehabilitation after brain damage," *Journal of Speech, Language, and Hearing Research*, vol. 51, no. 1, pp. S225–S239, 2008.

[8] A. Luft, R. Macko, L. Forrester, A. Goldberg, and D. F. Hanley, "Post-stroke exercise rehabilitation: what we know about retraining the motor system and how it may apply to retraining the heart," *Cleveland Clinic Journal of Medicine*, vol. 75, Supplement 2, pp. S83–S86, 2008.

[9] Cumberland Consensus Working Group, B. Cheeran, L. Cohen et al., "The future of restorative neurosciences in stroke: driving the translational research pipeline from basic science to rehabilitation of people after stroke," *Neurorehabilitation and Neural Repair*, vol. 23, no. 2, pp. 97–107, 2009.

Hindawi
Neural Plasticity
Volume 2018, Article ID 8105480, 15 pages
https://doi.org/10.1155/2018/8105480

Research Article

Quantification of Upper Limb Motor Recovery and EEG Power Changes after Robot-Assisted Bilateral Arm Training in Chronic Stroke Patients: A Prospective Pilot Study

Marialuisa Gandolfi,[1,2] **Emanuela Formaggio**,[3] **Christian Geroin**,[1,2] **Silvia Francesca Storti**,[4] **Ilaria Boscolo Galazzo**,[4] **Marta Bortolami**,[1,2] **Leopold Saltuari**,[5,6] **Alessandro Picelli**,[1,2] **Andreas Waldner**,[6,7] **Paolo Manganotti**,[8] **and Nicola Smania**[1,2]

[1]*Neuromotor and Cognitive Rehabilitation Research Centre (CRRNC), Department of Neuroscience, Biomedicine and Movement Sciences, University of Verona, Verona, Italy*
[2]*U.O.C Neurorehabilitation Unit, AOUI of Verona, Verona, Italy*
[3]*San Camillo Hospital IRCCS, Venice, Italy*
[4]*Department of Computer Science, University of Verona, Verona, Italy*
[5]*Department of Neurology, Hochzirl Hospital, 6170 Zirl, Austria*
[6]*Research Unit for Neurorehabilitation South Tyrol, 39100 Bolzano, Italy*
[7]*Department of Neurological Rehabilitation, Private Hospital Villa Melitta, Bolzano, Italy*
[8]*Clinical Unit of Neurology, Department of Medical Sciences, University Hospital and Health Services of Trieste, University of Trieste, Trieste, Italy*

Correspondence should be addressed to Marialuisa Gandolfi; marialuisa.gandolfi@univr.it

Received 18 June 2017; Revised 1 September 2017; Accepted 20 November 2017; Published 26 March 2018

Academic Editor: Vincent C. Cheung

Background. Bilateral arm training (BAT) has shown promise in expediting progress toward upper limb recovery in chronic stroke patients, but its neural correlates are poorly understood. *Objective*. To evaluate changes in upper limb function and EEG power after a robot-assisted BAT in chronic stroke patients. *Methods*. In a within-subject design, seven right-handed chronic stroke patients with upper limb paresis received 21 sessions (3 days/week) of the robot-assisted BAT. The outcomes were changes in score on the upper limb section of the Fugl-Meyer assessment (FM), Motricity Index (MI), and Modified Ashworth Scale (MAS) evaluated at the baseline (T_0), posttraining (T_1), and 1-month follow-up (T_2). Event-related desynchronization/synchronization were calculated in the upper alpha and the beta frequency ranges. *Results*. Significant improvement in all outcomes was measured over the course of the study. Changes in FM were significant at T_2, and in MAS at T_1 and T_2. After training, desynchronization on the ipsilesional sensorimotor areas increased during passive and active movement, as compared with T_0. *Conclusions*. A repetitive robotic-assisted BAT program may improve upper limb motor function and reduce spasticity in the chronically impaired paretic arm. Effects on spasticity were associated with EEG changes over the ipsilesional sensorimotor network.

1. Introduction

Poststroke upper limb impairment strongly influences disability and patients' quality of life [1, 2]. Considering that up to two-thirds of stroke survivors suffer from upper limb dysfunctions, one of the main goals of rehabilitation is to improve recovery of upper limb functioning. Many rehabilitation approaches have been put forward [3–5]. However, there is strong evidence that the conceptual evolution of stroke rehabilitation promotes high-intensity, task-specific, and repetitive training [3, 5, 6]. To this end, the application of robot-assisted therapy has steadily gained acceptance since the 1990s [7, 8]. Robotic devices, in fact, allow repetitive, interactive, high-intensity, and task-specific

upper limb training across all stages of recovery and neurological severity as well [6].

A meta-analysis has shown significant, homogeneous positive summary effect sizes (SESs) for upper limb motor function improvements and muscle strength with the use of elbow-wrist robots in a bilateral mode [5]. Although subgroup analysis revealed no significant differences between phases post stroke [5], bilateral arm training (BAT) has shown great promise in expediting progress toward post-stroke recovery of upper limb functioning even in the chronic phase [6, 9–11].

BAT is a form of training in which both upper limbs perform the same movements simultaneously and independently of each other [12]. It can be undertaken in different modes (in-phase, antiphase) and training modalities (i.e., active, passive, and active-passive) [13]. The beneficial effects of BAT are thought to arise from a coupling effect in which both limbs adopt similar spatio-temporal movement parameters leading to a sort of coordination [14]. Active-passive BAT of the wrist has been investigated in behavioral and neurophysiological studies [11, 15]. It consists of rhythmic, continuous bimanual mirror symmetrical movements during which the patient actively flexes and extends the "unaffected" wrist, while the device assists the movement of the "affected" wrist in a mirrored, symmetrical pattern via mechanical coupling [15–19]; that is, movement of the affected upper limb is facilitated by the unaffected one [12]. Previous studies have reported that this pattern of coordinated movement leads to improvements in upper limb function [11, 16, 19, 20] associated with an increase in ipsilesional corticomotor excitability [11]. In addition, passive BAT of the forearm and the wrist has been shown to lead to a sustained reduction of muscle tone in hemiparetic patients with upper limb spasticity [20].

Current evidence indicates that the neural correlates of BAT are poorly understood [13]. The limitations of previous studies are threefold. First, patient characteristics such as type and site of stroke lesion were not consistently reported [21], precluding full understanding of motor and neural responses to BAT. Second, different BAT modalities (i.e., in-phase, antiphase, active, and active-passive) combined or not with other interventions (i.e., functional tasks or free movements with rhythmic auditory cues) have been reported. As different training modalities are thought to exploit different clinical effects and neural mechanisms [22], the relationship between each of these specific modes (delivered as a single intervention) and brain activity patterns needs to be more precisely explored [13]. Finally, a wide range and variation of neurophysiological and neuroimaging measures have been used among studies.

Essentially, transcranial magnetic stimulation (TMS) and functional magnetic resonance imaging (fMRI) studies have been used to investigate the neural correlates of BAT. Strength and weakness might be acknowledged for both techniques when applied in a neurorehabilitation setting [23]. TMS is an important tool that fits in the middle of the functional biology continuum for assessment in stroke recovery. However, it has the disadvantage of not being as relevant as other biologic measures in gathering information on brain activity during different states (or tasks) [23], unless electroencephalography (EEG) is recorded simultaneously [24].

Functional imaging and related techniques ((fMRI), positron emission tomography (PET), EEG, magnetoencephalography (MEG), and near-infrared spectroscopy (NIRS)) are important tools to determine the effects of brain injury and how rehabilitation can change brain systems [23]. fMRI is the most widely used technique for studying brain function. Several fMRI studies have described movement-related changes in motor cortical activation during partial recovery of the affected limb in stroke patients [25], and many studies have described the effects of various rehabilitative treatments on motor activation.

fMRI shows difficulties when exploring brain functions during robot-assisted sensorimotor tasks because only a few devices are MRI compatible [26–28] and their use in the clinical setting is limited by regulation (i.e., CE marking).

The EEG technique, conversely, has considerable advantages over other methods in the rehabilitation setting [17, 18, 29] being portable and readily operable with different robotic devices. Finally, the higher temporal resolution of EEG than fMRI signals allows monitoring brain activity during movement execution [30–32]. EEG alpha and beta band powers decrease during motor execution over the premotor and primary sensorimotor cortex; at the end of the movement, a rebound of beta activity is observed over the ipsilesional side. These power changes are termed, respectively, event-related desynchronization (ERD)—that is, power band decrease—and event-related synchronization (ERS)—that is, power band increase [33].

To the best of our knowledge, no study has addressed changes in EEG power alongside changes in upper limb motor function after passive robot-assisted BAT (R-BAT). Therefore, the aim of this pilot study was to evaluate changes in both EEG power by investigating the topographical distribution of event ERD/ERS, and upper limb recovery of function after passive R-BAT in chronic stroke patients. Conducting a small-scale pilot study before the main study can enhance the likelihood of success of the main study. Moreover, information gathered in this pilot study would be used to refine or modify the research methodology and to develop large-scale studies [34]. The work hypothesis was that R-BAT would improve recovery of upper limb function and that these effects would be associated with an increase in activation of the ipsilesional hemisphere.

2. Methods

This study was a within-subject design. Seven right-handed male outpatients aged ≥ 18 years with first-ever stroke were recruited. Inclusion criteria were unilateral stroke (hemorrhagic or ischemic) as documented by radiologic evidence; at least 6 months from stroke; Medical Research Council (MRC) scale score ≤ 4 [35] evaluated at the wrist and finger extensors; and motor function stability assessed by means of a 2-week baseline evaluation.

Exclusion criteria were multi-infarctual cerebrovascular pathology; Mini-Mental State Examination (MMSE)

score ≤ 24/30 [36]; Modified Ashworth Scale (MAS) score > 4 [37] at the wrist and/or fingers; botulinum toxin injections in the 12 weeks prior to and/or during the study period; presence of metallic implants in the brain; previous brain surgery; use of medications altering cortical excitability or with a presumed effect on brain plasticity; and any other diagnosis having a major effect on upper limb function. Patients were not receiving any type of physical therapy for the affected upper limb during the study period. Table 1 presents patients' demographic and clinical data.

Control data from eight healthy volunteers (5 women; mean age 26.38 years ± SD 2.62 years), performing the same experimental motor paradigm, were gathered from our previous study [17]. The local ethics committee of the Verona University Department and Hospital (CE number 2366) approved the study. All participants provided written informed consent in accordance with the Declaration of Helsinki.

2.1. Assessments. Demographic and clinical data were collected at enrollment. Neurological severity and disability were assessed by the European Stroke Scale [38] and the Barthel Index [39], respectively. The precise site of stroke was identified by lesion mapping analysis using MRIcron software (http://www.mricro.com/mricron) (Table 1). MRI images were gathered from each patient, except for one (number 6) for digital imaging unavailability. Lesions were visually identified as having altered FLAIR signal intensity compared to corresponding contralateral tissue [40]. An expert clinical neurologist confirmed the lesion, and a trained image analyst traced all lesions visually identified using digital T1-weighted anatomical MRI scan. The ch2bet anatomical brain template provided with the MRIcron software was used to draw three-dimensional regions of interest (ROIs) [41]. For each patient, the ROI images were converted into volume of interest (VOI) images using MRIcron software (http://www.mricro.com/mricron). The regions of the brain that have sustained damage were computed and reported in Table 1.

Patients completed baseline assessment with primary and secondary outcome measures. Baseline values were obtained by averaging the baseline scores (T_0). The Fugl-Meyer motor assessment (FM) was the primary outcome measure [42–44]. It is a sensitive, reliable, and valid test to evaluate functional improvements in stroke studies on robotic upper limb rehabilitation (score range, 0–66; with higher scores indicating better performance) [42, 44]. Patients with a FM score < 18 were considered affected by severe-moderate upper limb paresis [19]. Although the minimal clinically important difference on the FM scale is not yet known in chronic stroke patients, a greater than 10-point (10%) change in FM motor scores was considered a clinically meaningful improvement [45].

The secondary outcomes were the Action Research Arm Test (ARAT) [46, 47] to evaluate upper limb function (score range, 0–57; with higher scores indicating better performance), the Motricity Index (MI) upper limb items (Bohannon et al. 1999) to evaluate upper limb strength (score range, 0–99; with higher scores indicating greater strength), the MAS [37] to evaluate upper limb spasticity (score range, 0–4; with higher scores indicating worse spasticity; total score, 0–16; with higher scores indicating worse spasticity), and the Barthel Index (BI) to evaluate disability.

Clinical assessments were repeated after training (T_1) and at 1-month follow-up (T_2). The same therapist, who was unaware of the nature of the study, assessed all patients. All outcome measures after training are expressed in relation to the baseline values.

2.2. Neurophysiological Measures and Motor Paradigm. EEG data were acquired using a video-EEG system (Ates Medica Device, Verona, Italy) and a cap (Electrical Geodesic Inc., Eugene, OR, USA) with 32 Ag/AgCl electrodes positioned according to a 10/20 international system. The reference was placed at Cz. The electromyographic (EMG) signal was recorded from the right and left flexor carpi radialis muscles with two surface Ag/AgCl electrodes in a belly tendon montage. This served to trigger the movement onset and to monitor movements required by the tasks (i.e., involuntary mirror movements and any other unspecific muscle activations). The EEG data were acquired at a rate of 250 Hz using the software package Geodesic EEG System on Neurotravel technology (Ates Medica Device and Electrical Geodesic Inc.).

The video-EEG was performed during a robot-assisted motor paradigm using the Bi-Manu-Track (BMT) (Rehastim Co, Berlin, Germany) [19, 20]. The protocol consisted of six tasks involving unilateral, bilateral, passive, and active movements of wrist flexion/extension [17, 18, 29]. In each protocol, six 20 s runs of rest alternating with six 20 s runs of execution were performed. Task execution was acoustically paced with a metronome at a frequency of 1 Hz. The metronome ticking continued during both activation and rest blocks to keep input constant. The subject was signaled to start and stop the task according to the experimenter's vocal instruction "start" and "stop," respectively. To perform the task correctly, each subject was trained for several minutes before the experiment.

EEG assessments were carried out at T_0, T_1, and T_2 during one-day experimental sessions in a quiet environment in the afternoon. The data were processed in MATLAB 7 (MathWorks, Natick, MA, USA) using scripts based on EEGLAB toolbox (Delorme and Makeig 2004), as well as a custom-made code created for this study. The EEG recordings were band-pass filtered from 1 to 30 Hz; visible artifacts were removed using an independent component analysis procedure [48], and data were processed using a common average reference. EMG signal was band-pass filtered from 10 to 450 Hz and rectified. The envelope was computed by low-pass filtering the signal (5 Hz). The threshold level for activity was identified for EMG by measuring the standard deviation of the signal during rest condition. The threshold level was set at two times this standard deviation. The time of EMG offset was identified as the intersection of the envelope signal with the threshold level. The EEG data of each rest and active run, selected by EMG signal, were divided into epochs of 2 s. Power spectral density (μV^2/Hz) was estimated using a fast Fourier transform (FFT) applied to 2 s period

Table 1: Demographic and clinical data.

Patient	Age	Gender	Hand preference (°)	Poststroke (months)	Type of stroke	Side of stroke	Postrehabilitation (months)	Lesion mapping analysis (Brodmann areas/white matter tracts)		ESS (0–100*)
1	61	M	+15	78	H	L	6	F, T, P	48, 40, 39, 6, 44, 45, 3, 7, 22, 41, 2, 42, 4, 19, 43, 37, 21, 47, 9, 46, 1, 18, 23, 10/41, 27, 29, 25, 33, 23, 17, 47, 21, 5	69
2	60	M	+23	61	I	L	6	F, T	48, 32, 46, 24, 11, 25, 45/23, 3, 4, 35, 17, 43, 25, 33	65
3	74	M	−18	80	I	L	12	F, T, P, O	44, 48, 46, 6, 45, 9, 4, 3, 32, 19/25, 41, 24	69
4	64	M	+24	20	I	L	6	T	48/25, 4, 19, 33, 43, 17, 27, 23, 41, 5	70
5	49	M	−16	21	I	L	6	F, T, P	48, 45, 44, 6, 46, 43, 4, 3, 47, 32, 9, 38, 22, 10/25, 23, 41, 4, 33, 43, 17, 3, 35	82
6	49	M	−15	123	H	L	18	F, P		79
7	56	M	+24	83	I	R	6	F, T, P, O	48, 37, 19, 20, 21, 18, 40, 6, 39, 22, 3, 38, 4, 2, 44, 47, 7, 41, 42, 43, 17, 34, 45, 1, 11, 36, 30, 28, 35, 27/42, 34, 26, 32, 30, 28, 40, 22, 46, 4, 24	64
Mean	59			66.57			8.57			71.14
SD	8.79			36.61			4.72			6.82

M: male; °Briggs and Nebes' laterality inventory; I: ischemic; H: hemorrhagic; R: right; L: left; SD: standard deviation; ESS: European Stroke Scale; F: frontal lobe; T: temporal lobe; P: parietal lobe; O: occipital lobe; (): range; *best performance. Brodmann areas and white matter tracts are reported in decreasing order according to the number of involved voxels.

and then averaged separately for each condition (rest and active). The recordings were Hamming-windowed to control for spectral leakage. A ERS/ERD procedure was used to quantify the changes in EEG power in the upper alpha (10–12 Hz) and the beta (13–30 Hz) frequency ranges. ERD/ERS transformation was defined as the percentage decrease/increase of power density during the task with respect to the baseline value (rest condition). Event-related power decreases, which represent a decrease in synchrony of the underlying neuronal populations and indicate cortical activation state, are expressed as negative values, whereas event-related power increases indicating a cortical idling state are expressed as positive values [33, 49]. The alpha and beta ERD/ERS maps were derived for all patients and used for individual analysis.

A laterality index (LI) [50], describing the contrast in amount of activation (i.e., ERD in alpha and beta bands) between the right and left hemisphere, was calculated during all movement tasks according to

$$\mathrm{LI} = \begin{cases} \dfrac{(|\mathrm{ERD_C}| - |\mathrm{ERD_I}|)}{(|\mathrm{ERD_C}| + |\mathrm{ERD_I}|)} & \text{if } \mathrm{ERD_C} < 0 \text{ and } \mathrm{ERD_I} < 0, \\ 0 & \text{if } \mathrm{ERD_C} > 0 \text{ and } \mathrm{ERD_I} > 0, \\ +1 & \text{if } \mathrm{ERD_C} < 0 \text{ and } \mathrm{ERD_I} > 0, \\ -1 & \text{if } \mathrm{ERD_C} > 0 \text{ and } \mathrm{ERD_I} < 0, \end{cases} \quad (1)$$

where ERDc is the C3 ERD value over the contralateral (left) sensorimotor (SM) area and I is the C4 ERD over the ipsilateral (right) SM area. LI can thus range from +1 (exclusively contralateral) to −1 (exclusively ipsilateral).

2.3. Intervention. The training consisted of twenty-one 50-minute individual sessions, 3 days/week (Monday, Wednesday, and Friday), for 7 consecutive weeks. The BMT is a robotic arm trainer that allows bimanual practice of 1 degree of freedom pronation and supination movements of the forearm and the wrist in dorsiflexion and volarflexion [19, 20]. It has been designed to train distal movements (elbow and wrist), which are an integral part of activities of daily living. The patients sat at a height-adjustable table with their elbows flexed at 90° and their forearms inserted in an arm trough in the midposition. Each hand grasped a handle. A strap kept the affected hand in place. The training protocol consisted of 5 minutes of upper limb mobilization and stretching exercises to enhance flexibility and facilitate positioning on the BMT, followed by 45 minutes of robot-assisted BAT. Two computer-controlled modes were trained. The passive-passive modes consisted of smooth passive movements driven by the robotic system at a preselected speed and range of motion (ROM). The passive mode is an accepted mobilization technique in the neurodevelopmental framework to improve joint, muscle, and tendon flexibility, as well as to reduce muscle tone [51]. In addition, functional imaging and neurophysiological studies have shown that passive hand movements in healthy controls and in stroke patients resulted in a similar activation of the corresponding sensorimotor cortical areas [17, 18, 52–54]. The active-passive mode consisted of passive movements of the affected upper limb driven by the unaffected side. It is an accepted rehabilitation technique with a facilitatory effect on the affected upper limb, as previously discussed.

During each session, the patients performed up to 800 repetitions as follows: 400 repetitions in passive-passive mode (200 prono/supination and 200 wrist flexion/extension) and 400 in active-passive mode (200 prono/supination and 200 wrist flexion/extension). One repetition included both movement directions (forearm prono/supination and wrist flexion/extension). Treatments were performed in the same room by the same therapists not involved in the assessment procedures. The therapists set up the device and remained within shouting distance in case of any problems. Training parameters (i.e., ROM, movement speed, and number of repetitions) were tailored to each patient's ability and progressively increased as the patient improved. The therapists recorded on the patient's chart the exercises performed during each treatment session, improvements observed, and any adverse events occurring during the study period. During the study, patients did not receive other rehabilitation treatments than scheduled in the current protocol. They were allowed performing activities of daily function and physical activity according to their upper limb function. No advices on home-based exercises or any other upper limb training were given.

2.4. Statistical Analysis. Descriptive statistics included mean, standard deviation, and median. Brodmann areas and white matter tracts involved from the brain damage were reported in decreasing order according to the number of involved voxels in Table 1. Coloured maps representing the brain lesion were generated onto the automated anatomical labeling (AAL), and the Johns Hopkins University white matter templates provided *i*th MRIcron software [41] and displayed in figures. Shapiro-Wilk and Levene tests were used to check the normality of distribution and the homogeneity of variance. Because clinical data gathered from clinical scales are not normally distributed, nonparametric tests were applied. The Friedman test was used to analyze changes in performance over time. Post hoc comparisons were carried out on differences in T_0-T_1 and T_0–T_2 scores using Wilcoxon signed-ranks tests.

Because the EEG data were normally distributed, parametric tests were used. Comparison of the control group versus each single patient was carried out using a z-test ($p < 0.1$). In detail, the statistical map defines the electrodes in which ERD/ERS values from a patient differ statistically from those of a reference population (control group). To compare patients and the reference population, which was acquired with only 21 EEG channels, 19 electrodes out of 30 were included in the statistical analyses (Fp1, Fp2, F7, F3, Fz, F4, F8, T3, C3, Cz, C4, T4, T5, P3, Pz, P4, T6, O1, and O2). A three-way analysis of variance (ANOVA) for repeated measures was applied to the relative power with the three factors: "time" (T_0, T_1, and T_2), "task" (unimanual and bimanual active and passive movements), and "channel" (19 electrodes). The sphericity assumption was assessed using

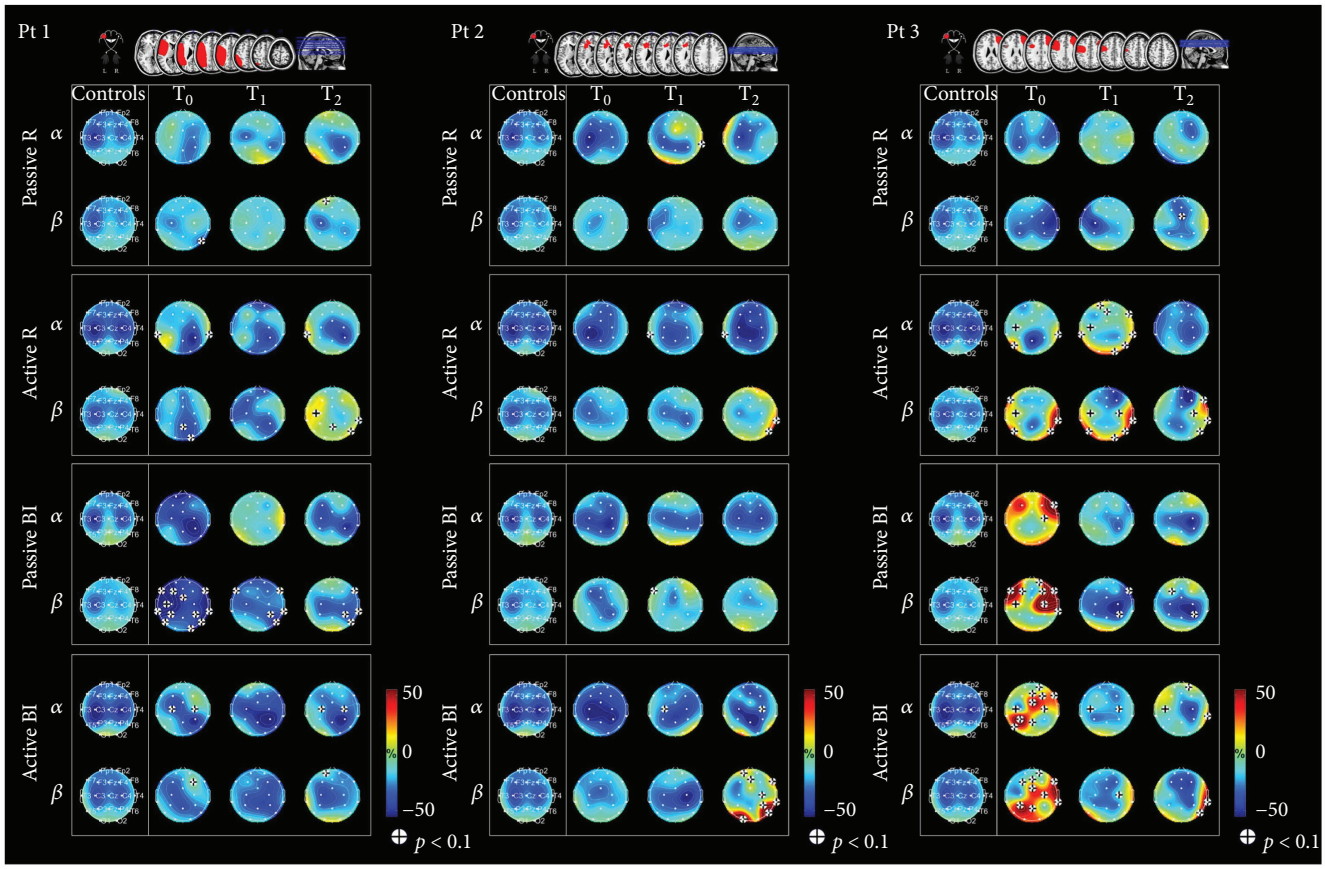

Figure 1: Lesions displayed on a magnetic resonance imaging brain template and topographic maps showing ERD/ERS values. ERD/ERS maps in the alpha and beta bands during passive and active movements with the affected hand and during bimanual passive and active movements (patient numbers 1, 2, and 3). Blue indicates maximal ERD. The *t*-test was applied individually for each patient in order to compare the ERD/ERS map of each patient to the mean ERD/ERS map of the controls ($p < 0.1$ ($|t| > 1.895$) indicated by (+)).

Mauchly's test, and Greenhouse Geisser corrections were undertaken when sphericity was violated. Statistical results were deemed significant if $p < 0.05$. A post hoc two-tailed *t*-test adjusted for multiple comparisons with the Bonferroni method was used whenever appropriate. Finally, the Pearson correlation coefficient was used to assess the relationships between LI and clinical scales (FM and MAS), and between ERD/ERS values and clinical scales (FM and MAS) at each evaluation time point (T_0, T_1, and T_2). $p < 0.05$ was considered statistically significant. Software statistics IBM SPSS (20.0) for Macintosh software (IBM, Armonk, NY, USA) was used.

3. Results

Five of the 7 patients were affected by moderate-to-severe upper limb paresis, and 2 by mild paresis (numbers 5 and 6). All 7 patients presented upper limb spasticity, 5 of which at the wrist (numbers 1, 2, 3, 4, and 7). All patients completed the R-BAT. No adverse events were reported. The regions of the brain that have sustained damage were summarized in Table 1. Stroke location was cortical-subcortical in all patients. However, brain lesion size and location varied among patients. The most damaged areas were the supplementary motor area, primary motor cortex, the primary somatosensory cortex, retrosubicular area, pars orbitalis, part of the inferior frontal gyrus, dorsolateral prefrontal cortex, inferior frontal gyrus, fusiform gyrus, the most rostral part of the superior and middle temporal gyrus, and the angular gyrus. White matter tracts included the anterior limb of the internal capsule, fasciculus fronto-occipitalis superior, the superior longitudinal fasciculus, external capsule, and superior corona radiate. ROIs were displayed in Figures 1, 2, and 3 (for details, see Tables 4, 5, 6, 7, and 8 in Supplementary Materials available here).

3.1. Primary Outcome. A significant improvement in FM scale was noted over time ($p = 0.008$) (for details, see Figure in Supplementary Materials. A greater than 10% change in FM scores at both T_0-T_1 and T_0–T_2 was observed in 4 patients (57%) (numbers 1, 2, 4, and 7) (Table 2).

Post hoc comparisons revealed significant effects between T_0 and T_2 by 2.85 (95% CI, 1.5 to 4.66) ($p = 0.002$). No statistically significant differences were noted between T_0 and T_1 (Table 3).

3.2. Secondary Outcomes. A significant improvement in MI ($p = 0.009$) and MAS ($p = 0.002$) scores over time was seen.

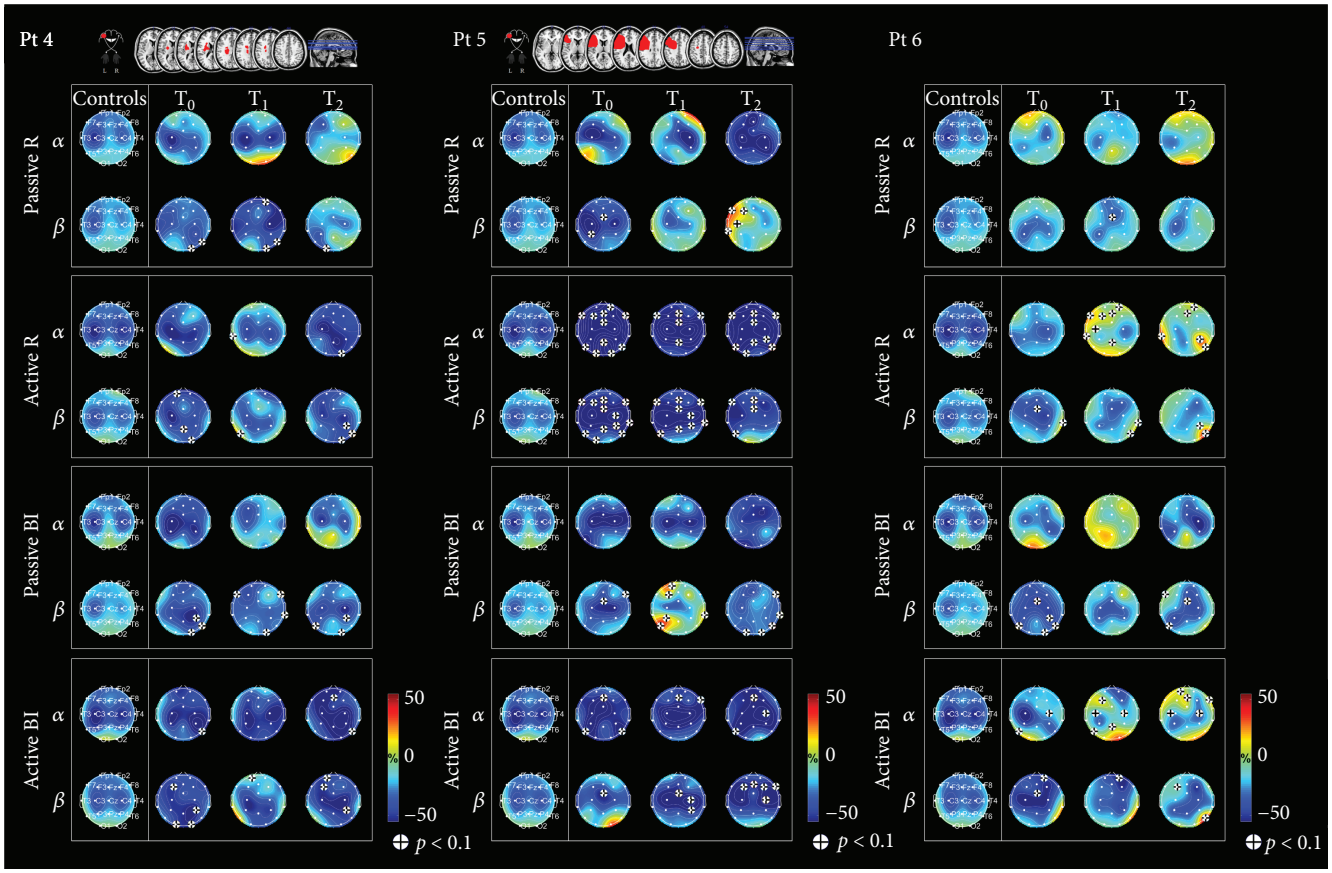

Figure 2: Lesions displayed on a magnetic resonance imaging brain template and topographic maps showing ERD/ERS values. ERD/ERS maps in the alpha and beta bands during passive and active movements with the affected hand and during bimanual passive and active movements (patient numbers 4, 5, and 6). Blue indicates maximal ERD. The *t*-test was applied individually for each patient in order to compare the ERD/ERS map of each patient to the mean ERD/ERS map of the controls ($p < 0.1$ ($|t| > 1.895$) indicated by (+)).

Improvement on the MI was recorded for five patients (71%) (numbers 1, 4, 5, 6, and 7) at T_1 and was maintained at T_2. No changes in performance on the MI were recorded for two patients (28%) (numbers 2 and 3). Post hoc comparison revealed significant changes on MAS between T_0-T_1 ($p = 0.017$) and T_0–T_2 ($p = 0.017$). No significant effects were observed on the ARAT, BI, and MI.

3.3. Neurophysiological Evaluation. One patient (number 7) was excluded from the EEG analysis because of artifacts during recording. ANOVA of the alpha and the beta relative powers showed significant main effects for the factor "channel" in both the alpha [$F(2.98,14.88) = 12.68$, $p < 0.001$] and the beta [$F(1.78,8.92) = 6.5$, $p < 0.05$] band. No significant main effects for the factors "time" and "task" were observed. Significant interactions between "time" and "channel" were also observed in the alpha [$F(36,180) = 1.47$, $p < 0.05$] and the beta [$F(36,180) = 1.596$, $p < 0.05$] range. In particular, significant differences were observed in O1 (T_0 versus T_1, $p < 0.001$), O2 (T_0 versus T_1, $p < 0.01$), T6 (T_0 versus T_1, $p < 0.05$), and 28 (T_1 versus T_2, $p < 0.05$) in alpha band and in F7 (T_0 versus T_1, $p < 0.05$) in beta band.

No mirror movements occurred during unimanual movements, as confirmed by EMG.

3.4. Passive Movement with the Affected Hand. Individual EEG results are summarized in Figures 1 and 2, which display lesions on a magnetic resonance imaging brain template and topographic maps showing ERD/ERS values. The first column represents the maps from healthy subjects (control), the other three represent individual maps at specific time points. Alpha and beta rhythm (first and second row, resp.) are reported for each task.

Bilateral alpha desynchronization was observed at T_0 in all patients except for patient number 1 who showed only contralesional ERD and for patient number 5 who showed ipsilesional ERD. At T_1, four different patterns of alpha ERD were observed: bilateral (patient numbers 1, 2, and 4), contralesional (patient number 5), ipsilesional (patient number 6), and anterior (patient number 3). At T_2, bilateral ERD was detected in 1 patient (number 5), contralesional ERD in 2 patients (numbers 1 and 3), and ipsilesional ERD in 3 patients (numbers 2, 4, and 6).

Bilateral beta desynchronization was observed at T_0 in all patients, except for 2 (numbers 1 and 2) who showed ipsilesional ERD. As compared with the controls, ERD was significantly decreased over the right temporal and occipital electrodes in 1 patient (number 4) and over C3 and electrode 28 in 1 patient (number 5). At T_1, the ERD pattern remained bilateral and different from the controls in the right temporal

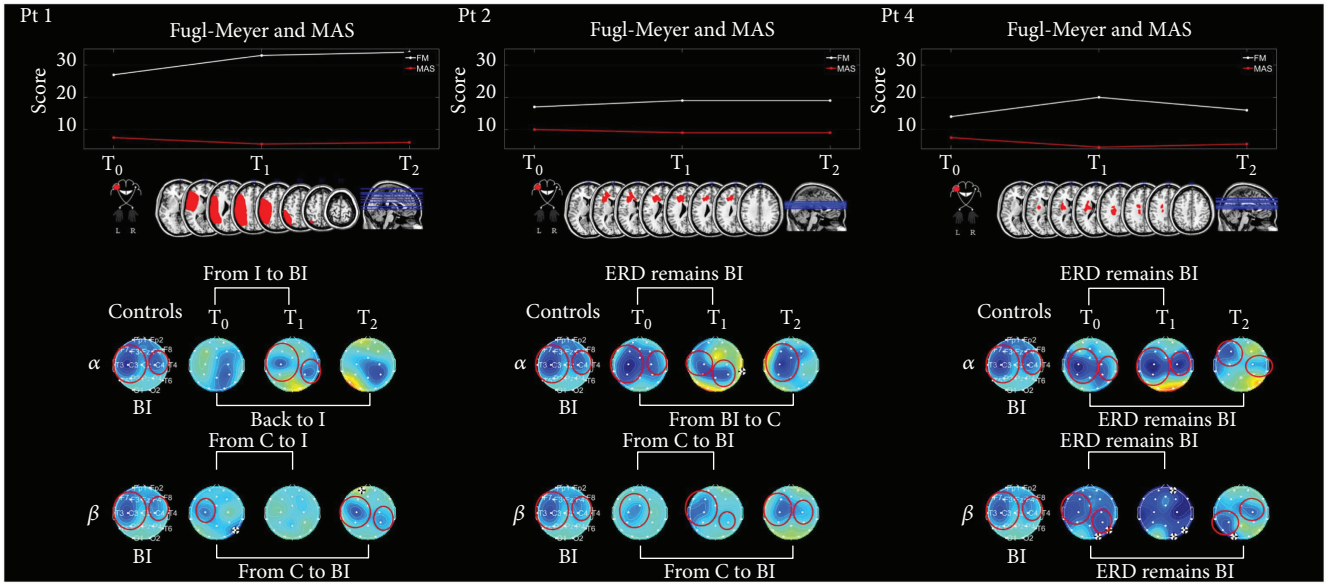

Figure 3: Fugl-Meyer and Modified Ashworth Scale scores, stroke lesions, and topographic maps showing ERD/ERS values during passive movement of the affected hand are reported for three representative patients (numbers 1, 2, and 4). Blue indicates maximal ERD. BI: bilateral ERD; C: ipsilesional ERD; I: contralesional ERD.

Table 2: Changes in primary and secondary outcome scores.

Patient	Fugl-Meyer (0–66)			Action Research Arm Test (0–57)			Motricity Index (0–100)			UL MAS (0–16)			Barthel Index (0–100)		
	T_0	T_1	T_2	T_0	T_1	T_2	T_0	T_1	T_2	T_0	T_1	T_2	T_0	T_1	T_2
1	27	33*	34*	2	2	2	39	47	47	7.5	5.5	6	90	90	90
2	17	19*	19*	0	0	0	33	33	33	10	9	9	90	90	90
3	33	33	34	16	16	16	65	65	65	6	4.5	4.5	85	85	85
4	14	20*	16*	0	0	0	28	44	39	7.5	4.5	5.5	95	100	100
5	61	63	64	33	53	55	72	84	76	3	1	1	80	85	90
6	50	54	53	27	35	41	76	99	92	1	0	0	100	100	100
7	14	17*	16*	2	2	2	39	44	44	8.5	6.5	7	90	90	90
Mean/median	30.86	34.14	33.71	11.43	15.43	16.57	50.29	59.43	56.57	7.5	4.5	5.5	90.00	91.43	92.14
SD/Q1–Q3	18.51	18.04	18.86	13.95	22.01	22.54	20.00	24.25	21.67	3–8.5	1–6.5	5.5–7	6.45	6.27	5.67

T_0: baseline assessment; T_1: after training; T_2: 1-month follow-up; UL: upper limb; MAS: Modified Ashworth Scale; *change in Fugl-Meyer score greater than 10%; (): range of score; SD: standard deviation; Q1–Q3: 1st quartile to 3rd quartile.

and occipital electrodes in 1 patient (number 4) and ipsilesional in 1 patient (number 2); anterior ERD was observed in 1 patient (number 1) and ipsilesional ERD in 3 patients (numbers 3, 5, and 6). As compared with the pattern observed in the controls, significant ERD over electrode 28 was noted in 1 patient (number 6). Three beta ERD patterns were observed at T_2: (i) ipsilesional ERD in 3 patients (numbers 1, 2, and 6); (ii) bilateral ERD in 1 patient (number 4) with significant predominance over the ipsilesional side; and (iii) significant ipsilesional synchronization was noted in 1 patient (number 5) and significant ERD over anterior and central areas in 1 patient (number 3). Fugl-Meyer scores, stroke lesions, and topographic maps showing ERD/ERS values during passive movement of the affected hand are reported for three representative patients (numbers 1, 2, and 4) in Figure 3.

3.5. Active Movement with the Affected Hand. Three different patterns of alpha desynchronization were observed at T_0: (i) bilateral ERD in 3 patients (numbers 2, 4, and 5); (ii) contralesional ERD in 2 patients (numbers 1 and 6); and (iii) ERD in central-posterior regions in 1 patient (number 3). These patterns remained unchanged at T_1. The distribution was maintained at T_2 in 4 patients (numbers 1, 2, 4, and 5), though widespread desynchronization was observed in 2 of them (numbers 4 and 5), with significant differences over the frontal regions as compared with the controls. Marked ERD on the contralesional side was observed in 1 patient (number 3). ERD became ipsilesional in 1 patient (number 6), with strong synchronization over the frontal electrodes and over T3, P4, and T6, as compared with the controls.

Three different patterns of beta ERD were observed at T_0: (i) bilateral in 4 patients (numbers 2, 4, 5, and 6), with

Table 3: Within-group training effects on clinical outcome measures.

	Friedman's two-way analysis of variance T_0–T_2	Post hoc comparisons T_0-T_1		Post hoc comparisons T_0–T_2	
	p value	p value	95% CI Mean (LB, UP)	p value	95% CI Mean (LB, UP)
Primary outcome					
Fugl-Meyer (0–66*)	0.008*	0.027	3.28 (1.23, 5.33)	0.017°	2.85 (1.05, 4.66)
Secondary outcomes					
Action Research Arm Test (0–57*)	n.s.	n.s.	4.00 (−3.08, 11.08)	n.s.	1.14 (−0.95, 3.24)
Motricity Index upper limb (0–100*)	0.009*	0.04	9.14 (1.28, 16.99)	0.04	6.28 (0.87, 11.69)
Barthel Index (0–100*)	n.s.	n.s.	1.42 (−0.82, 3.68)	n.s.	2.14 (−1.49, 5.78)
Modified Ashworth Scale (0–16*)	0.002*	0.017°	−1.78 (−2.43, −1.13)	0.02	−1.5 (−1.87, −1.12)
Stroke Impact Scale (0–800*)	n.s.	n.s.	11.18 (−19.19, 41.56)	n.s.	7.11 (−18.71, 32.94)

T_0: baseline assessment; T_1: after training; T_2: 1-month follow-up; CI: confidence interval; LB: lower bound; UP: upper bound; n.s.: not significant. *p value significant at ≤0.05; °p value significant at ≤0.025.

predominance over the ipsilesional side in 1 patient (number 2); (ii) there was a significant difference in central-posterior ERD in 1 patient (number 1) as compared with the controls, and (iii) in anterior-posterior ERD in 1 patient (number 3). These patterns remained unchanged at T_1. Desynchronization became more ipsilesional to movement in 2 patients (numbers 2 and 5) at T_2.

3.6. Bimanual Passive Movement. At T_0, bilateral alpha ERD was found in 5 patients (numbers 1, 2, 4, 5, and 6), more localized over C4 in 1 patient (number 1). One patient (number 3) showed central-parietal ERD. At T_1, bilateral desynchronization was maintained in 2 patients (numbers 2 and 5); ERD was localized at P4 in 2 patients (numbers 1 and 3), and over left central-anterior area in 1 patient (number 4), while ERS at P3 was observed in 1 patient (number 6). At T_2, a bilateral pattern was observed in all patients. One patient (number 3) showed a more localized ERD over C4.

Two patterns of beta ERD were observed at T_0: (i) bilateral in 4 patients (numbers 1, 4, 5, and 6), with significant predominance over C4 in 1 patient (number 4) and over the right posterior region in 1 patient (number 6), as compared with the controls and (ii) anterior-posterior ERD in 2 patients (numbers 2 and 3). A strong ERS was observed in 1 patient (number 3) over frontal areas and over right motor area. Four different patterns were found at T_1: (i) bilateral ERD in 3 patients (numbers 1, 4, and 6); (ii) significant ERD over the right SM in 1 patient (number 3); (iii) ERD over C3 and significant ERS over P3 in 1 patient (number 5); and (iv) ERD over F3, 28, and C3 in 1 patient (number 2). Bilateral ERD was found in all patients at T_2, with significant predominance over P4 in 3 patients (numbers 1, 3, and 4) and strong ERD localized over C3 in 1 patient (number 5).

3.7. Bimanual Active Movement. At T_0, bilateral alpha ERD was found in 4 patients (numbers 1, 2, 4, and 5) and it was significantly localized over C3 in 1 patient (number 1); ERD over the left SM was observed in 2 patients (numbers 3 and 6). The alpha maps at T_1 showed bilateral ERD in these 2 patients, with ERD over the right SM in patient number 3 and significant ERD over the left SM in patient number 6, as compared with the controls. Two patterns were observed at T_2: (i) bilateral ERD in 4 patients (numbers 2, 4, 5, and 6), which was more localized over the right side in 2 patients (numbers 2 and 5) and (ii) ERD over the right SM in 2 patients (numbers 1 and 3) differently from the controls.

At T_0, bilateral beta ERD was found in 3 patients (numbers 4, 5, and 6), more localized over the mesial region in 1 patient (number 5) and over F3, P4, O1, and O2 in 1 patient (number 4). ERD over C3 was observed in 3 patients (numbers 1, 2, and 3). At T_1, bilateral ERD was detected in all patients, with predominance over C4 in 3 patients (numbers 2, 5, and 6). Three different patterns were observed at T_2: (i) bilateral ERD in 3 patients (numbers 4, 5, and 6), with predominance over the left central-posterior electrodes in 1 patient (number 6); (ii) ERD over the left SM in 2 patients (numbers 1 and 2); and (iii) ERD over the right frontal-central electrodes in 1 patient (number 3).

3.8. Association between ERD/ERS Modulation and Clinical Scales. No significant correlation was observed between LI and clinical scales (MAS and FM) at each evaluation time point. The only statistically significant correlation between ERD/ERS and clinical scales was for the passive bimanual motor task, where beta ERD over left sensorimotor area was positively correlated with MAS at T_2 ($R = 0.8459$, $p < 0.05$). Nevertheless, EEG patterns and LI changes related to FM and MAS changes were observed over time. At T_0, the majority of patients showed bilateral or contralesional activation of the primary sensorimotor cortex on alpha band during passive movement of the affected hand, as shown also by LI (Figure 4). Three patients (numbers 2, 4, and 5) showed ipsilesional activation. After training, desynchronization moved from contralesional to ipsilesional (patient numbers 1 and 6), from bilateral to ipsilesional (patient number 3), and from ipsilesional to bilateral (patient number 4) or to contralesional (patient number 5), as quantified by LI. The

pattern remained ipsilesional in patient 2. These changes paralleled the improvements in the FM scores (Figure 3). No change in FM scores was noted in patient number 3, as confirmed by the anterior-posterior ERD. Regarding beta band, the 3 patients (numbers 4, 5, and 6) who showed bilateral activation before training moved to ipsilesional activation after training, as demonstrated also by the improvement in the MAS score at the wrist, in patient 3 desynchronization moved to contralesional to ipsilesional. At T_2, patient number 1 had values close to the pretreatment ones as shown by neurophysiological evaluation in alpha band, while an improvement was noted in 2 patients (numbers 4 and 6) as shown by both clinical and neurophysiological evaluation.

During active movement of the affected hand, neurophysiological results in alpha band remained unchanged from T_0 to T_2 in 4 patients (bilateral ERD in numbers 2, 4, and 5 and contralesional in number 1), and a shift from contralesional to ipsilesional ERD was noted in 1 patient (number 6), as confirmed (except for patient number 1) by clinical evaluation, where FM score improved from T_0 to T_2, and by LI changes. Modification from T_0 to T_2 in beta band desynchronization was observed in 3 patients in which ERD shifted from bilateral to the ipsilesional side (numbers 2 and 5) and to contralesional to ipsilesional side (number 3).

4. Discussion

The main finding of our study was a reduction in upper limb spasticity after passive robot-assisted bilateral arm training. This effect was associated, albeit not significantly, with changes in cortical oscillatory activity, as demonstrated by the ERD/ERS maps and LI.

The most common deficit after stroke is hemiparesis of the contralesional UL [55]. However, the manifestation of UL motor impairment includes also muscle weakness, impaired motor control, deficits in somatic sensations, pain, and changes in muscle tone [55]. Poststroke spasticity is a disabling symptom affecting 17 to 43% of patients in the chronic stages of the illness [56]. It is now clear that spasticity encompasses a broad spectrum of clinical conditions, the so-called spastic movement disorder (SMD) [57]. Interdisciplinary complex rehabilitation interventions represent the mainstay of poststroke care [6]. Rehabilitation procedures, in particular, play a pivotal role in the management of SMD [58].

So far, limited knowledge is available to describe what best represents the optimum rehabilitative procedure. From a theoretical point of view, the UL rehabilitation program should include motor rehabilitation, multisensory interaction, hemispheric subspecialization in motor activity, and electrical brain stimulation [59]. Based on the current level of evidence, a decisional tree for UL rehabilitation has been proposed as a clinical tool for selecting a specific patient's intervention [55]. According to the stage of stroke, the presence of hand movements and the presence of spasticity-specific rehabilitation approaches and adjuvant techniques have been recommended [55]. Muscle strengthening exercises, treatment of spasticity, constraint-induced movement therapy, and mirror therapy have been recommended as a main rehabilitation intervention. However, most of these procedures cannot be performed in severely impaired patients. To this end, technology-supported training can overcome difficulties and deliver high-dosage and high-intensity training even in severely impaired patients [60]. Coupling the bilateral approach to robot-assisted therapy may be relevant in the rehabilitation of patient unable to perform active tasks.

Passive robot-assisted BAT has been shown to improve upper limb motor function in subacute and chronic stroke patients [11, 13, 19, 20, 61]. Moreover, two studies have shown positive training effects on spasticity [19, 20] though neither included neurophysiological measures. A full review of the pathophysiology of spasticity after stroke is beyond this perspective. Nevertheless, the overall evidence that the hyper excitable stretch reflexes may depend on imbalance of supraspinal inhibitory and excitatory inputs and on secondary soft tissue changes in the paretic limb has been established [62]. From a clinical point of view, spasticity in patients with upper motor neuron syndrome can be divided into two components. On the one hand, it can be mediated by the stretch reflex, which corresponds to spasticity itself. On the other hand, hypertonia can depend on soft tissue changes, which are referred as "nonreflex hypertonia." Limb mobilization in patients with upper motor neuron syndrome is then essential to prevent and treat these two components [62].

Our findings are shared by a previous study by Hesse [20] and for the first time suggest that training effects could parallel specific changes in EEG power. Before training, passive movement of the affected hand resulted in bilateral or contralesional alpha and beta desynchronization of the primary sensorimotor cortex in the majority of patients, as quantified by LI (Figure 4).

After training, desynchronization shifted from bilateral to ipsilesional sensorimotor areas, and active movement of the affected hand shifted from contralesional to ipsilesional sensorimotor areas, as compared with pretreatment assessment. No significant correlation was observed between LI or ERD/ERS and clinical scales, but a marked trend was detected over time: changes in clinical scales, associated to a good recovery, paralleled with changes in LI values, which evidence modifications of ERD from contralesional to ipsilesional side.

Why R-BAT supports the observed findings remains a challenging question. The specific features of the training, in terms of type (passive, intensive, and repetitive) and duration (7 weeks), may have provided strong proprioceptive cueing by strengthening the neural pathways involved in upper limb function [63]. There is converging evidence that training protocols consisting of both active and passive movements (with or without visual feedback) tend to be more beneficial than passive movement alone in functional and neurophysiological outcomes [63, 64]. However, there is initial evidence suggesting that passive training may induce cortical reorganization, providing evidence for the notion that proprioceptive training could improve motor function [63]. Passive movements are a form of sensory stimuli (mainly proprioceptive input) that

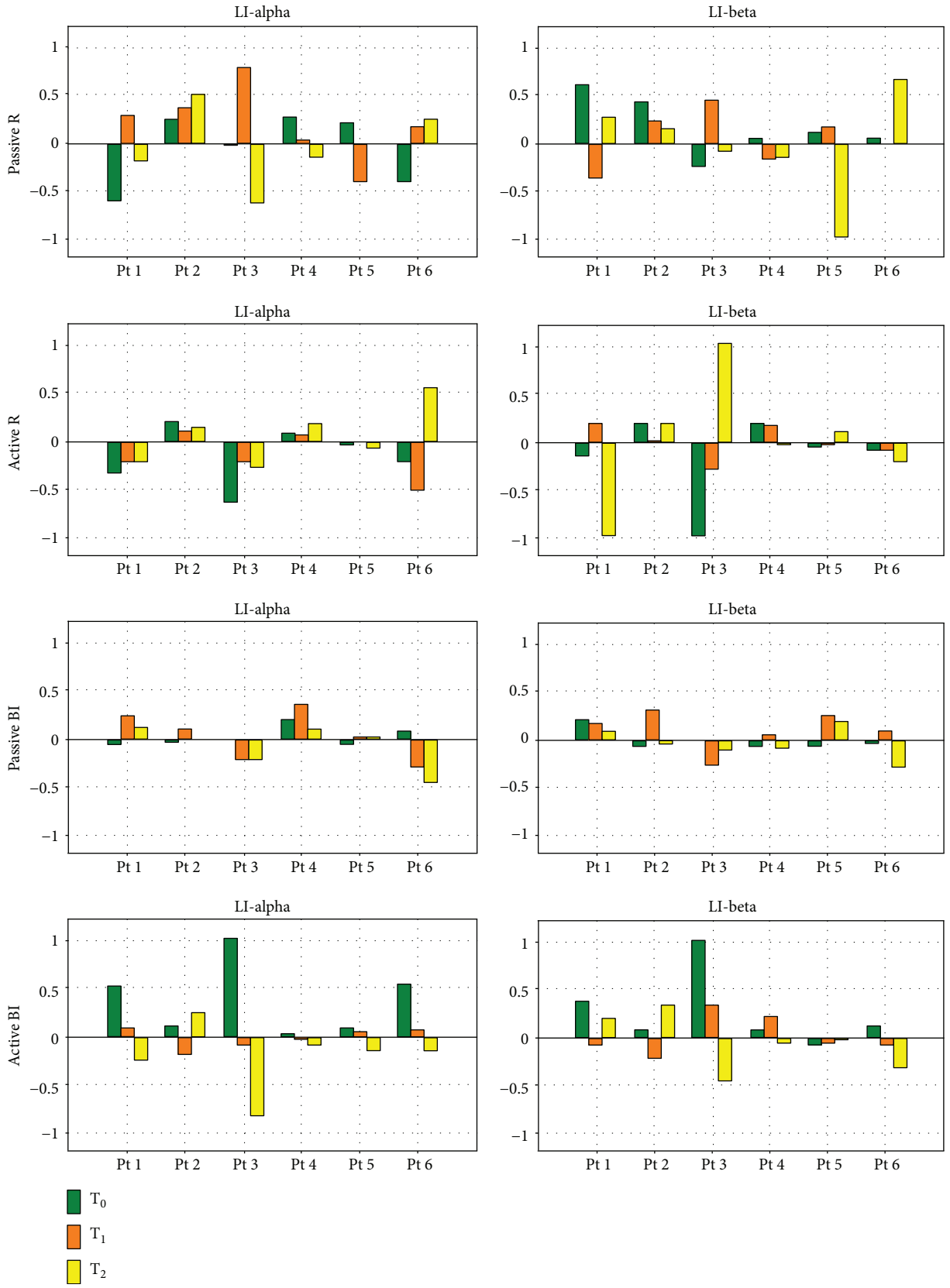

Figure 4: Laterality index (LI) in alpha and beta bands at each evaluation time point (T_0, T_1, and T_2). LI was calculated considering contralateral (ipsilesional) ERD as the C3 ERD value over the left sensorimotor area and ipsilateral (contralesional) ERD as the C4 ERD over the right sensorimotor area. LI > 0 indicates contralateral ERD and LI < 0 indicates ipsilateral ERD.

can activate the primary motor area (M1) and the primary somatosensory area (S1) through two mechanisms. The one is based on overlapping of the M1 and S1 maps, while the other is based on the fact that M1 receives somatosensory input directly from the thalamus [65]. This suggests that proprioceptive inputs are part of the motor control network during both the preparation and the execution of movement [63, 66, 67]. Robots might increase the sensorimotor experience by providing novel patient-environment interactions through passive and passive-mirrored repetitive training [68]. Note that training regimens lasting 6 weeks or longer tend to yield positive results [63].

The execution of bilateral pattern of movements might amplify these effects. In healthy controls, active-passive bilateral patterns of coordinated movement performed for 15 minutes disinhibit the M1 ipsilesional to the assisted upper limb and facilitate its excitability for at least 30 minutes [16]. In people with chronic stroke, daily application of active-passive R-BAT followed by motor practice was found to lead to a greater improvement in upper limb function as compared with motor practice alone [11]. These effects were associated with an increase in ipsilesional corticomotor excitability [11]. Passive R-BAT may facilitate cortical neural plasticity by two mechanisms. One consists of the simultaneous activation of both hemispheres, which is thought to facilitate activation of the damaged hemisphere by reducing transcallosal inhibition from the unaffected hemisphere. In this view, a rebalancing of interhemispheric inhibition would be enhanced [9, 11, 61, 69]. The other mechanism involves facilitation of the contralesional uncrossed corticospinal tract and spared indirect corticospinal pathways [22]. Finally, the training effects on muscle tone may be related to improvements in viscoelastic muscle properties [58].

To our knowledge, this is the first study that explores the effects of passive bilateral upper limb robot-aided rehabilitation by behavioral and EEG assessments in chronic stroke patients. So far, few studies have reported on the modulation of EEG cortical activity during robot-assisted tasks [17, 18, 29, 70, 71] and none have evaluated the effects of passive R-BAT on spasticity. The major advances in this study compared to our previous research is the investigation of neural correlates of behavioral changes after robot-assisted training in chronic stroke patients. Building on the results from our previous EEG studies on healthy subjects, few major novel aspects can be highlighted. Firstly, the feasibility of the EEG setup and motor paradigm was generated by movements in highly standardized robot-assisted paradigm to evaluate cortical activity in clinical setting. It allows for testing brain activity during specific rehabilitation tasks in different populations [72]. Second, the patients were in the chronic stage after stroke, which minimized the influence of confounding effects due to spontaneous recovery. In addition, a 2-week baseline assessment was performed to ensure motor function stability. Third, no combined treatments were associated with robotic training. In most previous studies, multiple modalities were combined in one training protocol, making it difficult to single out the effects of one specific modality [73] and to explore the neural correlates of specific robot-assisted training [74]. Finally, the training effects were evaluated at 1-month follow-up. Within this perspective, robotic devices can serve as highly standardized and reliable tools to inform the design of evaluation protocols and provide new insights into the dynamics of cortical reorganization promoted by rehabilitation.

The main limitation of the present study is the small sample size. Moreover, the lack of homogeneity between brain lesion size and location would have precluded statistically significant results. The ERD/ERS maps of the patients shown were different among themselves, and each map was also different with the control group in different ways. The current results varied across patients and precluded to conclude. According to these preliminary results, future studies would enroll larger sample size, and patients would be stratified according to lesion features. It would allow discussing EEG power changes after specific robot-assisted upper limb training (i.e., active, passive, unilateral, and bilateral). Other limitations are the lack of follow-up beyond 1 month and the lack of a control group receiving conventional therapy. Moreover, control group should be age-matched, in order to compare it to a group of subjects affected by stroke. However, since the peak frequency of the mu wave increases with age until maturation into adulthood, when it reaches its final and stable frequency of 8–13 Hz [75], the age of the subjects should not significantly affect the EEG desynchronization process during movement. These limitations notwithstanding, specific training effects on functional upper limb recovery and EEG power could be identified, as previously discussed.

5. Conclusion

The findings from the present pilot study may have implications for upper limb rehabilitation after stroke. Recovery may benefit from passive R-BAT program even years after the stroke event. Furthermore, bilateral repetitive robot-assisted training programs may sustain improvement in upper limb functioning in chronically impaired stroke patients and induce specific changes in the sensorimotor network. We speculate that the reduction in spasticity may have facilitated EEG changes over the ipsilesional sensorimotor network. The utility of a bilateral repetitive robot-assisted program as an adjuvant to physical therapy warrants further consideration.

Conflicts of Interest

The authors declare that they have no conflicts of interest.

Acknowledgments

This study was supported by James S. McDonnell Foundation Collaborative Award "Advancing the Science of Rehabilitation: Translating Neuroscience and Rehabilitation into Everyday Life" (no. 220020413).

Supplementary Materials

Figure: upper limb behavioral scores. Table 4: brain lesion mapping results in patient number 1. Table 5: brain lesion mapping results in patient number 2. Table 6: brain lesion mapping results in patient number 3. Table 7: brain lesion mapping results in patient number 4. Table 8: brain lesion mapping results in patient number 5. Table 9: brain lesion mapping results in patient number 7. *(Supplementary Materials)*

References

[1] G. Kwakkel, B. Kollen, and J. Twisk, "Impact of time on improvement of outcome after stroke," *Stroke*, vol. 37, pp. 2348–2353, 2006.

[2] P. Langhorne, F. Coupar, and A. Pollock, "Motor recovery after stroke: a systematic review," *The Lancet Neurology*, vol. 8, no. 8, pp. 741–754, 2009.

[3] L. Oujamaa, I. Relave, J. Froger, D. Mottet, and J. Y. Pelissier, "Rehabilitation of arm function after stroke. Literature review," *Annals of Physical and Rehabilitation Medicine*, vol. 52, no. 3, pp. 269–293, 2009.

[4] N. Smania, M. Gandolfi, S. Paolucci et al., "Reduced-intensity modified constraint-induced movement therapy versus conventional therapy for upper extremity rehabilitation after stroke: a multicenter trial," *Neurorehabilitation and Neural Repair*, vol. 26, no. 9, pp. 1035–1045, 2012.

[5] J. M. Veerbeek, E. van Wegen, R. van Peppen et al., "What is the evidence for physical therapy poststroke? A systematic review and meta-analysis," *PLoS One*, vol. 9, no. 2, article e87987, 2014.

[6] P. Langhorne, J. Bernhardt, and G. Kwakkel, "Stroke rehabilitation," *The Lancet*, vol. 377, no. 9778, pp. 1693–1702, 2011.

[7] J. Mehrholz, A. Hädrich, T. Platz, J. Kugler, and M. Pohl, "Electromechanical and robot-assisted arm training for improving generic activities of daily living, arm function, and arm muscle strength after stroke," *Cochrane Database of Systematic Reviews*, vol. 6, article CD006876, 2012.

[8] A. C. Lo, P. D. Guarino, L. G. Richards et al., "Robot-assisted therapy for long-term upper-limb impairment after stroke," *The New England Journal of Medicine*, vol. 362, no. 19, pp. 1772–1783, 2010.

[9] J. H. Cauraugh, K. Sang-Bum, and J. Summers, "Chronic stroke longitudinal motor improvements: cumulative learning evidence found in the upper extremity," *Cerebrovascular Diseases*, vol. 25, no. 1-2, pp. 115–121, 2008.

[10] W. R. Staines, W. E. McIlroy, S. J. Graham, and S. E. Black, "Bilateral movement enhances ipsilesional cortical activity in acute stroke: a pilot functional MRI study," *Neurology*, vol. 56, no. 3, pp. 401–404, 2001.

[11] C. M. Stinear, P. A. Barber, J. P. Coxon, M. K. Fleming, and W. D. Byblow, "Priming the motor system enhances the effects of upper limb therapy in chronic stroke," *Brain*, vol. 131, no. 5, pp. 1381–1390, 2008.

[12] K. C. Stewart, J. H. Cauraugh, and J. J. Summers, "Bilateral movement training and stroke rehabilitation: a systematic review and meta-analysis," *Journal of the Neurological Sciences*, vol. 244, no. 1-2, pp. 89–95, 2006.

[13] P. L. Choo, H. L. Gallagher, J. Morris, V. M. Pomeroy, and F. van Wijck, "Correlations between arm motor behavior and brain function following bilateral arm training after stroke: a systematic review," *Brain and Behavior*, vol. 5, no. 12, article e00411, 2015.

[14] S. P. Swinnen, "Intermanual coordination: from behavioural principles to neural-network interactions," *Nature Reviews Neuroscience*, vol. 3, no. 5, pp. 348–359, 2002.

[15] C. M. Stinear, M. A. Petoe, S. Anwar, P. A. Barber, and W. D. Byblow, "Bilateral priming accelerates recovery of upper limb function after stroke: a randomized controlled trial," *Stroke*, vol. 45, no. 1, pp. 205–210, 2014.

[16] W. D. Byblow, C. M. Stinear, M. C. Smith, L. Bjerre, B. K. Flaskager, and A. B. McCambridge, "Mirror symmetric bimanual movement priming can increase corticomotor excitability and enhance motor learning," *PLoS One*, vol. 7, no. 3, article e33882, 2012.

[17] E. Formaggio, S. F. Storti, I. Boscolo Galazzo et al., "Modulation of event-related desynchronization in robot-assisted hand performance: brain oscillatory changes in active, passive and imagined movements," *Journal of NeuroEngineering and Rehabilitation*, vol. 10, no. 1, p. 24, 2013.

[18] M. Gandolfi, E. Formaggio, C. Geroin et al., "Electroencephalographic changes of brain oscillatory activity after upper limb somatic sensation training in a patient with somatosensory deficit after stroke," *Clinical EEG and Neuroscience*, vol. 46, no. 4, pp. 347–352, 2015.

[19] S. Hesse, C. Werner, M. Pohl, S. Rueckriem, J. Mehrholz, and M. L. Lingnau, "Computerized arm training improves the motor control of the severely affected arm after stroke: a single-blinded randomized trial in two centers," *Stroke*, vol. 36, no. 9, pp. 1960–1966, 2005.

[20] S. Hesse, G. Schulte-Tigges, M. Konrad, A. Bardeleben, and C. Werner, "Robot-assisted arm trainer for the passive and active practice of bilateral forearm and wrist movements in hemiparetic subjects," *Archives of Physical Medicine and Rehabilitation*, vol. 84, no. 6, pp. 915–920, 2003.

[21] S. H. Kreisel, M. G. Hennerici, and H. Bäzner, "Pathophysiology of stroke rehabilitation: the natural course of clinical recovery, use-dependent plasticity and rehabilitative outcome," *Cerebrovascular Diseases*, vol. 23, no. 4, pp. 243–255, 2007.

[22] J. H. Cauraugh and J. J. Summers, "Neural plasticity and bilateral movements: a rehabilitation approach for chronic stroke," *Progress in Neurobiology*, vol. 75, no. 5, pp. 309–320, 2005.

[23] B. Crosson, A. Ford, K. M. McGregor et al., "Functional imaging and related techniques: an introduction for rehabilitation researchers," *Journal of Rehabilitation Research and Development*, vol. 47, no. 2, pp. vii–xxxiv, 2010.

[24] P. Manganotti, E. Formaggio, S. F. Storti et al., "Time-frequency analysis of short-lasting modulation of EEG induced by intracortical and transcallosal paired TMS over motor areas," *Journal of Neurophysiology*, vol. 107, no. 9, pp. 2475–2484, 2012.

[25] C. Calautti and J. C. Baron, "Functional neuroimaging studies of motor recovery after stroke in adults," *Stroke*, vol. 34, no. 6, pp. 1553–1566, 2003.

[26] R. Gassert, L. Dovat, G. Ganesh et al., "Multi-joint arm movements to investigate motor control with FMRI," in *2005 IEEE Engineering in Medicine and Biology 27th Annual Conference*, vol. 5, pp. 4488–4491, Shanghai, China, 2005.

[27] M. Hara, M. Gaëtan, Y. Akio et al., "Development of a 2-DOF electrostatic haptic joystick for MRI/fMRI applications," in

2009 IEEE International Conference on Robotics and Automation, pp. 1479–1484, Kobe, Japan, May 12–17, 2009.

[28] N. Yu, N. Estévez, M. C. Hepp-Reymond, S. S. Kollias, and R. Riener, "fMRI assessment of upper extremity related brain activation with an MRI-compatible manipulandum," *International Journal of Computer Assisted Radiology and Surgery*, vol. 6, no. 3, pp. 447–455, 2011.

[29] E. Formaggio, S. F. Storti, I. Boscolo Galazzo et al., "Time–frequency modulation of ERD and EEG coherence in robot-assisted hand performance," *Brain Topography*, vol. 28, no. 2, pp. 352–363, 2015.

[30] E. Formaggio, S. F. Storti, M. Avesani et al., "EEG and FMRI coregistration to investigate the cortical oscillatory activities during finger movement," *Brain Topography*, vol. 21, no. 2, pp. 100–111, 2008.

[31] E. Formaggio, S. F. Storti, R. Cerini, A. Fiaschi, and P. Manganotti, "Brain oscillatory activity during motor imagery in EEG-fMRI coregistration," *Magnetic Resonance Imaging*, vol. 28, no. 10, pp. 1403–1412, 2010.

[32] S. F. Storti, E. Formaggio, A. Beltramello, A. Fiaschi, and P. Manganotti, "Wavelet analysis as a tool for investigating movement-related cortical oscillations in EEG-fMRI coregistration," *Brain Topography*, vol. 23, no. 1, pp. 46–57, 2010.

[33] G. Pfurtscheller and A. Aranibar, "Event-related cortical desynchronization detected by power measurements of scalp EEG," *Electroencephalography and Clinical Neurophysiology*, vol. 42, no. 6, pp. 817–826, 1977.

[34] L. Thabane, J. Ma, R. Chu et al., "A tutorial on pilot studies: the what, why and how," *BMC Medical Research Methodology*, vol. 10, no. 1, p. 1, 2010.

[35] Medical Research Council, *Aids to Examination of the Peripheral Nervous System Memorandum*, Her Majesty's Stationery Office, London, UK, 1976.

[36] M. F. Folstein, S. E. Folstein, and P. R. McHugh, ""Mini-mental state". A practical method for grading the cognitive state of patients for the clinician," *Journal of Psychiatric Research*, vol. 12, no. 3, pp. 189–198, 1975.

[37] R. W. Bohannon and M. B. Smith, "Interrater reliability of a modified Ashworth scale of muscle spasticity," *Physical Therapy*, vol. 67, no. 2, pp. 206-207, 1987.

[38] L. Hantson, W. De Weerdt, J. De Keyser et al., "The European stroke scale," *Stroke*, vol. 25, no. 11, pp. 2215–2219, 1994.

[39] F. I. Mahoney and D. W. Barthel, "Functional evaluation: the Barthel index," *Maryland State Medical Journal*, vol. 14, pp. 61–65, 1965.

[40] H.-O. Karnath, J. Rennig, L. Johannsen, and C. Rorden, "The anatomy underlying acute versus chronic spatial neglect: a longitudinal study," *Brain*, vol. 134, no. 3, pp. 903–912, 2011.

[41] C. Rorden, H.-O. Karnath, and L. Bonilha, "Improving lesion-symptom mapping," *Journal of Cognitive Neuroscience*, vol. 19, no. 7, pp. 1081–1088, 2007.

[42] A. Deakin, H. Hill, and V. M. Pomeroy, "Rough guide to the Fugl-Meyer assessment: upper limb section," *Physiotherapy*, vol. 89, no. 12, pp. 751–763, 2003.

[43] A. R. Fugl-Meyer, L. Jääskö, I. Leyman, S. Olsson, and S. Steglind, "The post-stroke hemiplegic patient. 1. A method for evaluation of physical performance," *Scandinavian Journal of Rehabilitation Medicine*, vol. 7, no. 1, pp. 13–31, 1975.

[44] X. J. Wei, K. Y. Tong, and X. L. Hu, "The responsiveness and correlation between Fugl-Meyer assessment, motor status scale, and the action research arm test in chronic stroke with upper-extremity rehabilitation robotic training," *International Journal of Rehabilitation Research*, vol. 34, no. 4, pp. 349–356, 2011.

[45] D. J. Gladstone, C. J. Danells, and S. E. Black, "The Fugl-Meyer assessment of motor recovery after stroke: a critical review of its measurement properties," *Neurorehabilitation and Neural Repair*, vol. 16, no. 3, pp. 232–240, 2002.

[46] R. C. Lyle, "A performance test for assessment of upper limb function in physical rehabilitation treatment and research," *International Journal of Rehabilitation Research*, vol. 4, no. 4, pp. 483–492, 1981.

[47] J. H. Van der Lee, V. De Groot, H. Beckerman, R. C. Wagenaar, G. J. Lankhorst, and L. M. Bouter, "The intra- and interrater reliability of the action research arm test: a practical test of upper extremity function in patients with stroke," *Archives of Physical Medicine and Rehabilitation*, vol. 82, no. 1, pp. 14–19, 2001.

[48] T. P. Jung, S. Makeig, C. Humphries et al., "Removing electroencephalographic artifacts by blind source separation," *Psychophysiology*, vol. 37, no. 2, pp. 163–178, 2000.

[49] G. Pfurtscheller and C. Neuper, "Event-related synchronization of mu rhythm in the EEG over the cortical hand area in man," *Neuroscience Letters*, vol. 174, no. 1, pp. 93–96, 1994.

[50] R. T. Pivik, R. J. Broughton, R. Coppola, R. J. Davidson, N. Fox, and M. R. Nuwer, "Guidelines for the recording and quantitative analysis of electroencephalographic activity in research contexts," *Psychophysiology*, vol. 30, no. 6, pp. 547–558, 1993.

[51] P. M. Davies, *Steps to follow*, A Guide to the Treatment of Adult Hemiplegia, Springer Verlag, Berlin, 1985.

[52] I. Boscolo Galazzo, S. F. Storti, E. Formaggio et al., "Investigation of brain hemodynamic changes induces by active and passive movements: a combined arterial spin labeling-BOLD fMRI study," *Journal of Magnetic Resonance Imaging*, vol. 40, no. 4, pp. 937–948, 2014.

[53] S. F. Storti, E. Formaggio, P. Manganotti, and G. Menegaz, "Brain network connectivity and topological analysis during voluntary arm movements," *Clinical EEG and Neuroscience*, vol. 47, no. 4, pp. 276–290, 2016.

[54] C. Weiller, M. Jüptner, S. Fellows et al., "Brain representation of active and passive movements," *NeuroImage*, vol. 4, no. 2, pp. 105–110, 1996.

[55] S. M. Hatem, G. Saussez, M. Della Faille et al., "Rehabilitation of motor function after stroke: a multiple systematic review focused on techniques to stimulate upper extremity recovery," *Frontiers in Human Neuroscience*, vol. 10, p. 442, 2016.

[56] J. Wissel, A. Manack, and M. Brainin, "Toward an epidemiology of poststroke spasticity," *Neurology*, vol. 80, no. 3, Supplement 2, pp. S13–S19, 2013.

[57] J. M. Gracies, "Physical modalities other than stretch in spastic hypertonia," *Physical Medicine and Rehabilitation Clinics of North America*, vol. 12, pp. 769–792, 2001.

[58] N. Smania, A. Picelli, D. Munari et al., "Rehabilitation procedures in the management of spasticity," *European Journal of Physical and Rehabilitation Medicine*, vol. 46, no. 3, pp. 423–438, 2010.

[59] B. B. Johansson, "Current trends in stroke rehabilitation. A review with focus on brain plasticity," *Acta Neurologica Scandinavica*, vol. 123, no. 3, pp. 147–159, 2011.

[60] M. Sivan, R. J. O'Connor, S. Makower, M. Levesley, and B. Bhakta, "Systematic review of outcome measures used in

the evaluation of robot-assisted upper limb exercise in stroke," *Journal of Rehabilitation Medicine*, vol. 43, no. 3, pp. 181–189, 2011.

[61] J. W. Stinear and W. D. Byblow, "Rhythmic bilateral movement training modulates corticomotor excitability and enhances upper limb motricity poststroke: a pilot study," *Journal of Clinical Neurophysiology*, vol. 21, no. 2, pp. 124–131, 2004.

[62] C. Trompetto, L. Marinelli, L. Mori et al., "Pathophysiology of spasticity: implications for neurorehabilitation," *BioMed Research International*, vol. 2014, Article ID 354906, 8 pages, 2014.

[63] J. E. Aman, N. Elangovan, I. L. Yeh, and J. Konczak, "The effectiveness of proprioceptive training for improving motor function: a systematic review," *Frontiers in Human Neuroscience*, vol. 8, article 1075, 2015.

[64] I. A. Beets, M. Macé, R. L. Meesen, K. Cuypers, O. Levin, and S. P. Swinnen, "Active versus passive training of a complex bimanual task: is prescriptive proprioceptive information sufficient for inducing motor learning?," *PLoS One*, vol. 7, no. 5, article e37687, 2012.

[65] A. Canedo, "Primary motor cortex influences on the descending and ascending systems," *Progress in Neurobiology*, vol. 51, no. 3, pp. 287–335, 1997.

[66] C. Carel, I. Loubinoux, K. Boulanouar et al., "Neural substrate for the effects of passive training on sensorimotor cortical representation: a study with functional magnetic resonance imaging in healthy subjects," *Journal of Cerebral Blood Flow & Metabolism*, vol. 20, no. 3, pp. 478–484, 2000.

[67] S. H. Jang, Y. H. Kim, Y. Chang, B. S. Han, W. M. Byun, and C. H. Chang, "The predictive value of cortical activation by passive movement for motor recovery in stroke patients," *Restorative Neurology and Neuroscience*, vol. 22, no. 2, pp. 59–63, 2004.

[68] D. J. Reinkensmeyer, L. E. Kahn, M. Averbuch, A. McKenna-Cole, B. D. Schmit, and W. Z. Rymer, "Understanding and treating arm movement impairment after chronic brain injury: progress with the ARM guide," *Journal of Rehabilitation Research and Development*, vol. 37, no. 6, pp. 653–662, 2000.

[69] J. Cauraugh, N. Lodha, S. Naik, and J. Summers, "Bilateral movement training and stroke motor recovery progress: A structured review and meta-analysis," *Human Movement Science*, vol. 29, no. 5, pp. 853–870, 2010.

[70] E. Formaggio, S. Masiero, A. Bosco, F. Izzi, F. Piccione, and A. Del Felice, "Quantitative EEG evaluation during robot-assisted foot movement," *IEEE Transactions on Neural Systems and Rehabilitation Engineering*, vol. 25, no. 9, pp. 1633–1640, 2016.

[71] S. Mazzoleni, M. Coscia, G. Rossi, S. Aliboni, F. Posteraro, and M. C. Carrozza, "Effects of an upper limb robot-mediated therapy on paretic upper limb in chronic hemiparetic subjects: a biomechanical and EEG-based approach for functional assessment," in *2009 IEEE International Conference on Rehabilitation Robotics*, pp. 92–97, Kyoto, Japan, 2009.

[72] C. Stinear, "Prediction of recovery of motor function after stroke," *The Lancet Neurology*, vol. 9, no. 12, pp. 1228–1232, 2010.

[73] A. Basteris, S. M. Nijenhuis, A. H. Stienen, J. H. Buurke, G. B. Prange, and F. Amirabdollahian, "Training modalities in robot-mediated upper limb rehabilitation in stroke: a framework for classification based on a systematic review," *Journal of Neuroengineering and Rehabilitation*, vol. 11, no. 1, p. 111, 2010.

[74] D. L. Turner, A. Ramos-Murguialday, N. Birbaumer, U. Hoffmann, and A. Luft, "Neurophysiology of robot-mediated training and therapy: a perspective for future use in clinical populations," *Frontiers in Neurology*, vol. 4, p. 184, 2013.

[75] M. Berchicci, T. Zhang, L. Romero et al., "Development of mu rhythm in infants and preschool children," *Developmental Neuroscience*, vol. 33, no. 2, pp. 130–143, 2011.

Hindawi
Neural Plasticity
Volume 2018, Article ID 6125901, 15 pages
https://doi.org/10.1155/2018/6125901

Research Article

Motor Improvement of Skilled Forelimb Use Induced by Treatment with Growth Hormone and Rehabilitation Is Dependent on the Onset of the Treatment after Cortical Ablation

Margarita Heredia[1], **Jesús Palomero**[1], **Antonio de la Fuente**[1], **José María Criado**[1], **Javier Yajeya**[1], **Jesús Devesa**[2], **Pablo Devesa**[3], **José Luis Vicente-Villardón**[4] and **Adelaida S. Riolobos**[1]

[1]*Department of Physiology and Pharmacology, Neuroscience Institute of Castilla y León (INCyL), University of Salamanca, Salamanca, Spain*
[2]*Scientific Direction, Medical Centre Foltra, Teo, Spain*
[3]*Research and Development, Medical Centre Foltra, Teo, Spain*
[4]*Department of Statistics, University of Salamanca, Salamanca, Spain*

Correspondence should be addressed to Margarita Heredia; mheredia@usal.es and Jesús Devesa; devesa.jesus@gmail.com

Received 24 March 2017; Revised 20 December 2017; Accepted 8 January 2018; Published 20 March 2018

Academic Editor: Stuart C. Mangel

We previously demonstrated that the administration of GH immediately after severe motor cortex injury, in rats, followed by rehabilitation, improved the functionality of the affected limb and reexpressed nestin in the contralateral motor cortex. Here, we analyze whether these GH effects depend on a time window after the injury and on the reexpression of nestin and actin. Injured animals were treated with GH (0.15 mg/kg/day) or vehicle, at days 7, 14, and 35 after cortical ablation. Rehabilitation was applied at short and long term (LTR) after the lesion and then sacrificed. Nestin and actin were analyzed by immunoblotting in the contralateral motor cortex. Giving GH at days 7 or 35 after the lesion, but not 14 days after it, led to a remarkable improvement in the functionality of the affected paw. Contralateral nestin and actin reexpression was clearly higher in GH-treated animals, probably because compensatory brain plasticity was established. GH and immediate rehabilitation are key for repairing brain injuries, with the exception of a critical time period: GH treatment starting 14 days after the lesion. Our data also indicate that there is not a clear plateau in the recovery from a brain injury in agreement with our data in human patients.

1. Introduction

Brain repair after an injury involves a number of complex processes. Abundant evidence indicates that growth hormone (GH) administration, added to rehabilitation, can significantly contribute to the recovery of an acquired brain injury, both in animal models [1–9] and in human patients [10–15], regardless of whether the patient is GH-deficient (GHD) or not [14–18]. However, it is not clear whether there is a period of time after a brain injury during which GH can exert its positive effects for brain repair. While it seems logical that early GH administration and rehabilitation after brain damage should provide faster and better recovery [14–16], recent data from our group demonstrate that brain repair in humans can be achieved by administering GH together with rehabilitation even months or years after the injury happened [10, 16–18]. These data challenge the classical concept that there is a "plateau" for brain recovery following an injury after which few more positive improvements could be obtained.

In a previous work, we demonstrated, in rats, that GH administration, but not vehicle, given immediately after a severe lesion of the frontal motor cortex led to a significant improvement of the motor impairment induced by frontal cortical ablation of the dominant hemisphere. Therefore, their performance in the paw-reaching-for-food task was soon similar to that in sham-operated controls [19]. However, in the same study, despite intense rehabilitation, no significant changes were observed in motor function of animals receiving vehicle or GH 6 days after induction of a severe injury in the frontal motor cortex. This is perhaps because in this case, rehabilitation commenced 13 days after the lesion was produced, that is, almost at the end of the critical period of time in which rehabilitative therapies may achieve maximal efficiency in rats (5 to 14 days after an injury) [20]. It has been shown that rehabilitative therapies initiated during these days enhance dendritic growth in the undamaged motor cortex [20], but the heightened sensitivity to rehabilitation commencing early after the lesion declines with time [20].

In our previous study, we detected reexpression of nestin in the contralateral motor cortex only in injured rats treated with GH. This reexpression of nestin was clearly higher in animals receiving the hormone immediately after the injury than in rats in which GH treatment commenced 6 days after the injury occurred [19]. Since the substantial magnitude of the lesion made it impossible for the injured area to regenerate, we believe that the reexpression of nestin in the contralateral motor cortex of animals treated with GH (not observed in animals treated with vehicle) would be the factor responsible for explaining the differences in the recovery observed between the different groups of animals. Moreover, we deduced that GH administration has to be followed by early rehabilitation in order to obtain significant motor improvements [19].

Nestin expression is commonly used as a marker of neural stem and progenitor cells. However, nestin is expressed in many other nonneural progenitor cell types, such as developing muscle, endothelial cells, and reactive astrocytes, especially in the injured brain [21–26]. Therefore, it is likely that nestin reexpression in GH-treated rats played a significant role in mechanisms of brain plasticity, leading to the quick improvement observed in rats treated with GH and rehabilitation immediately after the lesion occurred. Meanwhile, the fact that the expression of this neural marker was lower in the contralateral cortex of GH-treated animals in which rehabilitation after GH administration commenced at the end of the critical period for maximal efficiency of rehabilitative therapy suggests that GH induces the reexpression of nestin. However, it also suggests that a number of factors (which are elevated towards the end of the critical period) can prevent GH expression from reaching the magnitude required to achieve significant brain plasticity after a brain injury.

It is well known that any damage to the adult brain generates an adaptative plasticity which depends on neurogenesis [27] and new axonal connections [28, 29]. It has been seen, in rodents, that stroke induces proliferation of newly born neurons in the subventricular zone (SVZ), migration of these immature neurons away from the SVZ, and localization within peri-infarct tissues. Immature neurons migrate after a stroke in close association with blood vessels and astrocytic processes [29]. This poststroke migration is very similar to the normal neuroblast migration in the rostral migratory stream. Immature neurons localize in the peri-infarct cortex in a neurovascular niche where neurogenesis is causally linked to angiogenesis through a number of vascular and neuronal growth factors including erythropoietin (EPO) [29]. Interestingly, most of these factors, if not all of them, are induced by GH [16]. However, despite the fact that for many years the expression of GH and its receptor has been detected in the brain [30]—where its neuroprotective role is well known [3]—the mechanisms by which the hormone acts and the time period during which these mechanisms may play a positive role still remain to be elucidated.

In this study, we analyzed whether the administration of GH immediately followed by rehabilitation in different periods of time after induction of severe ablation of the frontal motor cortex was able to induce significant motor improvements. That is, we studied whether there is a critical window of time for GH action, together with rehabilitation, in brain recovery after an injury in rats. Our results indicate that the administration of GH plus rehabilitation at days 7 or 35 after the lesion, but not rehabilitation alone, significantly improve the lost motor function. However, this did not occur when the GH treatment was given 14 days after the cortical ablation was produced, in spite of the fact that the rehabilitation commenced on that same day in the other GH-treated groups. In addition, our data also suggest that rehabilitation has to be performed immediately after GH therapy begins in order to achieve significant motor improvements. Moreover, in the motor cortex of the undamaged hemisphere, we observed an important reexpression of nestin and actin in GH-treated rats, but not in vehicle-treated or control animals, which probably indicates the development of compensatory mechanisms to achieve a functional recovery.

2. Materials and Methods

Thirty-five adult male Wistar rats (Charles River Laboratories, Spain), with body weight 200–220 g at the beginning of the experiments, were used for the behavioral and nestin/actin Western blot experiments. Animals were housed under controlled conditions of temperature (18–20°C) and natural light/dark cycles, at least 4 days prior to the experiments. They were fed with a normal chow diet and water *ad libitum*, except when the paw-reaching-for-food task was carried out. At this time, animals were maintained at 86–88% of their initial *ad libitum* weight. All experiments and procedures involved in this study were approved by the University of Salamanca Ethics Committee and were conducted in accordance with the animal care European guidelines (2010/63/EU) and Spanish regulations (Real Decreto 53/2013). In addition, every effort was made to minimize the suffering and number of animals used.

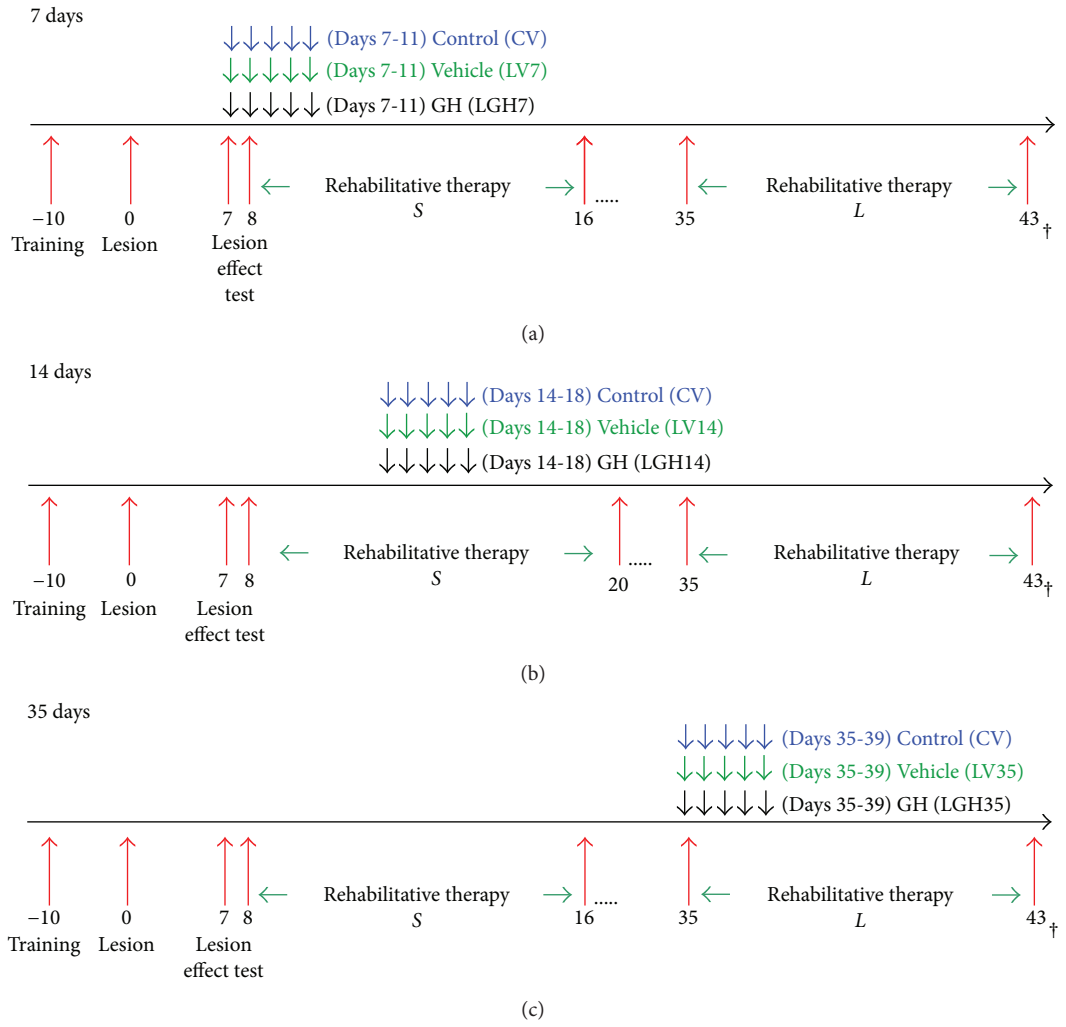

Figure 1: Schematic diagram of the experimental design. In (a), (b), and (c), −10 to 0 represent the days of training of the animals for paw-reaching-for-food task and to record the preferred forelimb (preoperative stage). In day 0, the motor cortex contraleral to the preferred limb was lesioned by aspiration. Arrows indicate the days during which GH or vehicle was given to each group of animals. Two groups of lesion animals (not GH treated) were given vehicle: in one group, it was administered on days 7 and 35 postablation (altogether called LV7/LV35 group) and in another group on day 14 (LV14 group) postablation. *S* indicates the days during which animals received short-term rehabilitative therapy, while *L* indicates the days during which animals received long-term rehabilitative therapy. 17 to 35 in (a), 21 to 35 in (b), and 17 to 35 in (c) correspond to resting period days (animals were kept in their cages without receiving any treatment). 43 correspond to the last day of long-term rehabilitative therapy.

2.1. Experimental Design for Behavioral Test. The experimental design consisted of the following phases:

(1) *Paw-reaching-for-food task. Presurgical phase.* Animals were trained in the paw-reaching test, and the preferred paw forelimb was recorded

(2) *Ablation of frontal motor cortex. Evaluation of the effectiveness of the lesion.* Anaesthetized animals were lesioned by aspiration in the motor cortex contralateral to the preferred paw or sham-operated. The effectiveness of the lesion was then verified at day 7 postablation

(3) *Treatment with GH or vehicle and rehabilitative therapies* (forced use of the affected paw) *at different times after cortical ablation. Evaluation of the paw-reaching-for-food responses*

(4) *Analysis of the nestin and actin expression in the motor cortex of the undamaged hemisphere by Western blot*

All surgical procedures and sacrifices were carried out under deep anesthesia with Equithesin (20 mg/kg, intraperitoneally). These study phases are shown schematically in Figure 1.

2.1.1. Paw-Reaching-for-Food Task. Presurgical Phase. Seven days after the arrival of animals, they were trained for the paw-reaching-for-food task: a specific motor test in which animals are conditioned to perform high-precision motor movements of extension and flexion of the forelimb fingers

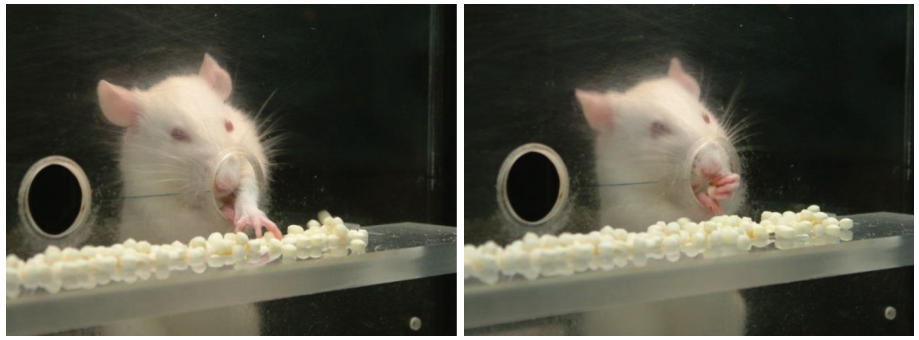

Figure 2: Consecutive photographs illustrating a rat in the test cage showing successful responses in the paw-reaching test during training in the presurgical phase. The design of the test cage prevented use of the tongue to retrieve food pellets or to rake the pellets.

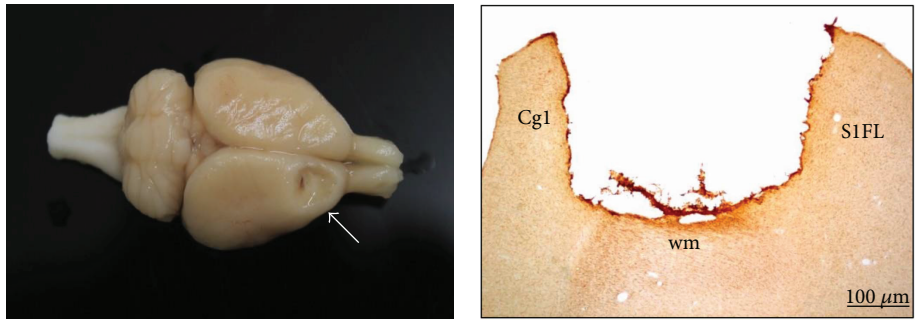

(a) (b)

Figure 3: (a) Photograph of an example of a rat brain with motor cortex ablation (white arrow). (b) Photomicrograph of a brain coronal section showing the motor cortex lesion. Cg1: cingulated cortex, area 1; S1FL: primary somatosensory cortex, forelimb; wm: white matter. Scale bar = 100 μm.

in order to obtain food. This test for fine motor skills has been widely used in previous studies from our group [19, 31–33]. Before carrying out the test, animals were housed individually and food was restricted until their body weight decreased to 86–88% of their previous *ad libitum* body weight. The design of the test cage has been described in previous studies of our laboratory [19, 31–33].

In the paw-reaching-for-food test, rats were required to extend a forelimb through the hole, grasp and retrieve a pellet from the groove, take it to their mouth, and eat it (Figure 2). Each time an animal succeeded in eating a pellet without dropping it was counted as a successful response, while any failure in the sequence for obtaining food was counted as an unsuccessful response.

In this presurgical phase, each experimental animal was placed in the test cage in individual sessions lasting 3 minutes for 10–12 sessions, in order to quantify the number of successful and unsuccessful responses with both paws. During this phase, the preferred paw (right or left) of each animal was established. The total number of responses (successful and unsuccessful with both paws) and the percentage of successful responses with the preferred paw with regard to the total number of responses were recorded.

This motor test was used in the presurgical phase to train the animals and to establish which was the preferred paw, after inducing the lesion (to test its efficiency) and also during the rehabilitative therapies (Figure 1).

2.1.2. Ablation of Frontal Motor Cortex. Each rat was placed in a stereotaxic apparatus and the skull exposed at the level of bregma. Animals were divided at random into two groups. One group ($n = 30$) was subjected to unilateral frontal cortex lesion. The other group ($n = 5$) was sham operated. Cortical ablation was performed, as in our previous work [19], at the coordinates indicated by Neafsey et al. [34], to remove the forelimb area of the motor cortex. A section of the skull was removed unilaterally 1 to 4 mm anterior to bregma and 1 to 3.5 mm lateral to the midline. The corpus callosum established the ventral limits of the lesion. Figure 3 shows an example of a motor cortex ablation.

Lesions were caused by aspiration in the hemisphere contralateral to the preferred paw determined in the presurgical phase. Under visual guidance, and using an operating microscope, meninges were removed and a glass pipette connected to an aspiration pump was gently introduced into the cortex to remove the tissue. Care was taken to spare the white matter underlying the cortex. Cortical ablation was severe and homogenous in size and localization and is similar to that made in previous studies from our group [19, 31–33]. Lesions were restricted to the primary and secondary motor cortex areas (M1 and M2), although in some cases, the cingulate cortex, area 1, (Cg1) was slightly affected (Figure 3(b)). After surgery, the skin was sutured.

Control animals were subjected to the same surgical process in the contralateral motor cortex to the preferred

forelimb, except for the lesion-inducing procedure itself (sham-operated group).

After surgery, the paw-reaching-for-food task established whether the lesion had been effective: either animals began to use their nonpreferred paw to reach for food, or the percentage of successful responses with the preferred paw was significantly decreased with regard to previous values in the presurgical phase.

2.1.3. Treatment with GH or Vehicle and Rehabilitative Therapies (Forced Use of the Affected Paw) at Different Times after Cortical Ablation. Evaluation of the Paw-Reaching-for-Food Responses. In three groups of injured animals, rhGH (Saizen, Merck; 0.15 mg/kg/day, subcutaneously) was administered for 5 consecutive days commencing on day 7, day 14, or day 35 after cortical ablation (Figure 1) (LGH7 group, $n = 7$; LGH14 group, $n = 6$; and LGH35 group, $n = 7$, resp.).

In order to minimize the number of animals used, according to the European guidelines, two other groups of lesion animals ($n = 5$ per group, not GH treated) were given vehicle (phosphate buffer saline 0.1 M, pH 7.4, PBS). In one of these groups, it was administered on day 7 and day 35 (altogether called LV7/LV35 group), and in the other group, on day 14 (LV14 group) postablation. Vehicle was administered for 5 days starting at each time point. For control purposes, the sham-operated animals received vehicle for 5 days starting on days 7, 14, and 35 after sham operation (CV group, $n = 5$). In this study, we did not include a group of sham-operated animals treated with GH, because this had been done in our previous work without finding differences between sham-operated animals treated with GH or vehicle [19]. GH or vehicle treatments were administered conjointly with the rehabilitation therapy (commencing on days 8 or 35; Figure 1).

Rehabilitative therapy consisted in inducing the forced use of the forelimb affected by the frontal motor cortex lesion (preferred paw), by attaching a removable plaster bracelet to the forelimb of the nonpreferred paw (undamaged paw, ipsilateral to the lesion), which prevented reaching food but not other movements. Therefore, animals could reach food only with the impaired paw (preferred paw, contralateral to the lesion) [19]. The animals wore the bracelet only during the test and not continuously. Rehabilitative therapy was carried out for 9 consecutive days in daily sessions of 3 minutes. Rehabilitative therapy was applied to all experimental groups (including sham-operated controls), at two different time points after cortical ablation: short-term rehabilitation and long-term rehabilitation.

Short-term rehabilitation commenced on day 8 after the lesion. The first rehabilitation period lasted 9 days in the LGH7, LGH35, and LV7/LV35 group and 13 days in the LGH14, LV14, and CV groups (*S* in Figure 1). Long-term rehabilitation commenced on day 35 after cortical ablation. This second rehabilitative therapy lasted 9 days (*L* in Figure 1).

During the period of time comprised between short- and long-term rehabilitation, the animals were kept in their cages and food and water were freely available (Figure 1).

2.1.4. Analysis of the Nestin and Actin Expression in the Motor Cortex of the Undamaged Hemisphere by Western Blot. Animals treated with GH or vehicle at 7, 14, or 35 days postablation, and sham-operated control animals were deeply anesthetized with Equithesin and sacrificed by decapitation. Brains were immediately removed, and a sample of the motor cortex from the undamaged hemisphere, approximately 3 mm^3, was dissected out, immediately snap-frozen in liquid nitrogen and then stored at −80°C. Motor cortex samples were individually homogenized in homogenization buffer 10 mM TRIS–HCl pH 7.4, 100 mM NaCl, 1 mM EDTA, 1 mM EGTA, 1% (*v*/*v*) Triton X-100, 10% (*v*/*v*) glycerol, 0.1% (*w*/*v*) dodecyl sodium sulfate, 0.5% (*w*/*v*) deoxycholate, and protease inhibitor cocktail (Sigma-Aldrich). Sample homogenates were centrifuged, and supernatants were collected in order to obtain the protein samples to be resolved by electrophoresis. Total protein content was determined using the bicinchoninic acid kit for protein determination (Sigma-Aldrich), and then samples were stored at −80°C until electrophoresis was performed. For electrophoresis, 30 μg of each protein sample was mixed with an equal volume of loading buffer (2X Laemmli Buffer). Then this mixture was incubated at 95°C for 10 min to obtain the loading samples, which were loaded in a SDS-PAGE gel (4–10% polyacrylamide) together with molecular weight protein markers (Bio-Rad). Then electrophoresis was performed (200 V for 45 min), and resolved proteins were transferred to a nitrocellulose membrane by applying 100 V, 350 mA for 60 min. No specific binding sites in the membranes were blocked by a 1-hour incubation with 5% (*w*/*v*) powdered nonfat milk. Membranes were incubated overnight at 4°C with the primary antibody diluted (1 : 1000) in TBS-T with 1% bovine serum albumin (BSA). The primary antibodies were anti-nestin (clone Rat 401, Millipore, MAB353) and anti-actin (polyclonal rabbit antibody, Sigma, A2103). Both anti-nestin antibody and anti-actin antibody were probed on independent membranes from independent gels. Membranes were incubated with the secondary antibodies, peroxidase-conjugated goat anti-mouse (Jackson ImmunoResearch, 115–035-174) (dilution 1 : 10,000), or donkey anti-rabbit (Amersham, NA934VS) (dilution1 : 10,000). Membranes were incubated with a chemiluminiscence reagent (ClarityTM Western ECL Blotting Substrate, Bio-Rad), and proteins were visualized by chemiluminiscence using a digital recording CCD imaging system (MicroChemi, Bio-Imaging Systems). Figure 4(a) shows digital images of nestin and actin. In addition, image densitometric analysis (using software ImageJ 1.46r, National Institute of Health, USA) was carried out to quantify the expression of nestin and actin in each motor cortex sample and presented in Figure 4(b), where each point identifies the expression of nestin and actin in motor cortex from an animal treated with GH, vehicle, or sham-operated control. In addition, the correlation coefficient (R) between nestin and actin was calculated. This coefficient indicates the direct relationship of the expression of both proteins in the different groups of animals.

2.2. Data Analysis. Statistical analysis was performed by using the Statview and SPSS programs. Each group of

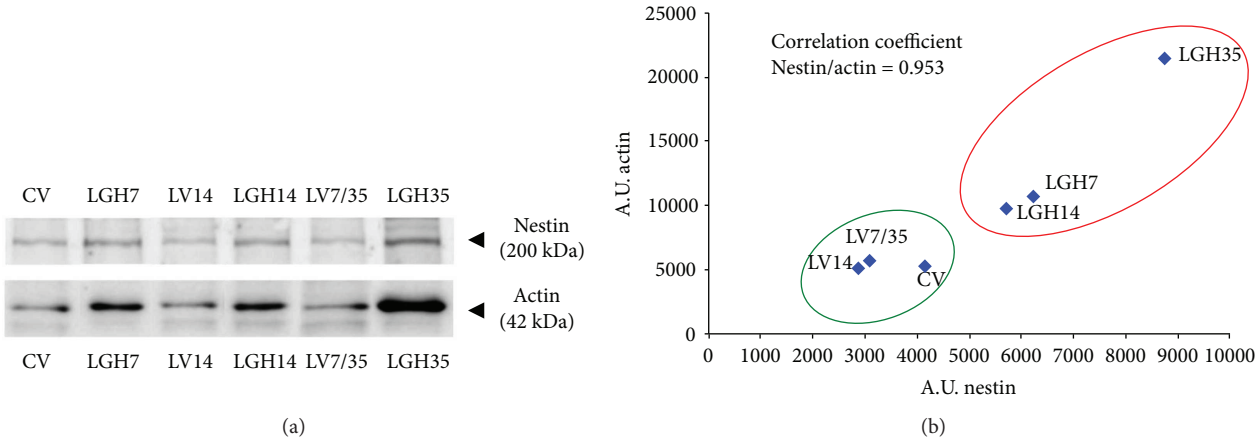

FIGURE 4: (a) Immunoblot images of nestin and actin expression in the motor cortex of the undamaged hemisphere, at 51 days postablation. Results show nestin and actin expression in homogenates of motor cortex samples from animals that were under different GH treatments (LGH7, LGH14, and LGH35) or controls (CV, LV14, and LV7/35). In each immunoblot band, either nestin or actin is identified with its corresponding GH-treated animal or control, and it comes from one animal in each case. Nestin and actin molecular weight, kilodaltons (kDa), is indicated. (b) Densitometric analysis of immunoblot images of nestin and actin displayed in (a). Arbitrary units (A.U.) of densitometry. Blue points represent the values (densitometric arbitrary units from immunoblot bands) of nestin and actin expression in each motor cortex sample that comes from one animal. Red underlined ellipse identifies samples from animals treated with GH, and green underlined ellipse identifies samples from control animals.

animals treated with GH at each time point was compared to the corresponding vehicle-treated group and sham-operated control group (CV). The percentage of successful responses with the preferred paw and the total number of responses (successful + unsuccessful with both paws) were compared. Fine motor skills results were analyzed by repeated ANOVA measures (group and session). Together with the P values, the eta squared (η^2) measure for the effect size was reported. Eta squared values higher than 0.26 are considered as strong effect size in the literature. When global ANOVA showed a significant difference among groups ($P \leq 0.05$), partial ANOVA comparing mean values and standard deviation of the different groups in each session was performed. To compare individual means, the Bonferroni post hoc test was used; $P < 0.016$ was the value considered as the limit for significance among groups. The relationship between the amount of nestin and actin detected in electrophoresed samples was calculated, after performing a densitometric analysis. The calculation of correlation coefficient from densitometric data was performed by Microsoft® Excel® software. The value of this coefficient indicates the direct relationship between the expression of nestin and actin in animals treated with GH or vehicle or sham-operated control.

3. Results

Figures 5, 6, and 7 show the results from the paw-reaching-for-food task at the three different time points of GH or vehicle treatment (7, 14, and 35 days postablation, resp.), during the different phases of the experiment: (a) mean percentages of successful responses obtained with the preferred paw with regard to the total number of responses; (b) average of the total number of responses (successful plus unsuccessful with both paws).

3.1. Presurgical Phase. In this phase, the ability to take food pellets from the groove and eat them was similar in all the rats. All rats displayed a stable strategy using a single forelimb to reach the pellets; thereby, a spontaneous limb preference was established during the training period. In all animals, limb preference was established at the fourth session, and the paw used was then considered the preferred paw. When the percentage of attempts using the right or left paw was between 85 and 100%, the rat was classified as right- or left-handed. It was considered that animals were well trained when the percentage of successful responses was ≥60% during two consecutive sessions. To distribute animals into the different experimental groups, the mean of results obtained in the two last sessions of this phase was taken. Therefore, both the percentage of successful responses (Figure 5(a), pre: $[F_{2,14} = 0.28, P \leq 0.7580]$, Figure 6(a), pre: $[F_{2,13} = 0.42, P \leq 0.6631]$, Figure 7(a), pre: $[F_{2,14} = 0.61, P \leq 0.5526]$) and the total number of responses (Figure 5(b), pre: $[F_{2,14} = 0.14, P \leq 0.8667]$, Figure 6(b), pre: $[F_{2,13} = 1{,}30, P \leq 0.3037]$, and Figure 7(b), pre: $[F_{2,14} = 2.68, P \leq 0.1033]$) were similar in all experimental groups.

3.2. Postablation Phase: Effectiveness of the Lesion. The lesions were large and homogenous in size and location and similar to the ones in previous studies from our group [19, 31–33] (Figure 3(a)). In all rats, the primary and secondary motor cortex areas (M1 and M2) were damaged. In some cases, the lesion extended slightly into the cingulate cortex, area 1, (Cg1) (Figure 3(b); a schematic representation of a cortical lesion by aspiration is shown in [19]).

The effectiveness of the lesion was tested on day 7 after ablation. ANOVA showed that significant differences existed in the percentage of successful responses between CV, LV7, and LGH7 groups (Figure 5(a) post, $F_{2,14} = 16.06$,

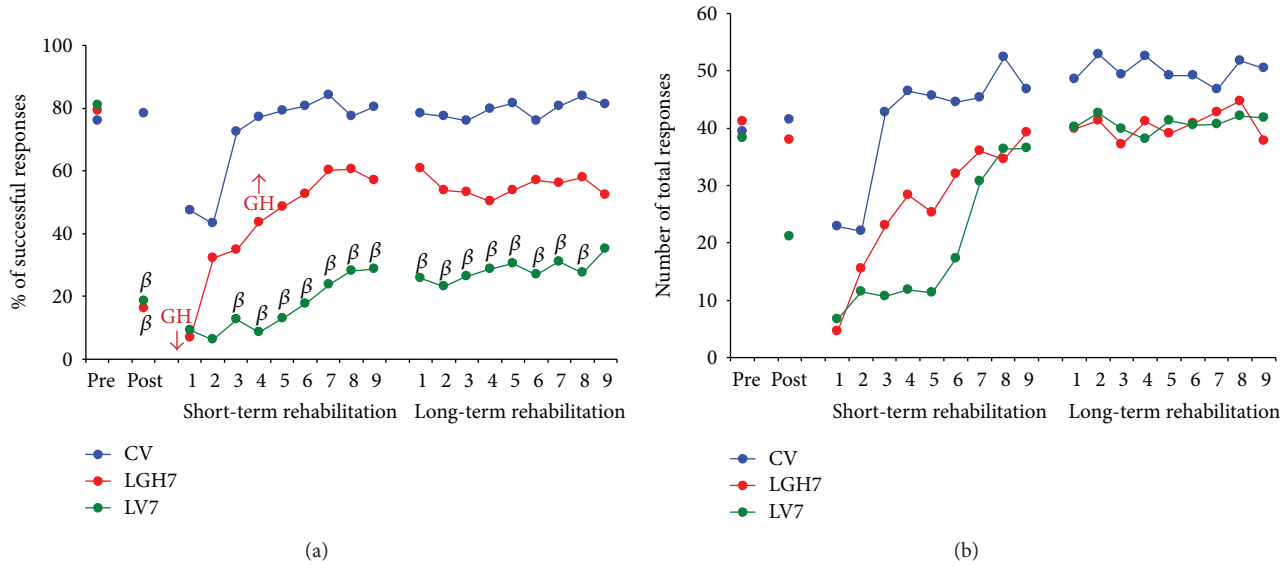

Figure 5: Animals treated with GH or vehicle at 7 days after cortical ablation. Behavioral results obtained in the paw-reaching-for-food task with the preferred paw (impaired paw) at the presurgical phase (PRE), postablation (POST), and rehabilitative therapies. (a) Mean percentage of successful responses (successful responses/total number of responses). (b) Mean of the total number of responses (successful and unsuccessful with both paws). The rehabilitative therapies consisted in the forced use of the impaired paw, in daily sessions for 3 min during 9 consecutive days (indicated in x-axis). No differences existed between LGH7 animals and sham-operated controls (CV), while a clear lack of successful responses was found in lesion animals treated with vehicle (LV7) as compared to both GH-treated animals and controls. Significant levels are obtained after comparison with sham-operated controls (CV). $\beta = P < 0.01$ (Bonferroni's test). GH arrows indicate when GH treatment commenced and finished in LGH7 animals.

$P \leq 0.0002$). The same thing happened when comparing CV, LV14, and LGH14 groups (Figure 6(a) post, $F_{2,13} = 35.22$, $P \leq 0.0001$), and CV, LV35, and LGH35 groups (Figure 7(a) post, $F_{2,14} = 24.08$, $P \leq 0.0001$). While the percentage of successful responses was preserved in the sham-operated control group (CV), these successful responses significantly decreased in all lesion animals (the Bonferroni post hoc test, $P \leq 0.0001$), as Figures 5, 6, and 7 show (A, post). The low percentage of successful responses was similar in all lesion animals. Some of these lesion animals changed their preferred paw, while others continued to use the preferred paw, but in all the cases, the number of successful responses clearly decreased. With regard to the total number of responses, global ANOVA showed that no significant differences existed between the different experimental groups (Figures 5, 6, and 7(b), post).

3.3. Treatment with GH Plus Rehabilitative Therapies

3.3.1. Treatment with GH 7 Days Postlesion Conjointly with Rehabilitative Therapy Produces Relevant Functional Improvement of the Motor Impairment Induced by the Cortical Ablation. The control group and animals treated with GH or vehicle at 7 days after cortical ablation underwent the first period of rehabilitative therapy, commencing on day 8 postlesion, in daily sessions of 3 min, for 9 consecutive days (Figure 1S). As described, it consisted in the forced use of the impaired paw (preferred paw) by means of a bracelet fitted on the nonpreferred paw. Repeated ANOVA measures (group and session) showed significant differences between groups ($F_{2,14} = 6.69$, $P \leq 0.009$, $\eta^2 = 0.489$) (Figure 5(a), short-term rehabilitation). In addition, given that in all groups, the number of successful responses was increasing along the rehabilitative sessions, a significant session effect was observed ($F_{8,112} = 9.36$, $P \leq 0.0001$, $\eta^2 = 0.401$). On the contrary, the group x session interaction was not significant ($F_{16,112} = 1.21$, $P \leq 0.2668$, $\eta^2 = 0.148$). Partial ANOVA tests showed significant differences among groups from the third to ninth rehabilitation sessions. As expected, the percentage of successful responses of the control group (CV) was similar during all sessions of this rehabilitation period, excepting the two first sessions in which they were lower (most likely due to the newness of the bracelet) and therefore not statistically different from animals with cortical ablation (Figure 5(a)). This lack of differences between groups in the two first sessions of rehabilitation agrees with the low number of total responses in these first two days observed in all groups (Figure 5(b)). However, interestingly, the Bonferroni post hoc test revealed that animals treated with GH 7 days postablation (LGH7) increased the percentage of successful responses along sessions, which became normal at the end of this rehabilitation period, similar to the percentage of successful responses in controls and remarkably higher than in lesion animals treated with vehicle (Figure 5(a)).

The total number of responses was similar in all the experimental groups. Therefore, no significant differences were observed among them ($F_{2,14} = 2.23$, $P \leq 0.1435$) (Figure 5(b)). However, since all groups progressively

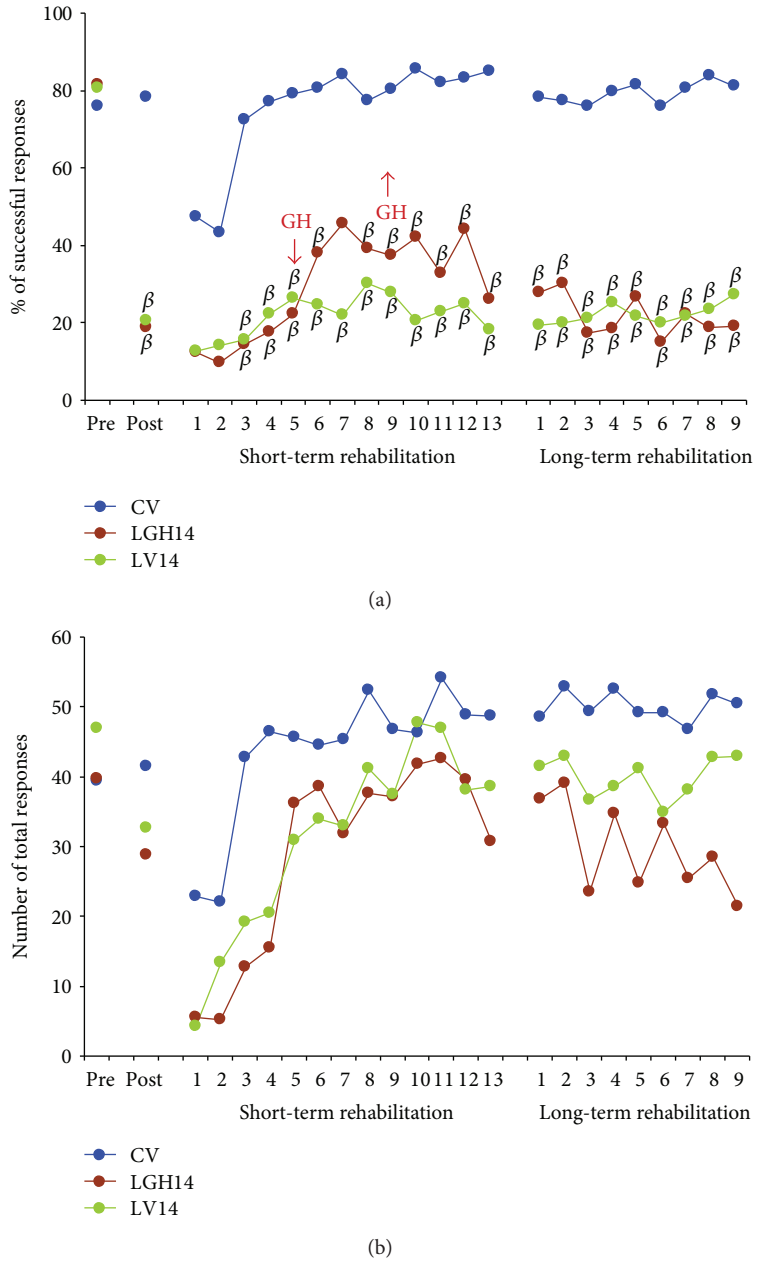

Figure 6: Animals treated with GH or vehicle at 14 days after cortical ablation. Behavioral results obtained in the paw-reaching-for-food task with the preferred paw (impaired paw) at the presurgical phase (PRE), postablation (POST), and rehabilitative therapies. (a) Mean percentage of successful responses (successful responses/total number of responses). (b) Mean of the total number of responses (successful and unsuccessful with both paws). The rehabilitative therapies consisted in the forced use of the impaired paw, in daily sessions for 3 min during 13 (short-term rehabilitation) and 9 (long-term rehabilitation) consecutive days (showed in x-axis). Significant levels (the Bonferroni post hoc test) indicated that both vehicle-treated animals (LV14) and GH-treated rats did not improve their percentage of successful responses in comparison to results obtained in the sham-operated control group (CV). $\beta = P < 0.01$; GH arrows indicate when GH treatment commenced and finished in LGH14 animals.

increased the number of total responses along the rehabilitative sessions, a clear session effect ($F_{8,112} = 14.62$, $P \leq 0.0001$) was shown. The group x session interaction was not significant ($F_{16,112} = 1.35$, $P \leq 0.1783$).

In the second period of rehabilitative therapy (Figure 1*L*, days 35 to 43 postablation) with the forced use of the impaired paw, global ANOVA demonstrated that significant differences existed among groups ($F_{2,14} = 5.55$, $P \leq 0.0168$, $\eta^2 = 0.442$). However, neither session effect ($F_{8,112} = 1.10$, $P = 0.366$, $\eta^2 = 0.073$) nor group x session interaction ($F_{16,112} = 1.02$, $P = 0.440$, $\eta^2 = 0.127$) was observed. The percentage of successful responses of animals treated with GH (LGH7) was similar to that of the control group in all 9 sessions, while no improvement was observed in lesion animals treated with vehicle on post hoc analyses (Figure 5(a), long-term rehabilitation). Thus,

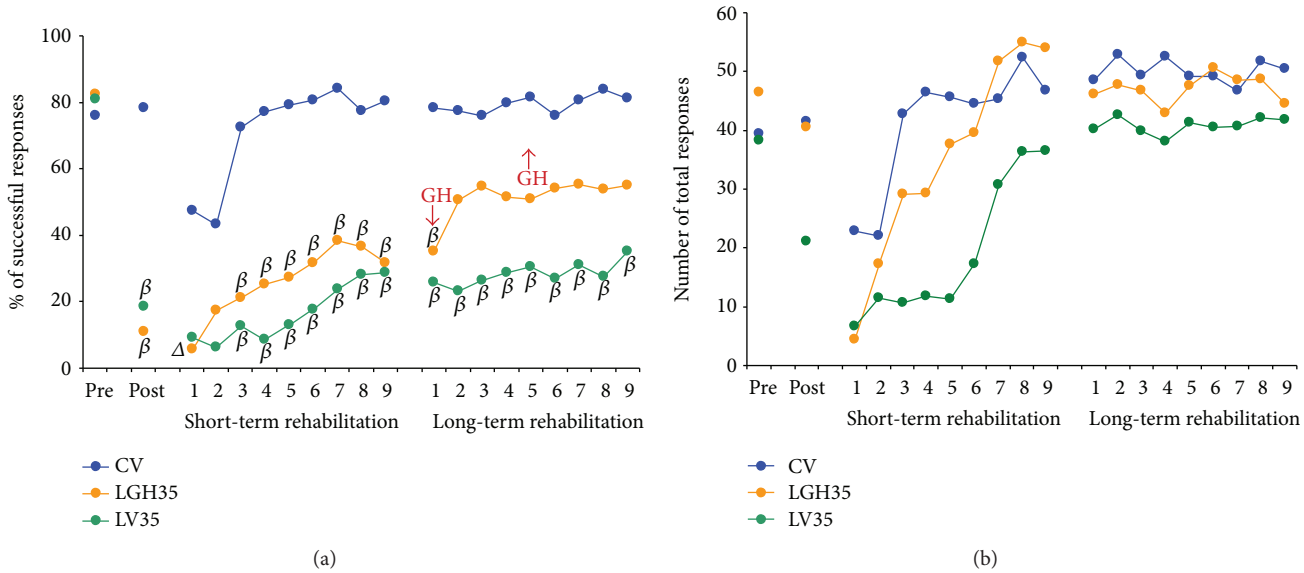

Figure 7: Animals treated with GH or vehicle at 35 days after cortical ablation. Behavioral results obtained in the paw-reaching-for-food task with the preferred paw (impaired paw) at the presurgical phase (PRE), postablation (POST), and rehabilitative therapies. (a) Mean percentage of successful responses (successful responses/total number of responses). (b) Mean of the total number of responses (successful and unsuccessful with both paws). The rehabilitative therapies consisted in the forced use of the impaired paw, in daily sessions for 3 min during 9 consecutive days indicated in (*x*-axis). GH-treated animals (LGH35) improved their percentage of successful responses after the second session, reaching a value no longer different to that of the sham-operated control group (CV), while vehicle-treated animals (LV35) did not change their low percentage of successful results. Significant levels are obtained after comparison with sham-operated controls (CV). $\beta = P < 0.01$; $\Delta = P < 0.05$ (Bonferroni's test). GH arrows indicate when GH treatment commenced and finished in LGH35 animals.

the functional improvement of the motor deficit reached in LGH7 animals at the end of the first rehabilitative period maintained an asymptotic value in all 9 sessions. With regard to the total number of responses (Figure 5(b)), global ANOVA showed no significant differences among groups ($F_{2,14} = 0.43$, $P \leq 0.654$). Neither session effect ($F_{8,112} = 0.61$, $P \leq 0.764$) nor group x session interaction ($F_{16,112} = 0.40$, $P \leq 0.977$) was observed.

3.3.2. Treatment with GH 14 Days after Cortical Ablation Does Not Induce Any Improvement. In this case, GH or vehicle treatment was administered on days 14 to 18 postablation, that is, after the beginning of the first rehabilitative therapy (Figure 1*S*). The first period of rehabilitation consisted in daily sessions of 3 min for 13 consecutive days: 4 rehabilitative sessions before treatment with GH or vehicle, 5 sessions conjointly with GH or vehicle treatment, and 4 rehabilitative sessions after being treated with GH or vehicle (Figure 1*S*). Global ANOVA (group and session) showed significant differences between groups ($F_{2,13} = 22.09$, $P \leq 0.0001$, $\eta^2 = 0.773$). In addition, a significant session effect was observed ($F_{12,156} = 6.14$, $P \leq 0.0001$, $\eta^2 = 0.321$), but the group x session interaction was not significant ($F_{24,156} = 1.11$, $P \leq 0.3369$, $\eta^2 = 0.146$). Partial ANOVA tests showed significant differences among groups from the third to the thirteenth rehabilitative sessions ($P \leq 0.005$). Again, with the same exception of sessions 1 and 2, both animals treated with GH or vehicle on day 14 postablation showed a significantly lower percentage of successful responses than control animals on post hoc analyses (Figure 6(a)). However, animals treated with GH showed a small increase in the percentage of successful responses from session 5 to session 12, coinciding with GH treatment, which tended to be higher than in lesion animals treated with vehicle, although the differences did not reach statistical significance (Figure 6(a)). The total number of responses was similar in all the experimental groups. Therefore, no significant differences were observed among them ($F_{2,13} = 1.90$, $P \leq 0.1882$) (Figure 6(b)). However, since all groups progressively increased the number of total responses along the rehabilitative sessions, a clear session effect ($F_{12,156} = 16.06$, $P \leq 0.0001$) existed.

In the second period of rehabilitative therapy (days 35 to 43 postablation) (Figure 6(a)), global ANOVA showed significant differences among groups ($F_{2,13} = 25.46$, $P \leq 0.0001$, $\eta^2 = 0.797$). However, neither session effect ($F_{8,104} = 1.02$, $P = 0.424$, $\eta^2 = 0.073$) nor group x session interaction ($F_{16,104} = 1.12$, $P = 0.346$, $\eta^2 = 0.147$) was observed. Animals treated with GH (LGH14) showed that the tendency observed during the days of GH administration disappeared. Therefore, their percentage of successful responses was similar to that of lesion animals treated with vehicle, and it was significantly lower than in control animals on post hoc analyses (Figure 6(a)). Hence, GH treatment starting on day 14 postlesion only slightly increased the percentage of successful responses during the days when the hormone was given, but this increase was no longer observed after interrupting GH treatment. With regard to the total number of responses (Figure 6(b)), no

significant differences among groups ($F_{2,13} = 2.94$, $P \leq 0.0882$), session effect ($F_{8,104} = 1.27$, $P = 0.267$), or group x session interaction ($F_{16,104} = 0.83$, $P = 0.6427$) were observed.

3.3.3. Treatment with GH 35 Days Postlesion Improves the Motor Impairment Induced by the Cortical Ablation. In this case, treatment with GH commenced on day 35 after the cortical ablation, coinciding with the second period of rehabilitation (Figure 1*L*). That is, in the first period of rehabilitation, animals in the LGH35 group had not received the GH treatment yet. In this first period of rehabilitation, global ANOVA showed significant differences among groups ($F_{2,14} = 16.87$, $P \leq 0.0002$, $\eta^2 = 0.707$). A significant session effect was observed ($F_{8,112} = 7.89$, $P \leq 0.0001$, $\eta^2 = 0.360$), but the group x session interaction was not significant ($F_{16,112} = 0.91$, $P \leq 0.5535$, $\eta^2 = 0.116$). Partial ANOVA showed significant differences among groups ($P \leq 0.0008$). Lesion animals (LGH35, LV35) presented a significantly lower percentage of successful responses than control animals (CV), once again with the exception of sessions 1 and 2 (Figure 7(a)). However, both lesion groups showed a slightly increasing trend in the percentage of successful responses along this first rehabilitative period (Figure 7(a)). No significant differences were observed in the total number of responses among the three groups ($F_{2,14} = 3.15$, $P \leq 0.741$) (Figure 7(b)). However, a session effect ($F_{8,112} = 16.90$, $P \leq 0.0001$) was shown. No significant group x session interaction was observed ($F_{16,112} = 1.67$, $P \leq 0.0612$).

In the second period of rehabilitative therapy (days 35 to 43 postlesion), coinciding with GH or vehicle treatment, animals were again obliged to use the paw affected by the cortical ablation. Global ANOVA demonstrated that significant differences existed among groups ($F_{2,14} = 7.82$, $P \leq 0.0052$, $\eta^2 = 0.528$) and also a session effect ($F_{8,112} = 2.44$, $P \leq 0.018$, $\eta^2 = 0.149$); however, no group-session interaction ($F_{16,112} = 1.21$, $P = 0.271$, $\eta^2 = 0.147$) was observed. The Bonferroni post hoc test revealed that animals treated with GH on day 35 after ablation (LGH35) showed a significant improvement of the motor impairment (Figure 7(a)). Therefore, excepting in session 1, during the rest of rehabilitative sessions, the percentage of successful responses was similar to that in control animals (Figure 7(a)) and notably higher than in lesion animals treated with vehicle in which no improvements were observed (Figure 7(a)). This significant improvement induced by administering GH and providing rehabilitation 35 days postablation was similar to that observed in animals treated with GH plus rehabilitation at 7 days after lesion. With respect to the total number of responses, global ANOVA showed no significant differences among groups ($F_{2,14} = 0.41$, $P \leq 0.667$) (Figure 7(b)). Neither session effect ($F_{8,112} = 0.59$, $P \leq 0.784$) nor interaction session group ($F_{16,112} = 0.57$, $P \leq 0.894$) was observed.

3.4.4. Animals Treated with GH Reexpress Nestin and Actin in the Motor Cortex of the Undamaged Hemisphere. Immunoblotting studies were carried out in motor cortex samples obtained 51 days after cortical ablation. In general, the results show that nestin expression in the motor cortex of the undamaged hemisphere was higher in animals treated with GH at 7, 14, or 35 days after the lesion (LGH7, LGH14, and LGH35) than in vehicle-treated animals (LV7/35, LV14) or sham-operated controls (CV) (Figure 4(a), Nestin). No differences were observed in nestin expression between vehicle-treated animals (LV14 and LV7/LV35) and controls (CV). We can highlight the fact that the rat treated with GH on day 35 after the lesion showed very high nestin expression in the motor cortex of the undamaged hemisphere (Figure 4(a), LGH35). This animal showed the highest functional improvement after motor cortex ablation compared with the other rats treated with GH. With regard to actin, the expression of this protein was similar in the control group (CV) and in vehicle-treated animals (LV14 and LV7/LV35). However, animals treated with GH (LGH7, LGH14, and LGH35) showed higher amount of actin expression, compared with samples from control and vehicle-treated animals (CV, LV14, and LV7/LV35) (Figure 4(a), actin). Figure 4(b) shows the densitometric quantification of nestin and actin expression from images shown in Figure 4(a), and these values have been plotted on a graphic that shows the association of nestin and actin expression. The coefficient of correlation between nestin and actin ($R = 0.953$) indicates that there is a very high relationship between the expression of these proteins. In fact, in some animals treated with GH, a strong correlation was observed between nestin and actin expression. Thus, samples from animals treated with GH show higher expression of nestin and actin (red underlined ellipse) than samples from control or vehicle-treated animals (green underlined ellipse). As it was mentioned above, the animal treated with GH on day 35 after the lesion showed the highest nestin and actin expression in the motor cortex of the undamaged hemisphere (Figure 4(b), LGH35), with good correlation with its functional improvement.

4. Discussion

We previously described in rats, for the first time, that after a severe lesion of the frontal motor cortex that produces a marked deficit in fine motor skills, early treatment with GH followed by rehabilitative therapy enabled the development of compensatory mechanisms in the contralateral undamaged hemisphere that allowed the functional recovery of the motor deficits resulting from the cortical ablation [19]. In that study, we also found that GH-treated animals showed a significant increase of nestin-positive cells in the intact contralateral motor cortex. This finding was also described for the first time, and we related it to the injury and the hormone since it was not found in vehicle-treated rats or sham-operated controls [19].

In this study, we tried to go further in the knowledge of these compensatory mechanisms and to know whether or not there is a window of time in which GH and rehabilitation are able to produce significant improvements after a severe cortical lesion. Our results demonstrate that GH plus rehabilitation treatment at day 7 or day 35 after the lesion lead to a remarkable functional improvement of the motor impairment induced by the lesion. By contrast, GH treatment on day 14 postablation did not induce any functional recovery.

Severe lesions of the motor cortex produce very important effects on the normal motor activity, affecting both the planning and organization of voluntary movements and their execution. The reason behind these effects is related to the limited capacity of the adult brain for self-repair after neuronal loss produced by an injury. In the case of cortical lesions, the alterations of axonal wirings produced by the trauma quickly led to a permanent functional impairment that caused severe behavioral deficits [31–33]. However, it is well known that any damage to the adult central nervous system generates adaptative brain plasticity. In fact, the adult brain is structurally dynamic [35–37], dendritic spines dynamically turn over in the adult brain [37, 38], and learning novel tasks are associated with a further increase in spine turnover [38]. Structural alterations that occur as a result of focal lesions in the brain have been identified, showing changes in axonal branching and growth [28]. Previous studies showed plasticity of the dendritic arborization in the cortex contralateral to a cortical lesion, and this is associated with improved skill in the limb unaffected by the lesion [39–41]. Another study has shown that rehabilitation can increase the numbers of dendritic spines and dendritic complexity in the cortical hemisphere contralateral to the brain lesion [42]. However, rehabilitation required several weeks of intensive training and practice of the impaired function, with rats undergoing 300–500 individual trials in order to regain about 60% of their prelesion skilled grasping ability [43]. This is concordant with our data in this study in which rats receiving only rehabilitation during a relatively short period of time were unable to reach any significant improvement in the paw affected by the cortical motor cortex ablation.

Animal studies indicate that many of the genes and proteins that are important for neuronal growth, synaptogenesis, and the proliferation of dendritic spines are expressed at their highest levels during early brain development and decline appreciably during ageing [44]. However, the second limited period of increased expression of these genes can be seen after a brain damage, such as what occurs in a stroke [45–47]. It seems that these new genetical reexpressions appear as an attempt to repair the damage occurred, since they have been seen surrounding the perilesional zone [48]. In spite of this, cases of significant damage, in which the repair is impossible because of the severity of the lesion, may lead to structural remodeling in some regions of the contralateral hemisphere [49, 50]. This agrees with our data in the present work and in our previous study [19]. We found remarkable nestin and actin reexpression in the contralateral undamaged frontal motor cortex in rats treated with GH and rehabilitation, but it was quite lower in animals receiving vehicle or in sham-operated controls.

Nestin is a class VI intermediate filament protein that, among other neural cells in the developing and adult central nervous system, was thought to be expressed exclusively in uncommitted neural progenitor cells (NPCs) and in endothelial cells [51–54], but it is also expressed in reactive astrocytes, especially after a brain injury [55]. After NPCs differentiate, nestin expression is usually replaced by the expression of neuronal or glial-specific markers. Since in our previous work, we detected remarkable nestin reexpression in the intact contralateral motor cortex of lesion animals treated with GH, but not in animals given vehicle or in sham-operated controls [19], and we assumed that this reexpression of nestin was related both to GH treatment and functional recovery. In that study, cells expressing nestin had the phenotype of neurons, but nestin immunoreactivity was detected in synaptic terminals outlining cell bodies of unlabeled neurons [19]. Therefore, it could be possible that these nestin-expressing neurons were already present and commenced to reexpress nestin after GH treatment and rehabilitative therapy, perhaps because of increased GH-receptor (GHR) expression and/or plasticity events leading to the remodeling of the undamaged contralateral motor cortex after the cortical ablation. We did not analyze whether GHR expression was upregulated in the contralateral intact cortex, but it has been recently described that during recovery from brain injury, there is an upregulation of GHR that may play a role in neuronal arborization and glial proliferation in the injured cortex [56].

The role of nestin in the central nervous system is not well known yet. It has been suggested that there is a selective distribution of nestin-expressing neurons in the cholinergic basal forebrain and regions of the brain involved in higher-order cognitive functions such as attention, learning, and memory, leading to the speculation that cell cycle and/or plasticity-related events may be involved in the expression of nestin by these neurons [26]. However, the authors themselves ruled out the hypothesis that in the normal brain the presence of nestin-expressing neurons may be due to the fact that these neurons had reentered the cell cycle and divided or that they arose from the division of another cell [26]. However, things may occur differently in an injured brain, as demonstrated by Nakatomi et al. [57]; their results, together with a number of other studies, showed that adult neural progenitors proliferate in situ in response to various insults, including trauma [58].

In mitotically active cells, nestin plays an important role, regulated by phosphorylation, in the assembly and disassembly of intermediate filaments, which contributes to remodeling the cytoskeleton of the cells. Nestin preferentially forms heterodimers with vimentin and alpha-internexin, possibly because these heterodimers are more stable than nestin homodimers. This is suggested by the fact that nestin contains a short N-terminal, a domain known to be essential for filament protein assembly [59] which inhibits filament formation *in vitro* when present at concentrations greater than 50% [60]. Thus, nestin may aid in linking intermediate filaments with each other, and with microtubules and microfilaments via the long C-terminal domain of nestin. Throughout the cell cycle, nestin colocalizes with the intracellular reorganization of vimentin filaments and aggregates and is essential for the mitotic disassembly of vimentin [61]. This suggests a role for nestin-mediated reorganization of the cytoskeleton during mitosis that is mediated in part by the upregulation of phosphorylation of Thr^{316} by cdc2 kinase [62].

Therefore, it seems logical to assume that the increased nestin reexpression we observed in the intact contralateral motor cortex of lesion animals treated with GH is related to

a structural remodeling of the cytoskeleton triggered by severe cortical damage and the administration of GH together with rehabilitation in order to develop compensatory mechanisms leading to the functional improvement observed in two groups (LGH7 and LGH35) of these animals, but not in LGH14 group, in spite of the fact that increased nestin reexpression was also observed in them.

With regard to actin expression, it followed a pattern of expression parallel to that of nestin in lesion animals treated with GH and rehabilitation, remarkably higher than in lesion animals given vehicle or sham-operated rats. In fact, a strong correlation was observed between nestin and actin expression in some animals treated with GH.

Actin is a multifunctional protein that forms microfilaments and participates in many important cellular processes, including cell motility, cell division, vesicle and organelle movements, cell signaling, and maintenance of cell junctions and cell shape. Dendritic spines are actin-rich protrusions from the dendritic shaft, considered to be the locus where most synapses occur, as they receive the vast majority of excitatory connections in the central nervous system (CNS). Since changes in spine shape and size are correlated with the strength of excitatory synapses, spine morphology directly reflects spine function [63]. Actin has been reported to be present in cell nuclei (where it regulates the transcription of several genes) and cell membranes. Although actin is one of the most evolutionary conserved eukaryotic proteins, it is expressed in mammals as at least six major different isoforms characterized by electrophoresis and amino acid sequence analysis. Four of them represent the differentiation markers of muscle tissues, and two are found in virtually all nonmuscle cells.

There are three α-actins (α-skeletal, α-cardiac, and α-smooth muscle), one β-actin (β-nonmuscle), and two γ-actins (γ-smooth muscle and γ-nonmuscle). Since actin isoforms show >90% overall sequence homology, we decided to use an anti-actin polyclonal antibody addressed against the N-terminal domain of the molecule, instead of a more specific β-actin antibody. The β-actin gene has been considered a housekeeping gene in the CNS; however, its expression changes according to external or internal factors. By using the N-terminal anti-actin polyclonal antibody, we attempted to detect by immunoblotting the total expression of different actin isoforms in the brain homogenates: α-smooth muscle actin (brain vessels induced to proliferate by the injury, GH, and rehabilitation), β-actin (neural cells), and the two isoforms of γ-actins (brain vessels and neural cells).

As it happened with nestin, the amount of actin detected by immunoblotting in the homogenates of the intact contralateral motor cortex was notably higher in GH-treated lesion animals than in rats treated with vehicle or sham operated, suggesting that this increased expression of actin was related to the development of compensatory mechanisms in the undamaged cortex for functional recovery. Moreover, as described before, the animal that showed the highest expression of nestin and actin (LGH35) achieved the highest functional improvement after the severe motor injury was induced. Therefore, it is likely that the increased expression of nestin and actin in the contralateral hemisphere reflects compensatory mechanisms that appear after the injury and GH plus rehabilitation for the functional recovery of the affected paw.

However, interestingly, despite the fact that nestin and actin also increased in LGH14 animals, these were unable to reach a significant number of successful responses in the paw-reaching-for-food task. In this case, short-term rehabilitation commenced at the same day after the lesion than in the other groups, but GH treatment (on day 14 postablation) commenced at the end of the "critical period of time" in which maximal efficiency during rehabilitative therapies could be obtained (5 to 14 days after injury) [20] (Figure 1*S*). In this LGH14 group, just after initiating GH administration, a tendency to increase the number of successful responses was observed, but it did not reach statistical significance and it disappeared once GH administration was interrupted (Figure 6(a)).

It has been shown that after a stroke, in rats, soon a number of positive factors are induced in the peri-infarct region [48]; among them a number of growth factors have been described [45, 64, 65]. These factors might facilitate the sprouting of new axons [27, 66, 67] and support the increased elaboration of dendrites and spines [39, 68]. However, balancing these positive signals, there is an induced expression of negative factors that either inhibit outgrowth or repel sprouting axons. Among these inhibiting factors, the protein NOGO-A [69–71] and extracellular matrix factors such as chondroitin sulphate proteoglycan [72] play a pivotal role. Most growth-inhibitory genes tend to be upregulated gradually towards the end of the "critical period of rehabilitation" (see [48], for a more detailed explanation). Although these positive and negative effects on cortical regeneration only have been seen in the zones surrounding the lesion, it is likely that they may affect other areas of the brain (i.e., the contralateral undamaged frontal motor cortex). On these bases, the lack of significant improvements observed when GH was given 14 days after the cortical ablation could be explained by the presence of these negative factors that oppose to regeneration. The detection of clear increases in the expression of nestin and actin in these LGH14 animals is not against this assumption; while cells try to remodel their cytoskeleton to establish new circuits, they could not be set correctly or there are not enough of them. Further studies will reveal whether administering GH together with rehabilitation for a longer time after this critical period of time in which no improvements are observed will produce significant recoveries, similar to those observed in LGH7 and LGH35 animals.

In summary, it is interesting to highlight here that despite the long time elapsed since the lesion was produced, improvements in LGH35 animals were similar to those observed in LGH7 animals. This indicates that there is not a plateau in rehabilitation after a brain injury and agrees with recent data from our group [17], showing that despite the time elapsed after the brain injury and its severity, GH plus rehabilitation led to an almost complete recovery of the functionality of a young man affected by a plane crash [17]. Moreover, the fact that in this case the right hemisphere had been

virtually lost in its entirety agrees with the idea that GH and rehabilitation lead to the development of compensatory mechanisms in the undamaged contralateral hemisphere, as we observed in this study. Therefore, if there is a time window during which GH plus rehabilitation cannot exert their positive effects on the brain repair after an injury, then this time window seems to be restricted in duration. Further studies will clarify this concept.

5. Conclusions

Our data allow us to conclude that GH is a very important factor in the repair of injured brains, but its administration has to be followed by immediate rehabilitation or accompanied by parallel rehabilitative therapy, in order to achieve functionally significant improvements. In the case of severe brain injuries, it is likely that GH administration and rehabilitation induce significant nestin and actin reexpression in the undamaged contralateral motor cortex. The amount of these reexpressed proteins seems to play a key role in the remodeling of the cytoskeleton of the cells and thus enable the development of compensatory brain plasticity which is responsible for the functional improvements observed. It remains uncertain whether GH administration together with rehabilitative therapy for a longer time after this critical period of time, in which no observed improvements would counteract the opposite negative effects of brain factors known to be released during this time. From our study, we cannot conclude whether there is a time window in which GH effects are counteracted by negative factors or it is a matter of doses. Lastly, our data indicate that there is not a plateau in recovery from a brain injury. Efforts have to be made to continue rehabilitative therapies after a brain injury beyond the time established in which no more recovery can be achieved.

Conflicts of Interest

The authors declare that there is no conflict of interests.

Acknowledgments

The excellent technical assistance of Javier Blanco and María José Almaraz is acknowledged. This research was supported by Foltra Foundation (Teo, Spain).

References

[1] A. Scheepens, E. S. Sirimanne, B. H. Breier, R. G. Clark, P. D. Gluckman, and C. E. Williams, "Growth hormone as a neuronal rescue factor during recovery from CNS injury," *Neuroscience*, vol. 104, no. 3, pp. 677–687, 2001.

[2] D. H. Shin, E. Lee, J. W. Kim et al., "Protective effect of growth hormone on neuronal apoptosis after hypoxia-ischemia in the neonatal rat brain," *Neuroscience Letters*, vol. 354, no. 1, pp. 64–68, 2004.

[3] N. D. Aberg, K. G. Brywe, and J. Isgaard, "Aspects of growth hormone and insulin-like growth factor-I related to neuroprotection, regeneration, and functional plasticity in the adult brain," *The Scientific World Journal*, vol. 6, pp. 53–80, 2006.

[4] J. Isgaard, D. Aberg, and M. Nilsson, "Protective and regenerative effects of the GH/IGF-I axis on the brain," *Minerva Endocrinologica*, vol. 32, no. 2, pp. 103–113, 2007.

[5] L. J. Christophidis, T. Gorba, M. Gustavsson et al., "Growth hormone receptor immunoreactivity is increased in the subventricular zone of juvenile rat brain after focal ischemia: a potential role for growth hormone in injury-induced neurogenesis," *Growth Hormone & IGF Research*, vol. 19, no. 6, pp. 497–506, 2009.

[6] P. Pathipati, A. Surus, C. E. Williams, and A. Scheepens, "Delayed and chronic treatment with growth hormone after endothelin-induced stroke in the adult rat," *Behavioural Brain Research*, vol. 204, no. 1, pp. 93–101, 2009.

[7] P. Devesa, P. Reimunde, R. Gallego, J. Devesa, and V. M. Arce, "Growth hormone (GH) treatment may cooperate with locally-produced GH in increasing the proliferative response of hippocampal progenitors to kainate-induced injury," *Brain Injury*, vol. 25, no. 5, pp. 503–510, 2011.

[8] R. C. Li, S. Z. Guo, M. Raccurt et al., "Exogenous growth hormone attenuates cognitive deficits induced by intermittent hypoxia in rats," *Neuroscience*, vol. 196, pp. 237–250, 2011.

[9] C. Alba-Betancourt, J. L. Luna-Acosta, C. E. Ramírez-Martínez et al., "Neuro-protective effects of growth hormone (GH) after hypoxia-ischemia injury in embryonic chicken cerebellum," *General and Comparative Endocrinology*, vol. 183, pp. 17–31, 2013.

[10] J. Devesa, P. Reimunde, A. Devesa et al., "Recovery from neurological sequelae secondary to oncological brain surgery in an adult growth hormone-deficient patient after growth hormone treatment," *Journal of Rehabilitation Medicine*, vol. 41, no. 9, pp. 775–777, 2009.

[11] W. M. High Jr, M. Briones-Galang, J. A. Clark et al., "Effect of growth hormone replacement therapy on cognition after traumatic brain injury," *Journal of Neurotrauma*, vol. 27, no. 9, pp. 1565–1575, 2010.

[12] P. Reimunde, A. Quintana, B. Castañón et al., "Effects of growth hormone (GH) replacement and cognitive rehabilitation in patients with cognitive disorders after traumatic brain injury," *Brain Injury*, vol. 25, no. 1, pp. 65–73, 2011.

[13] O. K. Moreau, C. Cortet-Rudelli, E. Yollin, E. Merlen, W. Daveluy, and M. Roseaux, "Growth hormone replacement therapy in patients with traumatic brain injury," *Journal of Neurotrauma*, vol. 30, no. 11, pp. 998–1006, 2013.

[14] J. Song, K. Park, H. Lee, and M. Kim, "The effect of recombinant human growth hormone therapy in patients with completed stroke: a pilot trial," *Annals of Rehabilitation Medicine*, vol. 36, no. 4, pp. 447–457, 2012.

[15] J. Devesa, P. Devesa, P. Reimunde, and V. Arce, "Growth hormone and kynesitherapy for brain injury recovery," in *Brain Injury - Pathogenesis, Monitoring, Recovery and Management*, A. Agrawal, Ed., pp. 417–454, InTech, Rijeka Croatia, 2012.

[16] J. Devesa, P. Reimunde, P. Devesa, M. Barberá, and V. Arce, "Growth hormone (GH) and brain trauma," *Hormones and Behavior*, vol. 63, no. 2, pp. 331–344, 2013.

[17] J. Devesa, G. Díaz-Getino, P. Rey et al., "Brain recovery after a plane crash: treatment with growth hormone (GH) and neurorehabilitation: a case report," *International Journal of Molecular Sciences*, vol. 16, no. 12, pp. 30470–30482, 2015.

[18] J. Devesa, H. Lema, E. Zas, B. Munín, P. Taboada, and P. Devesa, "Learning and memory recoveries in a young girl treated with growth hormone and neurorehabilitation," *Journal of Clinical Medicine*, vol. 5, no. 2, 2016.

[19] M. Heredia, A. Fuente, J. Criado, J. Jayeya, J. Devesa, and A. S. Riolobos, "Early growth hormone (GH) treatment promotes relevant motor functional improvement after severe frontal cortex lesion in adult rats," *Behavioural Brain Research*, vol. 247, pp. 48–58, 2013.

[20] J. Biernaskie, G. Chernenko, and D. Corbett, "Efficacy of rehabilitative experience declines with time after focal ischemic brain injury," *The Journal of Neuroscience*, vol. 24, no. 5, pp. 1245–1254, 2004.

[21] T.-S. Yu, G. Zhang, D. J. Liebl, and S. G. Kernie, "Traumatic brain injury-induced hippocampal neurogenesis requires activation of early nestin-expressing progenitors," *The Journal of Neuroscience*, vol. 28, no. 48, pp. 12901–12912, 2008.

[22] J. L. Ridet, S. K. Malhotra, A. Privat, and F. H. Gage, "Reactive astrocytes: cellular and molecular cues to biological function," *Trends in Neurosciences*, vol. 20, no. 12, pp. 570–577, 1997.

[23] S. Belachew, R. Chittajallu, A. A. Aguirre et al., "Postnatal NG2 proteoglycan-expressing progenitor cells are intrinsically multipotent and generate functional neurons," *The Journal of Cell Biology*, vol. 161, no. 1, pp. 169–186, 2003.

[24] A. Aguirre and V. Gallo, "Postnatal neurogenesis and gliogenesis in the olfactory bulb from NG2-expressing progenitors of the subventricular zone," *The Journal of Neuroscience*, vol. 24, no. 46, pp. 10530–10541, 2004.

[25] A. Yokoyama, A. Sakamoto, K. Kameda, Y. Imai, and J. Tanaka, "NG2 proteoglycan-expressing microglia as multipotent neural progenitors in normal and pathologic brains," *Glia*, vol. 53, no. 7, pp. 754–768, 2006.

[26] M. L. Hendrickson, A. J. Rao, O. N. Demerdash, and R. E. Kalil, "Expression of nestin by neural cells in the adult rat and human brain," *PLoS One*, vol. 6, no. 4, article e18535, 2011.

[27] J. J. Ohab and S. T. Carmichael, "Poststroke neurogenesis: emerging principles of migration and localization of immature neurons," *The Neuroscientist*, vol. 14, no. 4, pp. 369–380, 2008.

[28] N. Dancause, S. Barbay, S. B. Frost et al., "Extensive cortical rewiring after brain injury," *The Journal of Neuroscience*, vol. 25, no. 44, pp. 10167–10179, 2005.

[29] S. Li, J. J. Overman, D. Katsman et al., "An age-related sprouting transcriptome provides molecular control of axonal sprouting after stroke," *Nature Neuroscience*, vol. 13, no. 12, pp. 1496–1504, 2010.

[30] . Gossard, F. Dihl, G. Pelletier, P. M. Dubois, and G. Morel, "In situ hybridization to rat brain and pituitary gland of growth hormone cDNA," *Neuroscience Letters*, vol. 79, no. 3, pp. 251–256, 1987.

[31] A. S. Riolobos, M. Heredia, J. A. de la Fuente et al., "Functional recovery of skilled forelimb use in rats obliged to use the impaired limb after grafting the frontal cortex lesions with homotopic fetal cortex," *Neurobiology of Learning and Memory*, vol. 75, no. 3, pp. 274–292, 2001.

[32] M. Heredia, A. S. Riolobos, A. Fuente, J. M. Criado, and J. Yajeya, "Motor skill recovery through neural transplants in adult rats with frontal cortex damage," *Trauma*, vol. 20, pp. 137–143, 2009.

[33] M. Heredia, A. Fuente, J. M. Criado, L. Jiménez-Díaz, J. Yajeya, and A. S. Riolobos, "Transplant of encapsulated astrocyte ameliorate lesion-induced motor deficits in adults rats with frontal cortex injury," *Trauma*, vol. 22, pp. 281–288, 2011.

[34] E. J. Neafsey, E. L. Bold, G. Haas et al., "The organization of the rat motor cortex: a microstimulation mapping study," *Brain Research*, vol. 11, no. 1, pp. 77–96, 1986.

[35] H. W. Horch, A. Krüttgen, S. D. Portbury, and L. C. Katz, "Destabilization of cortical dendrites and spines by BDNF," *Neuron*, vol. 23, no. 2, pp. 353–364, 1999.

[36] J. T. Trachtenberg, B. E. Chen, G. W. Knott et al., "Long-term in vivo imaging of experience-dependent synaptic plasticity in adult cortex," *Nature*, vol. 420, no. 6917, pp. 788–794, 2002.

[37] A. Holtmaat and K. Svoboda, "Experience-dependent structural synaptic plasticity in the mammalian brain," *Nature Reviews. Neuroscience*, vol. 10, no. 9, pp. 647–658, 2009.

[38] G. Yang, F. Pan, and W. B. Gan, "Stably maintained dendritic spines are associated with lifelong memories," *Nature*, vol. 462, no. 7275, pp. 920–924, 2009.

[39] T. A. Jones and T. Schallert, "Use-dependent growth of pyramidal neurons after neocortical damage," *The Journal of Neuroscience*, vol. 14, no. 4, pp. 2140–2152, 1994.

[40] T. A. Jones, J. A. Kleim, and W. T. Greenough, "Synaptogenesis and dendritic growth in the cortex opposite unilateral sensorimotor cortex damage in adult rats: a quantitative electron microscopic examination," *Brain Research*, vol. 733, no. 1, pp. 142–148, 1996.

[41] T. A. Jones and T. Schallert, "Overgrowth and pruning of dendrites in adult rats recovering from neocortical damage," *Brain Research*, vol. 581, no. 1, pp. 156–160, 1992.

[42] C. J. Chu and T. A. Jones, "Experience-dependent structural plasticity in cortex heterotopic to focal sensorimotor cortical damage," *Experimental Neurology*, vol. 166, no. 2, pp. 403–414, 2000.

[43] L. Wang, J. M. Conner, A. H. Nagahara, and M. H. Tuszynski, "Rehabilitation drives enhancement of neuronal structure in functionally relevant neuronal subsets," *Proceedings of the National Academy of Sciences of the United States of America*, vol. 113, no. 10, pp. 2750–2755, 2016.

[44] B. Hattiangady, M. S. Rao, G. A. Shetty, and A. K. Shetty, "Brain-derived neurotrophic factor, phosphorylated cyclic AMP response element binding protein and neuropeptide Y decline as early as middle age in the dentate gyrus and CA1 and CA3 subfields of the hippocampus," *Experimental Neurology*, vol. 195, no. 2, pp. 353–371, 2005.

[45] S. T. Carmichael, I. Archibeque, L. Luke, T. Nolan, J. Momiy, and S. Li, "Growth-associated gene expression after stroke: evidence for a growth-promoting region in peri-infarct cortex," *Experimental Neurology*, vol. 193, no. 2, pp. 291–311, 2005.

[46] S. T. Carmichael, "Cellular and molecular mechanisms of neural repair after stroke: making waves," *Annals of Neurology*, vol. 59, no. 5, pp. 735–742, 2006.

[47] S. C. Cramer and M. Chopp, "Recovery recapitulates ontogeny," *Trends in Neurosciences*, vol. 23, no. 6, pp. 265–271, 2000.

[48] T. H. Murphy and D. Corbett, "Plasticity during stroke recovery: from synapse to behaviour," *Nature Reviews Neuroscience*, vol. 10, no. 12, pp. 861–872, 2009.

[49] J. Biernaskie, A. Szymanska, V. Windle, and D. Corbett, "Bihemispheric contribution to functional motor recovery of the affected forelimb following focal ischemic brain injury in rats," *The European Journal of Neuroscience*, vol. 21, no. 4, pp. 989–999, 2005.

[50] Y. Takatsuru, D. Fukumoto, M. Yoshitomo, T. Nemoto, H. Tsukada, and J. Nabekura, "Neuronal circuit remodeling in the contralateral cortical hemisphere during functional recovery from cerebral infarction," *The Journal of Neuroscience*, vol. 29, no. 32, pp. 10081–10086, 2009.

[51] U. Lendahl, L. B. Zimmerman, and R. D. G. McKay, "CNS stem cells express a new class of intermediate filament protein," *Cell*, vol. 60, no. 4, pp. 585–595, 1990.

[52] J. Dahlstrand, M. Lardelli, and U. Lendahl, "Nestin mRNA expression correlates with the central nervous system progenitor cell state in many, but not all, regions of developing central nervous system," *Developmental Brain Research*, vol. 84, no. 1, pp. 109–129, 1995.

[53] R. McKay, "Stem cells in the central nervous system," *Science*, vol. 276, no. 5309, pp. 66–71, 1997.

[54] M. S. Rao, "Multipotent and restricted precursors in the central nervous system," *The Anatomical Record*, vol. 257, no. 4, pp. 137–148, 1999.

[55] A. G. Douen, L. Dong, S. Vanance et al., "Regulation of nestin expression after cortical ablation in adult rat brain," *Brain Research*, vol. 1008, no. 2, pp. 139–146, 2004.

[56] I. Lavrnja, V. Ajdzanovic, S. Trifunovic et al., "Cortical ablation induces time-dependent changes in rat pituitary somatotrophs and upregulates growth hormone receptor expression in the injured cortex," *Journal of Neuroscience Research*, vol. 92, no. 10, pp. 1338–1349, 2014.

[57] H. Nakatomi, T. Kuriu, S. Okabe et al., "Regeneration of hippocampal pyramidal neurons after ischemic brain injury by recruitment of endogenous neural progenitors," *Cell*, vol. 110, no. 4, pp. 429–441, 2002.

[58] E. Gould and P. Tanapat, "Lesion-induced proliferation of neuronal progenitors in the dentate gyrus of the adult rat," *Neuroscience*, vol. 80, no. 2, pp. 427–436, 1997.

[59] K. Michalczyk and M. Ziman, "Nestin structure and predicted function in cellular cytoskeletal organisation," *Histology and Histopathology*, vol. 20, no. 2, pp. 665–671, 2005.

[60] P. M. Steinert, Y.-H. Chou, V. Prahlad et al., "A high molecular weight intermediate filament-associated protein in BHK-21 cells is nestin, a type VI intermediate filament protein," *The Journal of Biological Chemistry*, vol. 274, no. 14, pp. 9881–9890, 1999.

[61] Y. Chou, S. Khuon, H. Herrmann, and R. D. Goldman, "Nestin promotes the phosphorylation-dependent disassembly of vimentin intermediate filaments during mitosis," *Molecular Biology of the Cell*, vol. 14, no. 4, pp. 1468–1478, 2002.

[62] C. M. Sahlgren, A. Mikhailov, J. Hellman et al., "Mitotic reorganization of the intermediate filament protein nestin involves phosphorylation by cdc2 kinase," *The Journal of Biological Chemistry*, vol. 276, no. 19, pp. 16456–16463, 2001.

[63] A. Bellot, B. Guivernau, M. Tajes, M. Bosch-Morató, V. Valls-Comamaia, and F. J. Muñoz, "The structure and function of actin cytoskeleton in mature glutamatergic dendritic spines," *Brain Research*, vol. 1573, pp. 1–16, 2014.

[64] R. P. Stroemer, T. A. Kent, and C. E. Hulsebosch, "Neocortical neural sprouting, synaptogenesis, and behavioural recovery after neocortical infarction in rats," *Stroke*, vol. 26, no. 11, pp. 2135–2144, 1995.

[65] M. C. Comelli, D. Guidoli, M. S. Seren et al., "Time course, localization and pharmacological modulation of immediate early inducible genes, brain-derived neurotrophic factor and trkB messenger RNAs in the rat brain following photochemical stroke," *Neuroscience*, vol. 55, no. 2, pp. 473–490, 1993.

[66] C. E. Brown, K. Aminoltejari, H. Erb, I. R. Winship, and T. H. Murphy, "In vivo voltage-sensitive dye imaging in adult mice reveals that somatosensory maps lost to stroke are replaced over weeks by new structural and functional circuits with prolonged modes of activation within both the peri-infarct zone and distant sites," *The Journal of Neuroscience*, vol. 29, no. 6, pp. 1719–1734, 2009.

[67] S. T. Carmichael and M. F. Chesselet, "Synchropous neuronal activity is a signal for axonal sprouting after cortical lesions in the adult," *The Journal of Neuroscience*, vol. 22, no. 14, pp. 6062–6070, 2002.

[68] C. E. Brown, P. Li, J. D. Boyd, K. R. Delaney, and T. H. Murphy, "Extensive turnover of dendritic spines and vascular remodeling in cortical tissues recovering from stroke," *The Journal of Neuroscience*, vol. 27, no. 15, pp. 4101–4109, 2007.

[69] J. L. Cheatwood, A. J. Emerick, M. E. Schwab, and G. L. Kartje, "Nogo-A expression after focal ischemic stroke in the adult rat," *Stroke*, vol. 39, no. 7, pp. 2091–2098, 2008.

[70] J. K. Lee, J. E. Kim, M. Sivula, and S. M. Strittmatte, "Nogo receptor antagonism promotes stroke recovery by enhancing axonal plasticity," *The Journal of Neuroscience*, vol. 24, no. 27, pp. 6209–6217, 2004.

[71] C. M. Papadopoulos, S. Y. Tsai, J. L. Cheatwood et al., "Dendritic plasticity in the adult rat following middle cerebral artery occlusion and Nogo-A neutralization," *Cerebral Cortex*, vol. 16, no. 4, pp. 529–536, 2006.

[72] C. Hobohm, A. Günther, J. Grosche, S. Rossner, D. Schneider, and G. Brückner, "Decomposition and long-lasting downregulation of extracellular matrix in perineuronal nets induced by focal cerebral ischemia in rats," *Journal of Neuroscience Research*, vol. 80, no. 4, pp. 539–548, 2005.

Hindawi
Neural Plasticity
Volume 2018, Article ID 9828070, 7 pages
https://doi.org/10.1155/2018/9828070

Research Article

Acoustic Trauma Changes the Parvalbumin-Positive Neurons in Rat Auditory Cortex

Congli Liu,[1,2,3] Tao Xu,[1,2] Xiaopeng Liu,[4] Yina Huang,[4] Haitao Wang,[4] Bin Luo,[1,2] and Jingwu Sun[1,2]

[1]*Department of Otolaryngology-Head and Neck Surgery, Anhui Medical University Affiliated Anhui Provincial Hospital, Hefei 230001, China*
[2]*Department of Otolaryngology-Head and Neck Surgery, The First Affiliated Hospital of University of Science and Technology of China, Hefei 230001, China*
[3]*Department of Otolaryngology-Head and Neck Surgery, Lu'an People's Hospital, Lu'an Affiliated Hospital of Anhui Medical University, Lu'an 237000, China*
[4]*Auditory Research Laboratory, University of Science and Technology of China, Hefei 230027, China*

Correspondence should be addressed to Bin Luo; luobinsky@foxmail.com and Jingwu Sun; entsunjingwu@hotmail.com

Received 26 May 2017; Revised 3 October 2017; Accepted 26 November 2017; Published 8 February 2018

Academic Editor: Andrea Turolla

Acoustic trauma is being reported to damage the auditory periphery and central system, and the compromised cortical inhibition is involved in auditory disorders, such as hyperacusis and tinnitus. Parvalbumin-containing neurons (PV neurons), a subset of GABAergic neurons, greatly shape and synchronize neural network activities. However, the change of PV neurons following acoustic trauma remains to be elucidated. The present study investigated how auditory cortical PV neurons change following unilateral 1 hour noise exposure (left ear, one octave band noise centered at 16 kHz, 116 dB SPL). Noise exposure elevated the auditory brainstem response threshold of the exposed ear when examined 7 days later. More detectable PV neurons were observed in both sides of the auditory cortex of noise-exposed rats when compared to control. The detectable PV neurons of the left auditory cortex (ipsilateral to the exposed ear) to noise exposure outnumbered those of the right auditory cortex (contralateral to the exposed ear). Quantification of Western blotted bands revealed higher expression level of PV protein in the left cortex. These findings of more active PV neurons in noise-exposed rats suggested that a compensatory mechanism might be initiated to maintain a stable state of the brain.

1. Introduction

Acoustic overexposure, aging, and ototoxic drugs could lead to auditory disorders including hearing loss, hyperacusis, and tinnitus [1]. Hearing loss-induced elevation of neuronal activity and synchronization is closely related with impaired inhibition [2–4]. Cortical inhibition was contributed by nearly 20% interneurons which balance the excitation exerted by glutamatergic neurons. These GABAergic interneurons targeting different compartments of glutamatergic neurons play critical roles in sculpturing cortical circuits. GABA inhibition powerfully influences the frequency tuning curve and receptive field of auditory cortex neurons, and the impaired inhibition is implicated in many neurological disorders. Noise-induced increase of the excitability of principal neurons of auditory stations is largely documented [5–7], and now, the question is how the inhibitory neurons change in this process.

Compared with homogenous excitatory neurons, inhibitory neurons are more heterogeneous in terms of morphology, firing patterns, and calcium-binding proteins (CBP) expressed. CBP function as calcium sensor and buffer to regulate calcium signaling and homeostasis [8, 9]. Parvalbumin (PV), calbindin (CB), and calretinin (CR) are characteristic CBP of different subpopulations of interneurons. 20–25% of cortical GABAergic neurons express PV [10], and these

neurons belong to fast-spiking interneurons, which play a vital role in the synchrony and oscillation of neural networks. Recently, a layer-specific activity was reported in the noise-induced hearing loss animals as a result of change in cortical GABA neurons [11] and the deterioration of perineuronal nets enwrapping PV neurons [12].

In the present study, immunohistochemical staining and Western blotting assay were applied to quantitate the change of PV inhibitory neurons following chronic acoustic trauma. The findings hopefully advance our understanding of the neural mechanism underlying acoustic trauma-induced hearing loss at the cortical level.

2. Materials and Methods

The animal care and experimental procedures were in accordance with the guidelines set by the Institutional Animal Care and Use Committee of Anhui Medical University.

2.1. Subjects. 31 adult male Sprague-Dawley rats (200–250 g) were randomly divided into two groups, namely control group (8 rats for immunohistochemistry and 7 rats for Western blotting) and noise-exposed group (8 rats for immunohistochemistry and 8 rats for Western blotting).

2.2. Auditory Brainstem Evoked Responses. Auditory brainstem evoked responses (ABR) to clicks generated through RZ6 processor (Tucker-Davis Technologies, USA) were obtained (BioSigRZ, Tucker-Davis Technologies, USA) in anesthetized rats (chloral hydrate, 350 mg/kg, i.p.). Three platinum-coated electrodes were placed under the dermis, specifically the positive electrode in the vertex, the ground electrode in the apex nasi, and the negative electrode in the ipsilateral mastoidal dermis. A polyethylene tube of the electrostatic speaker (ED1, TDT) was plugged into the ear canal for sound delivery. Acoustic stimuli were presented at the rate of 10/sec from 100 dB to 5 dB SPL in a descending sequence at 5 dB steps until no discernible waveform was acquired. 1000 repeating stimuli were presented to generate the averaged response. ABR recordings for each ear of each rat were conducted before and on the 7th day after noise exposure.

2.3. Unilateral Noise Exposure. Anesthetized rats were unilaterally exposed to one octave band noise centered at 16 kHz with the peak intensity of 116 dB sound pressure level (SPL). The acoustic signal for generating noise was programmed with RpvdsEx v7 (Tucker-Davis Technologies, USA) and MatLab R2008a (MathWorks Inc., USA), generated with TDT System 3 hardware (RP 2.1, PA 5, ED 1, and HB 7), amplified through an amplifier (MATRX/M-640, USA), and presented via a free-field speaker (CP-75A, Shanghai Chuangmu). The noise was converted into electrical signals by a microphone (model 7016, ACO Pacific Inc., USA) and acquired by the TDT system for calibration of sound levels. One hour continuous noise exposure was conducted within a soundproof chamber. The amplified noise was presented via the speaker positioned 3 cm from the left ear canal, while the right ear was carefully plugged to preserve hearing and make a unilaterally noise-exposed animal model. The material of the plug was a kind of propenoic acid, commonly used to make ear mode in clinic, injected into the right external ear canal and ear nail through a syringe; this material could be turned into solid after ten minutes, and it could be easily pulled out from the external ear canal.

2.4. Immunohistochemical Staining. Several days after noise exposure, animals were anesthetized to be transcardically perfused with 0.1 M PBS (phosphate buffered saline) and 4% paraformaldehyde fixative. The brains were further postfixed for 6 h at 4°C. 30 μm thick coronal brain slices were cryosectioned with a freezing microtome (CM1950, Leica, Germany). Stereotaxic coordinates [13] were referred to select brain slices containing the auditory cortex. The hippocampus and the rhinal fissure were used as landmarks for locating the auditory cortex. In the coronal slice, we took the edge of the auditory cortex from 1 mm away from the rhinal fissure and we took the width of 1 mm as the auditory cortex. Every fifth section along rostral-caudal axis of the auditory cortex (AC) was collected to form a set of tissue samples. In addition, every one or two of five sets of samples and a total of ten samples of each animal were selected for staining.

Avidin-biotin-peroxidase method (ABC kit, Vector Labs) was adopted to stain PV protein in the 12-well culture plates. Free-floating sections were washed for 10 minutes (3 times) with Tris-Triton (pH 7.4), then incubated for 15 minutes with 10% normal goat serum to block nonspecific sites. Slices were incubated with primary antibody against PV (1 : 1000, PV235, Swant, Switzerland) overnight at 4°C. The secondary antibody (goat anti-mouse IgG, streptavidin-peroxidase kits, ZSJQ-BIO, Beijing, China) was used to biotinylate the primary antibody for 15 minutes, and additional 15 minutes incubation with avidin-biotin-peroxidase solution was performed to form the aggregates. Complete washes with Tris-Triton were done between each incubations. Finally, diaminobenzidine (DAB, ZLI9017, ZSJQ-BIO, Beijing, China) produced the dark brown color reaction to visualize PV neurons, and the sections were further mounted on slides, dehydrated, and coverslipped. The images were taken with a light microscope (ZEISS Axioskop 2 Plus, Germany). The PV neurons across all layers of the auditory cortex were counted with Image Pro Plus 6.0.

2.5. Western Blotting Assay. Coronal auditory cortex slices with the thickness of 300 μm were obtained in oxygenated (95% O_2/5% CO_2) ice-cold artificial cerebrospinal fluid (ACSF) with a vibratome (DTK-1000, DSK, Japan). ACSF contained the following (in mM): NaCl 129, KCl 3, $MgSO_4$ 1.3, KH_2PO_4 1.2, HEPES 3, D-glucose 10, $NaHCO_3$ 20, and $CaCl_2$ 2.4, with the pH 7.4 and osmolality of 300 Osmol/L. The auditory cortex was carefully dissected out with fine syringe needles from a total of five slices each animal.

Tissues were homogenized manually in a buffer (50 mM Tris, 150 mM NaCl, 0.1% SDS, 1% TritonX-100, and 0.5% sodium deoxycholate, pH 7.6) containing protease inhibitors (Cocktail, Roche, USA). Lysate was cleared at 12000g for 10 min at 4°C. The protein concentration of the supernatant was measured through a Bradford assay (Sangon SK3051, Shanghai, China) and quantified through a Biomate5

spectrophotometer (MDC SpectraMax 190, California, USA). 40 mg protein from each sample was added to 5x sample buffer and electrophoresed on 8% sodium dodecyl sulphate-polyacrylamide gel (SDS-PAGE) for 1 h at 120 V. Proteins were transferred from the gel to a 0.45 μm polyvinylidene fluoride- (PVDF-) Plus membrane (Bio-Rad Laboratories Inc., Minnetonka, USA) for 2 h at 260 mA. The target membrane was cut according to marker and blocked at room temperature for 1 h in Tris-buffered saline Tween (TBST, 10 mM Tris/HCl, 150 mM NaCl, 0.1% Tween-20, pH 7.6) containing 5% skim milk and then incubated in TBST containing the primary antibodies at room temperature for 1 h before keeping overnight at 4°C. Following three TBST washes (15 min each), the membrane was incubated in a secondary antibody for 1 h at room temperature. Following another TBST washes, the membrane was developed with an ECL kit (Bio-Rad Laboratories Inc., Minnetonka, USA). Images were acquired using Fusion solo gel imaging system (Vilber Lourmat, France) and were further analyzed using ImageJ (NIH, USA).

The primary antibodies for Western blotting included mouse monoclonal anti-PV (1 : 1000, Swant, Switzerland) and rabbit monoclonal anti-β-tubulin (1 : 1000, Cell signaling technology, USA). Secondary antibodies included horseradish peroxidase- (HRP-) conjugated goat anti-mouse and anti-rabbit IgG (1 : 5000, Biosharp, China). The expression level of proteins was quantified with the optic density of a band with ImageJ software, and PV/β-tubulin ratio was calculated.

2.6. Statistical Analysis. The cell density (cells/mm^2) was calculated from the PV-positive cells across all auditory cortex layers. SPSS 21.0 (IBM Corporation, Somers, NY) was used for data comparison and presentation. Paired and unpaired Student's t-test was taken to evaluate the statistical significance, and difference at the level of $p < 0.05$ was considered significant. All numerical values are expressed as mean ± SE (standard error), and GraphPad Prism software (San Diego, CA, USA) was used for graphs plotting.

3. Results

3.1. Noise Exposure Elevated ABR Threshold. At first, in order to make sure that all the subjects have a normal hearing before noise exposure, the ABR thresholds for clicks were determined (control group: right ear 19.00 ± 1.01 dB, left ear 18.33 ± 0.79 dB, $n = 15$; exposure group: right ear 18.75 ± 0.85 dB, left ear 17.19 ± 0.91 dB, $n = 16$). The threshold of noise-exposed ear was significantly elevated when the rats were examined 7 days after noise exposure paradigm (76.88 ± 1.01 dB, $p < 0.0001$, $n = 16$, Figure 1(e)), while that of the contralateral ears remained unaffected (18.13 ± 0.77 dB, $p > 0.05$, $n = 16$, Figure 1(e)), which indicated that rat model with unilateral hearing loss was successfully established. The ABR threshold of control group did not show any significant change (data not shown). Representative traces of ABR from each group of rats were shown in Figures 1(a)–1(d).

3.2. More Detectable PV Neurons in the Auditory Cortex of Noise-Exposed Rats. As shown in Figure 2, PV-positive neurons are distributed in all cortical layers except layer I. We observed higher density of PV-positive neurons in both sides of the auditory cortex (right AC 133.5 ± 2.21 neurons/mm^2 and left AC 162.5 ± 2.99 neurons/mm^2) of noise-exposed rats relative to control group (right AC 109.1 ± 2.77 neurons/mm^2 and left AC 110 ± 2.05 neurons/mm^2) ($p < 0.0001$, $n = 8$ for each group, unpaired Student's t-test), and the representative photomicrographs for each group and statistical results were shown in Figures 2 and 3, respectively. In the noise-exposed rats, the right AC and left AC are contralateral and ipsilateral side to the exposed ear, and we observed that the number of PV neurons in the left AC exceeds that of the right AC ($p < 0.0001$) after noise exposure.

3.3. Noise Exposure Upregulated the Expression Level of Cortical PV. Next, Western blotting was applied to quantify the PV protein level of the auditory cortex before and after noise exposure. On the 7th day following nose exposure, rats were sacrificed for collecting the target tissues, and PV/β-tubulin ratio was calculated to indicate the relative expression level of PV. The imaged gel bands from AC of exposed rats were heavier and broader, while those from AC of control rats were lighter and narrower (Figure 4). Statistically, noise exposure significantly upregulated the expression level of cortical PV protein, and the average PV expression level of both sides AC in exposed rats was 174.23% of that in control rats (Figure 5) ($p < 0.001$, $n = 7$ and 8 rats for control and experimental groups, resp.). Comparison between two hemispheres of AC from exposed rats showed that PV expression level of the right AC was 63.64% that of the left AC ($p < 0.001$, $n = 8$).

4. Discussion

In the present study, we investigated the effect of acoustic trauma on PV neurons of the auditory cortex, a subset of GABAergic inhibitory neurons. Acoustic trauma, aging, and ototoxic drugs permanently or temporarily produce the hearing deficit. Among these factors, noise exposure becomes more common [14, 15], and noise-induced hearing loss reorganizes the tonotopic maps and elevates the neuronal activity of the auditory cortex, causing other auditory disorders such as tinnitus and hyperacusis [16, 17]. The activity of the brain is influenced by GABAergic inhibition, and the imbalance of excitation and inhibition often occurs following noise exposure [2, 17–20]; hence, it is vital to understand the change of cortical PV neurons following acoustic trauma.

Noise-induced temporary and permanent auditory threshold shifts could be immediately observed depending on the intensity of noise [21–24]. Our noise exposure paradigm caused ABR threshold shift ranging from 45 to 65 dB on day 7 postexposure, which is similar to those reported previously [22, 25, 26]. The underlying mechanism can be acoustic trauma damaging cochlear hair cells [27], and these irreversible insults elevate the auditory threshold [28]. Consistently, the noise-exposed ear with

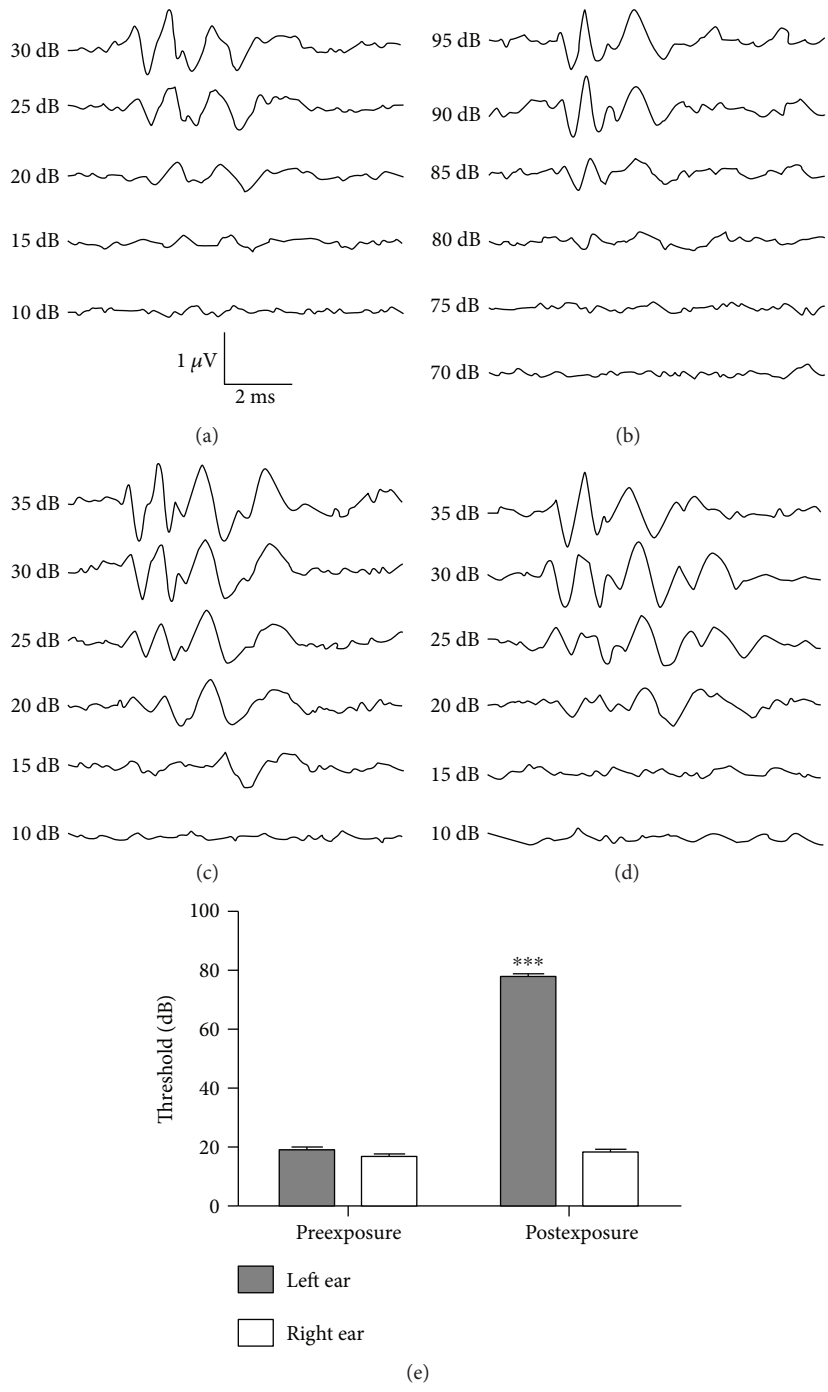

Figure 1: Auditory brainstem responses before and after noise exposure. (a, b) Representative ABR waveforms following acoustic trauma in noise-exposed group ((a) right ear; (b) left ear) and control group ((c) right ear; (d) left ear). (e) Group data showing that ABR threshold was elevated in the exposed ear of exposed group, but not in the unexposed ear and both ears of the control group. $^{***}p < 0.0001$.

elevated ABR threshold and unexposed ear with normal ABR threshold suggested that the impairment occurred in the ear exposed to noise.

Hearing loss changes the neuronal activities of different auditory stations, and the hypofunction of cortical inhibitory neurons is proposed to account for the overexcitability of auditory principal neurons. PV-containing neurons as the largest population of interneurons target the soma and proximal dendrites of pyramidal neurons to shape the receptive fields [29], process rapid-changing signals [30], and participate in the gamma-band oscillation [31, 32]. Proper function of the brain requires the inhibition mediated by GABA interneurons, and the lowered inhibition is considered to be involved in the hyperactivity of AC and inferior colliculus [33]. Initially, it was hypothesized that noise exposure would decrease the number of PV neurons and protein level of PV, but more PV neurons were detected in both sides of rats' AC. A recent research reported that in mice the cell

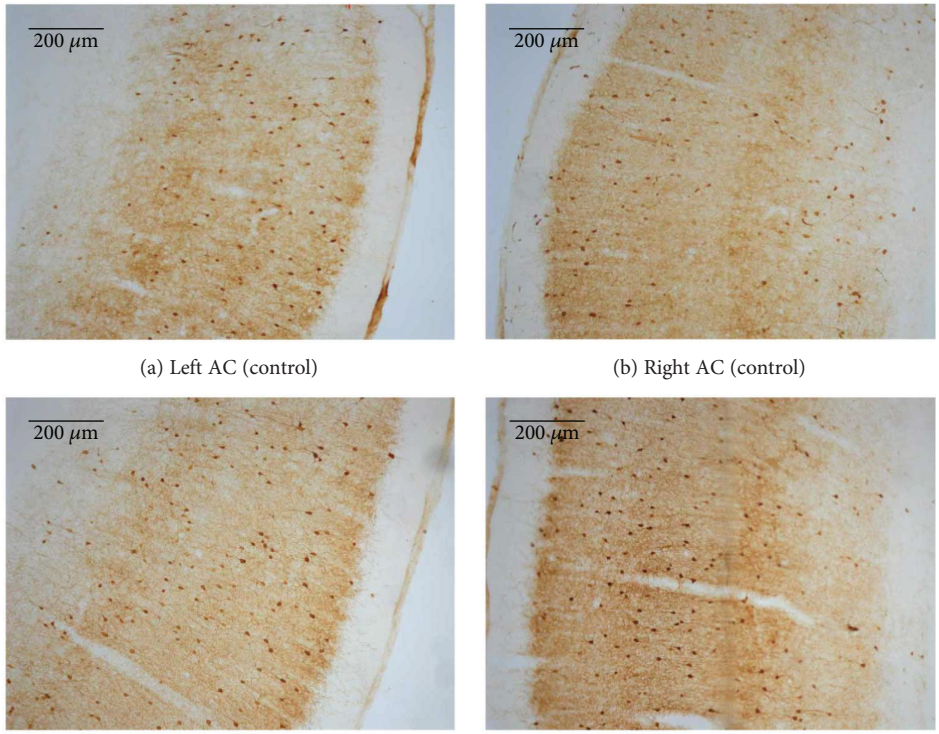

(a) Left AC (control) (b) Right AC (control)

(c) Left AC (noise-exposed group) (d) Right AC (noise-exposed group)

Figure 2: Photographs showing PV-immunoreactive neurons of auditory cortices. Representative immunostaining images of PV in the auditory cortex of a control rat ((a) left AC; (b) right AC) and a noise-exposed rat ((c) left AC; (d) right AC).

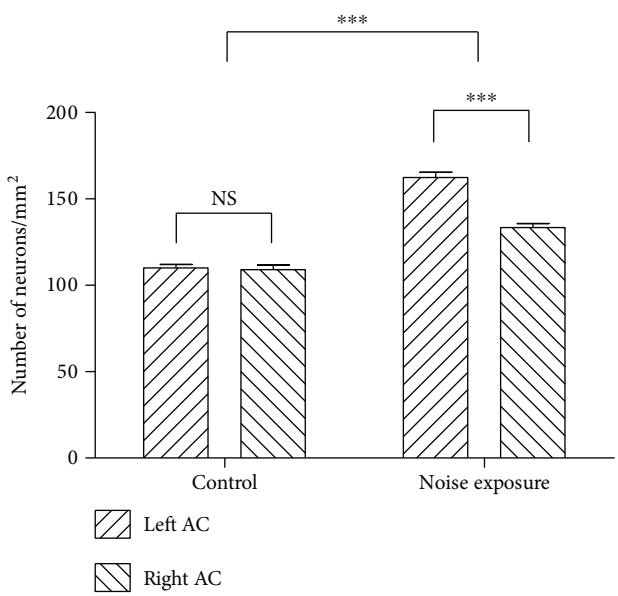

Figure 3: Statistical quantification shows the cell density of detectable PV-positive neurons. Noise exposure elevated the cell density of PV-positive neurons in both sides of the auditory cortex in noise-exposed rats (***$p < 0.0001$) with higher cell density in the left AC than in the right AC (***$p < 0.0001$).

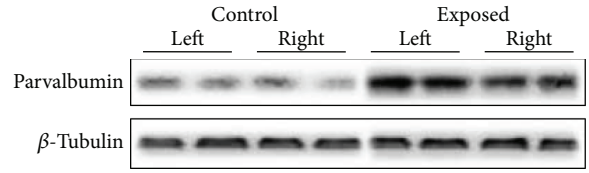

Figure 4: The representative Western blots from a control and a noise-exposed rat.

density of AC PV neurons following bilateral noise exposure indeed showed an increasing trend but having a minor difference [12]. This inconsistence might be a result of various subjects (rats versus mice) and noise exposure paradigm (116 dB unilateral exposure versus 103 dB bilateral exposure).

Quantitative analysis of Western blots of PV protein revealed that acoustic trauma elevated the expression level of PV protein, which is in accordance with more detectable PV neurons in noise-exposed rats. The apparent increase of PV neuron number is unlikely due to the neuronal proliferation in that mammalian adult neurons have already lost their ability of mitosis. The higher protein level and stronger immunoreactivity of PV in AC of noise-exposed rats observed in our experiment and increased evoked-to-spontaneous firing rate ratios in layer II/II PV neurons of AC demonstrated by Novak et al. [11] lead us to propose that a compensatory increase of PV proteins of AC in noise-exposed rats likely makes PV neurons more easily detected. The ipsilateral AC to noise exposure of the noise-exposed rats also underwent a similar change and this could be explained by the fact that binaural information converges on the auditory brain stem and some fibers from peripheral

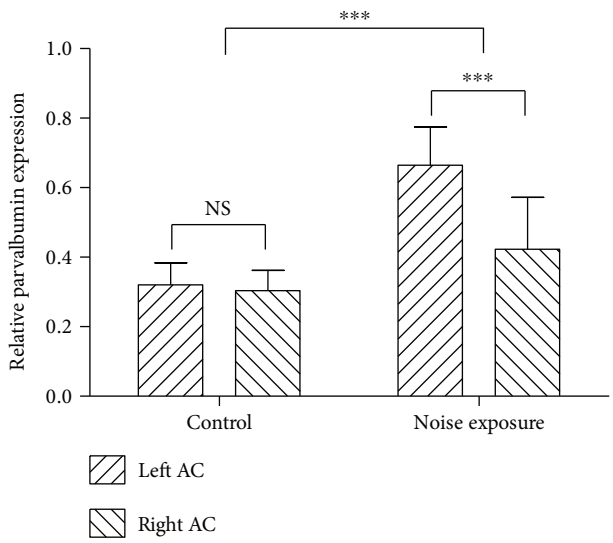

Figure 5: Quantification data showing relative expression levels of parvalbumin in control and noise-exposed rats. $^{***}p < 0.001$.

can cross to the contralateral central. One phenomenon which is difficult to explain is why the ipsilateral AC to noise exposure showed a more dramatic change. The surprising finding that the ipsilateral AC to noise exposure showed a more dramatic change could be explained by functional asymmetry between two hemispheres of the auditory cortex. In human being, left AC prevails in processing sound information [34, 35], and in the left ear noise-exposed gerbil [36], the primary AC of the left side was more activated than that of the right side. Similarly, if the activity of the left AC is higher than that of the right AC in our experimental rats, the compensatory mechanism would enable more PV activity in the left AC.

More PV protein expression possibly represents more activated state of cortical neurons, since PV protein, a marker of cellular metabolic level [37, 38], increased in cochlear nucleus and inferior colliculus of mice following noise exposure or sound stimulation [39, 40]. Logically, acoustic trauma-induced change of PV neurons could be suggested to promote cortical inhibition in the noise-exposed rats. However, the percentage of PV neurons of AC superficial layers declined in aged mice AC in a way different from those of noise-induced hearing loss mice [41].

Taken together, this study provided the evidence that acoustic trauma changed the PV neurons expression in rat auditory cortex, and the compensatory change of PV expression would help maintain the balance between excitation and inhibition. Our findings could develop our understanding of the behavior of inhibitory neurons following noise-induced hearing loss and help to develop the prevention or treatment strategies through targeting PV interneurons.

Conflicts of Interest

The authors declare that they have no conflict of interest.

Authors' Contributions

Congli Liu and Tao Xu contributed equally to this article.

Acknowledgments

This work was supported by National Natural Science Foundation of China (81470699, 81200741).

References

[1] L. E. Roberts, J. J. Eggermont, D. M. Caspary, S. E. Shore, J. R. Melcher, and J. A. Kaltenbach, "Ringing ears: the neuroscience of tinnitus," *Journal of Neuroscience*, vol. 30, no. 45, pp. 14972–14979, 2010.

[2] J. C. Milbrandt, T. M. Holder, M. C. Wilson, R. J. Salvi, and D. M. Caspary, "GAD levels and muscimol binding in rat inferior colliculus following acoustic trauma," *Hearing Research*, vol. 147, no. 1-2, pp. 251–260, 2000.

[3] W. H. A. M. Mulders and D. Robertson, "Hyperactivity in the auditory midbrain after acoustic trauma: dependence on cochlear activity," *Neuroscience*, vol. 164, no. 2, pp. 733–746, 2009.

[4] S. Seki and J. J. Eggermont, "Changes in spontaneous firing rate and neural synchrony in cat primary auditory cortex after localized tone-induced hearing loss," *Hearing Research*, vol. 180, no. 1-2, pp. 28–38, 2003.

[5] N. Pilati, C. Large, I. D. Forsythe, and M. Hamann, "Acoustic over-exposure triggers burst firing in dorsal cochlear nucleus fusiform cells," *Hearing Research*, vol. 283, no. 1-2, pp. 98–106, 2012.

[6] B. G. Peng, Q. X. Li, T. Y. Ren et al., "Group I metabotropic glutamate receptors in spiral ganglion neurons contribute to excitatory neurotransmissions in the cochlea," *Neuroscience*, vol. 123, no. 1, pp. 221–230, 2004.

[7] N. Pilati, M. J. Ison, M. Barker et al., "Mechanisms contributing to central excitability changes during hearing loss," *Proceedings of the National Academy of Sciences of the United States of America*, vol. 109, no. 21, pp. 8292–8297, 2012.

[8] M. Yanez, J. Gil-Longo, and M. Campos-Toimil, "Calcium binding proteins," *Calcium Signaling*, vol. 740, pp. 461–482, 2012.

[9] C. W. Heizmann, "Parvalbumin, and intracellular calcium-binding protein; distribution, properties and possible roles in mammalian cells," *Experientia*, vol. 40, no. 9, pp. 910–921, 1984.

[10] A. V. Zaitsev, G. Gonzalez-Burgos, N. V. Povysheva, S. Kröner, D. A. Lewis, and L. S. Krimer, "Localization of calcium-binding proteins in physiologically and morphologically characterized interneurons of monkey dorsolateral prefrontal cortex," *Cerebral Cortex*, vol. 15, no. 8, pp. 1178–1186, 2005.

[11] O. Novak, O. Zelenka, T. Hromádka, and J. Syka, "Immediate manifestation of acoustic trauma in the auditory cortex is layer specific and cell type dependent," *Journal of Neurophysiology*, vol. 115, no. 4, pp. 1860–1874, 2016.

[12] A. Nguyen, H. M. Khaleel, and K. A. Razak, "Effects of noise-induced hearing loss on parvalbumin and perineuronal net expression in the mouse primary auditory cortex," *Hearing Research*, vol. 350, pp. 82–90, 2017.

[13] G. Paxinos and C. Watson, *The Rat Brain in Stereotaxic Coordinates*, Academic Press, Australia, fifth edition, 2005.

[14] A. Kumar, K. Mathew, S. A. Alexander, and C. Kiran, "Output sound pressure levels of personal music systems and their effect on hearing," *Noise & Health*, vol. 11, no. 44, pp. 132–140, 2009.

[15] J. H. Peng, Z. Z. Tao, and Z. W. Huang, "Risk of damage to hearing from personal listening devices in young adults," *Journal of Otolaryngology*, vol. 36, no. 3, pp. 181–185, 2007.

[16] K. S. Kraus, D. Ding, H. Jiang, E. Lobarinas, W. Sun, and R. J. Salvi, "Relationship between noise-induced hearing-loss, persistent tinnitus and growth-associated protein-43 expression in the rat cochlear nucleus: does synaptic plasticity in ventral cochlear nucleus suppress tinnitus?," *Neuroscience*, vol. 194, pp. 309–325, 2011.

[17] W. H. Liao, T. Van Den Abbeele, P. Herman et al., "Expression of NMDA, AMPA and $GABA_A$ receptor subunit mRNAs in the rat auditory brainstem. II. Influence of intracochlear electrical stimulation," *Hearing Research*, vol. 150, no. 1-2, pp. 12–26, 2000.

[18] S. Dong, W. H. A. M. Mulders, J. Rodger, and D. Robertson, "Changes in neuronal activity and gene expression in guinea-pig auditory brainstem after unilateral partial hearing loss," *Neuroscience*, vol. 159, no. 3, pp. 1164–1174, 2009.

[19] J. Tan, L. Rüttiger, R. Panford-Walsh et al., "Tinnitus behavior and hearing function correlate with the reciprocal expression patterns of BDNF and Arg3.1/arc in auditory neurons following acoustic trauma," *Neuroscience*, vol. 145, no. 2, pp. 715–726, 2007.

[20] M. L. Zettel, W. E. O'Neill, T. T. Trang, and R. D. Frisina, "The effects of early bilateral deafening on calretinin expression in the dorsal cochlear nucleus of aged CBA/CaJ mice," *Hearing Research*, vol. 183, no. 1-2, pp. 57–66, 2003.

[21] J. Syka and N. Rybalko, "Threshold shifts and enhancement of cortical evoked responses after noise exposure in rats," *Hearing Research*, vol. 139, no. 1-2, pp. 59–68, 2000.

[22] C. A. Bauer, "Animal models of tinnitus," *Otolaryngologic Clinics of North America*, vol. 36, no. 2, pp. 267–285, 2003.

[23] J. L. Puel, J. Ruel, C. G. d'Aldin, and R. Pujol, "Excitotoxicity and repair of cochlear synapses after noise-trauma induced hearing loss," *Neuroreport*, vol. 9, no. 9, pp. 2109–2114, 1998.

[24] W. W. Clark, "Recent studies of temporary threshold shift (Tts) and permanent threshold shift (pts) in animals," *Journal of the Acoustical Society of America*, vol. 90, no. 1, pp. 155–163, 1991.

[25] J. G. Turner, T. J. Brozoski, C. A. Bauer et al., "Gap detection deficits in rats with tinnitus: a potential novel screening tool," *Behavioral Neuroscience*, vol. 120, no. 1, pp. 188–195, 2006.

[26] H. Wang, T. J. Brozoski, J. G. Turner et al., "Plasticity at glycinergic synapses in dorsal cochlear nucleus of rats with behavioral evidence of tinnitus," *Neuroscience*, vol. 164, no. 2, pp. 747–759, 2009.

[27] A. S. Nordmann, B. A. Bohne, and G. W. Harding, "Histopathological differences between temporary and permanent threshold shift," *Hearing Research*, vol. 139, no. 1-2, pp. 13–30, 2000.

[28] A. S. B. Edge and Z. Y. Chen, "Hair cell regeneration," *Current Opinion in Neurobiology*, vol. 18, no. 4, pp. 377–382, 2008.

[29] G. K. Wu, R. Arbuckle, B.h. Liu, H. W. Tao, and L. I. Zhang, "Lateral sharpening of cortical frequency tuning by approximately balanced inhibition," *Neuron*, vol. 58, no. 1, pp. 132–143, 2008.

[30] C. A. Atencio, T. O. Sharpee, and C. E. Schreiner, "Hierarchical computation in the canonical auditory cortical circuit," *Proceedings of the National Academy of Sciences of the United States of America*, vol. 106, no. 51, pp. 21894–21899, 2009.

[31] G. Buzsaki and A. Draguhn, "Neuronal oscillations in cortical networks," *Science*, vol. 304, no. 5679, pp. 1926–1929, 2004.

[32] M. Bartos, I. Vida, and P. Jonas, "Synaptic mechanisms of synchronized gamma oscillations in inhibitory interneuron networks," *Nature Reviews Neuroscience*, vol. 8, no. 1, pp. 45–56, 2007.

[33] J. F. Willott and S. M. Lu, "Noise-induced hearing loss can alter neural coding and increase excitability in the central nervous system," *Science*, vol. 216, no. 4552, pp. 1331–1334, 1982.

[34] B. Liu, Y. Feng, M. Yang et al., "Functional connectivity in patients with sensorineural hearing loss using resting-state MRI," *American Journal of Audiology*, vol. 24, no. 2, pp. 145–152, 2015.

[35] D. R. Moore, J. T. Devlin, J. Raley et al., "Effects of long term unilateral hearing loss on the lateralization of fMRI measured activation in human auditory cortex," *Plasticity and Signal Representation in the Auditory System*, vol. 46, no. 7, pp. 335–346, 2005.

[36] I. W. Stuermer and H. Scheich, "Early unilateral auditory deprivation increases 2-deoxyglucose uptake in contralateral auditory cortex of juvenile Mongolian gerbils," *Hearing Research*, vol. 146, no. 1-2, pp. 185–199, 2000.

[37] C. Batini, M. Palestini, M. Thomasset, and R. Vigot, "Cytoplasmic calcium buffer, calbindin-D28k, is regulated by excitatory amino-acids," *NeuroReport*, vol. 4, no. 7, pp. 927–930, 1993.

[38] M. R. Celio, L. Schärer, J. H. Morrison, A. W. Norman, and F. E. Bloom, "Calbindin immunoreactivity alternates with cytochrome c-oxidase-rich zones in some layers of the primate visual cortex," *Nature*, vol. 323, no. 6090, pp. 715–717, 1986.

[39] E. Idrizbegovic, N. Bogdanovic, and B. Canlon, "Modulating calbindin and parvalbumin immunoreactivity in the cochlear nucleus by moderate noise exposure in mice.: a quantitative study on the dorsal and posteroventral cochlear nucleus," *Brain Research*, vol. 800, no. 1, pp. 86–96, 1998.

[40] E. Idrizbegovic, N. Bogdanovic, and B. Canlon, "Sound stimulation increases calcium-binding protein immunoreactivity in the inferior colliculus in mice," *Neuroscience Letters*, vol. 259, no. 1, pp. 49–52, 1999.

[41] H. N. M. del Campo, K. R. Measor, and K. A. Razak, "Parvalbumin immunoreactivity in the auditory cortex of a mouse model of presbycusis," *Hearing Research*, vol. 294, no. 1-2, pp. 31–39, 2012.

Hindawi
Neural Plasticity
Volume 2018, Article ID 2782804, 10 pages
https://doi.org/10.1155/2018/2782804

Research Article

Bilateral Transcranial Direct Current Stimulation Reshapes Resting-State Brain Networks: A Magnetoencephalography Assessment

Giovanni Pellegrino[1], **Matteo Maran**[1], **Cristina Turco**[1], **Luca Weis**[1], **Giovanni Di Pino**[2], **Francesco Piccione**[1] and **Giorgio Arcara**[1]

[1]*San Camillo Hospital IRCCS, Venice, Italy*
[2]*NeXT: Neurophysiology and Neuroengineering of Human-Technology Interaction Research Unit, Campus Bio-Medico University, Rome, Italy*

Correspondence should be addressed to Giovanni Pellegrino; giovannipellegrino@gmail.com

Received 4 May 2017; Revised 11 September 2017; Accepted 2 October 2017; Published 11 January 2018

Academic Editor: Dario Farina

Transcranial direct current stimulation (tDCS) can noninvasively induce brain plasticity, and it is potentially useful to treat patients affected by neurological conditions. However, little is known about tDCS effects on resting-state brain networks, which are largely involved in brain physiological functions and in diseases. In this randomized, sham-controlled, double-blind study on healthy subjects, we have assessed the effect of bilateral tDCS applied over the sensorimotor cortices on brain and network activity using a whole-head magnetoencephalography system. Bilateral tDCS, with the cathode (−) centered over C4 and the anode (+) centered over C3, reshapes brain networks in a nonfocal fashion. Compared to sham stimulation, tDCS reduces left frontal alpha, beta, and gamma power and increases global connectivity, especially in delta, alpha, beta, and gamma frequencies. The increase of connectivity is consistent across bands and widespread. These results shed new light on the effects of tDCS and may be of help in personalizing treatments in neurological disorders.

1. Introduction

Transcranial direct current stimulation (tDCS) is a noninvasive neurostimulation technique capable of modulating brain excitability and inducing plastic phenomena outlasting the duration of the stimulation itself [1–3].

tDCS consists in the application of a weak homogeneous direct current over the scalp using two electrodes of different polarity (anode and cathode) connected to a stimulator, decreasing the cortical excitability under the cathode and increasing it under the anode [4]. Because of its ease of use, limited side effects, and low cost [5], tDCS has become very popular in the recent years and has been applied in a number of different frameworks, ranging from cognitive and social neuroscience [6] to clinical research [7]. tDCS application is now explored as a promising tool for the treatment of drug-resistant epilepsy [8] and, together with physical therapy, to boost brain plasticity and possibly to improve the outcome of disabled stroke patients [9–11].

As it happens for other noninvasive brain stimulation techniques, the mechanism by which tDCS is supposed to work is mainly related to the long-lasting changes of brain excitability [2, 12, 13]. However, change of excitability is disclosing only one aspect of tDCS effects, which surely involve modulation of neurotransmission [14], of brain activity [15], and of metabolism [16–18].

Despite the efficacy of both noninvasive and invasive brain stimulations in treating multiple neurological and psychiatric conditions being strictly dependent on their effects on resting-state brain networks [19], very little is known so far on tDCS effects on brain activity and connectivity.

In this study, we focused on the effects of tDCS on resting-state brain networks as assessed by magnetoencephalography (MEG). MEG is a noninvasive technique measuring

cortical magnetic activity with high temporal and spatial resolution [20–24]. Compared to other techniques such as EEG, MEG also owns the unique advantage of detecting signals without the application of electrodes on the scalp, thus allowing to place and to activate/deactivate tDCS without significant interference with the acquisition process.

We designed a sham-controlled, double-blind study where healthy subjects were scanned immediately before and after a 20-minute session of bihemispheric tDCS to investigate the effects of tDCS on the architecture of brain networks. Since both cathode and anode are active in producing cortical effects, the bihemispheric montage tested in this study exploits mechanisms of interhemispheric interaction to enhance the biological effects of tDCS [8, 9].

2. Materials and Methods

2.1. Participants and Experimental Design. We recruited 15 healthy subjects (mean age = 28.8 ± 3 (2 SE); 12 F) to participate in a randomized, sham-controlled, double-blind tDCS study (Figure 1). Each participant underwent two sessions of bihemispheric tDCS stimulation (sham and real). The two sessions were at least 20 h far apart. Before and after each tDCS session, we measured resting-state MEG data for about 5 minutes. All the subjects were right-handed as assessed by the Oldfield's Edinburgh inventory (91.13 ± 6.8) [25] and were free from medications. The fluctuations of vigilance were controlled by means of the Stanford Sleepiness Scale (SSS), which was administered before and after every MEG scan [26]. The experimental procedures were carried out at the MEG unit of the IRCCS San Camillo hospital in Venice, with the subjects lying down on a bed in a supine position in a quiet environment. Subjects were asked to keep their regular wake/sleep cycle before participation. All the procedures were performed in agreement with the 1964 Helsinki Declaration and its later amendments. This study was approved by the local ethics committee, and all participants provided a written informed consent.

2.2. tDCS. tDCS was delivered with a battery-powered stimulator connected to a pair of saline-soaked sponge electrodes having a surface of 35 cm^2. Real/sham stimulation was applied over the sensorimotor regions bilaterally, with the cathode (−) centered over C4 and the anode (+) centered over C3, where C3 and C4 are scalp positions according to the 10/20 international EEG system. This montage has been previously employed for clinical applications [8, 9]. Real stimulation lasted 20 minutes with 20 seconds of fade-in and fade-out, an intensity of 2 mA, and the current density was 0.057 mA/cm^2. For the sham stimulation, we employed the same setting except for the current, which was only applied for 20 seconds at the beginning and at the end of the stimulation with the aim of giving a slight tingling sensation that many subjects report for tDCS real stimulation.

2.3. MEG Data Acquisition and Preprocessing. MEG measures were acquired with a CTF MEG system (MISL, Vancouver, Canada) with 275 MEG gradiometers. Eye blinks, eye movements, and electrocardiogram (EKG) were recorded using bipolar electrodes, and the head position within the helmet was continuously monitored thanks to three localization coils placed on anatomical landmarks (the nasion and the left and right ear canals). The sampling rate was set to 1200 Hz. The acquisition lasted 5 minutes. Subjects were scanned with their eyes closed and were given the following instructions: "Clear your mind and stay relaxed." Before and after each MEG acquisition, the technician administered the Stanford Sleepiness Scale [26]. MEG data analysis was performed with Brainstorm toolbox [27], which is documented and freely available for download online under the GNU general public license (http://neuroimage.usc.edu/brainstorm). The preprocessing pipeline consisted of (1) third-order spatial gradient noise cancellation, (2) downsampling to 600 Hz, (3) signal space-separation (SSP), (4) epoching, (5) DC removal, and (6) bad sensor removal [22]. Artifacts related to heartbeat and eye movements were removed in step 3 of the pipeline using the SSP procedure [28, 29]. Resting-state signals were divided in step 4 into 20-second-lasting epochs. Each epoch was visually inspected, and those affected by artifacts were rejected.

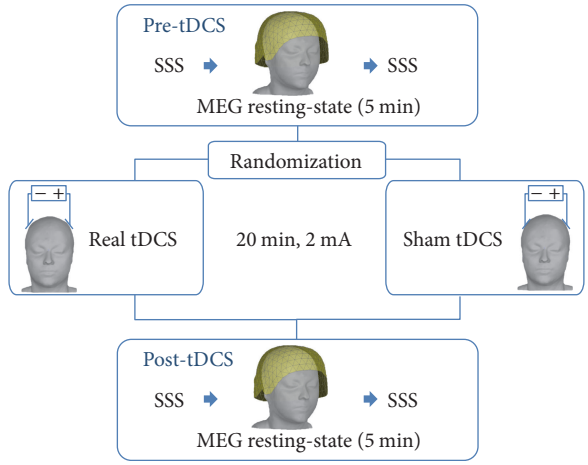

Figure 1: Experimental design.

2.4. Source Imaging. For each participant, we acquired an individual whole-head 3-dimensional sagittal T1-weighted-3D-TFE scan with a 1.5 T Achieva Philips scanner (Philips Medical Systems, best, Netherlands), with the following scan parameters: repetition time (TR) = 8.3 milliseconds, echo time (TE) = 4.1 milliseconds, flip angle = 8°, acquired matrix resolution (MR) = 288 × 288, and slice thickness (ST) = 0.87 mm. The cortical mesh of the "mid" cortical layer equidistant from white/grey matter interface and pial surface was segmented using FreeSurfer software [30], tasselled into 15,000 vertices, and then downsampled to 8000 vertices, whereas the reconstruction of the skull surface and the coregistration between patients' MRI and MEG data was performed with the Brainstorm toolbox [27]. The individual head model for source imaging was implemented with the OpenMEEG boundary element method (BEM) [31]. We only considered one cortical layer with a

conductivity of 0.33 S/m. The inverse problem was solved by using a whitened and depth-weighted linear L2-minimum norm estimate algorithm, with the estimated dipole orientations constrained to be normal to the cortex. A common imaging kernel was computed and then applied to obtain single epoch cortical reconstructions. Noise covariance for source reconstruction was obtained from an empty room recording of 2 minutes.

2.5. Brain Network Analysis: Resting-State Activity and Connectivity. To assess the changes in brain networks, we focused on two aspects: resting-state activity and connectivity.

Firstly, to have a general measure of resting-state activity, we focused on the spectral power of specific bands. Specifically, we calculated power spectrum density (PSD) at the source level. After inverting the signal onto the cortical surface, we computed the PSD for each cortical vertex in all the relevant frequency bands (delta: 2–4 Hz; theta: 5–7 Hz; alpha: 8–12 Hz; beta: 15–29 Hz; and gamma: 30–60 Hz).

We also focused on measuring resting-state connectivity across the brain, estimating the changes in coupling between two seeds beneath the tDCS electrodes and the rest of the cortex. We computed the phase locking value (PLV) [32], which is a very popular measure of brain synchronization commonly used to estimate nondirectional functional connectivity [33]. The connectivity analysis was performed considering two cortical seeds, underneath the cathode and the anode. They corresponded to the left and right primary sensorimotor hand regions. These regions were manually drawn by an expert neurologist (GP) onto the individual cortical surface using anatomical landmarks [34]. Each seed was extended about 10 cm^2. The signal within each seed was averaged, and the connectivity between such an average and every other cortical vertex was computed before and after tDCS. The same procedure was performed for the following frequency bands (delta: 2–4 Hz; theta: 5–7 Hz, alpha: 8–12 Hz; beta: 15–29 Hz, gamma: 30–60 Hz). To allow group analysis, PSD and PLV maps were projected onto standard MNI template [35] and spatially smoothed with full width at half maximum at 3 mm [36], which is the default value in Brainstorm for MEG and is compatible with the image resolution and distribution provided by the minimum norm estimate.

2.6. Statistical Analysis. Statistical analysis was performed using the IBM SPSS Statistics (ver. 24) and Matlab (Mathworks). After checking data distribution using the Kolmogorov and Smirnov test, Stanford Sleepiness Scale scores were modeled using a repeated measure ANOVA, with factor time (4 levels) and stimulation (2 levels) (Figure 1). For activity and connectivity analysis, after checking that the baseline (pre-tDCS) measures were not different between stimulations, the post-tDCS measures were expressed as percentage of the pre-tDCS according to the following formula (post-tDCS−pre-tDCS)/pre-tDCS $*$ 100. Post-tDCS variations of activity and connectivity were directly compared between the real and sham stimulations by means of t-statistics. This procedure was applied for each vertex of the cortical surface,

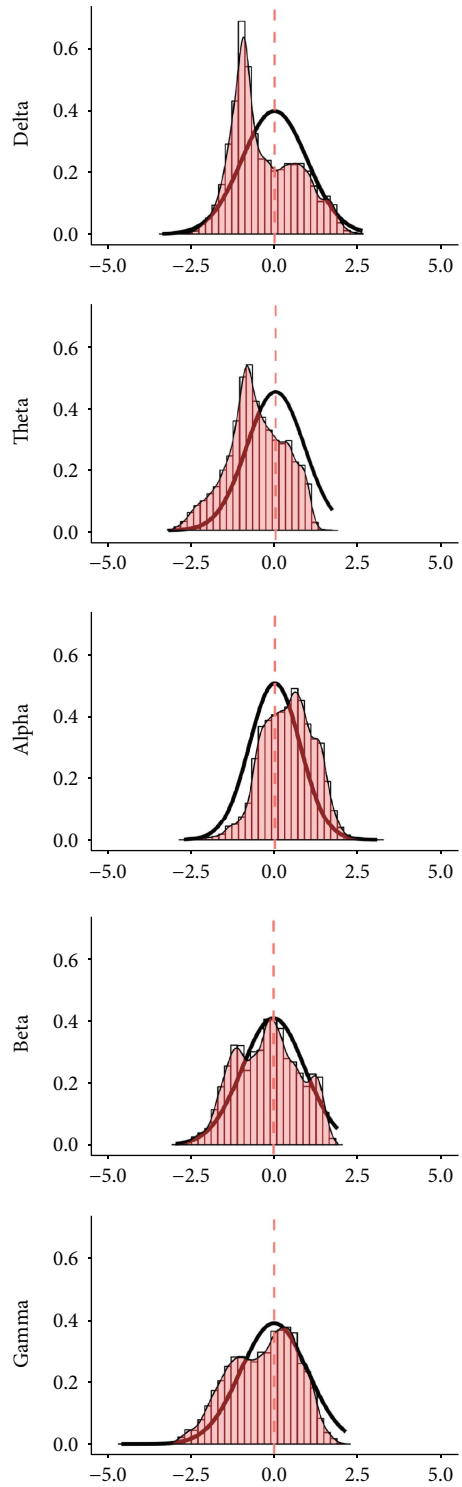

Figure 2: Resting-state activity (PSD) cortical t-value distribution. Histograms with red bars and the superimposed density plot with the thin line were calculated from the observed t-value distribution for the frequency bands under investigation. The tick black line shows a theoretical null-hypothesis distribution, with zero mean and zero median and the same variability of the empirical distribution. x-axes: t-value; y-axes: frequency of cortical vertices exhibiting a specific t-value expressed as proportion on the entire sample (intensity).

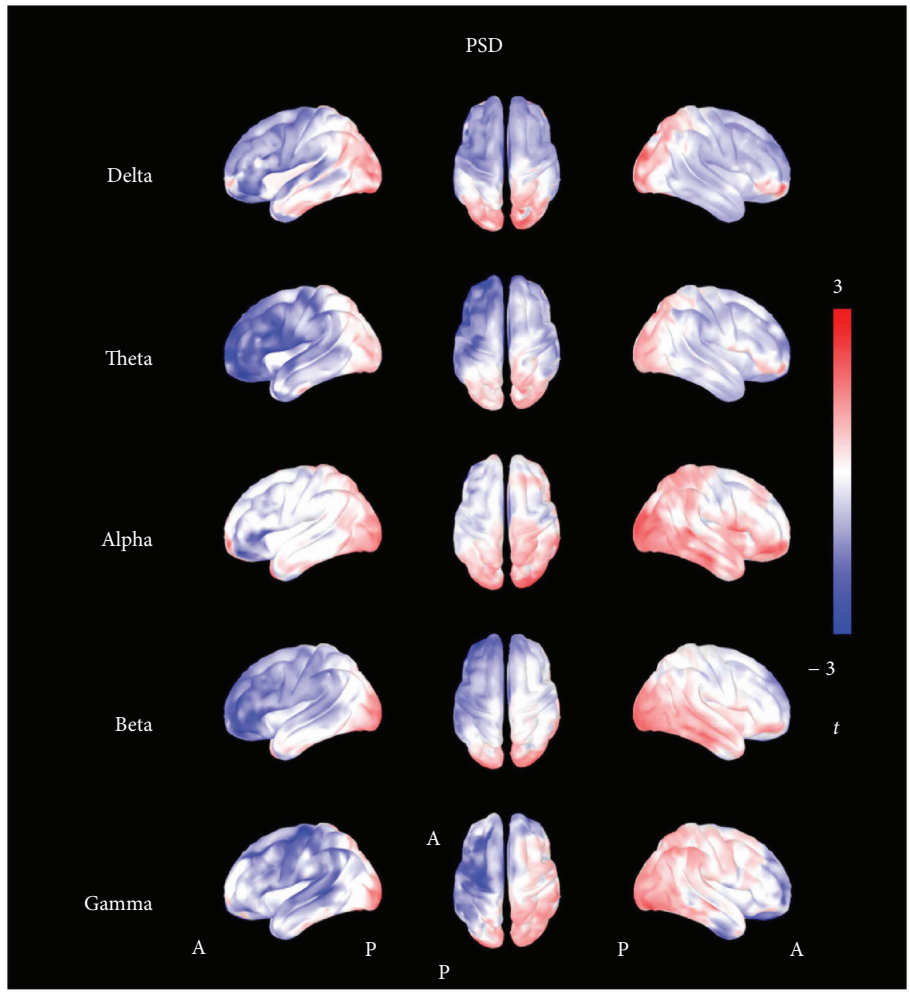

Figure 3: *t*-maps of resting-state activity (PSD). The figure shows the topographic distribution of *t*-values calculated for the power spectrum density (PSD). Shades of red colors indicate positive values, shades of blue colors indicate negative values, and shades of white indicate values toward zero. The *t*-maps show a global reduction of PSD in all frequency bands, mostly localized in the left frontal regions.

and it allowed to generate *t*-maps of real minus sham differences. In order to test whether tDCS was inducing a global increase or decrease of activity/connectivity, we applied a Wilcoxon test comparing the actual *t*-value distribution with a theoretical distribution with 0 mean and same variability as the one empirically found. In other words, we tested whether the distribution was significantly different from the one expected under the null hypothesis of no global tDCS effect. Then, we visually explored the spatial distribution of the effects. As further exploratory analysis of the topographic effects, we extracted average measures of PSD and PLV from regions of interest (ROIs) derived from a parcellation of the cortical surface implemented in Brainstorm [37] and we compared the real versus sham stimulations by means of *t*-tests. These results are reported in the Supplementary Materials (available here).

3. Results

All participants completed the experimental sessions, and none of them reported any problem or discomfort during the tDCS procedure or during the MEG recordings. Moreover, none of the participants reported to have clearly identified the real or sham session.

As for the sleepiness evaluation, the repeated measure ANOVA showed no significant factor stimulation nor time by stimulation interaction ($p > 0.200$ consistently). We did find a significant factor time [$F\ (3,42) = 6.596$, $p = 0.001$]. This effect was related to a sleepiness increase between the beginning and the end of the MEG resting-state scan. The size of the effect was small (about 1 point) and the average values at all time-points were always below 2.5, suggesting that subjects were awake during the entire study.

3.1. Resting-State Brain Activity (PSD). The results of the analysis on brain activity (i.e., PSD) are also reported in Figures 2 and 3. The analysis showed that all *t*-maps had a distribution significantly different from the theoretical null distribution [delta $U = 36.111^{*}10^{6}$; theta $U = 19.312 * 10^{6}$; alpha $U = 86.411 * 10^{6}$; beta $U = 44.582 * 10^{6}$; gamma $U = 38.501 * 10^{6}$, $p < 0.001$ consistently]. The empirical *t*-value distributions were mostly shifted to negative values for the delta, theta, beta, and gamma frequency bands, and only

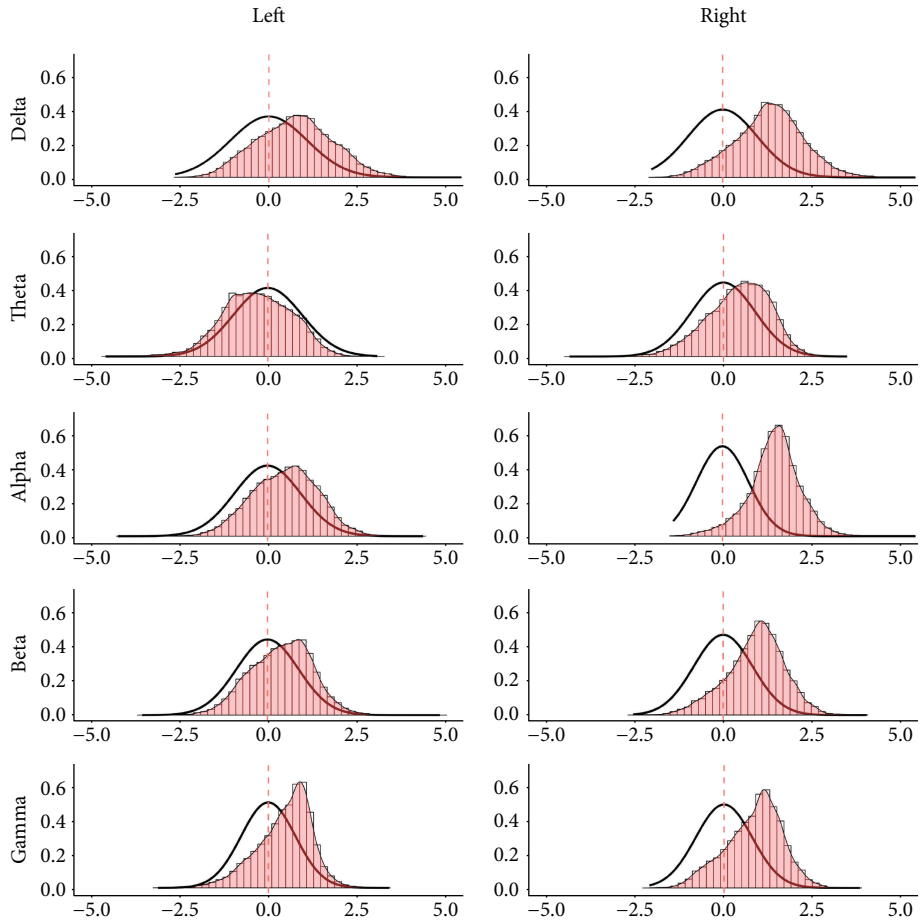

Figure 4: Resting-state connectivity (PLV) cortical t-value distribution. The figure shows the distribution of the t-values for the phase locking value maps calculated at the source level. The histogram with red bars and density plot with the thin line were calculated from the observed t-value distribution. The tick black line shows the theoretical null-hypothesis distribution, with zero mean and the same variability of the empirical distribution. Results are presented in an array divided in rows and columns (bands by seeds). x-axes: t-value; y-axes: frequency of cortical vertices exhibiting a specific t-value expressed as proportion on the entire sample (intensity).

slightly positively shifted for the alpha band (Figure 2). The effect was stronger for delta, theta and alpha band and, even if it was statistically significant, less evident for beta and gamma bands, whose curves of empiric distribution were very close to those theoretically generated.

The evaluation of the topographic distribution indicated a stronger effect, consistent across multiple frequency bands, in the left frontal regions, homolateral to the anode (+) (Figure 3). The ROI-based analysis confirmed such finding. The reader is referred to the supplementary materials for the ROI-based analysis of the spatial distribution of the effects.

3.2. Resting-State Brain Connectivity (PLV). The results of the analysis on brain connectivity (i.e., PLV) are also reported in Figures 4 and 5. The analysis showed that all t-maps had a distribution significantly different from the theoretical null distribution for both the left seed (under the anode) and right seed (under the cathode) [delta: left $U = 93.770^{*}10^{5}$, right $U = 109.13 * 10^{6}$; theta: left $U = 38.04 * 10^{6}$, right $U = 85.342 * 10^{6}$; alpha: left $U = 87.201 * 10^{6}$, right $U = 111.94 * 10^{6}$; beta: left $U = 83.063 * 10^{6}$, right $U = 10.489 * 10^{6}$; gamma: left $U = 90.813 * 10^{6}$, right $U = 10.414 * 10^{6}$, $p < 0.001$ consistently]. Figure 4 shows that the observed t-value distributions were shifted toward a positive effect, which indicates overall higher connectivity values after real stimulation as compared to sham. In particular, the distribution was positively shifted for both seeds in delta, alpha, beta, and gamma bands and in the theta frequency band for the right seed (see also the supplementary materials for results on ROIs). Only in the case of theta and left seed occurs a negative shift as compared to the theoretical null distribution. The evaluation of the topography of t-value distributions indicated widespread effects, involving regions remote from the anode and cathode (Figure 5).

4. Discussion

In this study, we have combined noninvasive brain stimulation and high-resolution magnetoencephalography (MEG) and provided evidence that bilateral tDCS reshapes resting-state brain networks.

During the last 20 years, noninvasive brain stimulation techniques have been exploited for the investigation and

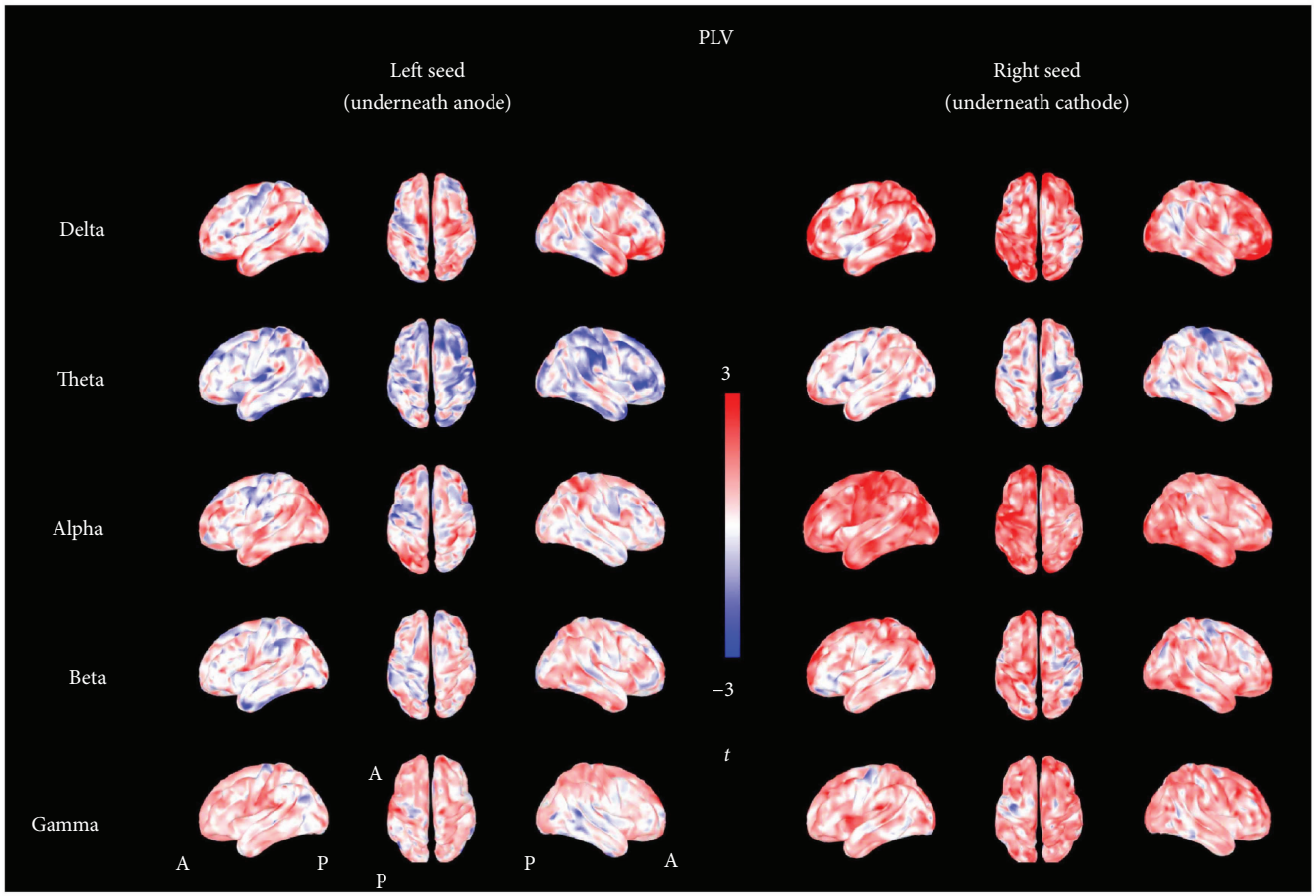

Figure 5: *t*-maps of resting-state connectivity (PLV). The figure shows the topographic distribution of *t*-values calculated for the phase locking value. Shades of red colors indicate positive values, shades of blue colors indicate negative values, and shades of white indicate values toward zero. An inspection of these maps shows a widespread increment of PLV values in all frequency bands.

treatment of a number of neurological disorders because of their ability of inducing LTP- and LTD-like plasticity phenomena.

Plasticity induction has been usually measured as changes of brain excitability [10, 38]. However, previous studies have demonstrated that both noninvasive brain stimulation and cortical plasticity are also associated with changes of brain rhythms and synchronization [39–41]. Conversely, robust and consistent evidence suggests that also neurological conditions translate into changes of brain activity and synchronization [41]. For instance, an impairment of cortical synchronization is often found at the first stages of neuropsychiatric conditions, up to the healthy subjects who own an increased risk [42–44]. More importantly, clinical recovery seems to be associated with changes of cortical rhythms and synchronization [45–47].

Our study was performed with a translational perspective and aimed at investigating the effects of bilateral tDCS on the healthy brain to better tailor treatment of neurological patients.

Both measures of brain activity and connectivity showed a significant tDCS-related modulation after real tDCS as compared to sham. Brain activity, as assessed by Power spectral density, is an indirect measure of cortical synchronization/desynchronization. Previous investigations of the tDCS effects on PSD have been largely performed with EEG and have provided conflicting results, in terms of the frequency bands and brain regions affected by the stimulation [48–55]. Our MEG study provides higher accuracy in the detection and modeling of cortical activity and supported a consistent and reduction of alpha, beta, and gamma power of the left frontal regions, ipsilateral to the anode and contralateral to the cathode. Changes in power can be related to an enhancement of the brain activation [56, 57] and are often found in neurological disorders, such as stroke [58] and epilepsy [41]. For these and other neurological disorders, tDCS application, rather being tailored on the base of the effect produced on brain excitability alone [8, 9], might benefit from taking into consideration the effects on brain activity and connectivity.

PSD results also confirm two additional relevant aspects in a translational perspective: (a) tDCS effects on cortical activity (PSD) depend upon the position of the anode and cathode [48] and (b) stronger effects are not necessarily confined under the region of stimulation but can involve remote regions. Our results on tDCS remote effects are in agreement with previous evidence from other approaches. Remote effects of brain stimulation have been indeed demonstrated

for several measures of brain function, such as brain activity [15], cortical excitability [59, 60], hemodynamic activity and connectivity as measured by BOLD signal [61], and behavioral measures [62].

The connectivity analysis was performed on the entire cortex, taking into account the two seeds located in the sensorimotor regions, under the cathode and anode. For both seeds and for all the frequency bands under investigations, we found a significant increase of the synchronization of tDCS-related cortical activity. Such effect was widespread and particularly evident in delta, alpha, beta, and gamma bands. PLV results displayed in Figure 5 (and also the ROI-based analysis reported in the supplementary material) suggest a more widespread, homogeneous, short- and long-range increase of connectivity, especially when considering the seed under the anode (+, increasing cortical excitability), and support the idea that the effects of the stimulation depend upon the interaction with networks rather than brain areas [19].

Very recently, and in agreement with our results, other groups have reported a global increase of EEG synchronization after tDCS [63] and diffuse changes of connectivity in post-tDCS fMRI [64]. Vecchio and collaborators have suggested that tDCS effects on cortical coherence are polarity dependent, mainly involve alpha band, and are characterized by a connectivity increase [65]. Beyond the differences of experimental design, similar findings are supported by the investigation of Mancini and colleagues [66].

The findings of this study arise from a very specific setting, characterized by bilateral stimulation performed on healthy subjects. In a translational perspective, it will be necessary to investigate how tDCS-related activity and connectivity changes are influenced by several individual factors, such as genetic pattern [67, 68], gender [69], spontaneous fluctuations of cortical activity and excitability [70] and, especially in patients, the effect of brain lesions [11], cortical degeneration [71], and the influence of medications [72]. It will also be crucial to address the time dynamics of the effects on brain networks, in order to tune appropriately the duration, frequency, and dose of tDCS.

5. Conclusions

tDCS is a noninvasive brain stimulation approach which is becoming very popular and currently exploited to treat neurological disorders. We have demonstrated that bilateral tDCS (left anode and right cathode) reduces left alpha, beta, and gamma power and increases global connectivity in delta, alpha, beta, and gamma frequencies, in a diffuse fashion. We have also demonstrated that, beyond the well-known effects on brain excitability, tDCS reshapes resting-state brain networks. This information can be of help to understand the plasticity phenomena induced by noninvasive brain stimulation and can be exploited to tailor the therapeutic intervention in patients affected by neurological conditions.

Conflicts of Interest

The authors declare that there is no conflict of interest regarding the publication of this paper.

Acknowledgments

The authors acknowledge the contribution of the participants and the kind support of the researchers of the MEG unit Fondazione IRCCS S. Camillo Hospital in Venice. This study has been supported by a Ministry of Health Operating Grant to the San Camillo IRCCS Venice. Giovanni Di Pino is supported by the European Research Council (ERC) Starting Grant 2015 RESHAPE: REstoring the Self with embodiable Hand ProsthesEs (ERC-2015-STG, Project no. 678908).

Supplementary Materials

The supplementary materials contain additional analyses conducted at ROI level, to test the regional effect of tDCS on PSD and on PLV measures. Eleven bilateral ROIs covering the whole cortex surface were selected from the automatic parcellation of Destrieux Atlas [1], as implemented in the Brainstorm Toolbox [2]. For each ROI a paired t-test was performed, comparing the effect of real tDCS with the effect of sham tDCS. The effect was calculated as percentage increase in the poststimulation as compared to the pre [(post − pre/pre) ∗ 100]. Importantly, the information provided in these tables is different from the information of the global analysis included in the manuscript. While the analysis in the manuscript tests whether there is a global effect of tDCS on the measures, these tables show if there are specific effects in the average value of the measure calculated for each specific ROI. Each table reports (1) the name of the ROI, the "L" or "R" at the end of the name which indicate if the ROI was in the left or right hemisphere; (2) the degrees of freedom of the test; (3) the t-value; (4) the effect size, calculated as Cohen's d; (5) the p value; (6) the significance of the p value with asterisks " ∗ " denoting values below 0.05; (7) the direction of the significant difference, with ">" indicating "Real > Sham" and "<" indicating "Real < Sham"; (8) the mean values of the effect in the real condition (SD enclosed in parenthesis); (9) the mean values for the effect in the sham condition (SD enclosed in parenthesis). (*Supplementary Materials*)

References

[1] U. Ziemann, W. Paulus, M. A. Nitsche et al., "Consensus: motor cortex plasticity protocols," *Brain Stimulation*, vol. 1, no. 3, pp. 164–182, 2008.

[2] V. Di Lazzaro, F. Ranieri, P. Profice et al., "Transcranial direct current stimulation effects on the excitability of corticospinal axons of the human cerebral cortex," *Brain Stimulation*, vol. 6, no. 4, pp. 641–643, 2013.

[3] F. Ranieri, M. V. Podda, E. Riccardi et al., "Modulation of LTP at rat hippocampal CA3-CA1 synapses by direct current stimulation," *Journal of Neurophysiology*, vol. 107, no. 7, pp. 1868–1880, 2012.

[4] M. A. Nitsche, L. G. Cohen, E. M. Wassermann et al., "Transcranial direct current stimulation: state of the art 2008," *Brain Stimulation*, vol. 1, no. 3, pp. 206–223, 2008.

[5] C. Poreisz, K. Boros, A. Antal, and W. Paulus, "Safety aspects of transcranial direct current stimulation concerning healthy

subjects and patients," *Brain Research Bulletin*, vol. 72, no. 4–6, pp. 208–214, 2007.

[6] C. C. Ruff, G. Ugazio, and E. Fehr, "Changing social norm compliance with noninvasive brain stimulation," *Science*, vol. 342, no. 6157, pp. 482–484, 2013.

[7] A. R. Brunoni, M. A. Nitsche, N. Bolognini et al., "Clinical research with transcranial direct current stimulation (tDCS): challenges and future directions," *Brain Stimulation*, vol. 5, no. 3, pp. 175–195, 2012.

[8] G. Assenza, C. Campana, F. Assenza et al., "Cathodal transcranial direct current stimulation reduces seizure frequency in adults with drug-resistant temporal lobe epilepsy: a sham controlled study," *Brain Stimulation*, vol. 10, no. 2, pp. 333–335, 2017.

[9] V. Di Lazzaro, M. Dileone, F. Capone et al., "Immediate and late modulation of interhemipheric imbalance with bilateral transcranial direct current stimulation in acute stroke," *Brain Stimulation*, vol. 7, no. 6, pp. 841–848, 2014.

[10] G. Di Pino, G. Pellegrino, G. Assenza et al., "Modulation of brain plasticity in stroke: a novel model for neurorehabilitation," *Nature Reviews Neurology*, vol. 10, no. 10, pp. 597–608, 2014.

[11] G. Di Pino, G. Pellegrino, F. Capone, and V. Di Lazzaro, "Human cerebral cortex metaplasticity and stroke recovery," *Austin Journal of Cerebrovascular Disease & Stroke*, vol. 1, no. 2, 2014.

[12] M. A. Nitsche and W. Paulus, "Excitability changes induced in the human motor cortex by weak transcranial direct current stimulation," *The Journal of Physiology*, vol. 527, no. 3, pp. 633–639, 2000.

[13] N. Lang, M. A. Nitsche, M. Dileone et al., "Transcranial direct current stimulation effects on I-wave activity in humans," *Journal of Neurophysiology*, vol. 105, no. 6, pp. 2802–2810, 2011.

[14] C. J. Stagg, V. Bachtiar, and H. Johansen-Berg, "The role of GABA in human motor learning," *Current Biology*, vol. 21, no. 6, pp. 480–484, 2011.

[15] F. Notturno, L. Marzetti, V. Pizzella, A. Uncini, and F. Zappasodi, "Local and remote effects of transcranial direct current stimulation on the electrical activity of the motor cortical network," *Human Brain Mapping*, vol. 35, no. 5, pp. 2220–2232, 2014.

[16] N. Lang, H. R. Siebner, N. S. Ward et al., "How does transcranial DC stimulation of the primary motor cortex alter regional neuronal activity in the human brain?," *European Journal of Neuroscience*, vol. 22, no. 2, pp. 495–504, 2005.

[17] C. J. Stagg and M. A. Nitsche, "Physiological basis of transcranial direct current stimulation," *The Neuroscientist*, vol. 17, no. 1, pp. 37–53, 2011.

[18] C. S. Herrmann, S. Rach, T. Neuling, and D. Strüber, "Transcranial alternating current stimulation: a review of the underlying mechanisms and modulation of cognitive processes," *Frontiers in Human Neuroscience*, vol. 7, 2013.

[19] M. D. Fox, R. L. Buckner, H. Liu, M. M. Chakravarty, A. M. Lozano, and A. Pascual-Leone, "Resting-state networks link invasive and noninvasive brain stimulation across diverse psychiatric and neurological diseases," *Proceedings of the National Academy of Sciences of the United States of America*, vol. 111, no. 41, pp. E4367–E4375, 2014.

[20] N. von Ellenrieder, G. Pellegrino, T. Hedrich et al., "Detection and magnetic source imaging of fast oscillations (40–160 Hz) recorded with magnetoencephalography in focal epilepsy patients," *Brain Topography*, vol. 29, no. 2, pp. 218–231, 2016.

[21] G. Pellegrino, A. Machado, N. von Ellenrieder et al., "Hemodynamic response to interictal epileptiform discharges addressed by personalized EEG-fNIRS recordings," *Frontiers in Neuroscience*, vol. 10, 2016.

[22] G. Pellegrino, T. Hedrich, R. Chowdhury et al., "Source localization of the seizure onset zone from ictal EEG/MEG data," *Human Brain Mapping*, vol. 37, no. 7, pp. 2528–2546, 2016.

[23] T. Hedrich, G. Pellegrino, E. Kobayashi, J. M. Lina, and C. Grova, "Comparison of the spatial resolution of source imaging techniques in high-density EEG and MEG," *NeuroImage*, vol. 157, pp. 531–544, 2017.

[24] R. A. Chowdhury, G. Pellegrino, Ü. Aydin et al., "Reproducibility of EEG-MEG fusion source analysis of interictal spikes: Relevance in presurgical evaluation of epilepsy," *Human Brain Mapping*, 2017.

[25] R. C. Oldfield, "The assessment and analysis of handedness: the Edinburgh inventory," *Neuropsychologia*, vol. 9, no. 1, pp. 97–113, 1971.

[26] E. Hoddes, V. Zarcone, H. Smythe, R. Phillips, and W. C. Dement, "Quantification of sleepiness: a new approach," *Psychophysiology*, vol. 10, no. 4, pp. 431–436, 1973.

[27] F. Tadel, S. Baillet, J. C. Mosher, D. Pantazis, and R. M. Leahy, "Brainstorm: a user-friendly application for MEG/EEG analysis," *Computational Intelligence and Neuroscience*, vol. 2011, Article ID 879716, 13 pages, 2011.

[28] S. Taulu and J. Simola, "Spatiotemporal signal space separation method for rejecting nearby interference in MEG measurements," *Physics in Medicine and Biology*, vol. 51, no. 7, pp. 1759–1768, 2006.

[29] C. Tesche, M. A. Uusitalo, R. J. Ilmoniemi, M. Huotilainen, M. Kajola, and O. Salonen, "Signal-space projections of MEG data characterize both distributed and well-localized neuronal sources," *Electroencephalography and Clinical Neurophysiology*, vol. 95, no. 3, pp. 189–200, 1995.

[30] A. M. Dale, B. Fischl, and M. I. Sereno, "Cortical surface-based analysis: I. segmentation and surface reconstruction," *NeuroImage*, vol. 9, no. 2, pp. 179–194, 1999.

[31] A. Gramfort, T. Papadopoulo, E. Olivi, and M. Clerc, "OpenMEEG: opensource software for quasistatic bioelectromagnetics," *Biomedical Engineering Online*, vol. 9, no. 1, p. 45, 2010.

[32] J.-P. Lachaux, E. Rodriguez, J. Martinerie, and F. J. Varela, "Measuring phase synchrony in brain signals," *Human Brain Mapping*, vol. 8, no. 4, pp. 194–208, 1999.

[33] S. Aydore, D. Pantazis, and R. M. Leahy, "A note on the phase locking value and its properties," *NeuroImage*, vol. 74, pp. 231–244, 2013.

[34] E. Raffin, G. Pellegrino, V. di Lazzaro, A. Thielscher, and H. R. Siebner, "Bringing transcranial mapping into shape: sulcus-aligned mapping captures motor somatotopy in human primary motor hand area," *NeuroImage*, vol. 120, pp. 164–175, 2015.

[35] J. Mazziotta, A. Toga, A. Evans et al., "A four-dimensional probabilistic atlas of the human brain," *Journal of the American Medical Informatics Association*, vol. 8, no. 5, pp. 401–430, 2001.

[36] K. J. Worsley, J. E. Taylor, F. Carbonell et al., "SurfStat: a Matlab toolbox for the statistical analysis of univariate and

multivariate surface and volumetric data using linear mixed effects models and random field theory," *NeuroImage*, vol. 47, article S102, 2009.

[37] C. Destrieux, B. Fischl, A. Dale, and E. Halgren, "Automatic parcellation of human cortical gyri and sulci using standard anatomical nomenclature," *NeuroImage*, vol. 53, no. 1, pp. 1–15, 2010.

[38] M. Tombini, G. Pellegrino, P. Pasqualetti et al., "Mobile phone emissions modulate brain excitability in patients with focal epilepsy," *Brain Stimulation*, vol. 6, no. 3, pp. 448–454, 2013.

[39] G. Assenza, G. Pellegrino, M. Tombini, G. di Pino, and V. di Lazzaro, "Wakefulness delta waves increase after cortical plasticity induction," *Clinical Neurophysiology*, vol. 126, no. 6, pp. 1221–1227, 2015.

[40] F. Vecchio, M. Tombini, P. Buffo et al., "Mobile phone emission increases inter-hemispheric functional coupling of electroencephalographic alpha rhythms in epileptic patients," *International Journal of Psychophysiology*, vol. 84, no. 2, pp. 164–171, 2012.

[41] G. Pellegrino, M. Tombini, G. Curcio et al., "Slow activity in focal epilepsy during sleep and wakefulness," *Clinical EEG and Neuroscience*, vol. 48, no. 3, pp. 200–208, 2017.

[42] M. Maran, T. Grent, and P. J. Uhlhaas, "Electrophysiological insights into connectivity anomalies in schizophrenia: a systematic review," *Neuropsychiatric Electrophysiology*, vol. 2, no. 1, p. 6, 2016.

[43] P. J. Uhlhaas and W. Singer, "Neuronal dynamics and neuropsychiatric disorders: toward a translational paradigm for dysfunctional large-scale networks," *Neuron*, vol. 75, no. 6, pp. 963–980, 2012.

[44] K. M. Larsen, G. Pellegrino, M. R. Birknow et al., "22q11. 2 deletion syndrome is associated with impaired auditory steady-state gamma response," *Schizophrenia Bulletin*, article sbx058, 2017.

[45] G. Pellegrino, L. Tomasevic, M. Tombini et al., "Inter-hemispheric coupling changes associate with motor improvements after robotic stroke rehabilitation," *Restorative Neurology and Neuroscience*, vol. 30, no. 6, pp. 497–510, 2012.

[46] G. Di Pino, C. Porcaro, M. Tombini et al., "A neurally-interfaced hand prosthesis tuned inter-hemispheric communication," *Restorative Neurology and Neuroscience*, vol. 30, no. 5, pp. 407–418, 2012.

[47] M. Tombini, G. Pellegrino, F. Zappasodi et al., "Complex visual hallucinations after occipital extrastriate ischemic stroke," *Cortex*, vol. 48, no. 6, pp. 774–777, 2012.

[48] N. Accornero, M. Capozza, L. Pieroni, S. Pro, L. Davi, and O. Mecarelli, "EEG mean frequency changes in healthy subjects during prefrontal transcranial direct current stimulation," *Journal of Neurophysiology*, vol. 112, no. 6, pp. 1367–1375, 2014.

[49] T. W. Boonstra, S. Nikolin, A. C. Meisener, D. M. Martin, and C. K. Loo, "Change in mean frequency of resting-state electroencephalography after transcranial direct current stimulation," *Frontiers in Human Neuroscience*, vol. 10, p. 270, 2016.

[50] J. Choe, B. A. Coffman, D. T. Bergstedt, M. D. Ziegler, and M. E. Phillips, "Transcranial direct current stimulation modulates neuronal activity and learning in pilot training," *Frontiers in Human Neuroscience*, vol. 10, p. 34, 2016.

[51] K. E. Hoy, N. W. Bailey, S. L. Arnold, and P. B. Fitzgerald, "The effect of transcranial direct current stimulation on gamma activity and working memory in schizophrenia," *Psychiatry Research*, vol. 228, no. 2, pp. 191–196, 2015.

[52] A. L. Mangia, M. Pirini, and A. Cappello, "Transcranial direct current stimulation and power spectral parameters: a tDCS/EEG co-registration study," *Frontiers in Human Neuroscience*, vol. 8, p. 601, 2014.

[53] J. Miller, B. Berger, and P. Sauseng, "Anodal transcranial direct current stimulation (tDCS) increases frontal-midline theta activity in the human EEG: a preliminary investigation of non-invasive stimulation," *Neuroscience Letters*, vol. 588, pp. 114–119, 2015.

[54] G. F. Spitoni, R. L. Cimmino, C. Bozzacchi, L. Pizzamiglio, and F. di Russo, "Modulation of spontaneous alpha brain rhythms using low-intensity transcranial direct-current stimulation," *Frontiers in Human Neuroscience*, vol. 7, p. 529, 2013.

[55] A. Thibaut, C. Russo, L. Morales-Quezada et al., "Neural signature of tDCS, tPCS and their combination: comparing the effects on neural plasticity," *Neuroscience Letters*, vol. 637, pp. 207–214, 2017.

[56] G. Pfurtscheller and F. L. Da Silva, "Event-related EEG/MEG synchronization and desynchronization: basic principles," *Clinical Neurophysiology*, vol. 110, no. 11, pp. 1842–1857, 1999.

[57] F. L. da Silva, "EEG and MEG: relevance to neuroscience," *Neuron*, vol. 80, no. 5, pp. 1112–1128, 2013.

[58] G. Assenza, F. Zappasodi, P. Pasqualetti, F. Vernieri, and F. Tecchio, "A contralesional EEG power increase mediated by interhemispheric disconnection provides negative prognosis in acute stroke," *Restorative Neurology and Neuroscience*, vol. 31, no. 2, pp. 177–188, 2013.

[59] N. Lang, M. A. Nitsche, W. Paulus, J. C. Rothwell, and R. N. Lemon, "Effects of transcranial direct current stimulation over the human motor cortex on corticospinal and transcallosal excitability," *Experimental Brain Research*, vol. 156, no. 4, pp. 439–443, 2004.

[60] K. Boros, C. Poreisz, A. Münchau, W. Paulus, and M. A. Nitsche, "Premotor transcranial direct current stimulation (tDCS) affects primary motor excitability in humans," *European Journal of Neuroscience*, vol. 27, no. 5, pp. 1292–1300, 2008.

[61] R. Polanía, W. Paulus, and M. A. Nitsche, "Modulating cortico-striatal and thalamo-cortical functional connectivity with transcranial direct current stimulation," *Human Brain Mapping*, vol. 33, no. 10, pp. 2499–2508, 2012.

[62] B. W. Vines, D. G. Nair, and G. Schlaug, "Contralateral and ipsilateral motor effects after transcranial direct current stimulation," *Neuroreport*, vol. 17, no. 6, pp. 671–674, 2006.

[63] T. Kunze, A. Hunold, J. Haueisen, V. Jirsa, and A. Spiegler, "Transcranial direct current stimulation changes resting state functional connectivity: a large-scale brain network modeling study," *NeuroImage*, vol. 140, pp. 174–187, 2016.

[64] R. Lindenberg, M. M. Sieg, M. Meinzer, L. Nachtigall, and A. Flöel, "Neural correlates of unihemispheric and bihemispheric motor cortex stimulation in healthy young adults," *NeuroImage*, vol. 140, pp. 141–149, 2016.

[65] F. Vecchio, M. C. Pellicciari, F. Miraglia, D. Brignani, C. Miniussi, and P. M. Rossini, "Effects of transcranial direct current stimulation on the functional coupling of the sensorimotor cortical network," *NeuroImage*, vol. 140, pp. 50–56, 2016.

[66] M. Mancini, D. Brignani, S. Conforto, P. Mauri, C. Miniussi, and M. C. Pellicciari, "Assessing cortical synchronization

during transcranial direct current stimulation: a graph-theoretical analysis," *NeuroImage*, vol. 140, pp. 57–65, 2016.

[67] V. Di Lazzaro, G. Pellegrino, G. di Pino et al., "Val66Met BDNF gene polymorphism influences human motor cortex plasticity in acute stroke," *Brain Stimulation*, vol. 8, no. 1, pp. 92–96, 2015.

[68] G. Di Pino, G. Pellegrino, F. Capone et al., "Val66Met BDNF polymorphism implies a different way to recover from stroke rather than a worse overall recoverability," *Neurorehabilitation and Neural Repair*, vol. 30, no. 1, pp. 3–8, 2016.

[69] V. Di Lazzaro, G. Pellegrino, G. di Pino et al., "Human motor cortex functional changes in acute stroke: gender effects," *Frontiers in Neuroscience*, vol. 10, 2016.

[70] F. Giambattistelli, L. Tomasevic, G. Pellegrino et al., "The spontaneous fluctuation of the excitability of a single node modulates the internodes connectivity: a TMS-EEG study," *Human Brain Mapping*, vol. 35, no. 4, pp. 1740–1749, 2014.

[71] R. Dubbioso, G. Pellegrino, A. Antenora et al., "The effect of cerebellar degeneration on human sensori-motor plasticity," *Brain Stimulation*, vol. 8, no. 6, pp. 1144–1150, 2015.

[72] D. Landi, S. Vollaro, G. Pellegrino et al., "Oral fingolimod reduces glutamate-mediated intracortical excitability in relapsing–remitting multiple sclerosis," *Clinical Neurophysiology*, vol. 126, no. 1, pp. 165–169, 2015.

Hindawi
Neural Plasticity
Volume 2017, Article ID 2758097, 12 pages
https://doi.org/10.1155/2017/2758097

Review Article

Low-Frequency Repetitive Transcranial Magnetic Stimulation for Stroke-Induced Upper Limb Motor Deficit: A Meta-Analysis

Lan Zhang,[1,2] Guoqiang Xing,[1,3] Shiquan Shuai,[1] Zhiwei Guo,[1] Huaping Chen,[1] Morgan A. McClure,[1] Xiaojuan Chen,[4] and Qiwen Mu[1,5]

[1]*Department of Imaging & Imaging Institute of Rehabilitation and Development of Brain Function, The Second Clinical Medical College of North Sichuan Medical College, Nanchong Central Hospital, Nanchong 637000, China*
[2]*Department of Radiology, Langzhong People's Hospital, Nanchong 637000, China*
[3]*Lotus Biotech.com LLC., John Hopkins University-MCC, Rockville, MD 20850, USA*
[4]*North Sichuan Medical College, Nanchong 637000, China*
[5]*Peking University Third Hospital, Beijing 100080, China*

Correspondence should be addressed to Qiwen Mu; muqiwen99@yahoo.com

Received 19 July 2017; Accepted 1 October 2017; Published 21 December 2017

Academic Editor: Andrea Turolla

Background and Purpose. This meta-analysis aimed to evaluate the therapeutic potential of low-frequency repetitive transcranial magnetic stimulation (LF-rTMS) over the contralesional hemisphere on upper limb motor recovery and cortex plasticity after stroke. *Methods*. Databases of PubMed, Medline, ScienceDirect, Cochrane, and Embase were searched for randomized controlled trials published before Jun 31, 2017. The effect size was evaluated by using the standardized mean difference (SMD) and a 95% confidence interval (CI). Resting motor threshold (rMT) and motor-evoked potential (MEP) were also examined. *Results*. Twenty-two studies of 1 Hz LF-rTMS over the contralesional hemisphere were included. Significant efficacy was found on finger flexibility (SMD = 0.75), hand strength (SMD = 0.49), and activity dexterity (SMD = 0.32), but not on body function (SMD = 0.29). The positive changes of rMT (SMD = 0.38 for the affected hemisphere and SMD = −0.83 for the unaffected hemisphere) and MEP (SMD = −1.00 for the affected hemisphere and SMD = 0.57 for the unaffected hemisphere) were also significant. *Conclusions*. LF-rTMS as an add-on therapy significantly improved upper limb functional recovery especially the hand after stroke, probably through rebalanced cortical excitability of both hemispheres. Future studies should determine if LF-rTMS alone or in conjunction with practice/training would be more effective. *Clinical Trial Registration Information*. This trial is registered with unique identifier CRD42016042181.

1. Introduction

Stroke is a global disease with high rates of long-term disability [1]. Around the world, 25%–74% of stroke survivors require different levels of assistance for daily living mainly due to upper limb hemiplegia [2]. In search for better therapies, scientists have been trying to understand the relationship between stroke motor recovery and cortical reorganization [3]. The equilibrium of cortical excitability between the two hemispheres is often disrupted after stroke. In the affected hemisphere, both the cortical excitability and the homonymous motor representation of the affected hemisphere decrease; whereas the excitability in the unaffected hemisphere increases [4].

Repetitive transcranial magnetic stimulation (rTMS) is a noninvasive stimulation to induce electrical currents in the brain tissues. Currently, rTMS is being explored as a novel therapy in modulating cortical excitability to improve motor functions in stroke patients [5]. Of the two forms of rTMS, high-frequency rTMS (HF-rTMS > 1.0 Hz), applied over the ipsilesional hemisphere, facilitates cortical excitability [6], whereas, low-frequency rTMS (LF-rTMS ≤ 1.0 Hz), applied over the contralesional hemisphere, decreases cortical excitability [7].

The effect of rTMS is primarily determined by the stimulation frequency [8] and targeted region [3]. Although both LF-rTMS and HF-rTMS could treat motor dysfunction in poststroke patients, LF-rTMS is considered safer and superior to HF-rTMS in motor function recovery [9–12]. Lomarev et al. [13] reported increased risk for seizures by HF-rTMS of 20–25 Hz. To date, the majority of rTMS trials on motor recovery after stroke used the protocol of LF-rTMS with 1 Hz. In comparison, the HF-rTMS studies involved only a small number of trials and applied varied frequency protocols (3 Hz to 25 Hz). According to Cho et al. [14], the primary motor cortex (M1) forms a main part of the motor cortices and contributes to the high order control of motor behaviors. Until now, most studies about the efficacy of LF-rTMS on functional rehabilitation have focused on the M1. In healthy subjects, LF-rTMS applied over the M1 increased the resting motor threshold (rMT) and decreased the motor-evoked potential (MEP) size of the ipsilateral hemisphere, suggesting a suppressive effect of LF-rTMS in the intact M1 [15].

Multiple studies have investigated the therapeutic effect of LF-rTMS after stroke [8, 16–19], with the outcomes of pinch force [19–22], grip force [10, 22–25], finger tapping [8, 9, 26–29], and overall function [15, 30–34]. Other studies also explored the impact of rTMS on cortical excitability [10, 18, 19, 26]. However, inconsistent reports exist regarding the benefits of LF-rTMS: Some studies showed no beneficial effect of LF-rTMS [16, 23, 29] and one study reported worsening effects of LF-rTMS such as decreased finger-tapping speed; [35] other investigators proposed that inhibition of the contralesional motor areas may lead to deterioration of the function of the unaffected hand [24, 26]. Although a few previous meta-analyses had investigated the therapeutic effect of rTMS after stroke [11, 36–38], they focused on the mixed effect of combined LF-rTMS and HF-rTMS interventions or on the combined outcomes of varying motor measurements. So far, there is a lack of in-depth systematic meta-analysis about the efficacy of LF-rTMS on upper limb function recovery.

The primary objective of this study was to evaluate the effects of LF-rTMS on upper limb motor recovery after stroke in several aspects: "finger flexibility," "hand strength," "activity dexterity," and "body function level." The effects of LF-rTMS on motor cortex excitability which were represented by MEP and rMTin poststroke patients were also evaluated.

2. Methods

2.1. Protocol. Our meta-analysis followed the PRISMA statement.

2.2. Search Strategy. The databases of PubMed, ScienceDirect, Embase, and the Cochrane Library were searched for randomized controlled trials published before June 31, 2017. The search terms were "stroke/cerebrovascular accident, repetitive transcranial magnetic stimulation/rTMS, and upper limb/hand." The search was limited to human studies. Manual searches of the reference lists of the pertinent articles were also conducted to identify relevant articles [11, 36].

2.3. Study Selection. The preliminary screening was based on the title and abstract. As there were several separate aims of the paper, the articles with either any motor function assessment or MEP/rMT outcomes were all considered. Two reviewers independently assessed the eligibility of the literature. If there was a disagreement, the two reviewers checked the full text of the article and discussed with each other to reach an agreement. The selected articles were then assessed in their entirety. Studies were included if they met the following criteria: (1) they were randomized controlled trials; (2) they have ≥five patients in a trial; (3) the patients were adults (≥18 yrs); (4) the focus was on the effects on the upper limb in poststroke patients; (5) the types of intervention were LF-rTMS over the contralesional M1; (6) the outcomes were on continuous scales that evaluated the motor function of upper limb or cortical excitability; and (7) they were published in peer-reviewed English journals.

2.4. Quality Appraisal. Each included study was individually assessed by two reviewers according to a modified checklist of Moher et al. [39] that provided the following criteria: (1) blinding procedure (0 indicated a nonblind or no-mention procedure, 1 or 2 represented single blind or double blind, resp.); (2) dropout number; (3) description of baseline demographic data (was recorded as 1 if described, if not as 0); (4) point estimate and variability (was denoted as 1 if provided); and (5) description of adverse events (was recorded as the number and type of adverse event).

2.5. Data Extraction. A standard form was jointly designed by two reviewers for collecting the relevant data from each study for the following information: (1) patient characteristics; (2) trial design; (3) rTMS protocol; (4) outcome measures; (5) the duration of follow-up; and (6) mean difference and standard deviation (SD) of the scores immediately (short term) and chronically (long term) after the interventions (assessment within one day after the last rTMS session was considered as short-term outcome; assessment at one month or longer after the last rTMS session was considered long-term outcome [40]). Statistical analysis used the data of between different interventions. If the changes in scores of both groups were not clearly defined, the mean and SD of the scores after intervention for both groups were extracted on the premise of no statistical differences in baseline between the two groups. If the outcome was expressed only as a graph, the software GetData Graph Digitizer 2.25 (http://getdata-graph-digitizer.com/) was used to extract the required data.

2.6. Data Synthesis and Analysis. To elaborate the therapeutic effect of LF-rTMS on upper extremity recovery after stroke, the motor measures were categorized into four subclasses according to a previous study [41] of upper limb outcome measures in stroke rehabilitation: "finger flexibility," "hand strength," "activity dexterity," and "body function level." The results of the finger tapping were pooled to evaluate finger flexibility. The results of pinch force and grip force were pooled to evaluate hand strength. The results of action research arm test (ARAT), Wolf motor function test (WMFT), Jebsen-Taylor test (JTT), and nine-hole peg test

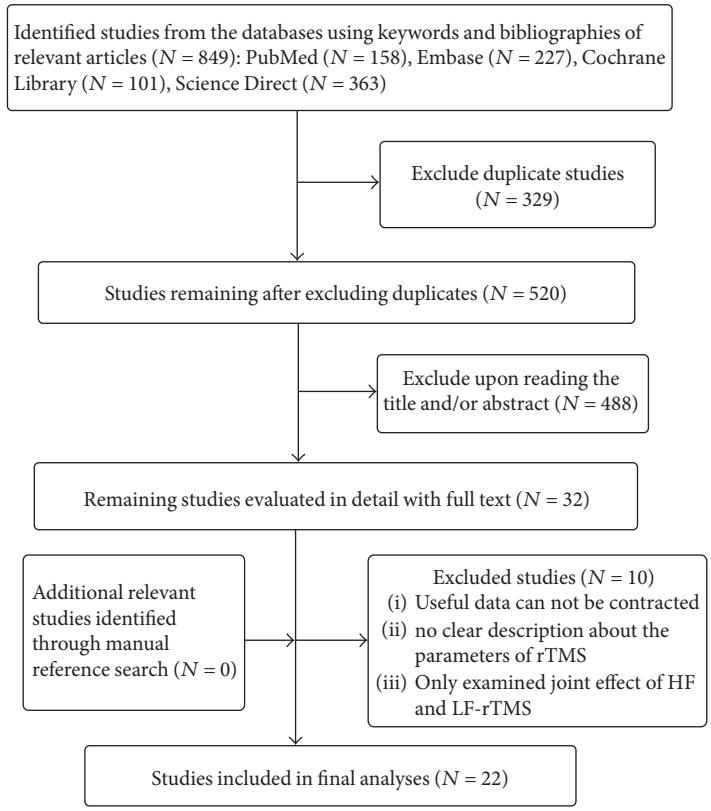

Figure 1: Selection process flow diagram.

(NHPT) were pooled to evaluate activity dexterity. The results of upper extremity Fugl-Meyer Assessment (FMA) were pooled to evaluate body function. For evaluating cortical excitability, the results of the rMT and MEP in both hemispheres were extracted [42, 43].

The meta-analysis was performed by using the Review Manager Software version 5.2 (Cochrane Collaboration, Oxford, England) with the formulation Hedges' g [44]. Data were described as mean ± SD. For the outcomes using different scales, we refer to the Cochrane Hand Book (Cochrane Collaboration, Oxford, England). The effect size of LF-rTMS was expressed by the standardized mean difference (SMD) with a 95% confidence interval (CI). The heterogeneity was tested by using the I^2 test [45]. If a significant heterogeneity was found ($I^2 \geq 50\%$), the random effect model was applied; otherwise, a fixed model was used. In addition, the trim and fill method [46] was constructed by using STATA/SE version 11.0 (STATA Corporation, Texas, USA) to test publication bias. The value of statistical significance was set at $P < 0.05$. Finally, effect sizes were classified as small (<0.2), medium (0.2–0.8), or large (>0.8) [47]. Sensitivity analysis was conducted to investigate the impact of lesion site, timing of stimulation from stroke onset, and other characteristics on the results.

3. Results

3.1. Study Identification. Of the total 849 studies found after the initial database search, 22 studies were identified ($N = 619$) finally. The flow diagram of the selection process is shown in Figure 1.

All of the included studies applied 1 Hz rTMS over the contralesional M1. Except one study [15] that included patients with severe motor deficits and one study [21] that included patients with mild to severe deficit, all the others recruited patients with mild to moderate motor deficits. Most studies excluded the patients with other neuropsychiatric comorbidities such as aphasia, spatial neglect, or visual field deficit. Five studies [20, 24–27] used LF-rTMS as monotherapy and gained significant effect size; the others used LF-rTMS as cotherapy of active training, that is, in most of the studies, patients were also undergoing other treatments and training in both the rTMS and control groups. The details of the included studies and the results of quality assessment are shown in Tables 1 and 2 separately.

3.2. Motor Function Measurement

3.2.1. Finger Flexibility. Six studies ($N = 176$) [8–10, 27–29] assessed the short-term finger flexibility. LF-rTMS had a high medium mean effect size of 0.75 (95% CI = 0.44–1.06; $P < 0.001$) without heterogeneity ($I^2 = 0\%$) (fixed-effect model) (Figure 2(a)). The SMD for long term was 0.53 (95% CI, 0.12–0.94; $P = 0.01$) without heterogeneity ($I^2 = 0\%$).

3.2.2. Hand Strength. Eleven studies ($N = 227$) [9, 10, 17–25] evaluated short-term hand strength that showed a medium effect size of LF-rTMS therapy (SMD = 0.49; 95% CI = 0.22–0.76; $P < 0.001$; and $I^2 = 12\%$) in the fixed-effect model

Table 1: Characteristics of the selected studies.

Study	*N* (Exp/Ctr)	Mean age	Time poststroke	Lesion site	Trial design	rTMS protocol	Outcome measurement		Follow-up	Combined training/practice
							Motor function	Neurophysiology		
Takeuchi et al. [19]	10/10	59 Y	6–60 m	Subcortical	P	1.0 Hz, 90% rMT, 1500 pulses × 1 days	Pinch force	rMT, MEP		Motor training
Fregni et al. [26]	10/5	56 Y	6–120 m	(13/15) Subcortical	P	1.0 Hz, 100% rMT, 1500 pulses × 5 days	PPT, JTT	rMT		
Liepert et al. [24]	12/12	63 Y	<2 wks	Subcortical	C	1.0 Hz, 90% rMT, 1200 pulses × 1 days	NHPT, grip force			
Takeuchi et al. [18]	10/10	62.3 Y	7–121 m	Subcortical	P	1.0 Hz, 90% rMT, 1500 pulses × 1 days	Pinch force	rMT, MEP		Motor training
Dafotakis et al. [20]	12/12	45.5 Y	1–4 m	Subcortical	C	1.0 Hz, 100% rMT, 600 pulses × 1 days	Pinch force			
Nowak et al. [27]	15/15	46 Y	1–4 m	Subcortical	C	1.0 Hz, 100% rMT, 600 pulses × 1 days	Finger tapping,			
Khedr et al. [10]	12/12	57.9 Y	1-2 wks	Nonspecified	P	1.0 Hz, 100% rMT, 900 pulses × 5 days	Finger tapping, grip force	MEP	3 m	Passive movement
Emara et al. [8]	20/20	54 Y	2–13.5 m	Nonspecified	P	1.0 Hz, 110%–120% rMT, 1500 pulses × 10 days	Finger tapping		3 m	Physical therapy
Theilig et al. [15]	12/12	61 Y	2 wks–58 m	Nonspecified	P	1.0 Hz, 100% rMT, 900 pulses × 10 days	WMFT	MEP		Extensor activity
Takeuchi et al. [17]	9/9	61.5 Y	62–71.9 m	Subcortical	P	1.0 Hz, 90% rMT, 1200 pulses × 1 days	Pinch force	MEP		Motor training
Conforto et al. [21]	15/15	55.8 Y	5–45 days	Nonspecified	P	1.0 Hz, 90% rMT, 1500 pulses × 10 days	Pinch force, JTT		1 m	Rehabilitation treatment
Seniow et al. [30]	20/20	63.4 Y	12–129 days	Nonspecified	P	1.0 Hz, 90% rMT, 1800 pulses × 15 days	FMA		3 m	Motor training
Sasaki et al. [9]	11/9	65 Y	6–29 days	Nonspecified	P	1.0 Hz, 90% rMT, 1800 pulses × 5 days	Finger tapping, grip force			Motor training
Higgins et al. [22]	6/5	66.2 Y	18–315 m	Not reported	P	1.0 Hz, 110% rMT, 1.200 pulses × 8 days	Pinch force		1 m	Task-oriented training
Sung et al. [28]	15/12	63.2 Y	3–12 m	Nonspecified	P	1.0 Hz, 90% rMT, 600 pulses × 10 days	Finger tapping, WMFT	rMT, MEP		Occupational therapy
Wang et al. [32]	17/15	62.6 Y	2–6 m	Nonspecified	P	1.0 Hz, 90% rMT, 600 pulses × 10 days	WMFT	rMT, MEP		Task-oriented training
Rose et al. [23]	11/10	64.6 Y	7–150 m	Not reported	P	1.0 Hz, 100% rMT, 1200 pulses × 16 days	Grip force, FMA	rMT, MEP	1 m	Functional task practice
Galvão et al. [31]	10/10	61 Y	>6 m	Not reported	P	1.0 Hz, 90% rMT, 1500 pulses × 10 days	FMA		1 m	Physical therapy

Table 1: Continued.

Study	*N* (Exp/Ctr)	Mean age	Time poststroke	Lesion site	Trial design	rTMS protocol	Outcome measurement		Follow-up	Combined training/practice
							Motor function	Neurophysiology		
Ludemann-Podubecka et al. [29]	20/20	67 Y	0.25–4 m	Nonspecified	P	1.0 Hz, 100% rMT, 900 pulses × 15 days	Finger tapping, WMFT	MEP	6 m	Task-oriented training
Zheng et al. [33]	55/53	66 Y	<1 m	Nonspecified	P	1.0 Hz, 90% rMT, 1800 pulses × 24 days	FMA, WMFT			Occupational therapy
Matsuura et al. [25]	10/10	73. Y	<1 m	Subcortical	P	1.0 Hz, 100% rMT, 1200 pulses × 5 days	Grip force, FMA			
Du et al. [34]	23/23		3 days–1 m	Nonspecified	P	1.0 Hz, 110–120% rMT, 1200 pulses × 20 days	FMA		6 m	Motor exercises

Ctr: control group; Exp: experimental group; P: parallel sham control; C: crossover sham control; FMA: Fugl-Meyer assessment; ARAT: action research arm test; JTT: Jebsen-Taylor test; m: month; MEP: motor-evoked potential; NHPT: nine-hole peg test; PPT: purdue pegboard test; rMT: resting motor threshold; wk: week; Y: years; WMFT: Wolf motor function test.

Table 2: Quality appraisal of the selected articles.

Study	Blind process	Description of baseline data	Dropout	Point estimate and variability	Overall quality appraisal score
Takeuchi et al. [19]	2	1	0	0	3
Fregni et al. [26]	2	1	0	1	4
Liepert et al. [24]	2	0	0	1	3
Takeuchi et al. [18]	2	1	0	0	3
Dafotakis et al. [20]	0	1	0	1	2
Nowak et al. [27]	0	1	0	1	2
Khedr et al. [10]	2	1	0	1	4
Emara et al. [8]	2	1	0	1	4
Theilig et al. [15]	2	1	0	0	3
Takeuchi et al. [17]	1	1	0	1	3
Conforto et al. [21]	2	1	1	0	2
Seniow et al. [30]	2	1	7	0	2
Sasaki et al. [9]	0	1	0	0	1
Higgins et al. [22]	1	1	2	0	1
Sung et al. [28]	2	1	0	1	4
Wang et al. [32]	2	1	0	1	4
Rose et al. [23]	2	1	3	0	2
Galvão et al. [31]	2	1	0	0	3
Ludemann-Podubecka et al. [29]	2	1	0	0	3
Zheng et al. [33]	2	1	4	0	2
Matsuura et al. [25]	2	1	0	1	4
Du et al. [34]	2	1	0	1	4

In the case of any dropout, the total score will be subtracted by 1.

(Figure 2(b)). No significant treatment effect was found for long-term effect: SMD = 0.38; 95% CI = −0.36 to 1.13; $P = 0.31$; and $I^2 = 58\%$.

3.2.3. Upper Limb Activity Dexterity. The pooled outcomes of ten trials ($N = 299$) [15, 21, 23, 24, 26, 28, 29, 32, 33] were used to evaluate the short-term upper limb activity dexterity. The result of the fixed-effect model showed a medium effect size of 0.32 (95% CI = 0.09–0.55; $P = 0.006$) without heterogeneity ($I^2 = 0\%$) (Figure 2(c)). No significant long-term treatment effect was found: SMD = 0.14; 95% CI = −0.22 to 0.49; $P = 0.45$; and $I^2 = 0\%$.

3.2.4. Body Function Level. The pooled results from seven studies ($N = 313$) [23, 25, 28, 30–34] for short-term effect of LF-rTMS on body function level showed a nonsignificant mean effect size of 0.29 (95% CI = −0.06–0.64; $P = 0.10$) (random effect model) due to the presence of heterogeneity ($I^2 = 52\%$) (Figure 2(d)). No significant long-term effect of LF-rTMS was found on body function [23, 30, 31]: SMD = 0.10; 95% CI = −0.70 to 0.90; $P = 0.80$; and $I^2 = 77\%$.

3.2.5. Comparison of the Motor Effect Sizes. The short-term effectiveness of LF-rTMS appears to follow this descending order: finger ability is greater than hand strength which is greater than the activity dexterity and greater than body function. A similar long-term therapeutic effect of LF-rTMS was observed (Figure 3).

3.3. Neurophysiologic Measurement

3.3.1. MEPs in Both Hemispheres. Four studies ($N = 122$) [10, 28, 32, 34] were pooled to explore the effects of LF-rTMS on MEPs in the affected hemisphere; and eight studies ($N = 200$) [10, 15, 17–19, 23, 29, 34] were pooled for MEPs in the unaffected hemisphere, by using the fixed effect model with the amplitude of the MEPs. The results showed a significant enhancing effect of MEP in the affected hemisphere (SMD = 0.38, 95% CI = 0.02–0.74; $P = 0.04$) without heterogeneity ($I^2 = 0\%$) (Figure 4(a)) and a highly significant suppressing effect of MEP in the unaffected hemisphere (SMD = −0.83, 95% CI = −1.13 to −0.54; $P < 0.0001$), without significant heterogeneity ($I^2 = 18\%$) (Figure 4(b)).

3.3.2. rMTs in Both Hemispheres. Four studies ($N = 121$) [26, 28, 32, 34] assessed the effect of LF-rTMS on rMT of the affected hemisphere by using the fixed-effect model that showed a large suppressing effect size (SMD = −1.00, 95% CI = −1.90 to −0.11; $P = 0.03$; $I^2 = 79\%$) (Figure 4(c)). LF-rTMS, however, induced an enhancing effect on rMT at a trend level in the unaffected hemisphere (SMD = 0.57; 95% CI = 0.04–1.10; $P = 0.03$; and $I^2 = 56\%$) (Figure 4(d)).

3.4. Publication Bias. Funnel plots conducted with the trim and fill method for the included studies were illustrated in Figure 2. The trim and fill analyses showed that only the

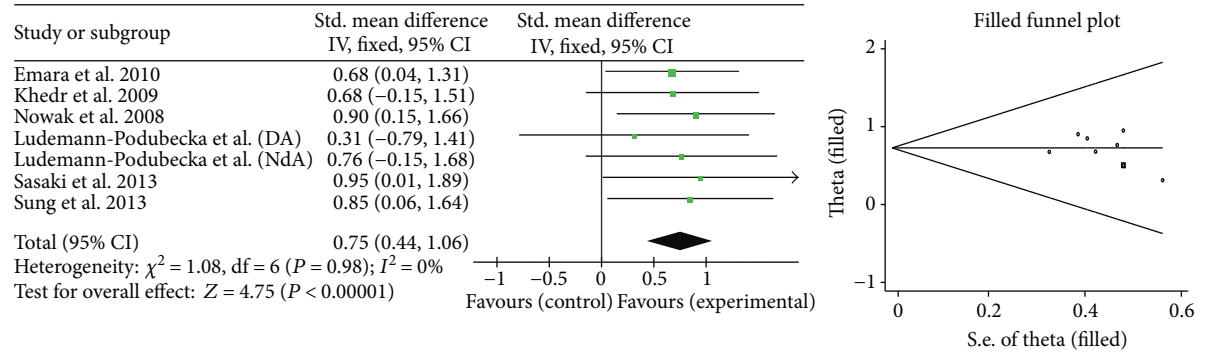

(a) Finger flexibility

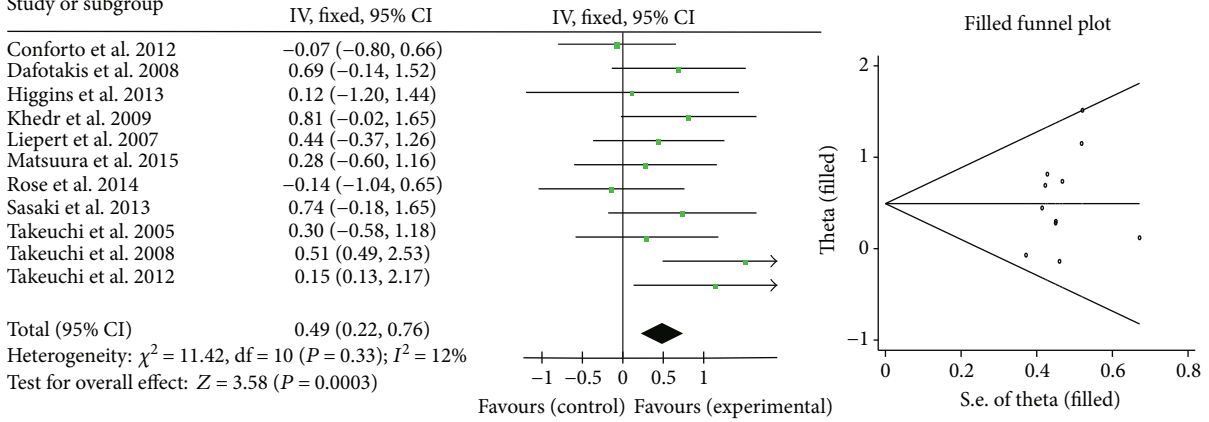

(b) Hard strength

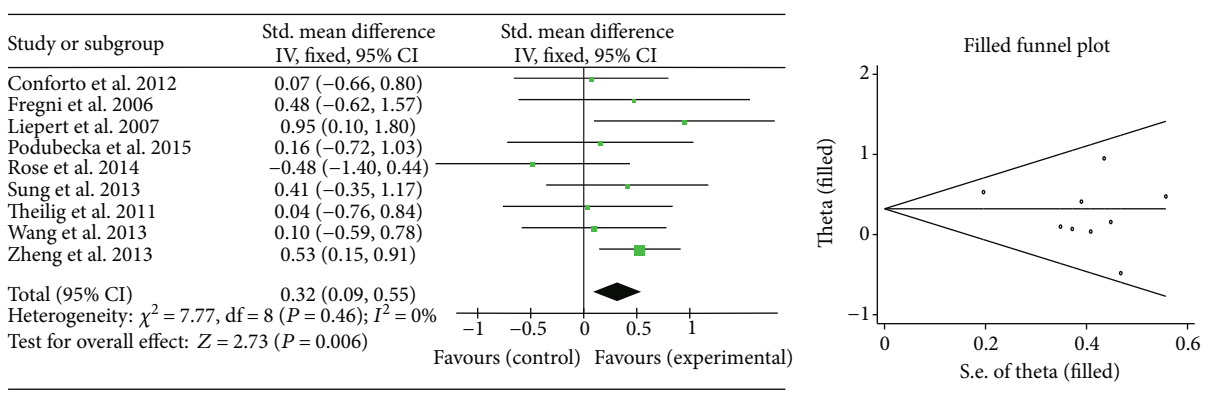

(c) Activity dexterity

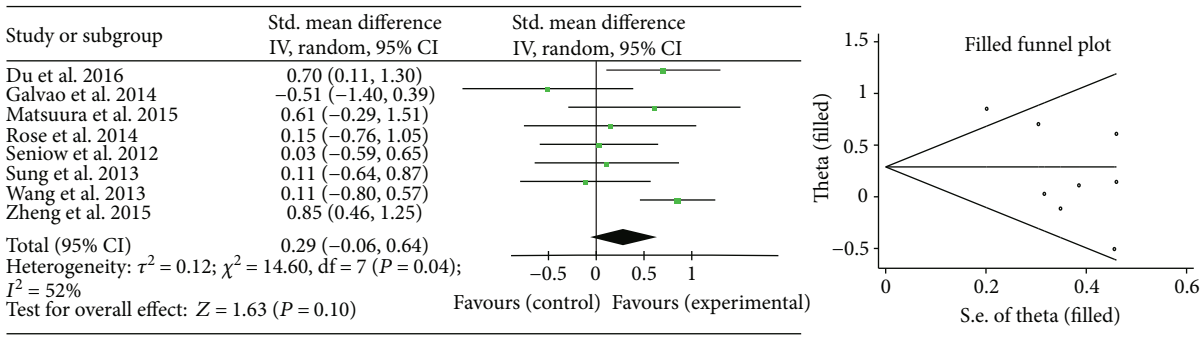

(d) Body function level

Figure 2: Forest plots of the short-term effect and the funnel plot analyses using the trim and fill method.

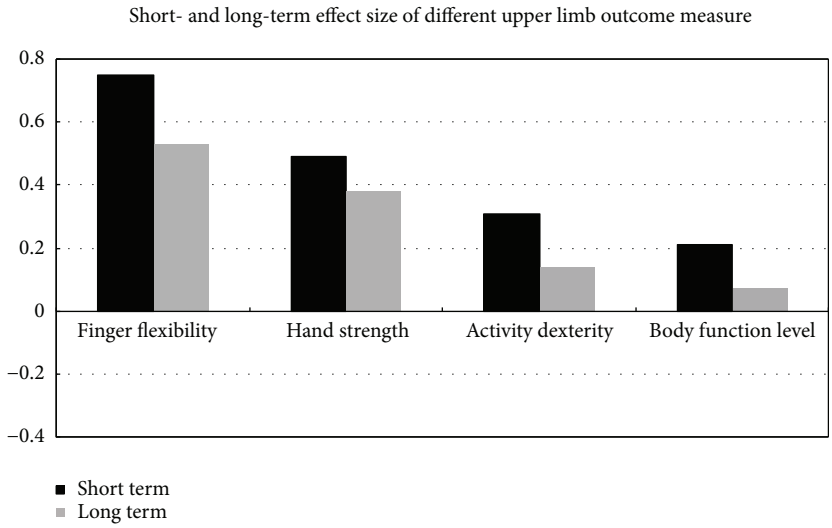

Figure 3: The bars show the pooled effect sizes of various upper extremity measure outcomes.

"finger flexibility" subclass had one study trimmed and the effect size was only slightly affected (adjusted effect size = 0.73, 0.43–1.02); no deletion or trimming occurred to other three subclasses and the effect sizes were unchanged.

3.5. Sensitivity Analyses. The lesion site and poststroke duration were matched between the four subgroups in two sensitivity analyses. One of the sensitivity analyses excluded eight trials that only involved subcortical stroke [17–20, 24–27] (based on the above four categories of motor function, SMD were 0.72, 0.28, 0.26, and 0.15) and the other excluded nine trials [10, 17–19, 22–24, 26, 31] that only involved acute/chronic stroke (<two weeks/>six months) [11] (SMD were 0.76, 0.36, 0.32, and 0.33), whereas the third sensitivity analysis only included rTMS plus motor training cotherapy after excluding five trials [20, 24–27] that did not specify potential cotherapy. The results were SMD = 0.72, 0.50, 0.26, and 0.15 (online-only data Supplement Figures I, II, and III).

4. Discussion

The present analysis provides the evidence that LF-rTMS applied over the contralesional M1 was effective for upper limb motor recovery, probably through modulating cortical excitability in poststroke patients. Although most of the trial participants were also undergoing other trainings, the trainings were carried out in both groups (rTMS group and control group) which could partially offset the impact of training on results. However, it is still not clear if the efficacy of LF-rTMS was due to its own function or its synergistic effect with other trainings. And more researches are needed in this direction.

These upper limb motor recoveries follow the previously reported four different effects of LF-rTMS on finger dexterity, hand strength, activity dexterity, and body function level [41]. Based on this classification, the short-term effectiveness of LF-rTMS appears to follow this descending order: finger ability is greater than hand strength and is greater than activity dexterity. The improvement in body function did not reach a significant level. A similar long-term therapeutic effect of LF-rTMS was observed, that is, rTMS not only produced short-term acute clinical effects but also maintained such motor improvement at the distal of the affected upper limb than at the proximal end (Figure 3).

Long-term efficacy is more important than short-term efficacy, because long-lasting beneficial effect of rTMS on upper limb motor function is a more reliable indicator for a successful clinic intervention. It is noted that although the descending trends of the various motor classifications were consistent between short term and long term—the effect size was larger at short term than at long term. Based on the follow-up data and because of the difference between the short-term and long-term effect size of LF-rTMS, it was inferred that LF-rTMS can not only produce better functional improvements but also accelerate this process in stroke patients. In other words, at short term, LF-rTMS stimulates the speed and degree of the motor recovery; whereas, at long term, LF-rTMS further maintains and improves the degree of recovery. Further research is required to test this hypothesis.

Different motor scales measured the domains differently. A better understanding of the different outcome measures and accurate interpretation of the results can help guide more efficient rehabilitation of the patient under different clinical conditions. For example, finger tapping and grip force could inform more about fine finger manipulation tasks and grasping abilities, respectively, whereas the FMA represents mixed measures, with most items (87%) related to the body structure domain [41]. Discrepancy exists in the literature. One early study showed no significant effect of LF-rTMS on upper limb coordination in motor outcomes [30]. Another study found no significant effect of LF-rTMS on the whole arm movements except for grip force [23]. Other studies, however, reported marked motor improvements of the finger and hand after LF-rTMS therapy [10, 17–20].

Although the mechanism is unknown, the results of this analysis may provide some explanations. It is known that the adaptive reorganization of stroke-induced motor deficit

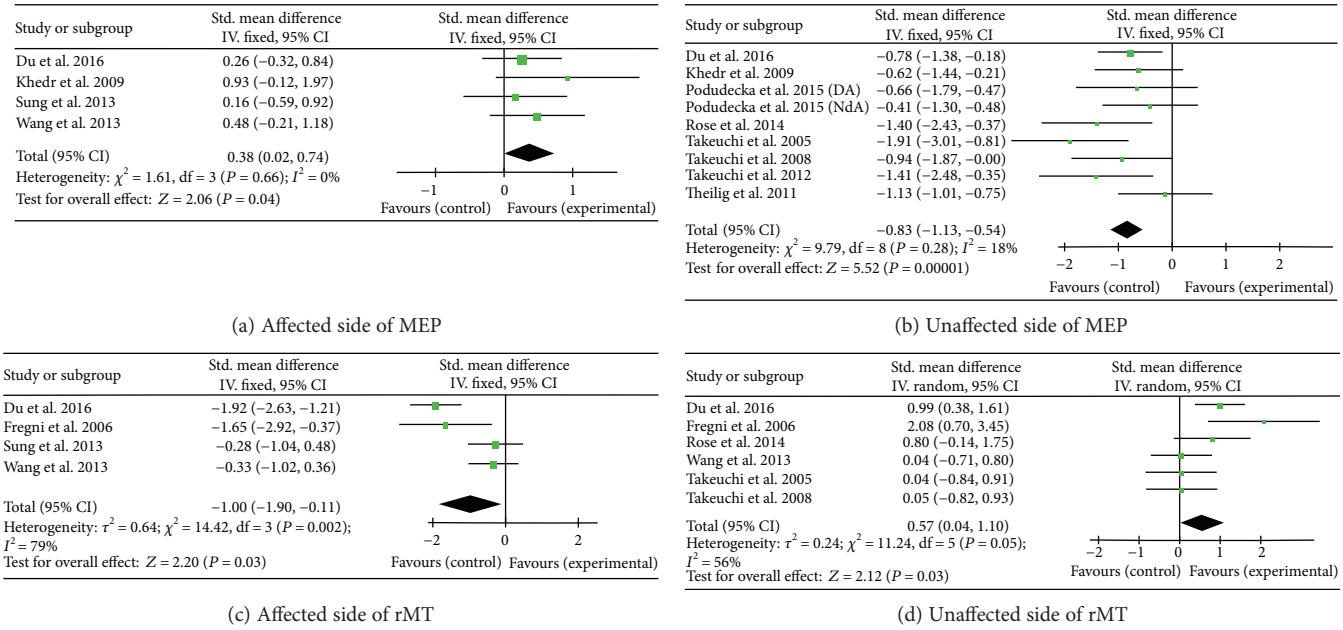

(a) Affected side of MEP

(b) Unaffected side of MEP

(c) Affected side of rMT

(d) Unaffected side of rMT

Figure 4: Forest plots of the mean effect sizes for MEP and rMT between the affected hand and unaffected hand. MEP: motor-evoked potential; rMT: resting motor threshold.

follows the patterns of from-the-proximal-to-distal limb and the distal limb especially the upper limb which is the most difficult to rehabilitate after stroke according to the neurodevelopment treatment [48]. The results of this meta-analysis indicate that LF-rTMS may be more effective in targeting the distal limb. One explanation for the discrepancy is that the LF-rTMS of our included trials was directed at the M1 which contributes to the high order control of motor behaviors [3]. It is known that the hand movement representation of the cortex coordinates upper limb movements through forearm muscle-controlled wrist, elbow, and shoulder [10]. Another possibility is that the speed and dexterity of finger movement are controlled primarily by corticospinal projections that are often damaged after stroke [10], but they are more readily targeted and influenced by rTMS application on the corticospinal projections. In contrast, combined activities that depend on both corticospinal and brain stem spinal pathways are less influenced by rTMS [10].

To avoid the possibility that some significant outcomes might be due to a high initial motor control, only the data of intergroup differences were analyzed. In our analysis, except one study [15] that recruited patients with severe motor deficits, all other studies recruited patients with mild-to-moderate motor deficits who did not show substantial functional disparity in both hand and arm motor outcomes. As such, our current findings may only apply to those patients of mild-to-moderate stroke. Besides, the sensitivity analysis of the trials which involved only the active training plus LF-rTMS versus those LF-rTMS without training produced similar results as the original combined results. Therefore, rTMS could indeed make further improvement on the hand flexibility which is considered the most difficult part of upper limb motor rehabilitation and which has limited success using the traditional training rehabilitation techniques alone [48].

There is evidence that cortical reorganization occurs during motor recovery of stroke [49]. The shift of balance in cortical activation between the two hemispheres has been vigorously investigated in stroke patients [3]. Compared with most other therapies, the curative effect of rTMS on stroke is based upon the activity changes of the cortex. Decreasing the excitability of corticospinal neurons, as reflected in the cumulative increase of rMT and decrease of MEP in the unaffected hemisphere, has been found associated with motor recovery [50]. However, a previous meta-analysis [36] did not show significant motor cortex improvements though a trend of positive changes in the MEP and MT groups was found. This may be due to the fact that both the LF-rTMS and HF-rTMS studies were included in the meta-analysis which included only very limited number of studies. In this current study, the LF-rTMS induced a highly significant suppressing effect on MEP in the contralesional hemisphere and a significant enhancing effect on MEP in the ipsilesional hemisphere. However, because only three trials evaluated MEP of the ipsilesional hemisphere, more studies are required to reach a reliable conclusion. A similar regulatory effect of cortical excitation exists for the results of rMT, but enhanced rMT only at a trend level in the contralesional hemisphere. These pooled effects were in agreement with the previous reports of the positive effect of LF-rTMS in modulating cortical excitability after stroke [26, 28, 32].

It is known that rTMS could enhance the motor function recovery of paretic upper limbs [51]. Increasing factors are shown to influence the effects that should be investigated in order to optimize the therapeutic effect of rTMS. A number of studies have been done in this regard. It is recognized that valid comparable measurement across studies is required to

compare the effect of different interventions. So far, however, there is no consensus yet regarding the best outcome measures for evaluating hand function rehabilitation. FMA is one of the most common outcome measures used by 36% of the studies that reported hand motor rehabilitation. Santisteban et al. [41] suggested that homogenous outcome measures were critical for across study efficacy evaluation of different rehabilitation techniques and feasibility of meta-analyses that were missing in earlier assessments for upper limb motor function. This present study demonstrates that it is possible to evaluate the motor outcomes at four different levels that can specify different motor recoveries of the various parts of the upper limb following LF-rTMS.

A recent study showed that differences in patients' characters and stimulation parameters such as age, gender, lesion location, and timing from stroke onset as well as frequency of rTMS could influence the effects of rTMS on upper extremity motor recovery [51]. However, the exact stimulation parameter for different patients remains to be experimentally determined. For example, one recent study demonstrated age-dependent motor cortical plasticity in LF-rTMS-treated patients, but not in HF-rTMS-treated stroke patients [51]. Another study showed that HF-rTMS was more beneficial for motor improvement than LF-rTMS in the early phase [52], but not in the late phase of stroke [10]. Thus, the optimal protocols of rTMS for different types of upper limb rehabilitation still need to be elucidated by large cohort studies and big data analysis.

Recently, Meyer et al. [53] reported that somatosensory impairments are negatively associated with motor recovery in the upper limb. This suggests that the level of the remaining sensorimotor control may play a role in neurorehabilitation. To date, most of the published rTMS studies on motor recovery in stroke patients have not reported on sensorimotor coimpairments and most of the studies excluded patients with neuropsychiatric comorbidities such as aphasia, spatial neglect, or visual field deficit which are positively correlated with the severity of somatosensory deficits [53]. Accordingly, it may be inferred that the present results would hardly be affected by mild to moderate sensorimotor impairment, but for the more severe sensorimotor impairment, proof-of-principle studies would be necessary. In addition, consensus in outcome measurement, validation of rTMS frequency, treatment timing and duration, and lesion sites in different age groups of male and female patients could refine the current findings.

Some limitations exist in this study. First, several uncontrollable variables of the patients such as age, gender, side of onset, severity of motor deficit, and sensorimotor impairment may confound the results. Second, variations in the number of trial days (i.e., session numbers) and stimulus intensity of rTMS interventions may affect the results. Especially, the more number of rTMS trial days and increased number of pulses could be more effective [54]. Of the four functional outcome categories of this study, the "hand strength" measurement group received the least numbers of rTMS sessions and pulses. This was followed by the "finger flexibility" group. "Activity dexterity" and "body function level" groups shared similar more numbers of rTMS sessions and pulses. It is possible that the outcome differences among the four outcome groups could still exist if each group had received equal numbers of rTMS sessions and pulses. Moreover, studies published in non-English journals were not included in this analysis.

5. Conclusion

This meta-analysis indicates that LF-rTMS applied over the contralesional M1 has significant add-on therapeutic effect on upper limb motor dysfunction especially the functional recovery of the hand in patients with mild-moderate stroke. Future studies should verify whether cotherapy of LF-rTMS plus training will induce better hand motor rehabilitation than that of rTMS or training monotherapy.

Conflicts of Interest

The authors declare that they have no conflicts of interest.

Acknowledgments

This work was supported by the National Natural Science Foundation of China (no. 81271559) and the State Administration of Foreign Experts Affairs, China (no. SZD201516, no. SZD201606).

Supplementary Materials

Supplementary Figure I: sensitivity analysis examining whether the result was influenced by lesion site. Supplementary Figure II: sensitivity analysis examining whether the result was influenced by combining training. Supplementary Figure III: sensitivity analysis examining whether the result was influenced by time post stroke. *(Supplementary Materials)*

References

[1] R. Bonita, N. Solomon, and J. B. Broad, "Prevalence of stroke and stroke-related disability. Estimates from the Auckland stroke studies," *Stroke*, vol. 28, no. 10, pp. 1898–1902, 1997.

[2] J. M. Veerbeek, G. Kwakkel, E. E. Van Wegen, J. C. Ket, and M. W. Heymans, "Early prediction of outcome of activities of daily living after stroke: a systematic review," *Stroke*, vol. 42, no. 5, pp. 1482–1488, 2011.

[3] Q. Tang, G. Li, T. Liu et al., "Modulation of inter hemispheric activation balance in motor-related areas of stroke patients with motor recovery: systematic review and meta-analysis of fMRI studies," *Neuroscience & Biobehavioral Reviews*, vol. 57, pp. 392–400, 2015.

[4] N. S. Ward and L. G. Cohen, "Mechanisms underlying recovery of motor function after stroke," *Archives of Neurology*, vol. 61, no. 12, pp. 1844–1848, 2004.

[5] P. M. Rossini and S. Rossi, "Transcranial magnetic stimulation: diagnostic, therapeutic, and research potential," *Neurology*, vol. 68, no. 7, pp. 484–488, 2007.

[6] A. Pascual-Leone, A. Amedi, F. Fregni, and L. B. Merabet, "The plastic human brain cortex," *Annual Review of Neuroscience*, vol. 28, no. 1, pp. 377–401, 2005.

[7] F. Maeda, J. P. Keenan, J. M. Tormos, H. Topka, and A. Pascual-Leone, "Modulation of corticospinal excitability by repetitive transcranial magnetic stimulation," *Clinical Neurophysiology*, vol. 111, no. 5, pp. 800–805, 2000.

[8] T. Emara, R. Moustafa, N. Elnahas et al., "Repetitive transcranial magnetic stimulation at 1 Hz and 5 Hz produces sustained improvement in motor function and disability after ischemic stroke," *European Journal of Neurology*, vol. 17, no. 9, pp. 1203–1209, 2010.

[9] N. Sasaki, S. Mizutani, W. Kakuda, and M. Abo, "Comparison of the effects of high- and low-frequency repetitive transcranial magnetic stimulation on upper limb hemiparesis in the early phase of stroke," *Journal of Stroke and Cerebrovascular Diseases*, vol. 22, no. 4, pp. 413–418, 2013.

[10] E. M. Khedr, M. R. Abdel-Fadeil, A. Farghali, and M. Qaid, "Role of 1 and 3 Hz repetitive transcranial magnetic stimulation on motor function recovery after acute ischemic stroke," *European Journal of Neurology*, vol. 16, no. 12, pp. 1323–1330, 2009.

[11] W. Y. Hsu, C. H. Cheng, K. K. Liao, I. H. Lee, and Y. Y. Lin, "Effects of repetitive transcranial magnetic stimulation on motor functions in patients with stroke a meta-analysis," *Stroke*, vol. 43, no. 7, pp. 1849–1857, 2012.

[12] N. Takeuchi, T. Tada, M. Toshima, Y. Matsuo, and K. Ikoma, "Repetitive transcranial magnetic stimulation over bilateral hemispheres enhances motor function and training effect of paretic hand in patients after stroke," *Journal of Rehabilitation Medicine*, vol. 41, no. 13, pp. 1049–1054, 2009.

[13] M. P. Lomarev, D. Y. Kim, S. P. Richardson, B. Voller, and M. Hallett, "Safety study of high-frequency transcranial magnetic stimulation in patients with chronic stroke," *Clinical Neurophysiology*, vol. 118, no. 9, pp. 2072–2075, 2007.

[14] S. H. Cho, H. K. Shin, Y. H. Kwon et al., "Cortical activation changes induced by visual biofeedback tracking training in chronic stroke patients," *NeuroRehabilitation*, vol. 22, pp. 77–84, 2007.

[15] S. Theilig, J. Podubecka, K. Bosl, R. Wiederer, and D. A. Nowak, "Functional neuromuscular stimulation to improve severe hand dysfunction after stroke: does inhibitory rTMS enhance therapeutic efficiency?," *Experimental Neurology*, vol. 230, no. 1, pp. 149–155, 2011.

[16] M. B. Iyer, N. Schleper, and E. M. Wassermann, "Priming stimulation enhances the depressant effect of low-frequency repetitive transcranial magnetic stimulation," *Journal of Neuroscience*, vol. 23, no. 34, pp. 10867–10872, 2003.

[17] N. Takeuchi, T. Tada, Y. Matsuo, and K. Ikoma, "Low-frequency repetitive TMS plus anodal transcranial DCS prevents transient decline in bimanual movement induced by contralesional inhibitory rTMS after stroke," *Neurorehabilitation and Neural Repair*, vol. 26, no. 8, pp. 988–998, 2012.

[18] N. Takeuchi, T. Tada, M. Toshima, T. Chuma, Y. Matsuo, and K. Ikoma, "Inhibition of the unaffected motor cortex by 1 Hz repetitive transcranial magnetic stimulation enhances motor performance and training effect of the paretic hand in patients with chronic stroke," *Journal of Rehabilitation Medicine*, vol. 40, no. 4, pp. 298–303, 2008.

[19] N. Takeuchi, T. Chuma, Y. Matsuo, I. Watanabe, and K. Ikoma, "Repetitive transcranial magnetic stimulation of contralesional primary motor cortex improves hand function after stroke," *Stroke*, vol. 36, no. 12, pp. 2681–2686, 2005.

[20] M. Dafotakis, C. Grefkes, S. B. Eickhoff, H. Karbe, G. R. Fink, and D. A. Nowak, "Effects of rTMS on grip force control following subcortical stroke," *Experimental Neurology*, vol. 211, no. 2, pp. 407–412, 2008.

[21] A. B. Conforto, S. M. Anjos, G. Saposnik et al., "Transcranial magnetic stimulation in mild to severe hemiparesis early after stroke: a proof of principle and novel approach to improve motor function," *Journal of Neurology*, vol. 259, no. 7, pp. 1399–1405, 2012.

[22] J. Higgins, L. Koski, and H. Xie, "Combining rTMS and task-oriented training in the rehabilitation of the arm after stroke: a pilot randomized controlled trial," *Stroke Research and Treatment*, vol. 2013, Article ID 539146, 8 pages, 2013.

[23] D. K. Rose and C. Patten, "Does inhibitory repetitive transcranial magnetic stimulation augment functional task practice to improve arm recovery in chronic stroke?," *Stroke Research and Treatment*, vol. 2014, Article ID 305236, 10 pages, 2014.

[24] J. Liepert, S. Zittel, and C. Weiller, "Improvement of dexterity by single session low-frequency repetitive transcranial magnetic stimulation over the contralesional motor cortex in acute stroke: a double-blind placebo-controlled crossover trial," *Restorative Neurology and Neuroscience*, vol. 25, no. 5-6, pp. 461–465, 2007.

[25] A. Matsuura, K. Onoda, H. Oguro, and S. Yamaguchi, "Magnetic stimulation and movement-related cortical activity for acute stroke with hemiparesis," *European Journal of Neurology*, vol. 22, no. 12, pp. 1526–1532, 2015.

[26] F. Fregni, P. S. Boggio, A. C. Valle et al., "A sham-controlled trial of a 5-day course of repetitive transcranial magnetic stimulation of the unaffected hemisphere in stroke patients," *Stroke*, vol. 37, no. 8, pp. 2115–2122, 2006.

[27] D. A. Nowak, C. Grefkes, M. Dafotakis et al., "Effects of low-frequency repetitive transcranial magnetic stimulation of the contralesional primary motor cortex on movement kinematics and neural activity in subcortical stroke," *Archives of Neurology*, vol. 65, no. 6, pp. 741–747, 2008.

[28] W. H. Sung, C. P. Wang, C. L. Chou, Y. C. Chen, Y. C. Chang, and P. Y. Tsai, "Efficacy of coupling inhibitory and facilitatory repetitive transcranial magnetic stimulation to enhance motor recovery in hemiplegic stroke patients," *Stroke*, vol. 44, no. 5, pp. 1375–1382, 2013.

[29] J. Ludemann-Podubecka, K. Bosl, S. Theilig, R. Wiederer, and D. A. Nowak, "The effectiveness of 1 Hz rTMS over the primary motor area of the unaffected hemisphere to improve hand function after stroke depends on hemispheric dominance," *Brain Stimulation*, vol. 8, no. 4, pp. 823–830, 2015.

[30] J. Seniow, M. Bilik, M. Lesniak, K. Waldowski, S. Iwanski, and A. Czlonkowska, "Transcranial magnetic stimulation combined with physiotherapy in rehabilitation of poststroke hemiparesis: a randomized, double-blind, placebo-controlled study," *Neurorehabilitation and Neural Repair*, vol. 26, no. 9, pp. 1072–1079, 2012.

[31] S. C. B. Galvão, R. B. C. Dos Santos, P. B. Dos Santos, M. E. Cabral, and K. Monte-Silva, "Efficacy of coupling repetitive transcranial magnetic stimulation and physical therapy to reduce upper-limb spasticity in patients with stroke: a randomized controlled trial," *Archives of Physical Medicine and Rehabilitation*, vol. 95, no. 2, pp. 222–229, 2014.

[32] C. P. Wang, P. Y. Tsai, T. F. Yang, K. Y. Yang, and C. C. Wang, "Differential effect of conditioning sequences in coupling inhibitory/facilitatory repetitive transcranial magnetic stimulation for post-stroke motor recovery," *CNS Neuroscience & Therapeutics*, vol. 20, no. 4, pp. 355–363, 2014.

[33] C. J. Zheng, W. J. Liao, and W. G. Xia, "Effect of combined low-frequency repetitive transcranial magnetic stimulation and virtual reality training on upper limb function in subacute stroke: a double-blind randomized controlled trail," *Journal of Huazhong University of Science and Technology [Medical Sciences]*, vol. 35, pp. 248–254, 2015.

[34] J. Du, L. Tian, W. Liu et al., "Effects of repetitive transcranial magnetic stimulation on motor recovery and motor cortex excitability in patients with stroke: a randomized controlled trial," *European Journal of Neurology*, vol. 23, no. 11, pp. 1666–1672, 2016.

[35] L. Jancke, H. Steinmetz, S. Benilow, and U. Ziemann, "Slowing fastest finger movements of the dominant hand with low-frequency rTMS of the hand area of the primary motor cortex," *Experimental Brain Research*, vol. 155, no. 2, pp. 196–203, 2004.

[36] Q. Le, Y. Qu, Y. Tao, and S. Zhu, "Effects of repetitive transcranial magnetic stimulation on hand function recovery and excitability of the motor cortex after stroke: a meta-analysis," *American Journal of Physical Medicine & Rehabilitation*, vol. 93, no. 5, pp. 422–430, 2014.

[37] E. M. Khedr and N. A. Fetoh, "Short- and long-term effect of rTMS on motor function recovery after ischemic stroke," *Restorative Neurology and Neuroscience*, vol. 28, no. 4, pp. 545–559, 2010.

[38] Z. Hao, D. Wang, Y. Zeng, and M. Liu, "Repetitive transcranial magnetic stimulation for improving function after stroke," *Cochrane Database of Systematic Reviews*, vol. 31, article CD008862, 2013.

[39] D. Moher, K. F. Schulz, and D. Altman, "The consort statement: revised recommendations for improving the quality of reports of parallel-group randomized trials," *Journal of the American Medical Association*, vol. 285, no. 15, pp. 1987–1991, 2001.

[40] C. L. Chung and M. K. Mak, "Effect of repetitive transcranial magnetic stimulation on physical function and motor signs in Parkinson's disease: a systematic review and meta-analysis," *Brain Stimulation*, vol. 9, no. 4, pp. 475–487, 2016.

[41] L. Santisteban, M. Teremetz, J. P. Bleton, J. C. Baron, M. A. Maier, and P. G. Lindberg, "Upper limb outcome measures used in stroke rehabilitation studies: a systematic literature review," *PLoS One*, vol. 11, no. 5, article e0154792, 2016.

[42] M. V. Sale, N. C. Rogasch, and M. A. Nordstrom, "Different stimulation frequencies alter synchronous fluctuations in motor evoked potential amplitude of intrinsic hand muscles—a TMS study," *Frontiers in Human Neuroscience*, vol. 10, p. 100, 2016.

[43] K. Funase, T. S. Miles, and B. R. Gooden, "Trial-to-trial fluctuations in h-reflexes and motor evoked potentials in human wrist flexor," *Neuroscience Letters*, vol. 271, no. 1, pp. 25–28, 1999.

[44] R. J. Grissom and J. J. Kim, *Effect Sizes for Research: A Broad Practical Approach*, Lawrence Erlbaum Associates Publishers, Mahwah, NJ, USA, 2005.

[45] J. P. Higgins and S. G. Thompson, "Quantifying heterogeneity in a meta-analysis," *Statistics in Medicine*, vol. 21, no. 11, pp. 1539–1558, 2002.

[46] S. J. Duval and R. L. Tweedie, "Trim and fill: a simple funnel-plot based method of accounting for publication bias in meta-analysis," *Biometrics*, vol. 56, no. 2, pp. 455–463, 2000.

[47] J. Cohen, *Statistical Power Analysis for the Behavioral Sciences*, Academic Press, New York NY, USA, 1977.

[48] B. Bobath and FCSP, Cofounder, Centre, *Adult Hemiplegia: Evaluation and Treatment*, William Heinemann, London, England, 2nd edition, 1978.

[49] T. L. Sutcliffe, W. C. Gaetz, W. J. Logan, D. O. Cheyne, and D. L. Fehlings, "Cortical reorganization after modified constraint-induced movement therapy in pediatric hemiplegic cerebral palsy," *Journal of Child Neurology*, vol. 22, no. 11, pp. 1281–1287, 2007.

[50] M. Hallett, "Transcranial magnetic stimulation: a primer," *Neuron*, vol. 55, no. 2, pp. 187–199, 2007.

[51] S. Y. Kim and S. B. Shin, "Factors associated with upper extremity functional recovery following low-frequency repetitive transcranial magnetic stimulation in stroke patients," *Annals of Rehabilitation Medicine*, vol. 40, no. 3, pp. 373–382, 2016.

[52] C. Kim, H. E. Choi, H. Jung, B. J. Lee, K. H. Lee, and Y. J. Lim, "Comparison of the effects of 1 Hz and 20 Hz rTMS on motor recovery in subacute stroke patients," *Annals of Rehabilitation Medicine*, vol. 38, no. 5, pp. 585–591, 2014.

[53] S. Meyer, N. D. Bruyn, C. Lafosse et al., "Somatosensory impairments in the upper limb poststroke: distribution and association with motor function and visuospatial neglect," *Neurorehabilitation and Neural Repair*, vol. 30, no. 8, pp. 731–742, 2016.

[54] D. R. De Jesus, G. P. Favalli, S. S. Hoppenbrouwers et al., "Determining optimal rTMS parameters through changes in cortical inhibition," *Clinical Neurophysiology*, vol. 125, no. 4, pp. 755–762, 2014.

Hindawi
Neural Plasticity
Volume 2017, Article ID 7876507, 6 pages
https://doi.org/10.1155/2017/7876507

Research Article

Transcutaneous Vagus Nerve Stimulation Combined with Robotic Rehabilitation Improves Upper Limb Function after Stroke

Fioravante Capone,[1,2] Sandra Miccinilli,[3] Giovanni Pellegrino,[4] Loredana Zollo,[5] Davide Simonetti,[5] Federica Bressi,[3] Lucia Florio,[1] Federico Ranieri,[1] Emma Falato,[1] Alessandro Di Santo,[1] Alessio Pepe,[1] Eugenio Guglielmelli,[5] Silvia Sterzi,[3] and Vincenzo Di Lazzaro[1,2]

[1]*Unit of Neurology, Neurophysiology, Neurobiology, Department of Medicine, Università Campus Bio-Medico di Roma, Via Álvaro del Portillo 21, 00128 Rome, Italy*
[2]*Fondazione Alberto Sordi-Research Institute for Ageing, Via Álvaro del Portillo 5, 00128 Rome, Italy*
[3]*Unit of Physical and Rehabilitation Medicine, Department of Medicine, Università Campus Bio-Medico di Roma, Via Álvaro del Portillo 21, 00128 Rome, Italy*
[4]*San Camillo Hospital IRCCS, Venice, Italy*
[5]*Unit of Biomedical Robotics and Biomicrosystems, Department of Engineering, Università Campus Bio-Medico di Roma, Via Álvaro del Portillo 21, 00128 Rome, Italy*

Correspondence should be addressed to Fioravante Capone; f.capone@unicampus.it

Received 12 June 2017; Revised 21 October 2017; Accepted 26 October 2017; Published 10 December 2017

Academic Editor: Dario Farina

The efficacy of standard rehabilitative therapy for improving upper limb functions after stroke is limited; thus, alternative strategies are needed. Vagus nerve stimulation (VNS) paired with rehabilitation is a promising approach, but the invasiveness of this technique limits its clinical application. Recently, a noninvasive method to stimulate vagus nerve has been developed. The aim of the present study was to explore whether noninvasive VNS combined with robotic rehabilitation can enhance upper limb functionality in chronic stroke. Safety and efficacy of this combination have been assessed within a proof-of-principle, double-blind, semirandomized, sham-controlled trial. Fourteen patients with either ischemic or haemorrhagic chronic stroke were randomized to robot-assisted therapy associated with real or sham VNS, delivered for 10 working days. Efficacy was evaluated by change in upper extremity Fugl–Meyer score. After intervention, there were no adverse events and Fugl–Meyer scores were significantly better in the real group compared to the sham group. Our pilot study confirms that VNS is feasible in stroke patients and can produce a slight clinical improvement in association to robotic rehabilitation. Compared to traditional stimulation, noninvasive VNS seems to be safer and more tolerable. Further studies are needed to confirm the efficacy of this innovative approach.

1. Introduction

Upper limb impairment is a common consequence of stroke with a deep impact on patient's quality of life. Since the efficacy of standard rehabilitative therapy is limited, alternative strategies are needed. Robot-assisted rehabilitation can be useful in stroke patients because it allows an intensive as well as task-specific training characterized by high repetition of movements in a strongly motivating environment [1–3]. Several studies have explored the possibility to potentiate the effect of robotic therapy by the association with noninvasive human brain stimulation techniques, such as repetitive transcranial magnetic stimulation (rTMS), that can induce neuroplasticity via long-term potentiation-/depression- (LTP-/LTD-) like phenomena [4]. Although intriguing, the evidence in support of this strategy remains low [5, 6].

Indeed, the literature analysis of the published data seems to demonstrate that the association of rTMS with robotic training has the same clinical gain derived from robotic therapy alone. Moreover, rTMS is contraindicated in patients who suffered from haemorrhagic stroke for the risk of inducing seizures [7]. For these reasons, there is great interest in the development of alternative techniques of neuromodulation that can foster the effect of robotic therapy.

Vagus nerve stimulation (VNS) is approved as adjunctive treatment for refractory epilepsy and depression but is currently under investigation for a wide range of neurological diseases [8]. In particular, recent studies have demonstrated that VNS paired with rehabilitation significantly improves forelimb strength and movement speed in rat models of ischemic [9] and haemorrhagic stroke [10]. VNS is believed to enhance the benefits of rehabilitation by promoting neuroplasticity [11]. Preliminary data [12] have showed that such approach is also feasible in patients; however, the diffusion of this technique is limited by its invasiveness. Indeed, VNS requires the surgical implantation of a stimulator of the cervical branch of the vagus nerve. Recently, it has been proposed a noninvasive technique that consists of transcutaneous stimulation of the vagus nerve (tVNS) in external auditory channel at the inner side of the tragus. Both neuroimaging [13] and neurophysiological [14] studies have demonstrated that the effect of tVNS on brain activity is quite similar to the effect induced by traditional, invasive VNS.

The aim of the present study was to explore whether tVNS can enhance the benefit induced by robotic rehabilitation on motor function of the upper limb in chronic stroke. Safety and efficacy of this combination have been assessed within a proof-of-principle, double-blind, semirandomized, sham-controlled trial.

2. Material and Methods

The study was performed accordingly to the Declaration of Helsinki and was approved by the Local Ethics Committee. The study was proposed to patients attending the outpatient clinic for cerebrovascular disorders of Campus Bio-Medico University Hospital. Inclusion criteria were as follows: (a) first-ever, ischemic or haemorrhagic stroke at least 1 year earlier; (b) hand function impairment; (c) and ability to give informed consent and comprehend instructions. Exclusion criteria were as follows: (a) previous surgical intervention on vagus nerve; (b) low hearth rate (<60 bpm); (c) cognitive impairment or any substantial decrease in alertness, language reception, or attention that might interfere with understanding instructions for motor testing; (d) apraxia; (e) excessive pain in any joint of the paretic extremity; (f) advanced liver, kidney, cardiac, or pulmonary disease; (g) history of significant alcohol or drug abuse; (h) depression or use of neuropsychotropic drugs such as antidepressants or benzodiazepines; (i) and pregnancy.

Fourteen patients with either ischemic or haemorrhagic chronic stroke were randomized to robot-assisted therapy associated with real or sham tVNS, delivered for 10 working days. Efficacy was evaluated by change in upper extremity Fugl–Meyer assessment (FMA) score. To assess safety, during the stimulation, heart rate (HR) and blood pressure (BP) were monitored. Moreover, to test the tolerability of tVNS, subjects were questioned about the presence of unpleasant sensations or other discomforts. Each day, patients received a session of robotic therapy immediately following the real or sham stimulation. All patients were evaluated at baseline (baseline) and just after the two weeks of treatment (post). At baseline, to evaluate neurological impairment and disability, we also included the following scales: National Institute of Health Stroke Scale (NIHSS), Rankin Scale, Barthel Index, and Modified Ashworth Scale. Spasticity was assessed by Modified Ashworth Scale at four different joints of affected arm: the shoulder, elbow, wrist, and fingers. For each patient, a cumulative score was obtained by summing the scores obtained in the four joints. The cumulative score ranges from 0 (no spasticity) to 16 (maximum spasticity, i.e., score 4 in all the considered joints).

The stimulation of the auricular branch of the vagus nerve was performed through an electric stimulator (Twister—EBM) and two Ag-AgCl electrodes (5 mm in diameter) placed in the left external acoustic meatus at the inner side of the tragus. For sham stimulation, electrodes were attached to the left ear lobe, an anatomical area that is outside the innervation of the auricular branch of the vagus nerve. tVNS was delivered as trains lasting 30 s and composed by 600 pulses (intratrain pulse frequency = 20 Hz; pulse duration = 0.3 ms) repeated every 5 min for 60 min. The intensity of stimulation was individually adjusted to a level ranging above the detection threshold and below the pain threshold. To reduce the risk of cardiac side effects, only the left ear was stimulated because vagal fibers to the heart are supposed to originate from the right side [15].

Robotic therapy was delivered at proximal or at distal segment of the affected limb according to the degree of impairment and the choice of the physician. The InMotion2 shoulder-elbow system (Interactive Motion Technologies Inc.) [16] was used for proximal limb segments and the InMotion3 wrist system (Interactive Motion Technologies Inc.) [17] for the treatment of distal segments. InMotion2 robot consists of a direct-drive mechanism that provides two translational degrees of freedom for elbow and forearm motion. Robot movement is enabled thanks to an impedance control that guides or perturbs the patient's movement. The InMotion3 robot enables unilateral wrist training characterized by low endpoint inertia and friction. Flexion-extension and radial-ulnar deviation are guaranteed thanks to two side-mounted actuators connected to a differential mechanism, while pronation-supination is actuated by another DC motor. An impedance control is implemented to assist patient's movement. Each day of robotic treatment consisted of three sessions of 320 assisted point-to-point movements, from the center to eight outbound targets, interspersed by four sessions of 16 unassisted recorded point-to-point movements. Robot assistance at each session was tuned on patients' performance during the 16 point-to-point sessions. During training, patients were required to move with a self-paced speed in a maximum time slot of 3 s. Robotic treatment was delivered daily for 10 consecutive working days, immediately after the end of real or sham tVNS. A physical and

rehabilitation medicine doctor attended and assisted patients during treatment. During the intervention period, patients did not receive any additional physical therapy. Pharmacological therapy was also unchanged. Researchers randomizing patients and researchers delivering tVNS were not involved in outcome assessments and data analysis; moreover, rehabilitation doctors, patients, and researchers involved in data analysis were blind to the type of tVNS delivered (i.e., sham or real), in order to obtain a double-blind study design.

2.1. Statistics. Statistical analysis was performed using the IBM SPSS Statistics (Ver. 24). After checking that the baseline clinical measures were not different between groups, postintervention FMA of the two groups was expressed as percentage of baseline scores and compared by means of Mann–Whitney test.

In order to assess the safety of the stimulation, we measured systolic blood pressure, diastolic blood pressure, and heart rate, before and after each stimulation, every day, for ten days. For each of these measures, we performed a mixed-model repeated ANOVA with days (ten levels) and prepost (2 levels) as within subject factors and group (two levels: real and sham) as between subject factor. Correction for sphericity violations and multiple comparisons were applied as needed.

3. Results

Seven patients were randomized to robot-assisted therapy associated with real tVNS and seven patients to robot-assisted therapy associated with sham tVNS. One sham patient withdrew consent before the first session of treatment. Another sham patient withdrew because of difficulty in reaching the hospital after the second day of treatment. Data of these patients were not included in the analysis. Thus, a total of 12 patients completed the study: 7 real (mean age: 53.7 ± 15.6 years, 4 males) and 5 sham (mean age: 55.6 ± 15.9 years, 3 males). The real and sham groups were not significantly different regarding age, sex, type of stroke (haemorrhagic versus ischemic), and side of lesion. Time elapsed from stroke onset and clinical status at baseline (in particular, FMA score) were different between the two groups, but this difference was not statistically significant ($p > 0.200$ consistently) (Table 1).

The treatment was safe and tolerable. There were no adverse events, unpleasant sensations, or other discomforts. None of the patients required to stop stimulation. For systolic BP, the ANOVA mixed model showed no significant main effects nor significant interactions with the factor days ($p > 0.200$ consistently). We however found a significant prepost by group interaction ($F(1.9) = 7.335$, $p = 0.024$) which was largely related to the intergroup systolic pressure difference ($F(1.9) = 9.986$, $p = 0.012$), as no prepost significant differences were found within each group. This analysis unveiled that the two groups had an average significant systolic blood pressure differences but the stimulation has no significant effect on this parameter (Figure 1). Similar behaviour showed the diastolic blood pressure, for which we only found a significant prepost *group interaction ($F(1.9) = 7.328$, $p = 0.024$).

Table 1: Demographic and clinical characteristics of the patients at baseline.

	Real ($N = 7$)	Sham ($N = 5$)	p value
Age (years)	53.71 ± 5.88	55.60 ± 7.12	1.00[a]
Sex (M)	4	3	0.447[b]
Months since stroke	93.71 ± 38.81	46.00 ± 21.85	0.432[a]
Fugl–Meyer	22.29 ± 3.51	32.60 ± 6.43	0.268[a]
NIHSS	6.14 ± 1.50	4.80 ± 0.74	0.639[a]
Barthel Index	72.14 ± 9.81	81.00 ± 9.00	0.639[a]
Modified Rankin	2.86 ± 0.40	2.20 ± 0.58	0.432[a]
Modified Ashworth Scale cumulative score	6.86 ± 1.16	5.40 ± 1.32	0.343[a]

All data are expressed as mean ± standard error. [a]Mann–Whitney test; [b]chi-square test.

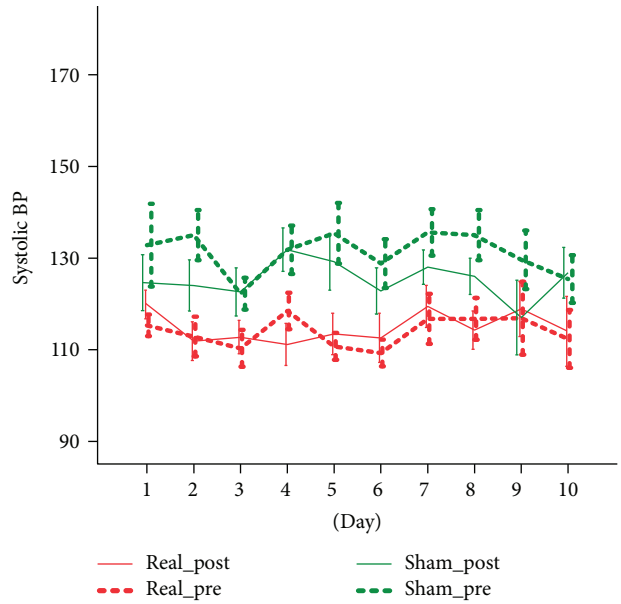

Figure 1: The effect of tVNS on systolic BP.

No significant group differences nor prepost differences in each group were found (Figure 2). For the HR measure, we only found a significant prepost main effect ($F(1.9) = 32.497$, $p < 0.001$) that was confirmed in both groups and corresponded to a mild and not clinically relevant reduction of heart rate (2.3 bpm in the real group and 4.7 bpm in the sham group) (Figure 3).

After intervention, FMA scores were significantly better in the real group as compared to the sham group (Mann–Whitney $U = 5.00$, $p = 0.048$) (Figure 4). Individual data, including the kind of treatment (robotics and VNS), the intensity of VNS, and the changes in FMA, HR, and blood pressure are reported in Table 2.

4. Discussion

This is the first study that has evaluated the feasibility of tVNS in chronic both ischemic and haemorrhagic stroke

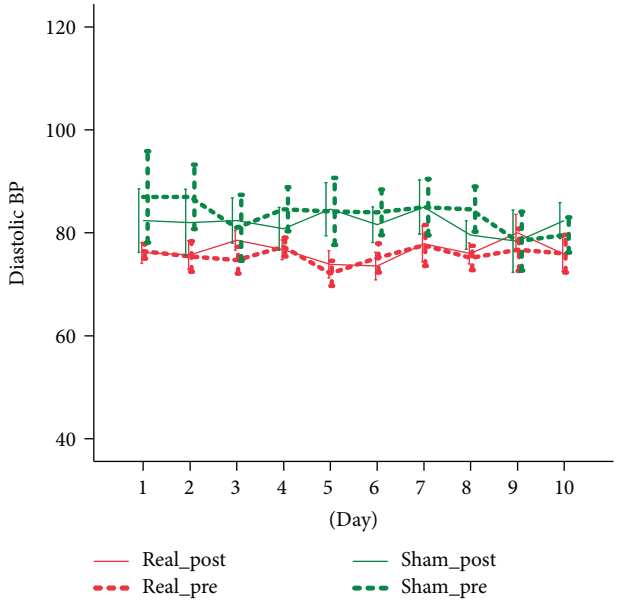

Figure 2: The effect of tVNS on diastolic BP.

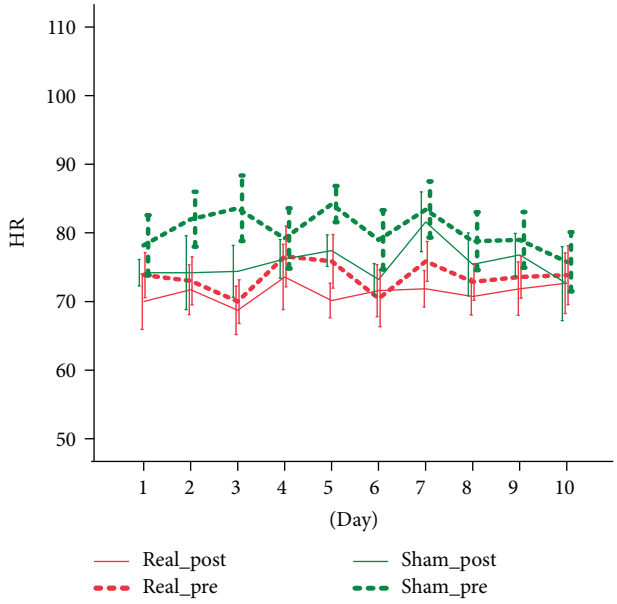

Figure 3: The effect of tVNS on HR.

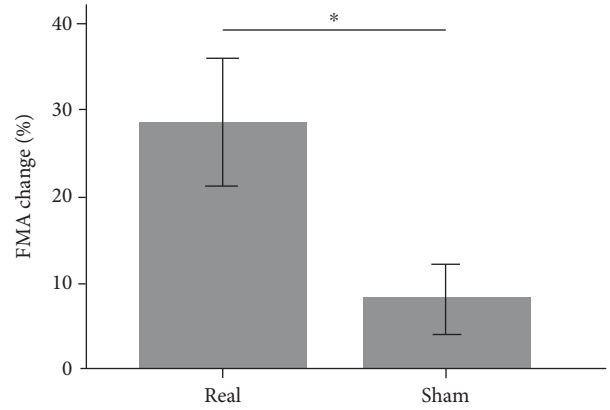

Figure 4: Effect of tVNS on FMA scores. The FMA score improved significantly ($^*p = 0.048$) more in the real group than in the sham group. FMA is expressed as percentage change with respect to baseline.

patients. Our data demonstrate that tVNS is safe and, combined to robot-assisted rehabilitation, can induce a slight but significant improvement of arm functionality. The treatment was well tolerated, and no adverse events or discomforts were reported from patients. In particular, we have not recorded any side effect that can occur with invasive VNS such as vocal cord palsy, dysphagia, nausea, taste disturbance, hoarseness, or neck tingling [12]. Since vagus nerve influences cardiac activity [18], we have carefully monitored HR and BP during tVNS session in order to identify any potential cardiovascular harm. We have not observed any clinically significant change in cardiovascular parameters throughout the stimulation. A slight and asymptomatic reduction of HR was observed both in the real and in the sham groups. Because this was present in both groups, it was not related to tVNS and thus represents an unspecific change that might be related to different causes such as patient relaxation during the course of the study. In a previous, randomized, placebo-controlled, double-blind study on ten healthy subjects [14], we have showed that tVNS does not change HR and BP. Similar results have been obtained from Shim et al. [19] that have treated thirty patients with refractory chronic tinnitus. Taken together, these findings suggest that tVNS is a safe technique that does not negatively influence cardiac functionality and can be used in stroke patients.

Even though this was a proof-of-principle study mainly aimed to demonstrate the feasibility of tVNS, our results suggest that the combination of vagal stimulation and robotic rehabilitation can improve arm functionality in chronic stroke patients. Indeed, both real and sham patients improved after the intervention but the change in FMA was significantly higher for the real group (5.4 versus 2.8 points; $p = 0.048$). This change, although slight, is considered clinically significant in chronic patients [20], especially in those with severe impairment of upper limb function [2]. A potential benefit of invasive VNS in chronic stroke has been recently described both in animal model [21] and in patients [12]. In a rat model of chronic stroke, Khodaparast et al. [21] have demonstrated that VNS paired with rehabilitative training significantly improves recovery of forelimb function compared to rehabilitation alone. Interestingly, ischemic lesion size is not reduced by VNS. According to the authors, this finding suggests that, in chronic stroke, VNS promotes recovery through a mechanism independent of neuroprotection, most likely by inducing neuroplasticity. This idea is further supported by additional experimental data showing that VNS increases levels of brain-derived neurotrophic factor (BDNF) and neurotransmitters such as noradrenaline linked to neuroplasticity and recovery after brain lesion [22, 23].

The feasibility of VNS in chronic stroke patients has been recently evaluated by a clinical trial involving twenty-one patients randomized to VNS plus rehabilitation or

Table 2: Effect of treatment on upper limb functionality and cardiovascular parameters.

Patient	Age	Gender	Stroke	Type of robot	Stimulation	VNS range intensity	FMA PRE	FMA POST	HR PRE	HR POST	sBP PRE	sBP POST	dBP PRE	dBP POST
1	44	M	Isch	InMotion2	Real	2.5–3.2	26	28	69.2	67.0	122.5	126.0	83.0	83.5
2	73	M	Isch	InMotion2	Real	5.1–9.0	31	39	63.4	60.6	117.0	120.5	74.0	75.5
3	54	F	Isch	InMotion3	Real	2.2-3.5	15	25	77.4	70.0	116.0	117.8	76.3	75.5
4	67	M	Isch	InMotion3	Real	1.2–2.8	20	26	74.8	74.6	125.0	124.9	80.6	82.6
5	26	F	Haem	InMotion3	Real	1.6–2.0	13	16	78.2	76.6	104.7	106.0	71.1	71.5
6	52	F	Haem	InMotion3	Real	2.0–7.0	14	17	85.1	84.6	105.0	106.1	71.3	73.1
7	60	M	Isch	InMotion3	Real	1.1–4.0	37	43	67.1	65.8	108.7	103.5	73.8	74.0
Mean	53.7					**2.0–4.5**	**22.3**	**27.7**	**73.6**	**71.3**	**114.1**	**115.0**	**75.7**	**76.5**
8	70	M	Isch	InMotion2	Sham	1.5–8.0	18	19	75.9	72.0	129.0	121.0	76.8	74.8
9	42	F	Haem	InMotion2	Sham	1.6–9.0	25	25	92.3	85.3	141.5	130.5	89.5	87.0
10	75	M	Isch	InMotion3	Sham	3.0–5.0	56	61	77.1	71.5	116.5	116.5	70.0	71.0
11	41	F	Isch	InMotion3	Sham	4.0–9.0	30	37	80.5	76.2	134.7	134.0	88.9	87.9
12	50	M	Haem	InMotion3	Sham	4.0–5.0	34	35	75.8	73.0	134.1	124.4	92.5	88.9
Mean	55.6					**2.8–7.2**	**32.6**	**35.4**	**80.3**	**75.6**	**131.2**	**125.3**	**83.5**	**81.9**

Isch: ischemic; Haem: haemorrhagic; FMA: Fugl–Meyer assessment; HR: heart rate; sBP: systolic blood pressure; dBP: diastolic blood pressure. PRE refers to values recorded immediately before VNS session and POST to values recorded immediately after the end of VNS session. VNS range intensity is expressed in mA.

rehabilitation alone [12]. VNS has been performed by a surgically implanted device producing stimulation paired with rehabilitative exercises. The authors reported some minor adverse effects related to stimulating device, but no serious adverse events were observed. Arm functionality, measured by FMA, improved in both groups but more in the VNS group (between-group difference, 5.7 points). In this trial, VNS was delivered simultaneously with the rehabilitative training. Indeed, animal studies [21] have demonstrated that the timing of VNS-rehabilitation coupling is essential because recovery does not improve when VNS follows rehabilitation. This result supports the idea that the synergistic effect of VNS and rehabilitation depends on neuroplasticity, a timing-dependent phenomenon. Our study extends this concept demonstrating that also noninvasive VNS delivered before rehabilitation can ameliorate arm functionality. As described for rTMS, tVNS could increase the effect of rehabilitation by producing a priming effect on subsequent motor training [24].

Although intriguing, the results of our study, in particular the effect on FMA, should be considered cautiously. Indeed, the present study has some important limitations such as the small sample size, the use of different kind of robotic training, and the lack of a long-term follow-up.

5. Conclusions

Our pilot study confirms that VNS is feasible and safe in stroke patients and can produce a slight clinical improvement in association to robotic rehabilitation. Compared to traditional, invasive stimulation, tVNS seems to be safer and more tolerable. Further studies are needed to confirm efficacy and unveil the mechanisms of action of this innovative approach.

Conflicts of Interest

The authors declare that they have no conflicts of interest.

References

[1] G. B. Prange, M. J. A. Jannink, C. G. M. Groothuis-Oudshoorn, H. J. Hermens, and M. J. IJzerman, "Systematic review of the effect of robot-aided therapy on recovery of the hemiparetic arm after stroke," *Journal of Rehabilitation Research & Development*, vol. 43, no. 2, pp. 171–184, 2006.

[2] A. C. Lo, P. D. Guarino, L. G. Richards et al., "Robot-assisted therapy for long-term upper-limb impairment after stroke," *The New England Journal of Medicine*, vol. 362, no. 19, pp. 1772–1783, 2010.

[3] V. Klamroth-Marganska, J. Blanco, K. Campen et al., "Three-dimensional, task-specific robot therapy of the arm after stroke: a multicentre, parallel-group randomised trial," *The Lancet Neurology*, vol. 13, no. 2, pp. 159–166, 2014.

[4] G. Di Pino, G. Pellegrino, G. Assenza et al., "Modulation of brain plasticity in stroke: a novel model for neurorehabilitation," *Nature Reviews Neurology*, vol. 10, no. 10, pp. 597–608, 2014.

[5] A. Pollock, S. E. Farmer, M. C. Brady et al., "Interventions for improving upper limb function after stroke," *Cochrane Database of Systematic Reviews*, vol. 11, article CD010820, 2014.

[6] V. Di Lazzaro, F. Capone, G. Di Pino et al., "Combining robotic training and non-invasive brain stimulation in severe upper limb-impaired chronic stroke patients," *Frontiers in Neuroscience*, vol. 10, p. 88, 2016.

[7] M. Cogné, C. Gil-Jardiné, P. A. Joseph, D. Guehl, and B. Glize, "Seizure induced by repetitive transcranial magnetic stimulation for central pain: adapted guidelines for post-stroke patients," *Brain Stimulation*, vol. 10, no. 4, pp. 862–864, 2017.

[8] D. A. Groves and V. J. Brown, "Vagal nerve stimulation: a review of its applications and potential mechanisms that

mediate its clinical effects," *Neuroscience and Biobehavioral Reviews*, vol. 29, no. 3, pp. 493–500, 2005.

[9] N. Khodaparast, M. P. Kilgard, R. Casavant et al., "Vagus nerve stimulation during rehabilitative training improves forelimb recovery after chronic ischemic stroke in rats," *Neurorehabilitation and Neural Repair*, vol. 30, no. 7, pp. 676–684, 2015.

[10] S. A. Hays, N. Khodaparast, D. R. Hulsey et al., "Vagus nerve stimulation during rehabilitative training improves functional recovery after intracerebral hemorrhage," *Stroke*, vol. 45, no. 10, pp. 3097–3100, 2014.

[11] S. A. Hays, I. I. R. L. Rennaker, and M. P. Kilgard, "Targeting plasticity with vagus nerve stimulation to treat neurological disease," *Progress in Brain Research*, vol. 207, pp. 275–299, 2013.

[12] J. Dawson, D. Pierce, A. Dixit et al., "Safety, feasibility, and efficacy of vagus nerve stimulation paired with upper-limb rehabilitation after ischemic stroke," *Stroke*, vol. 47, no. 1, pp. 143–150, 2016.

[13] T. Kraus, K. Hosl, O. Kiess, A. Schanze, J. Kornhuber, and C. Forster, "BOLD fMRI deactivation of limbic and temporal brain structures and mood enhancing effect by transcutaneous vagus nerve stimulation," *Journal of Neural Transmission*, vol. 11, pp. 1485–1493, 2007.

[14] F. Capone, G. Assenza, G. Di Pino et al., "The effect of transcutaneous vagus nerve stimulation on cortical excitability," *Journal of Neural Transmission*, vol. 122, no. 5, pp. 679–685, 2015.

[15] C. B. Nemeroff, H. S. Mayberg, S. E. Krahl et al., "VNS therapy in treatment-resistant depression: clinical evidence and putative neurobiological mechanisms," *Neuropsychopharmacology*, vol. 31, no. 7, pp. 1345–1355, 2006.

[16] H. I. Krebs, N. Hogan, M. L. Aisen, and B. T. Volpe, "Robot-aided neurorehabilitation," *IEEE Transactions on Rehabilitation Engineering*, vol. 6, no. 1, pp. 75–87, 1998.

[17] H. I. Krebs, B. T. Volpe, D. Williams et al., "Robot-aided neurorehabilitation: a robot for wrist rehabilitation," *IEEE Transactions on Neural Systems and Rehabilitation Engineering*, vol. 15, no. 3, pp. 327–335, 2007.

[18] J. H. Coote, "Myths and realities of the cardiac vagus," *The Journal of Physiology*, vol. 591, no. 17, pp. 4073–4085, 2013.

[19] H. J. Shim, M. Y. Kwak, Y. H. An, D. H. Kim, Y. J. Kim, and H. J. Kim, "Feasibility and safety of transcutaneous vagus nerve stimulation paired with notched music therapy for the treatment of chronic tinnitus," *Journal of Audiology & Otology*, vol. 19, no. 3, pp. 159–167, 2015.

[20] S. J. Page, G. D. Fulk, and P. Boyne, "Clinically important differences for the upper extremity Fugl-Meyer scale in people with minimal to moderate impairment due to chronic stroke," *Physical Therapy*, vol. 92, no. 6, pp. 791–798, 2012.

[21] N. Khodaparast, M. P. Kilgard, R. Casavant et al., "Vagus nerve stimulation during rehabilitative training improves forelimb recovery after chronic ischemic stroke in rats," *Neurorehabilitation and Neural Repair*, vol. 30, no. 7, pp. 676–684, 2016.

[22] P. Follesa, F. Biggio, G. Gorini et al., "Vagus nerve stimulation increases norepinephrine concentration and the gene expression of BDNF and bFGF in the rat brain," *Brain Research*, vol. 1179, pp. 28–34, 2007.

[23] Q. Gu, "Neuromodulatory transmitter systems in the cortex and their role in cortical plasticity," *Neuroscience*, vol. 111, no. 4, pp. 815–835, 2002.

[24] P. Profice, F. Pilato, M. Dileone et al., "Use of transcranial magnetic stimulation of the brain in stroke rehabilitation," *Expert Review of Neurotherapeutics*, vol. 7, no. 3, pp. 249–258, 2007.

Hindawi
Neural Plasticity
Volume 2017, Article ID 4281532, 12 pages
https://doi.org/10.1155/2017/4281532

Research Article

Interhemispheric Pathways Are Important for Motor Outcome in Individuals with Chronic and Severe Upper Limb Impairment Post Stroke

Kathryn S. Hayward,[1,2,3] Jason L. Neva,[1] Cameron S. Mang,[4] Sue Peters,[4] Katie P. Wadden,[4] Jennifer K. Ferris,[4] and Lara A. Boyd[1,5]

[1]*Department of Physical Therapy, University of British Columbia, Vancouver, BC, Canada V6T 1Z3*
[2]*Stroke Division, Florey Institute of Neuroscience and Mental Health, University of Melbourne, Melbourne, VIC 3084, Australia*
[3]*NHMRC Centre of Research Excellence in Stroke Rehabilitation and Brain Recovery, Melbourne, VIC 3084, Australia*
[4]*Graduate Program in Rehabilitation Sciences, Faculty of Medicine, University of British Columbia, Vancouver, BC, Canada V6T 1Z3*
[5]*Djavad Mowafaghian Centre for Brain Health, University of British Columbia, Vancouver, BC, Canada V6T 1Z3*

Correspondence should be addressed to Lara A. Boyd; lara.boyd@ubc.ca

Received 23 March 2017; Revised 27 June 2017; Accepted 8 August 2017; Published 16 November 2017

Academic Editor: Annalena Venneri

Background. Severity of arm impairment alone does not explain motor outcomes in people with severe impairment post stroke. *Objective*. Define the contribution of brain biomarkers to upper limb motor outcomes in people with severe arm impairment post stroke. *Methods*. Paretic arm impairment (Fugl-Meyer upper limb, FM-UL) and function (Wolf Motor Function Test rate, WMFT-rate) were measured in 15 individuals with severe (FM-UL ≤ 30/66) and 14 with mild–moderate (FM-UL > 40/66) impairment. Transcranial magnetic stimulation and diffusion weight imaging indexed structure and function of the corticospinal tract and corpus callosum. Separate models of the relationship between possible biomarkers and motor outcomes at a single chronic (≥6 months) time point post stroke were performed. *Results*. Age ($\Delta R^2$0.365, $p = 0.017$) and ipsilesional-transcallosal inhibition ($\Delta R^2$0.182, $p = 0.048$) explained a 54.7% ($p = 0.009$) variance in paretic WMFT-rate. Prefrontal corpus callous fractional anisotropy (PF-CC FA) alone explained 49.3% ($p = 0.007$) variance in FM-UL outcome. The same models did not explain significant variance in mild–moderate stroke. In the severe group, k-means cluster analysis of PF-CC FA distinguished two subgroups, separated by a clinically meaningful and significant difference in motor impairment ($p = 0.049$) and function ($p = 0.006$) outcomes. *Conclusion*. Corpus callosum function and structure were identified as possible biomarkers of motor outcome in people with chronic and severe arm impairment.

1. Introduction

Upper limb impairment post stroke is a devastating personal experience [1], and it remains challenging to prognosticate outcome [2]. To date, clinical measures administered early (<7 days post stroke) appear to be the best predictors of recovery of upper limb impairment and function [2]. However, there are important limitations to the use of clinical measures in people with severe upper limb impairment. First, a large amount of variability in motor outcome and recovery remains unexplained in people with severe upper limb impairment when only clinical measures are used during acute [2], subacute [3], and chronic [4] phases of recovery. Second, clinical measures do not provide information about the underlying neurobiology that may underpin outcome [5].

Increasing work suggests that brain biomarkers may be important to help better understand motor outcome and recovery of people with severe impairment after stroke [5–7]. A brain biomarker is an indicator of disease state that

can be used as a measure of underlying molecular/cellular processes that may be difficult to measure directly in humans and could be used to understand outcome or predict recovery or treatment response [8]. While the ultimate goal for the field of stroke recovery is to identify brain biomarker/s in the early stages post stroke that can prognosticate potential for motor recovery [9], conducting longitudinal studies to this end is extremely time consuming and expensive. Cross-sectional studies, even in the chronic stage, are an important preliminary step that can identify possible brain biomarkers, which may be subsequently used to inform longitudinal studies [9].

The corticospinal tract (CST) has been identified as a biomarker of upper limb motor outcome in the chronic phase. Corticospinal tract indicators of poor outcome include (i) absence of an ipsilesional motor evoked potential (MEP) tested with transcranial magnetic stimulation (TMS) [7], (ii) poor integrity of CST streamlines indicated by low fractional anisotropy (FA) indexed with diffusion-weighted imaging (DW-MRI) [10], or (iii) high asymmetry between contralesional and ipsilesional CST FA [11]. Past work has also demonstrated that individuals with severe motor impairment and poor integrity of the CST achieve less meaningful motor recovery in the chronic phase [12]. However, there is emerging evidence that data characterizing the CST alone cannot fully explain the spectrum of outcomes that individuals with severe motor impairment after stroke may experience [13–15]. While a meta-analysis of individuals with severe upper limb impairment demonstrated that the presence of a MEP was associated with significantly less arm impairment (higher Fugl-Meyer upper limb score, FM-UL) [7], similar FM-UL scores were noted in people with and without a MEP. Collectively, this suggests that other structures may contribute to motor outcome after stroke.

Focus on the CST as the only biomarker of upper limb motor outcome post stroke neglects the fact that the motor system operates as a network [16, 17]. Research suggests that remote regions in the motor network may be biomarkers of motor outcome in people with severe upper limb impairment [7, 10, 18–21]. There is evidence that the corpus callosum structure (e.g., indexed using DW-MRI) and function (e.g., indexed using TMS) contribute to motor outcome in the chronic phase post stroke. This work suggests that the prefrontal corpus callosum structure (DW-MRI) and function (transcallosal inhibition using TMS) may be a compensatory network to support paretic upper limb movement [10, 22–24].

To date, no work has investigated the combined contribution of the CST and corpus callosum to motor outcome in a cohort of individuals with severe upper limb impairment. The first aim of this cross-sectional study was to define the contribution of the CST and corpus callosum, using measures of both function (from TMS) and structure (from DWI) to upper limb impairment and function in individuals with chronic and severe stroke (FM-UL $\leq$ 30/66). The second aim was to determine if the biomarker(s) identified in our first aim could distinguish motor outcome subgroups within a group of people with clinically severe upper limb impairment. These findings were compared to a control group who had mild–moderate arm impairment (FM-UL > 40/66). Based on past work [10, 11], we hypothesised that indices of the brain structure (DWI) would explain the greatest variance in motor function and impairment in people with severe motor impairment. Further, we expected that identified brain biomarkers would be unique to the severe group as compared to the mild–moderate group.

2. Materials and Methods

Twenty-nine adults with severe ($n = 15$) or mild–moderate ($n = 14$) upper limb impairment after stroke were studied. All were in the chronic phase post stroke (>6 months) [25]. Participants were recruited by convenience sampling from the community and local postings. Inclusion criteria were (1) clinically diagnosed first middle cerebral artery stroke on MRI, (2) residual hemiparesis involving the upper limb, and (3) greater than 12 months post stroke. Exclusion criteria were (1) age < 18 or >85 years, (2) contraindication to TMS or MRI, (3) unable to follow yes/no commands, (4) concomitant neurological or psychiatric disease (beyond stroke), or (5) musculoskeletal disorder interfering with upper limb motor assessment. Ethical approval was received from University of British Columbia and all participants provided written informed consent in accordance with the Declaration of Helsinki.

All participants underwent two assessment sessions: (1) clinical and neurophysiological (TMS) testing and (2) neuroimaging (3T MRI) at the University of British Columbia MRI Research Centre, Vancouver, British Columbia, Canada. In addition, demographic and stroke characteristics were collected from the participants, including stroke date and age at stroke onset.

2.1. Clinical Assessment. Valid and reliable tests of upper limb impairment and function were administered by licensed physical therapists that were independent of neuroimaging and neurophysiological assessment collection and analysis. All examiners were trained in the collection of these measures; inter-rater accuracy was confirmed to be >90% by an experienced examiner. The FM-UL was performed to index upper limb impairment. It consists of 33 items rated on a scale from 0 to 2, totalling a possible 66 points [26], where higher scores indicate less motor impairment. We defined participants with a FM-UL score of ≤30 as having severe upper limb impairment [27]. The Wolf Motor Function Test rate (WMFT-rate) [28] indexed upper limb function. It is a valid and reliable measure that has been validated across individuals with a range of upper limb impairment [29]. The test consists of 15 timed movement tasks using the paretic upper limb. Movement time for each task was used to calculate the task rate (WMFT-rate): 60 seconds/time to complete task (in seconds). If an individual could not perform the task in 120 seconds, a mean rate of 0 was given for that task. The average rate of function was calculated across all tasks; faster rates indicate better function [30].

2.2. Transcranial Magnetic Stimulation (TMS) Assessment. All TMS sessions were completed with the participant seated comfortably in a height-adjustable chair. TMS was delivered using a figure-of-eight-shaped coil (Magstim 70 mm P/N 9790, Magstim Co., UK) connected to a Magstim 200^2 stimulator (Magstim Co., UK). The anatomical T_1 scan for each individual was coregistered to digitized landmarks to enable integration of coil and participant brain anatomy data using the Brainsight™ software package (Rogue Research Inc.), and thus real-time position monitoring. Electromyography (EMG) was collected bilaterally from the participant's extensor carpi radialis (ECR) muscle with 3 cm-diameter circular surface recording electrodes (Covidien, Mansfield, MA) to index TMS-elicited MEPs and ongoing muscle activity. EMG data were collected using LabChart software (LabChart 7.0) and sampled at 2000 Hz, preamplified (1000x) and band-pass filtered at 10–1000 Hz using PowerLab data acquisition system and two bioamplifiers (AD instruments, Colorado Springs, CO). Data were recorded in a 450 ms sweep from 100 ms before to 350 ms after TMS delivery. The "hotspot" for eliciting MEPs in the contralateral extensor carpi radialis (ECR) was found by positioning the coil over the scalp region overlying the hand/forearm representation within the M1 [31]. Standard procedures for determining resting motor threshold (RMT) were performed [32]. TMS pulses were delivered at a random rate between 0.15 and 0.2 Hz during MEP and TCI assessment. When no ipsilesional hotspot was identified ($n = 13$), the location for stimulation was inferred from either (1) the mirrored location of the contralesional hemisphere hotspot or (2) the location of the hand knob identified on the anatomical T_1 scan.

For TCI assessment, participants were asked to squeeze a handgrip dynamometer (ADInstruments, Colorado Springs, CO) to produce an active isometric contraction in the arm ipsilateral to the identified ECR hotspot. The force signal was digitized and presented on a computer screen in front of the participant for real-time feedback to maintain a constant level of force production during testing. Twelve single TMS pulses were delivered at 150% RMT over the ECR hotspot while participants maintained a unilateral background muscle contraction of 50% maximum grip force output with the ipsilateral hand. When no ipsilesional MEP was identified, TMS pulses were delivered at 80% maximum stimulator output. A custom MATLAB script (MathWorks, Natick, MA) was used to identify the transient reduction in volitional EMG activity elicited by TMS applied over the M1 ipsilateral to the active muscle (termed the ipsilateral silent period or iSP) for each participant.

2.3. Processing Ipsilateral Silent Period (iSP). To calculate the iSP, EMG data from each hemisphere were full-wave rectified and averaged for each participant. Mean prestimulus EMG amplitude (100 ms prior to TMS delivery) was defined as baseline muscle activity. The onset of the iSP was defined as the poststimulus time point where the rectified EMG signal fell below prestimulus mean EMG and continued to decrease to less than two standard deviations below this level. The iSP offset was defined as the point at which the EMG signal resumed the level of the prestimulus mean activity consistently for a minimum of 2 ms [33]. All data points between the onset and offset comprised the iSP (Figure 1). The magnitude of iSP was defined as the average EMG level during the iSP (iSP_{mean}) relative to the mean prestimulus EMG (iSP_{mean}/pre-$stim_{mean}$) [34]. Smaller ratio values indicate larger iSP magnitude and greater TCI generated from the stimulated hemisphere to the contralateral (active) hemisphere. The iSP evoked when TMS was delivered over the contralesional and ipsilesional hemispheres which are termed contralesional-TCI and ipsilesional-TCI, respectively. See Figures 1(a), 1(b), 1(c), 1(d), and 1(e). Two researchers (JN/CM) completed TCI data processing. Twenty-five percent of data were randomly crosschecked; we noted >90% accuracy between personnel.

2.4. MRI Acquisition. All MRIs were acquired at the University of British Columbia MRI Research Centre on a Philips Achieva 3.0 T whole-body MRI scanner (Phillips Healthcare, Andover, MD) using an eight-channel sensitivity encoding head coil (SENSE factor = 2.4) and parallel imaging. A high-resolution T1-weighted anatomical scan (TR = 7.47 ms, TE = 3.65 ms, flip angle $\theta = 6^\circ$, FOV = 256 × 256 mm, 160 slices, and 1 mm^3 isotropic voxel) was collected to determine lesion location. A single high-angular resolution diffusion imaging (HARDI) scan was subsequently performed using a single-shot echo planar imaging (EPI) sequence (TR = 7096 ms, TE = 60 ms, FOV = 224 × 224 mm, 70 slices, and voxel dimensions = 2.2 × 2.2 × 2.2 mm^3). Diffusion weighting was applied across 60 independent noncollinear orientations ($b = 700$ s/mm^2), along with a single unweighted image ($b = 0$ s/mm^2).

2.5. Preprocessing. DWI data were first visually inspected for excessive motion artifact or instrumental noise using quality assurance tools available in the diffusion MRI software package ExploreDTI v4.2.2 (http://www.exploredti.com) [35]. For all images, signal intensity was modulated and the b-matrix rotated [36]. Imaging data were then corrected for motion and distortion with images in native space for corpus callosum (CC) and corticospinal (CST) tractography. Constrained spherical deconvolution (CSD) was used to model diffusion behaviour [37]. CSD was chosen as it is robust in the presence of multiple fibre populations (estimated to occur in greater than 90% of white matter voxels in the brain [38]) as it does not make assumptions regarding uniform diffusion of water within a voxel [37, 39] and is more sensitive in the severely damaged brain [40]. CSD-based deterministic whole-brain fibre tractography was initiated at each voxel using the following parameters: seedpoint resolution of 2 mm^3, 0.2 mm step size, maximum turning angle of >40°, and fibre length range of 50–500 mm [41]. Tractography employed a fibre alignment by continuous tracking algorithm approach [42] with FA values extracted from reconstructed streamlines. FA is a quantitative, unit-less measure of diffusion behaviour of water in the brain influenced by microstructural properties of white matter and is the most commonly reported measure of white matter microstructural properties after stroke [43]. All regions of interest were hand drawn by experienced

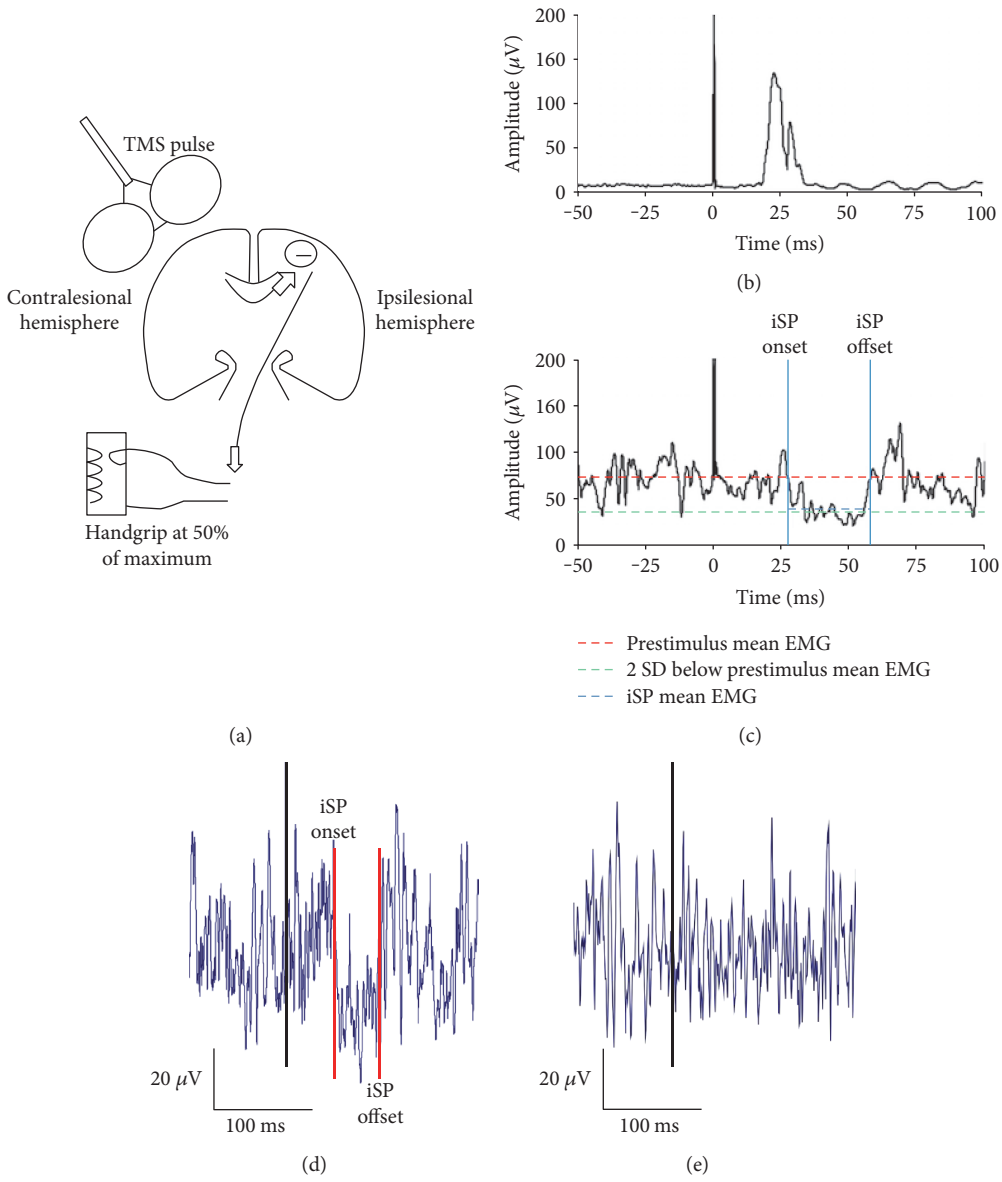

Figure 1: TMS-evoked TCI. (a) A schematic diagram of TMS-evoked TCI. Participants maintain a unilateral voluntary background muscle contraction in the arm ipsilateral to the TMS coil. A single TMS pulse is delivered to the motor cortex. The TMS pulse activates transcallosal pathways which transmit an inhibitory signal (−) to the active motor cortex. This elicits a transient quiescence in the background EMG in the active muscle. In the present example, TMS is delivered over the contralesional hemisphere to elicit the contra-iSP. TCI was also evoked with TMS delivered over the ipsilesional hemisphere to elicit the ipsi-iSP. (b) and (c) Rectified EMG data collected during a TMS session from a representative participant with mild to moderate impairment. (b) The motor evoked potential collected from the contralateral ECR muscle during the TCI procedure. (c) The EMG activity and iSP collected simultaneously from the ipsilateral ECR muscles. The iSP_{mean} ratio was calculated as: iSP mean EMG (blue line)/prestimulus mean EMG (red line). For ease of viewing, only 150 ms of the total 450 ms recording window is displayed. (d) and (e) Representative TCI output from the cohort of individuals with severe arm impairment. (d) The output from an individual when TCI was present. (e) The output from an individual when TCI was not present.

personnel (KH/JN/CM). We have previously established the inter-rater reliability of our processing and analysis procedures [40, 44].

2.6. Corticospinal Tract. Two regions of interest (ROIs) were drawn and applied to extract streamlines from the entire length of the CST. Firstly, a ROI was delineated in each hemisphere in the axial plane [45] as a "SEED" ROI around the posterior limb of the internal capsule at the level of the anterior commissure, a region through which motor fibres descend [45]. Secondly, a logical "AND" ROI was constructed in each hemisphere, around the CST at the level of the pons. The "AND" function introduced the requirement that only fibres passing through both the "SEED" and "AND" ROIs would be included for fibre tracking, similar to previous work [10]. On the basis of these ROIs, subsequent tract reconstructions of descending CST streamlines were produced and mean FA was calculated across the entire length of the

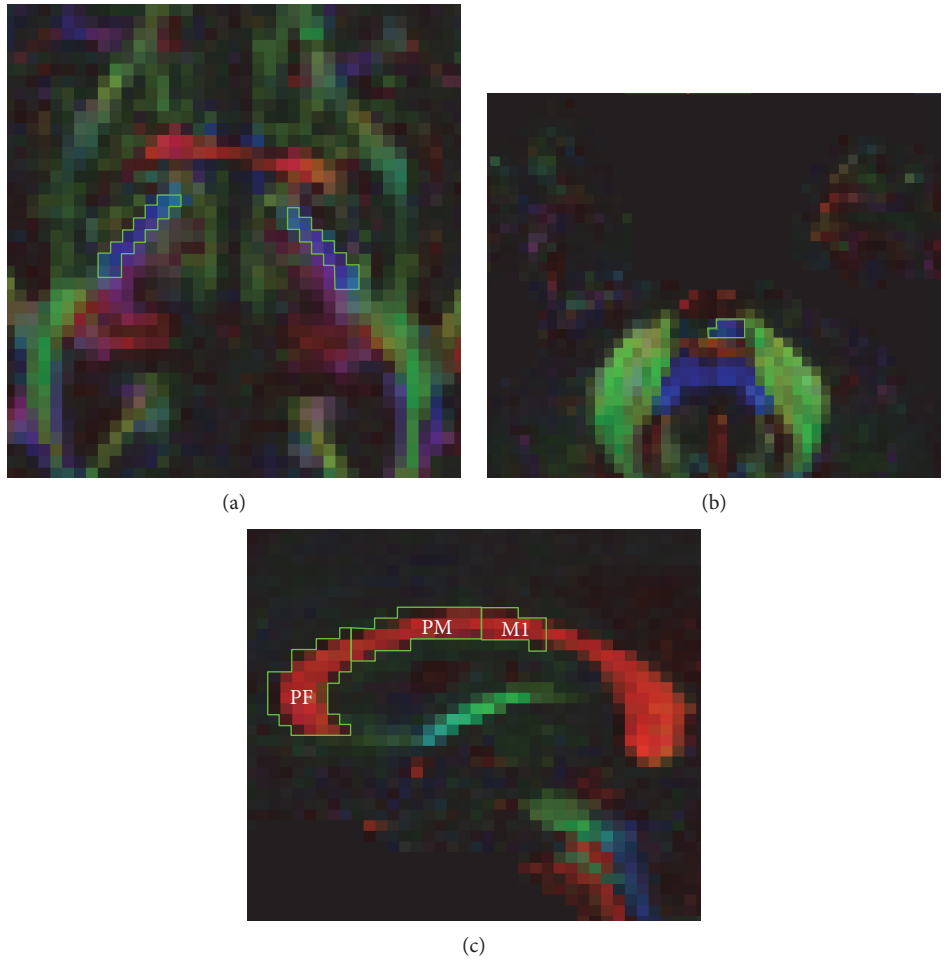

Figure 2: Representative regions of interest drawn on FA MAPS in ExploreDTI of an individual with severe arm impairment. Corticospinal tract regions of interest were drawn in the axial plane at the level of the (a) anterior commissure, and (b) pons as defined by Mang et al. [10]. (c) Corpus callosum regions of interest were drawn in the midsagittal plane according to a geometric partitioning scheme for regions I, II, and III according to Hofer and Frahm [46].

reconstruction. To compute the asymmetry index (equation: contralesional CST FA − ipsilesional CST FA/contralesional CST FA + ipsilesional CST FA). Figures 2(a) and 2(b) illustrate the CST ROIs in ExploreDTI.

2.7. Corpus Callosum. Callosal subregion ROIs were manually delineated in the midsagittal plane according to a geometric partitioning scheme [46]. Based on previous findings [10] and anatomical relevance [46], for this analysis, only streamlines projecting to subregion I (prefrontal, PF-CC), subregion II (premotor, PM-CC), and subregion III (primary motor, M1-CC) were extracted. Using each subregion ROI separately as a "SEED," interhemispheric streamlines passing these subregions of the corpus callosum were isolated and mean FA was calculated across the entire length of the reconstructed streamlines. Figure 2(c) illustrates the CC ROIs in Explore DTI.

2.8. Statistical Analysis. The primary dependent variable of interest was paretic WMFT-rate and the secondary dependent variable of interest was paretic FM-UL. Spearman's correlation coefficients (rho) were determined for the following variables in individuals with severe impairment: age, months since stroke onset, ipsilesional MEP (yes/no), ipsilesional-TCI, contralesional-TCI, ipsilesional CST FA, contralesional CST FA, PF-CC FA, PM-CC FA, and M1-CC FA. All variables with a $p < 0.05$ were considered to be significantly correlated with each dependent measure, while all variables with a $p < 0.1$ were considered to have a trending correlation with each dependent measure. A stepwise regression model was then performed for each dependent measure in individuals with severe impairment; all variables entered were at least $p < 0.1$. Separate stepwise regression models with these variables were performed for individuals with severe impairment and individuals with mild–moderate impairment. The stepping criteria was $p < 0.05$ to add and $p > 0.1$ to remove variables. We did not correct for multiple comparisons on the principle that the restrictiveness of Bonferroni correction could hinder initial exploratory studies with low participant numbers [47–49]. All statistics were performed in SPSS v23.0.

To determine if a variable identified in the stepwise regression model was able to differentiate levels of impairment and function within the severely impaired group, we

Table 1: Summary of group demographics and stroke characteristics.

	$n = 15$ severe	$n = 14$ mild–moderate
Age, year, mean (SD)	58.3 ± 12	68.3 ± 9.2
Gender, n = male : female	8 : 7	11 : 3
Lesion location, n = subcortical : cortical	9 : 6	11 : 3
Affected hemisphere, n = left : right	8 : 7	6 : 9
Affected arm, n = left : right	7 : 8	9 : 6
Months post stroke, mean (SD)	61.6 ± 50.0	80.1 ± 70.6
Fugl-Meyer upper limb, mean (SD), /66	16.7 ± 6.6	58.3 ± 4.0
Wolf Motor Function Test, rate, mean (SD)	10.6 ± 5.5	42.2 ± 12.0

used a two-group k-means cluster analysis. This approach provides a hypothesis-free classification of participants according to a variable of interest. It was performed when a single variable in isolation explained a significant amount of the variance in impairment or function. The mean difference between clusters was used to define higher and lower motor outcome clusters. To confirm that clusters differentiated meaningful subgroups based on model allocation, we investigated if clusters were separated by a minimal clinically important difference in motor impairment or function. For impairment, mean FM-UL scores for identified clusters should be separated by at least 5.75 points [50], and for motor function, mean WMFT-rate scores for identified clusters should be separated by >10% difference between groups [51]. Independent sample t-tests indicated descriptively the cluster analyses' goodness-of-fit ($p < 0.05$). Based on cluster model allocation, specificity and sensitivity of the algorithm for impairment and function outcomes were determined.

3. Results

Fifteen individuals with chronic, severe upper limb impairment (FM-UL mean 17 ± 7) and 14 individuals with chronic, mild–moderate upper limb impairment (FM-UL mean 58 ± 4) were evaluated. Table 1 outlines the group summary demographic, motor impairment and function outcomes, and Table 2 contains information on dependent and independent variables for each individual participant.

3.1. Upper Limb Function (WMFT-Rate). Age (rho = −0.682, $p = 0.005$) and PF-CC (rho = 0.609, $p = 0.016$) were significantly associated with paretic WMFT-rate, while contralesional-CST (rho = 0.486, $p = 0.066$) and ipsilesional-TCI (rho = 0.447, $p = 0.095$) showed a trend towards significance. The stepwise regression model identified age (R^2 change 0.365, $p = 0.017$) and ipsilesional-TCI (R^2 change 0.182, $p = 0.048$) to explain 54.7% ($p = 0.009$) of the variance in paretic WMFT-rate (Figures 3(a) and 3(b)). The same model was performed in individuals with mild–moderate upper limb impairment and no variables emerged to significantly explain variance of paretic WMFT-rate in this group ($p > 0.05$).

3.2. Upper Limb Impairment (FM-UL). PF-CC (rho = 0.658, $p = 0.008$), PM-CC (rho = 0.747, $p = 0.001$), and M1-CC (rho = 0.715, $p = 0.003$) were significantly associated with FM-UL. The stepwise regression model identified PF-CC as significantly explaining 49.3% of the variance in FM-UL ($p = 0.007$) (Figure 3(c)). The same model was performed in a cohort of individuals with mild–moderate upper limb impairment and no variables emerged to significantly explain the variance of the paretic FM-UL ($p > 0.05$).

3.3. Cluster Analysis. k-means cluster analysis was performed using PF-CC FA. Two clusters were identified: cluster A mean PF-CC FA = 0.384 and cluster B mean PF-CC FA = 0.298. The midpoint between clusters was 0.341 (Figure 4(a)), with modeling allocating individuals with a PF-CC FA above the midpoint labeled as cluster A, higher outcome, and PF-CC FA below the midpoint labeled as cluster B, lower outcome. The clusters represented clinically relevant groups (Figure 4(b)), demonstrated by clinically meaningful and significant differences between groups for motor impairment (FM-UL mean difference 6.6 points, $t = 2.174$, df 13, $p = 0.049$) and motor function (WMFT-rate mean difference 7.3 repetitions, $t = 3.316$, df 13, $p = 0.006$). Based on this clustering, specificity was 43%, but sensitivity was 88% for FM-UL. For WMFT-rate, specificity was 86% and sensitivity was 88%.

4. Discussion

Ipsilesional TCI from M1 (function) and prefrontal corpus callosum (structure) explained significant variance in motor outcome at a single chronic time point in individuals with severe upper limb impairment post stroke. Contrary to our hypothesis, a structural index derived from DWI did not explain greatest variance in upper limb function. Rather, interhemispheric inhibition indexed from the ipsilesional to contralesional M1 with TCI, along with younger age, explained the most variance in motor function. An index of brain structure (PF-CC FA) did explain the greatest amount of variance in arm impairment, and this variable was associated with function. Building upon these findings, a cluster analysis using PF-CC FA identified two clusters that were separated by a clinically meaningful and significant difference in motor impairment and function. While it is unlikely that one variable will accurately prognosticate all individuals, it appears that interhemispheric communication is an important consideration to understand motor outcomes in the chronic phase.

Table 2: Individual participant demographics and stroke characteristics.

ID	Stroke location	MSS	Age	FM-UL	WMFT-rate, NP	WMFT-rate, P	L MEP Rest	L TCI mean	NL TCI mean	PF-CC FA	PM-CC FA	M1-CC FA	L CST FA	NL CST FA
1	Subcortical	41	63	23	71.5	10.3	0	0.64	0.66	0.40	0.40	0.41	0.39	0.52
2	Cortical	91	61	16	83.0	11.7	0	0.73	0.74	0.23	0.13	0.20	0.31	0.49
3	Cortical	85	62	8	53.9	9.6	0	0.64	0.84	0.28	0.25	0.30	0.36	0.50
4	Cortical	94	57	7	50.6	9.6	0	0.52	—	0.30	0.29	0.34	0.35	0.45
5	Cortical	22	51	16	50.6	1.5	0	0.49	0.80	0.33	0.36	0.42	0.46	0.51
6	Cortical	25	69	11	46.6	0.9	0	0.64	0.81	0.30	0.29	0.30	0.33	0.50
7	Subcortical	21	65	15	45.7	9.3	0	0.60	0.80	0.36	0.35	0.35	0.37	0.46
8	Subcortical	22	57	16	75.9	17.1	0	0.82	0.83	0.38	0.40	0.41	0.45	0.53
9	Subcortical	94	36	11	61.0	14.3	0	0.88	0.80	0.37	0.29	0.22	0.26	0.49
10	Subcortical	145	64	16	62.8	9.9	1	0.79	0.91	0.35	0.36	0.43	0.47	0.50
11	Subcortical	23	72	16	71.8	7.9	0	0.76	0.93	0.28	0.36	0.38	0.45	0.42
12	Subcortical	33	33	18	146.8	20.1	0	0.74	—	0.41	0.42	0.42	0.33	0.55
13	Subcortical	47	51	29	62.3	19.0	0	0.72	0.77	0.40	0.41	0.43	0.44	0.58
14	Cortical	160	57	30	27.4	12.1	1	0.80	0.89	0.41	0.41	0.45	0.43	0.47
15	Subcortical	21	77	18	32.6	6.4	0	0.85	0.59	0.32	0.32	0.37	0.40	0.49
Mean	—	61.6	58.3	16.7	62.8	10.7	—	0.71	0.80	0.34	0.33	0.36	0.39	0.50
SD	—	47.0	12.02	6.6	27.9	5.5	—	0.12	0.10	0.05	0.08	0.08	0.06	0.04
Min	—	21.0	33.0	7.0	27.4	0.9	—	0.49	0.59	0.28	0.13	0.20	0.26	0.42
Max	—	160.0	77.0	30.0	146.8	20.1	—	0.88	0.93	0.41	0.42	0.45	0.47	0.58
1	Subcortical	155	76	49	48.17	34.11	1	1.00	0.68	0.32	0.29	0.36	0.39	0.52
2	Subcortical	23	60	54	54.77	39.90	1	0.62	0.67	0.32	0.32	0.42	0.51	0.51
3	Cortical	270	59	55	44.71	23.98	1	0.56	0.74	0.38	0.29	0.33	0.38	0.51
4	Subcortical	83	71	56	64.21	52.01	1	0.65	0.53	0.37	0.38	0.42	0.41	0.44
5	Cortical	94	64	56	55.27	46.88	1	1.00	0.67	0.36	0.22	0.13	0.42	0.48
6	Subcortical	15	69	57	62.82	52.99	1	0.69	0.63	0.40	0.41	0.45	0.45	0.53
7	Subcortical	82	67	59	79.77	62.95	1	0.65	0.67	0.34	0.33	0.40	0.46	0.52
8	Subcortical	142	73	60	76.42	57.58	1	0.57	0.61	0.40	0.37	0.40	0.39	0.49
9	Subcortical	35	85	60	40.72	34.49	1	0.44	0.69	0.34	0.31	0.35	0.41	0.49
10	Subcortical	18	79	61	54.93	45.00	1	1.00	1.00	0.33	0.33	0.40	0.45	0.49
11	Subcortical	81	76	62	63.57	64.07	1	0.78	0.82	0.37	0.36	0.41	0.45	0.41
12	Cortical	67	65	62	52.35	44.44	1	1.00	0.52	0.35	0.37	0.35	0.35	0.48
13	Subcortical	20	62	62	64.96	58.65	1	0.68	1.00	0.37	—	0.44	0.44	0.43
14	Subcortical	37	50	63	61.49	58.16	1	0.62	0.55	0.38	0.39	0.38	0.47	0.49
Mean	—	80.0	68.0	58.3	58.9	48.2	—	0.73	0.69	0.36	0.34	0.37	0.41	0.49
SD	—	71.0	9.2	4.0	11.1	12.0	—	0.19	0.15	0.03	0.05	0.08	0.06	0.03
Min	—	15.0	50.0	49.0	40.7	24.0	—	0.44	0.52	0.32	0.22	0.13	0.31	0.43
Max	—	270.0	85.0	63.0	79.8	64.1	—	1.00	1.00	0.40	0.41	0.45	0.51	0.53

CST: corticospinal tract; FA: fractional anisotropy; FM-UL: Fugl-Meyer upper limb; M1-CC: primary motor corpus callosum; min: minimum; max: maximum; MSS: months since stroke; L: ipsilesional; NL: contralesional; NP: nonparetic; P: paretic; PF-CC: prefrontal corpus callosum; PM-CC: premotor corpus callosum; SD: standard deviation; WMFT: Wolf Motor Function Test rate.

4.1. Prefrontal Corpus Callosum Structure Differentiated Motor Outcome Experienced by People with Severe Upper Limb Impairment. Structural integrity of the prefrontal segment of the corpus callosum (PF-CC) explained motor outcome over and above ipsilesional corticospinal tract integrity in people with chronic and severe upper limb impairment. Given that the CST had sustained significant damage, coupled with a higher probability of prefrontal areas surviving after stroke [52], it is perhaps not surprising that structures in the prefrontal region would emerge as the principal explanatory variable. Failure of CST streamlines alone to be related to better outcome in individuals with severe stroke is consistent with our recent individual patient data review [7] and other empirical work [14, 21]. Importantly, PF-CC structural integrity differentiated individuals with chronic and severe upper limb impairment after stroke

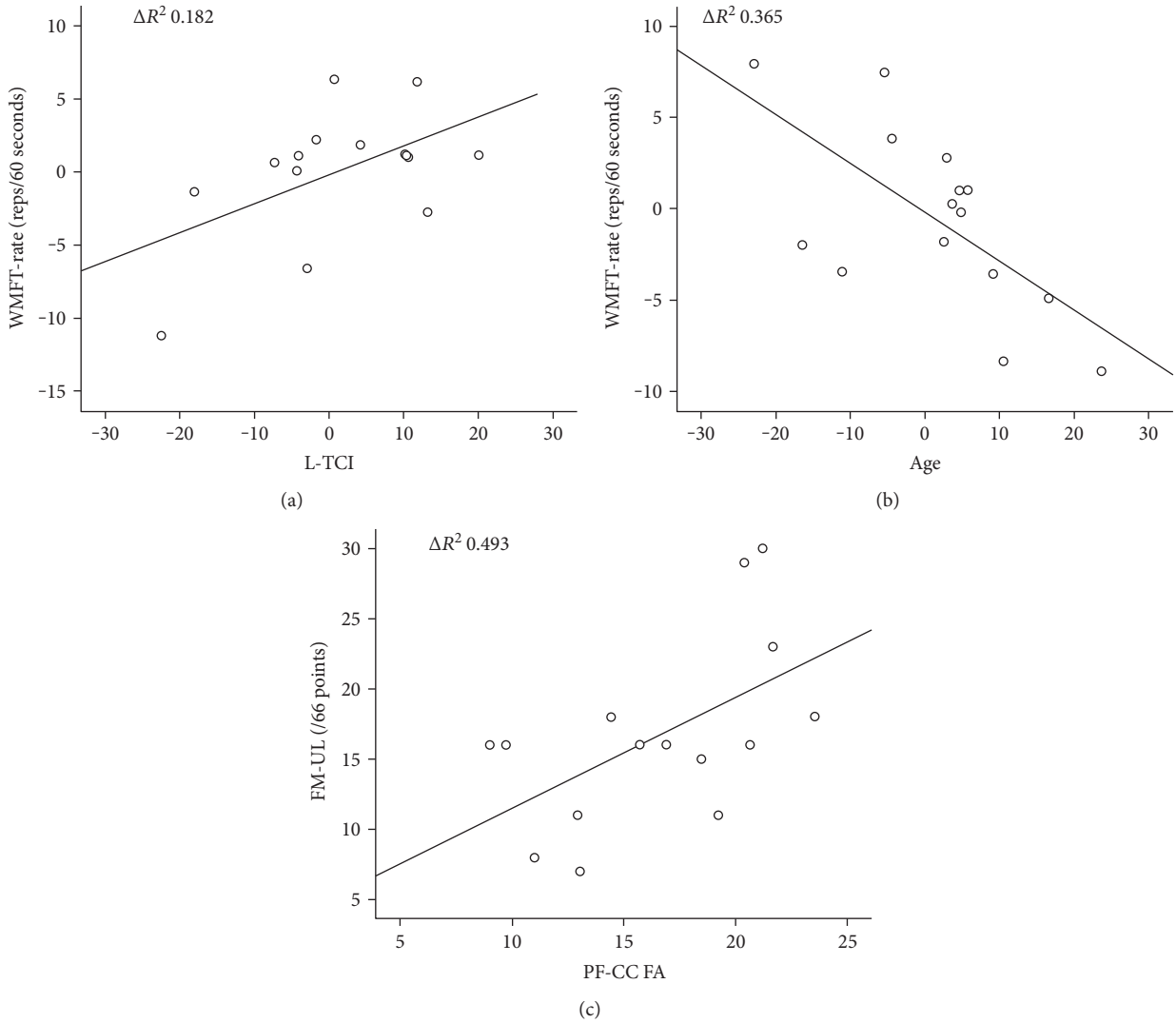

Figure 3: Partial plots for stepwise multiple linear regression model for the cohort of individuals with severe upper limb impairment, $n = 15$. (a) Wolf Motor Function Test rate and transcallosal inhibition from ipsilesional M1 to contralesional M1; (b) Wolf Motor Function Test rate and age; and (c) Fugl-Meyer upper limb assessment, prefrontal corpus callosum. WMFT-rate: Wolf Motor Function Test rate; L-TCI: lesioned transcallosal inhibition; FM-UL: Fugl-Meyer upper limb; PF-CC FA: prefrontal corpus callosum fractional anisotropy.

into two subgroups that were separated by a clinically meaningful difference in motor impairment and function outcome scores. This identifies a biological state in the chronic phase that could be tested in acute stroke trials in the future. Such data would enable evaluation of whether structural integrity in the PF-CC is critical in the acute stage or if it reflects a compensatory pattern that emerges with time post stroke.

4.2. How May the Prefrontal Corpus Callosum Contribute to Better Outcome after Severe Stroke? The emergence of the prefrontal corpus callosum may represent a compensatory pathway that can mediate motor outcomes in people with chronic and severe upper limb impairment after stroke. Building on evidence from the current study and previous studies of humans with [22] and without stroke [10], as well as nonhuman primates [53, 54], we propose a theoretical framework that underpins our findings.

Firstly, prefrontal regions of the brain are remotely connected to M1. A study of rhesus monkeys demonstrated that prefrontal regions of the brain (including regions 46, 9, 46v, and 46d) have projections to the premotor cortex (regions 6d, 6v) and subsequently the primary motor cortex (region 4) [54]. In humans, we cannot establish this multistep pathway. However, inhibitory signals are able to be sent from dorsolateral prefrontal cortex to M1 (within hemisphere) and between hemispheres, that is, the ipsilateral dorsolateral prefrontal cortex to the contralateral M1 in healthy young and healthy older individuals [55], as well as people with mild to severe arm impairment after stroke [56]. Therefore, it is possible that a pathway originating in the prefrontal area and ending in the primary motor area exists to be exploited.

Secondly, signals from the primary motor cortex can descend peripherally to the ipsilateral upper limb. Studies of CST architecture demonstrate that 10–15% of CST fibres

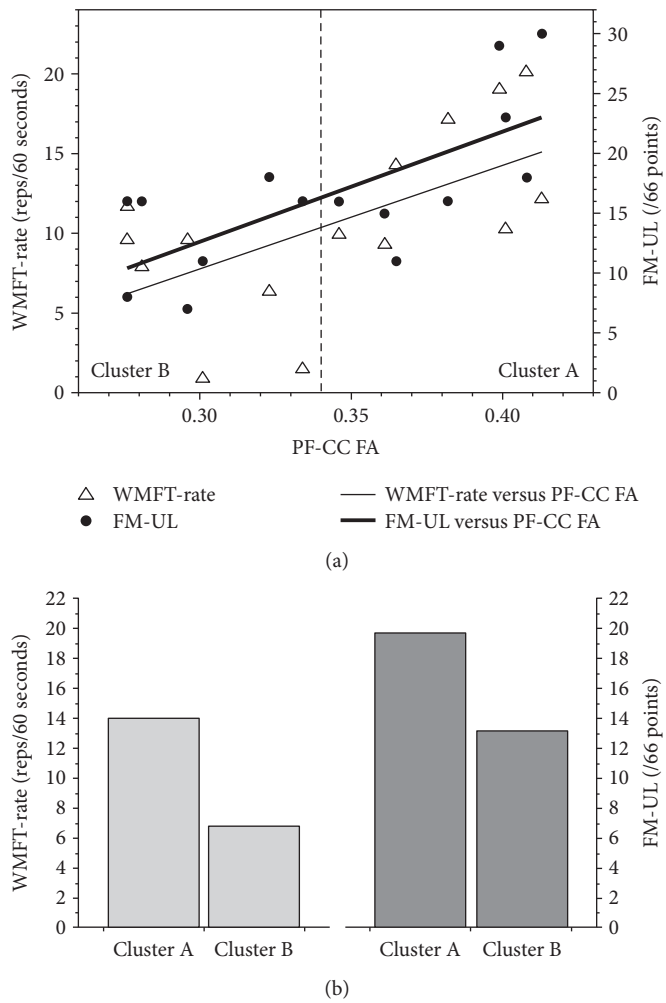

Figure 4: (a) From the group of individuals with severe arm impairment ($n = 15$), k-means cluster analysis of PF-CC FA identified two groups: cluster A, higher outcome, and cluster B, lower outcome. (b) Between group differences for cluster A and cluster B were significant for function (Wolf Motor Function Test rate (WMFT-rate), $p = 0.006$) and impairment (Fugl-Meyer upper limb (FM-UL), $p = 0.049$). PF-CC: prefrontal corpus callosum; FA: fractional anisotropy; WMFT-rate: Wolf Motor Function Test rate; FM-UL: Fugl-Meyer upper limb.

do not cross the midline in the brainstem and form the anterior CST [57]. Tracking these fibres peripherally indicates that they remain ipsilateral to innervate the proximal arm musculature. Individuals post stroke that exhibit little sparing of the ipsilesional CST may benefit from tapping into this anatomical redundancy as it may be the only remaining means by which paretic motor output may be produced [13]. Indeed, proximal movements are more likely to return to the paretic upper limb after severe stroke [4, 58, 59]. Our data show that higher FA from the contralateral CST (indexed with DW-MRI) was associated with higher motor function, suggesting that this pathway may be used to enable motor outcomes in the paretic limb of those with severe motor impairment after stroke.

Thirdly, less inhibition from the ipsilesional to contralesional M1, which was associated with better motor function (higher WMFT-rate) in people with severe impairment, could also support access to uncrossed, anterior CST fibres. This fits with previous work which found that suppression of contralesional M1 activity, through interventions such as inhibitory repetitive TMS, may be contraindicated for individuals with major disruption of the ipsilesional CST [60].

Taken together, interhemispheric communication (structural PF-CC indexed using DW-MRI and functional TCI indexed from TMS) may support a compensatory mechanism that helps to overcome poor ipsilesional CST integrity. Our findings provide a preliminary framework to test in a nonhuman primate model and in longitudinal studies of humans with severe upper limb impairment post stroke. If found to be reliable, they may provide a potential cortical target for noninvasive brain stimulation techniques, such as repetitive TMS or transcranial direct current stimulation, that attempt to amplify functionally relevant brain regions.

4.3. Strengths and Limitations. This study represents an important advance in our understanding of the biological state of the brain in the chronic stage in a cohort of individuals with severe upper limb impairment. However, it has several limitations. Firstly, our design is cross-sectional and conducted in the chronic phase post stroke. We did not have

access to information about participant status early post stroke. As such, it does not enable us to understand if our finding is a recovery-mediated outcome that reflects the system's best effort to respond to motor limitations. A longitudinal design that recruits participants early post stroke (e.g., within the first 7–28 days post stroke) and follows participants at meaningful time points (e.g., 3–6 and 12 months post stroke) is required to answer this question [25]. Secondly, we performed a k-means cluster on the same small cohort of severe stroke participants to confirm the findings of the regression analysis. This provided capacity to confirm that there were two groups in the current data based on PF-CC FA, but our data cannot be used to confirm a cut point or for individual prognostication. A larger, independent sample with longitudinal data from multiple sites is required to achieve this objective. Thirdly, the streamlines evaluated are reconstructions; they do not definitively establish whether structural connections provide afferent or efferent input, to or from a target region. As such, we only hypothesise the potential cascade of signals from the information collated. Fourth, our collection of TCI involved a handgrip contraction that generated EMG activity in both wrist extensors and flexors, which may have resulted in an underestimation of iSP due to reciprocal inhibition between the flexors and extensors in the nervous system. However, the individuals in this study had severe upper limb impairment and were unable to perform isolated wrist extension; therefore, whole handgrip contraction was employed. Finally, as is the case for all diffusion imaging studies, the number of streamlines extracted is based on reconstruction of imaging data derived from an algorithm computed with the software (*Explore DTI 4.2.2*) and errors related to midline shift, physiological noise, and microstructural changes in brain tissue may have influenced microstructural properties extracted. These limitations may collectively increase the risk of type 1 bias.

5. Conclusion

The data in this study suggest that the interhemispheric communication may support motor outcomes in individuals with severe and chronic upper limb impairment after stroke. The prefrontal areas could be a target for interventional studies that attempt to enable motor recovery of people with severe upper limb impairment. Further investigation is required to determine the role of PF-CC early post stroke and in mediating recovery.

Conflicts of Interest

The authors declare that they have no conflicts of interest.

Authors' Contributions

Kathryn S. Hayward, Jason L. Neva, Sue Peters, Katie P. Wadden, and Lara A. Boyd conceived the study; Jason L. Neva, Katie P. Wadden, Cameron S. Mang, and Jennifer K. Ferris collected the data; Kathryn S. Hayward, Jason L. Neva, Cameron S. Mang, and Lara A. Boyd analysed the data; Kathryn S. Hayward, Jason L. Neva, Cameron S. Mang, and Lara A. Boyd performed statistical analyses; Kathryn S. Hayward principally wrote the paper; and all authors reviewed and critiqued the paper.

Acknowledgments

This work was funded by a grant from the Canadian Institutes of Health Research (CIHR) (MOP-106651 to Lara A. Boyd). Kathryn S. Hayward was supported by the Heart and Stroke Foundation Canada, Michael Smith Foundation for Health Research (MSFHR), British Columbia, Canada (15980), and National Health and Medical Research Council of Australia (1088449); Jason L. Neva was supported by CIHR and MSFHR; Cameron S. Mang and Katie P. Wadden were supported by Natural Sciences and Engineering Research Council; Sue Peters and Jennifer K. Ferris were supported by CIHR; and Lara A. Boyd was supported by the Canada Research Chairs and the MSFHR (CI-SCH-01796).

References

[1] R. N. Barker and S. G. Brauer, "Upper limb recovery after stroke: the stroke survivors' perspective," *Disability and Rehabilitation*, vol. 27, pp. 1213–1223, 2005.

[2] C. Winters, M. W. Heymans, E. E. van Wegen, and G. Kwakkel, "How to design clinical rehabilitation trials for the upper paretic limb early post stroke?," *Trials*, vol. 17, p. 468, 2016.

[3] C. L. Koh, S. L. Pan, J. S. Jeng et al., "Predicting recovery of voluntary upper extremity movement in subacute stroke patients with severe upper extremity paresis," *PLoS One*, vol. 10, article e0126857, 2015.

[4] R. N. Barker, S. G. Brauer, and R. G. Carson, "Training of reaching in stroke survivors with severe and chronic upper limb paresis using a novel nonrobotic device: a randomized clinical trial," *Stroke*, vol. 39, pp. 1800–1807, 2008.

[5] N. S. Ward, "Does neuroimaging help to deliver better recovery of movement after stroke?," *Current Opinion in Neurology*, vol. 28, pp. 323–329, 2015.

[6] C. M. Stinear, P. A. Barber, M. Petoe, S. Anwar, and W. D. Byblow, "The PREP algorithm predicts potential for upper limb recovery after stroke," *Brain*, vol. 135, pp. 2527–2535, 2012.

[7] K. S. Hayward, J. Schmidt, K. R. Lohse et al., "Are we armed with the right data? Pooled individual data review of biomarkers in people with severe upper limb impairment after stroke," *NeuroImage: Clinical*, vol. 13, pp. 310–319, 2017.

[8] J. Bernhardt, K. Borschmann, L. Boyd et al., "Moving rehabilitation research forward: developing consensus statements for rehabilitation and recovery research," *International Journal of Stroke*, vol. 11, pp. 454–458, 2016.

[9] L. A. Boyd, K. S. Hayward, N. S. Ward et al., "Biomarkers of stroke recovery: consensus-based core recommendations from the stroke recovery and rehabilitation roundtable," *International Journal of Stroke*, vol. 12, pp. 480–493, 2017.

[10] C. S. Mang, M. R. Borich, S. M. Brodie et al., "Diffusion imaging and transcranial magnetic stimulation assessment of transcallosal pathways in chronic stroke," *Clinical Neurophysiology*, vol. 10, pp. 1951–1971, 2015.

[11] C. M. Stinear, P. A. Barber, P. R. Smale, J. P. Coxon, M. K. Fleming, and W. D. Byblow, "Functional potential in chronic stroke patients depends on corticospinal tract integrity," *Brain*, vol. 130, pp. 170–180, 2007.

[12] R. M. Levy, R. L. Harvey, B. M. Kissela et al., "Epidural electrical stimulation for stroke rehabilitation: results of the prospective, multicenter, randomized, single-blinded Everest trial," *Neurorehabilitation and Neural Repair*, vol. 30, pp. 107–119, 2016.

[13] R. N. Barker, S. G. Brauer, B. K. Barry, T. J. Gill, and R. G. Carson, "Training-induced modifications of corticospinal reactivity in severely affected stroke survivors," *Experimental Brain Research*, vol. 221, pp. 211–221, 2012.

[14] J. M. Rondina, C. H. Park, and N. S. Ward, "Brain regions important for recovery after severe post-stroke upper limb paresis," *Journal of Neurology, Neurosurgery, and Psychiatry*, vol. 88, no. 9, pp. 737–743, 2017.

[15] K. S. Hayward, S. G. Brauer, K. L. Ruddy, D. Lloyd, and R. G. Carson, "Repetitive reaching training combined with transcranial random noise stimulation in stroke survivors with chronic and severe arm paresis is feasible: a pilot, triple-blind, randomised case series," *Journal of Neuroengineering and Rehabilitation*, vol. 14, p. 46, 2017.

[16] R. J. Nudo and G. W. Miliken, "Reorganization of movement representations in primary motor cortex following focal ischemic infarcts in adult squirrel monkeys," *Journal of Neurophysiology*, vol. 75, pp. 2144–2149, 1996.

[17] R. J. Nudo, E. J. Plautz, and S. B. Frost, "Role of adaptive plasticity in recovery of function after damage to motor cortex," *Muscle & Nerve*, vol. 8, pp. 1000–1019, 2001.

[18] K. P. Wadden, T. S. Woodward, P. D. Metzak et al., "Compensatory motor network connectivity is associated with motor sequence learning after subcortical stroke," *Behavioural Brain Research*, vol. 286, pp. 136–145, 2015.

[19] S. K. Meehan, B. Randhawa, B. Wessel, and L. A. Boyd, "Implicit sequence-specific motor learning after subcortical stroke is associated with increased prefrontal brain activations: an fMRI study," *Human Brain Mapping*, vol. 32, pp. 290–303, 2011.

[20] J. M. Rondina, M. Filippone, M. Girolami, and N. S. Ward, "Decoding post-stroke motor function from structural brain imaging," *Neuroimage: Clinical*, vol. 12, pp. 372–380, 2016.

[21] C. H. Park, N. Kou, and N. S. Ward, "The contribution of lesion location to upper limb deficit after stroke," *Journal of Neurology, Neurosurgery & Psychiatry*, vol. 87, pp. 1283–1286, 2016.

[22] K. L. Ruddy, A. Leemans, and R. G. Carson, "Transcallosal connectivity of the human cortical motor network," *Brain Structure and Function*, vol. 222, pp. 1243–1252, 2016.

[23] U. Puh, A. Vovk, F. Sevsek, and D. Suput, "Increased cognitive load during simple and complex motor tasks in acute stage after stroke," *International Journal of Psychophysiology*, vol. 63, pp. 173–180, 2007.

[24] H. M. Sisti, M. Geurts, J. Gooijers, M. H. Heitger, K. Caeyenberghs, and I. A. Beets, "Microstructural organization of corpus callosum projections to prefrontal cortex predicts bimanual motor learning," *Learning & Memory*, vol. 19, pp. 351–357, 2012.

[25] J. Bernhardt, K. S. Hayward, G. Kwakkel et al., "Agreed definitions and a shared vision for new standards in stroke recovery research: the stroke recovery and rehabilitation roundtable taskforce," *International Journal of Stroke*, vol. 12, pp. 444–450, 2017.

[26] A. R. Fugl-Meyer, L. Jaasko, I. Leyman, S. Olsson, and S. Steglind, "The post-stroke hemiplegic patient. 1. A method for evaluation of physical performance," *Scandinavian Journal of Rehabilitation Medicine*, vol. 7, pp. 13–31, 1975.

[27] B. H. Dobkin and S. T. Carmichael, "The specific requirements of neural repair trials for stroke," *Neurorehabilitation and Neural Repair*, vol. 30, pp. 470–478, 2016.

[28] S. L. Wolf, P. A. Catlin, M. Ellis, A. L. Archer, B. Morgan, and A. Piacentino, "Assessing Wolf Motor Function Test as outcome measure for research in patients after stroke," *Stroke*, vol. 32, pp. 1635–1639, 2001.

[29] T. Hodics, L. G. Cohen, and S. C. Cramer, "Functional imaging of intervention effects in stroke motor rehabilitation," *Archives of Physical Medicine and Rehabilitation*, vol. 87, pp. 36–42, 2006.

[30] T. M. Hodics, K. Nakatsuka, B. Upreti, A. Alex, P. S. Smith, and J. C. Pezzullo, "Wolf Motor Function Test for characterizing moderate to severe hemiparesis in stroke patients," *Archives of Physical Medicine and Rehabilitation*, vol. 93, pp. 1963–1967, 2012.

[31] T. A. Yousry, U. D. Schmid, H. Alkadhi et al., "Localization of the motor hand area to a knob on the precentral gyrus. A new landmark," *Brain*, vol. 120, Part 1, pp. 141–157, 1997.

[32] P. M. Rossini, A. Berardelli, G. Deuschl et al., "Applications of magnetic cortical stimulation. The International Federation of Clinical Neurophysiology," *Electroencephalography and Clinical Neurophysiology-Supplement*, vol. 52, pp. 171–185, 1999.

[33] B. W. Fling and R. D. Seidler, "Task-dependent effects of interhemispheric inhibition on motor control," *Behavioural Brain Research*, vol. 226, pp. 211–217, 2012.

[34] P. Jung and U. Ziemann, "Differences of the ipsilateral silent period in small hand muscles," *Muscle & Nerve*, vol. 34, pp. 431–436, 2006.

[35] A. Leemans, B. Jeurissen, J. Sijbers, and D. K. Jones, "ExploreDTI: a graphical toolbox for processing, analyzing and visualizing diffusion MR data," in *Proceedings of the 17th Annual Meeting of the International Society of Magnetic Resonance in Medicine*, p. 3537, Honolulu, Hawaii, 2009.

[36] A. Leemans and D. K. Jones, "The B-matrix must be rotated when correcting for subject motion in DTI data," *Magnetic Resonance in Medicine*, vol. 61, pp. 1336–1349, 2009.

[37] J. D. Tournier, F. Calamante, and A. Connelly, "Robust determination of the fibre orientation distribution in diffusion MRI: non-negativity constrained super-resolved spherical deconvolution," *NeuroImage*, vol. 35, pp. 1459–1472, 2007.

[38] B. Jeurissen, A. Leemans, J. D. Tournier, D. K. Jones, and J. Sijbers, "Investigating the prevalence of complex fiber configurations in white matter tissue with diffusion magnetic resonance imaging," *Human Brain Mapping*, vol. 34, pp. 2747–2766, 2013.

[39] S. Farquharson, J. D. Tournier, F. Calamante et al., "White matter fiber tractography: why we need to move beyond DTI," *Journal of Neurosurgery*, vol. 118, pp. 1367–1377, 2013.

[40] A. M. Auriat, M. R. Borich, N. J. Snow, K. P. Wadden, and L. A. Boyd, "Comparing a diffusion tensor and non-tensor approach to white matter fiber tractography in chronic stroke," *Neuroimage: Clinical*, vol. 7, pp. 771–781, 2015.

[41] Y. D. Reijmer, A. Leemans, S. M. Heringa et al., "Improved sensitivity to cerebral white matter abnormalities in

Alzheimer's disease with spherical deconvolution based tractography," *PLoS One*, vol. 7, 2012.

[42] S. Mori, B. J. Crain, V. P. Chacko, and P. C. van Zijl, "Three-dimensional tracking of axonal projections in the brain by magnetic resonance imaging," *Annals of Neurology*, vol. 45, pp. 265–269, 1999.

[43] S. H. Jang, S. H. Ahn, J. Sakong et al., "Comparison of TMS and DTT for predicting motor outcome in intracerebral hemorrhage," *Journal of Neurological Sciences*, vol. 290, pp. 107–111, 2010.

[44] N. J. Snow, S. Peters, M. R. Borich et al., "A reliability assessment of constrained spherical deconvolution-based diffusion-weighted magnetic resonance imaging in individuals with chronic stroke," *Journal of Neuroscience Methods*, vol. 257, pp. 109–120, 2016.

[45] J. H. Hong, S. M. Son, and S. H. Jang, "Somatotopic location of corticospinal tract at pons in human brain: a diffusion tensor tractography study," *NeuroImage*, vol. 51, pp. 952–955, 2010.

[46] S. Hofer and J. Frahm, "Topography of the human corpus callosum revisited—comprehensive fiber tractography using diffusion tensor magnetic resonance imaging," *NeuroImage*, vol. 32, pp. 989–994, 2006.

[47] S. Nakagawa, "A farewell to Bonferroni: the problems of low statistical power and publication bias," *Behavioural Ecology*, vol. 15, pp. 1044-1045, 2004.

[48] S. J. Pocock, "Clinical trials with multiple outcomes: a statistical perspective on their design, analysis, and interpretation," *Controlled Clinical Trials*, vol. 18, pp. 530–545, 1997.

[49] J. R. Carey, H. Deng, B. T. Gillick et al., "Serial treatments of primed low-frequency rTMS in stroke: characteristics of responders vs. nonresponders," *Restorative Neurology and Neuroscience*, vol. 32, pp. 323–335, 2014.

[50] S. J. Page, G. D. Fulk, and P. Boyne, "Clinically important differences for the upper-extremity Fugl-Meyer scale in people with minimal to moderate impairment due to chronic stroke," *Physical Therapy*, vol. 92, pp. 791–798, 2012.

[51] J. H. Van der Lee, R. C. Wagenaar, G. J. Lankhorst, T. W. Vogelaar, W. L. Deville, and L. M. Bouter, "Forced use of the upper extremity in chronic stroke patients: results from a single-blind randomised clinical trial," *Stroke*, vol. 30, pp. 2369–2375, 1999.

[52] E. B. Plow, D. Cunningham, N. Varnerin, and A. Machado, "Rethinking stimulation of the brain in stroke rehabilitation: why higher motor areas might be better alternatives for patients with greater impairments," *The Neuroscientist*, vol. 21, pp. 225–240, 2015.

[53] D. Badre and M. D'Esposito, "Is the rostro-caudal axis of the frontal lobe hierarchical?," *Nature Reviews Neuroscience*, vol. 10, pp. 659–669, 2009.

[54] H. Barbas and D. N. J. Pandya, "Architecture and frontal cortical connections of the premotor cortex (area 6) in the rhesus monkey," *Journal of Computational Neuroscience*, vol. 256, pp. 211–228, 1987.

[55] Z. Ni, C. Gunraj, A. J. Nelson et al., "Two phases of interhemispheric inhibition between motor related cortical areas and the primary motor cortex in human," *Cerebral Cortex*, vol. 19, pp. 1654–1665, 2009.

[56] J. L. Neva, K. S. Hayward, K. E. Brown, L. NHM, C. S. Mang, and L. A. Boyd, "Transcallosal inhibition elicited from non-primary motor cortex in individuals with chronic stroke," in *World Congress of NeuroRehabilitation 2016, Conference Proceedings*, Philadelphia, PA, USA, 2016.

[57] P. I. Yakovlev and P. Rakic, "Patterns of decussation of bulbar pyramids and distribution of pyramidal tracts on two sides of the spinal cord," *Transactions in American Neurology Association*, vol. 91, pp. 366-367, 1966.

[58] K. S. Hayward, R. N. Barker, D. Lloyd, S. G. Brauer, S. A. Horsley, and R. G. Carson, "SMART arm with outcome-triggered electrical stimulation: a pilot randomized clinical trial," *Topics in Stroke Rehabilitation*, vol. 20, pp. 289–298, 2013.

[59] K. S. Hayward, S. S. Kuys, R. N. Barker, and S. G. Brauer, "Can stroke survivors with severe upper arm disability achieve a clinically important change in arm function during inpatient rehabilitation? A multicentre, prospective, observational study," *NeuroRehabilitation*, vol. 35, pp. 773–779, 2014.

[60] L. V. Bradnam, C. M. Stinear, P. A. Barker, and W. D. Byblow, "Contralesional hemisphere control of the proximal paretic upper limb following stroke," *Cerebral Cortex*, vol. 22, pp. 2662–2671, 2012.

Hindawi
Neural Plasticity
Volume 2017, Article ID 8721240, 11 pages
https://doi.org/10.1155/2017/8721240

Research Article

For Better or Worse: The Effect of Prismatic Adaptation on Auditory Neglect

Isabel Tissieres, Mona Elamly, Stephanie Clarke, and Sonia Crottaz-Herbette

Neuropsychology and Neurorehabilitation Service, Centre Hospitalier Universitaire Vaudois (CHUV) and University of Lausanne, Lausanne, Switzerland

Correspondence should be addressed to Sonia Crottaz-Herbette; Sonia.Crottaz-Herbette@chuv.ch

Received 29 May 2017; Accepted 8 August 2017; Published 12 September 2017

Academic Editor: Andrea Turolla

Patients with auditory neglect attend less to auditory stimuli on their left and/or make systematic directional errors when indicating sound positions. Rightward prismatic adaptation (R-PA) was repeatedly shown to alleviate symptoms of visuospatial neglect and once to restore partially spatial bias in dichotic listening. It is currently unknown whether R-PA affects only this ear-related symptom or also other aspects of auditory neglect. We have investigated the effect of R-PA on left ear extinction in dichotic listening, space-related inattention assessed by diotic listening, and directional errors in auditory localization in patients with auditory neglect. The most striking effect of R-PA was the alleviation of left ear extinction in dichotic listening, which occurred in half of the patients with initial deficit. In contrast to nonresponders, their lesions spared the right dorsal attentional system and posterior temporal cortex. The beneficial effect of R-PA on an ear-related performance contrasted with detrimental effects on diotic listening and auditory localization. The former can be parsimoniously explained by the SHD-VAS model (shift in hemispheric dominance within the ventral attentional system; Clarke and Crottaz-Herbette 2016), which is based on the R-PA-induced shift of the right-dominant ventral attentional system to the left hemisphere. The negative effects in space-related tasks may be due to the complex nature of auditory space encoding at a cortical level.

1. Introduction

Unilateral spatial neglect tends to include distinct auditory deficits, which are often referred to as auditory neglect and are investigated with a variety of experimental paradigms [1]. The key feature of auditory neglect, impaired attention to left-sided stimuli, has been initially revealed in tasks of *dichotic listening*. In this paradigm, simultaneous auditory stimuli are presented to either ear; extinction or significant decrease in reporting stimuli presented to the left ear has been considered as a manifestation of auditory neglect [2, 3]. Although often present in auditory neglect, left ear extinction on dichotic listening has been also reported in two conditions which are unrelated to neglect. Left ear extinction is a key feature of the callosal disconnection syndrome [4, 5] and is associated with lesions of the splenium and isthmus of the corpus callosum [6, 7]. Furthermore, contralateral ear extinction has been reported to occur as often after left as right hemispheric lesions, when the damage extended to auditory-related structures [8]. The ambiguity in the interpretation of left ear extinction as a sign of auditory neglect has led to the introduction of the *diotic listening paradigm*, which consists of two simultaneous stimuli presented to the right or left by means of interaural time differences. Extinction or significant decrease in reporting stimuli lateralized to the left and/or bilateral decrease in reported stimuli is a characteristic of the right hemispheric lesions and depends critically on the integrity of basal ganglia [9–11]. *Auditory mislocalization* and in particular systematic directional errors to the ipsilesional side are believed to be another manifestation of auditory neglect [12–14]. Particularly striking symptom is *alloacusis*, that is, the misplacement of auditory stimuli across the midline. The three key features of auditory neglect, left-sided extinction on dichotic or diotic listening, and the distortion of auditory space perception can occur independently of each other and involve distinct neural networks; very likely, they correspond to different types of auditory neglect [9–11]. The three key features of auditory neglect

are often associated with visuospatial neglect symptoms [1, 10, 11, 14], which are treated with different approaches, including prismatic adaptation [15–22].

Prismatic adaptation has gained much interest, partly because of its well-documented effect on visuospatial neglect [15–22]. It consists of a visuomotor task during which the subject points to visual targets while wearing glasses mounted with right-deviating prisms. After an initial phase, when the subject overshoots the targets to the right, the pointing becomes correct. After the removal of the prisms, the first trials show pointing errors to the left, referred to as the aftereffect [20]. A series of neuroimaging studies was carried out in normal subjects to investigate neural mechanisms underlying the effect of R-PA on visual attention. The stages of visuomotor adaptation were shown to involve the posterior parietal cortex and the cerebellum on the right side [23–27]. An overall effect of a brief exposure to R-PA is the change of visuospatial representations in the inferior parietal lobule (IPL) in both hemispheres. As demonstrated in a recent study, the representation of the left, center, and right visual fields is enhanced in the left IPL and the representation of the right visual field decreased in the right IPL [28]. Thus, R-PA appears to shift the right-dominant ventral attentional system to the left hemisphere; in neglect, this shift is likely to restore the alerting input to the dorsal attentional system on either side and contribute thus to the alleviation of attentional deficits in visuospatial neglect [29].

Several lines of evidence suggest that visual and auditory attention relies on a supramodal attentional network. Activation studies have shown that in the context of spatial and nonspatial attentional tasks visual and auditory stimuli involve the same cortical regions and hence most likely a shared attentional network [30–33]. Similarly, the frequent cooccurrence of visual and auditory attentional deficits in unilateral neglect was proposed to reflect the supramodal nature of the syndrome [1, 34]. Further support comes from two studies which reported that R-PA alleviates specific symptoms of auditory neglect. A first study focused on the effect of R-PA on dichotic listening and reported in a group of 6 patients an alleviation of left ear extinction on dichotic listening, without affecting general arousal [35]. A second study investigated the effect of R-PA on spatial gradients in visual and auditory target detection and described in a group of 12 patients an overall improvement of auditory target detection, without restoring the spatial gradient of attention [36]. It is currently unknown whether R-PA affects other symptoms of auditory neglect.

The effect of R-PA on specific symptoms of auditory neglect may rely on the shift of the right-dominant ventral attentional system to the left IPL, as postulated in the SHD-VAS model for visuospatial attention [37]. If so, the alleviation of auditory neglect symptoms would depend on the integrity of the right dorsal attentional system and its access to the left IPL. We have investigated how R-PA affects key features of auditory neglect, namely performance on dichotic and diotic listening and auditory localization, and what the underlying anatomical constraints are. We hypothetized that the restoration of the alerting input from ventral attentional system via the left IPL may alleviate auditory neglect symptoms if the remaining parts of the involved network are intact. Thus, we postulated that for the effect of R-PA to occur, the dorsal attentional system (within the right hemisphere) and the afferent interhemispheric pathway from the left IPL need to be intact. We have expected that these mechanisms are likely to play a role in dichotic and diotic listening tasks. We did not expect a systematic improvement of sound localization performance, because of the great complexity in auditory space encoding (for detailed description see discussion [38–40]).

2. Methods

2.1. Participants. Ten consecutive stroke patients with unilateral spatial neglect and without history of psychiatric or previous neurological affections participated in this study (6 men, mean age 59.6 years ± 7.1; Table 1). The inclusion criteria were (i) a first unilateral right hemispheric ischemic stroke; (ii) normal or corrected to normal visual acuity, compatible with performing visual tasks without prescription glasses (so that prisms can be worn); and (iii) normal hearing thresholds at a tonal audiometry and less than 12 dB difference between the ears (average across all frequencies). All patients sustained an ischemic infarction in the territory of the right middle cerebral artery (Figure 1) and presented at the time of testing visuospatial and auditory neglect. The mean delay between the R-PA and the stroke was 95 days ± 34. The patients were recruited among the patients of the Neuropsychology and Neurorehabilitation clinic of the Lausanne University Hospital (CHUV), and all provided an informed consent. Seventeen normal subjects served as control population for comparing the aftereffect in the ecological R-PA paradigm used here with the aftereffect observed in a shorter version R-PA used in a previous study (8 men, mean age 26.5 years ± 3.6; [28]). The study was conducted in accordance with the Declaration of Helsinki (1964) and was approved by the Ethic Committee of the Canton de Vaud, Switzerland.

2.2. Prismatic Adaptation. The ecological R-PA paradigm involved an adaptation phase during which the subject wore prisms which deviated the entire visual field 10° to the right (as in previous studies [17, 18, 20, 29, 41, 42]). The adaptation phase lasted 30 minutes during which the subject carried out a sequence of six different visuomotor activities, three of which resulted in sound production: (i) playing a sequence of 3 tones on a colour-coded xylophone according to the colours on a card shown by the experimenter; (ii) ringing 3 coloured bells in a sequence chosen from a group of 7 according to the colours on a card shown by the experimenter; (iii) placing five cups according to the pattern shown by the experimenter; (iv) picking up one bell identified by its colour among seven bells and ringing it; (v) placing a token in a column (among five) which the experimenter designated by its number (Puissance4® game); and (vi) placing Scrabble® tokens in the correct order to form three-letter words presented visually by the experimenter. Each activity lasted 5 minutes. The movements during these activities are slower than simple pointing movements in the classical adaptation;

Table 1: Patients' characteristics including the delay between the stroke and the testing session. STG: superior temporal gyrus; MTG: middle temporal gyrus; IFG: inferior frontal gyrus; IPL: inferior parietal lobule; SMG: supramarginal gyrus; AG: angular gyrus; SPL: superior parietal lobule; ITG: inferior temporal gyrus; HG: Heschl gyrus; TTG: transverse temporal gyrus; GP: globus pallidus; SFG: superior frontal gyrus.

Patient	Sex	Age	Handedness	Neurological and neuropsychological deficits	Regions involved in lesion	Delay (days)	Lesion vol (cm^3)
P1	M	53	Right	Left hemisyndrome (upper and lower limbs), multimodal neglect, nonspatial attentional deficits, executive dysfunction	STG, MTG, insula, IFG, temporal pole, putamen, caudate, precentral	54	135.4
P2	M	59	Right	Left unilateral homonymous hemianopia, severe multimodal neglect, executive dysfunction	STG, MTG, precentral, postcentral, IPL, IFG, insula, SMG, temporal pole, putamen, MFG, AG	80	182.6
P3	F	64	Right	Mild multimodal neglect and nonspatial attentional deficits	Insula, STG, temporal pole, MTG, putamen, IFG, caudate	59	93.1
P4	M	51	Left	Left hemisyndrome (upper and lower limbs), multimodal neglect, visuospatial apraxia, deficits in working memory and calculation, executive dysfunction	MFG, IFG, MTG, STG, precentral, postcentral, insula, SMG, temporal pole, occipital, putamen, precuneus, AG, SPL, ITG, HG, TTG, caudate	154	202.6
P5	M	57	Right	Horner syndrome on the right side, left unilateral homonymous hemianopia, severe multimodal neglect, nonspatial attentional deficits, deficit in anterograde episodic memory, executive dysfunction	Middle occipital, cuneus, superior occipital, MTG, cuneus, precuneus, AG, calarine	121	19.7
P6	M	59	Right	Left hemisyndrome (predominantly upper limb), left unilateral homonymous hemianopia, multimodal neglect, nonspatial attentional deficits, visuospatial apraxia, deficit in anterograde episodic memory, executive dysfunction	IFG, MFG, STG, precentral, insula, putamen, postcentral, temporal pole, precentral, MTG	89	118.7
P7	F	69	Right	Severe visuospatial neglect, nonspatial attentional deficits, mild executive dysfunction	IFG, MFG, STG, insula, putamen, temporal pole, MTG	122	70.6
P8	F	73	Right	Multimodal neglect, visuospatial apraxia, deficit in anterograde episodic memory, executive dysfunction	Insula, STG, IFG, putamen, MTG, HG, TTG	60	44.1
P9	M	58	Right	Left hemisyndrome (upper and lower limbs), severe multimodal neglect, deficit in anterograde episodic memory, executive dysfunction	Insula, putamen, caudate, GP, thalamus	127	382.0
P10	F	53	Right	Visuospatial neglect, nonspatial attentional deficits	MFG, STG, IFG, MTG, IPL, insula, postcentral, precentral, SMG, AG, precuneus, putamen, caudate, temporal pole, thalamus, hippocampus, parahippocampal gyrus, SFG	84	38.1

to reach the total number of movements which was shown to be critical for maximal adaptation to occur [43], we increased the duration of the adaptation phase to 30 minutes.

The aftereffect of R-PA, that is, visuomotor pointing error which occurs during the first pointing after the removal of the prisms, was assessed as in the previous studies [17, 18, 20, 37, 41, 42]. Briefly, the subject's head was positioned on chinrest and two black dots placed at a distance of 57 cm 14° to the left or to the right of his body midline; the proximal two-thirds of the distance between the subject and the dots were hidden. When positioned in the apparatus, the subject was asked to look at one of the dots, close his eyes, and point to the dot; this procedure was repeated twice for each dot. The aftereffect was expressed in degrees, corresponding to the average of the four measures. All patients performed the ecological R-PA paradigm, and all but one (P6) were tested for visuo-pointing errors before and after R-PA. P6 was not able to perform the aftereffect measure because he could not maintain the eyes closed during the pointing.

2.3. Evaluation of Auditory Neglect

2.3.1. Dichotic Listening Task. The dichotic listening task consisted of thirty pairs of disyllabic words presented simultaneously, one word to the left and another to the right ear (same paradigm as in [9, 11, 44]). The subjects were instructed to be attentive to both ears and to report both words. Performance was assessed by the total number of

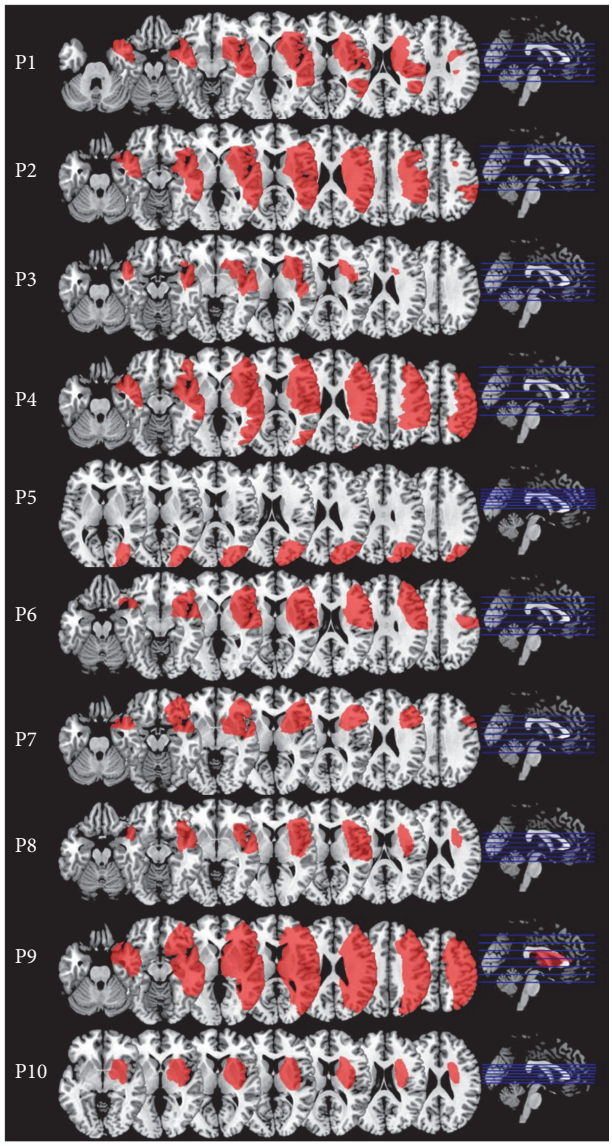

Figure 1: Lesions of individual patients displayed on axial slices of a normalized MRI template (positions of the slices in blue).

correct responses for each ear and by the lateralization index (right minus left ear, divided by right plus left ear, multiplied by 100). The performance of a control population was published previously [9]. The mean number of items reported for the right ear stimuli was 29.2 (SD = 1.685) and for the left ear stimuli 28.85 (SD = 2.74); the number of items reported for the left versus right ears did not differ significantly ($p = 0.1004$). The mean lateralization index was 0.986 (SD = 4.45).

2.3.2. Diotic Listening Task. The diotic listening task consisted of thirty pairs of words presented simultaneously. Both words were presented at the same intensity level to both ears, but one was lateralized to the right hemispace and the other one to the left hemispace, using interaural time difference of 1 ms (same paradigm as in [9, 11, 44]). For both tasks, performance was assessed by the total number of correct responses for each side separately and by the lateralization index (right minus left side, divided by right plus left side, multiplied by 100). The performance of a control population was published previously [9]. The mean number of items reported for the right space was 26.15 (SD = 4.632) and for the left space 24.867 (SD = 5.02). There was a significant advantage for the right space ($p = 0.0001$). The mean lateralization index was 3.521 (SD = 5.96).

2.3.3. Auditory Localization Task. The auditory localization task comprised 60 stimuli which were lateralized with interaural time differences (same paradigm as in [9, 11, 44–51]. The stimuli were bumblebee sounds, ranging from 20 to 10,000 Hz presented during 2 s including 100 ms rising and falling times. Five different azimuthal positions (12 sounds at each position) were simulated by interaural time differences (ITD), creating one central (no ITD) and four lateral positions, two in each hemispace. For the lateral positions, the ITD was 0.3 ms or 1 ms. The task consisted in indicating precisely the perceived position of the blumblebee on a graduated semicircle affixed on the headphone (from 0° at the vertex to 90° at each ear) with the right index finger. The overall performance of auditory localization was assessed by the relative positions attributed to two consecutive stimuli (global score). Responses were counted as correct when the position of the sound was indicated to the left or to the right of the previous stimulus in agreement with the difference in ITD or within ±10° of the previous location for identical stimuli; the maximal number of correct responses was 59. To quantify directional bias, more specific measures were used: (i) the number and the direction of alloacusis and (ii) the discrimination between neighbouring positions, by means of *t*-test between reported positions of nearby lateralizations (LL versus L; R versus RR). The performance of a control population was published previously [9, 44]. The mean global score was 57.15 (SD = 1.79). The mean for the central stimulus was −0.09° (SD = 4.5°). The mean index of response bias was 0.00 (SD = 0.74). Control subjects never exhibited alloacusis. Ten percent of control subjects failed to discriminate the two positions within one hemispace, never within both hemispaces.

2.4. Evaluation of Visuospatial Neglect. All patients were assessed for visuospatial aspects of neglect using the bells test and the line bisection task ("Batterie d'évaluation de la négligence spatiale" (BEN)) [52], as well as the evaluation of unilateral extinction for visual and tactile stimuli, search for neglect symptoms in visual target detection, graphical production, and motor performance (as in [9–11, 44, 50, 51]).

2.5. Statistical Analysis of Behavioural Data. Behavioural data from the dichotic and diotic tasks were tested for normality using the Shapiro-Wilk normality test, and due to the nonnormality of the distribution, the effect of R-PA was evaluated at the group level by a repeated measures nonparametric *F*-test. This method, used in a previous study [53], is a bootstrapping of the subjects (with replacement) and permutation of the within-subject factors. An *F* value is calculated on each cycle, for each randomization.

Table 2: Performance in dichotic and diotic listening tasks before (pre-R-PA) and after (post-R-PA) exposure to R-PA, listing the number of words reported for the left and right ears as well as the lateralization index. Scores outside the normal range are highlighted in bold.

	Dichotic listening task						Diotic listening task					
	Pre-R-PA			Post-R-PA			Pre-R-PA			Post-R-PA		
Patient	Left	Right	Lat. index	Left	Right	Lat. index	Left	Right	Lat. index	Left	Right	Lat. index
P1	**1**	30	**93.6**	**4**	29	**75.8**	**10**	**13**	13.0	15	26	**26.8**
P2	**3**	29	**81.3**	**4**	30	**76.5**	22	21	−2.3	20	22	4.8
P3	**19**	29	**20.8**	29	29	0.0	25	26	2.0	27	28	1.8
P4	**15**	27	**28.6**	**15**	27	**28.6**	18	24	14.3	16	29	**28.9**
P5	**19**	29	**20.8**	25	30	9.1	19	24	11.6	29	28	−1.8
P6	**22**	28	**12.0**	26	29	5.5	23	27	8.0	24	26	4.0
P7	29	30	1.7	30	30	0.0	25	27	3.9	28	30	3.5
P8	**20**	30	**20**	26	30	7.1	20	19	−2.6	24	27	5.9
P9	**7**	30	**62.2**	**2**	30	**87.5**	17	20	5.6	17	19	5.6
P10	29	28	−1.8	30	29	−1.7	26	27	1.9	28	29	1.8

Repeating this for 1000 cycles generates an empirical distribution of F values from which a corresponding p value is obtained. These analyses were processed using Python (Python Software Foundation, https://www.python.org/). For the dichotic listening task factors, ear (left, right) and session (pre- and post-R-PA) were used, for diotic listening side (left, right) and session (pre- and post-R-PA).

2.6. Lesion Analysis. Lesions were outlined on MRI ($n = 4$) or CT scan ($n = 6$) anatomical sequences using the Medical Imaging Interaction Toolkit (MITK) software (http://mitk.org). The superposition of the lesions was calculated using Statistical Parametric Mapping (SPM12, Wellcome Department of Cognitive Neurology, London, UK).

3. Results

3.1. Rightward Prismatic Adaptation and Its Aftereffects. The visuomotor effect of R-PA was evaluated by the presence of the aftereffect, that is, leftward deviation in pointing immediately after prism removal. Seventeen control subjects performed the ecological R-PA paradigm; their mean aftereffect was −8.55° (SD = 2.61°), which is within the range of aftereffects obtained with a shorter version of the R-PA paradigm in a previous study [28]. All but one patient (P6) were able to perform the pointing measures before and after R-PA, and all presented the expected leftward shift. The mean aftereffect was −5.88° (SD = 3.28°).

3.2. Dichotic Listening. The effect of R-PA was evaluated at a group level by a repeated measures nonparametric F-test [53]. The number of items reported for either ear yielded a significant main effect of ear ($F(1, 9) = 11.12$, $p = 0.002$) and a significant main effect of session ($F(1, 9) = 5.13$, $p = 0.023$), but only a trend for the interaction ($F(1, 9) = 3.36$, $p = 0.056$). The lateralization index did not differ significantly between pre- and post-R-PA (Wilcoxon signed-rank test, $Z = -1.481$, $p = 0.139$).

At an individual level, we have identified 8 patients who had a significant decrease of the left ear reporting and an abnormal lateralization index prior to R-PA (Table 2). After R-PA, 4 patients (P3, P5, P6, and P8) normalized their performance on dichotic listening, both in terms of items reported for the left ear and lateralization index. Four other patients (P1, P2, P4, and P9) did not improve their performance and presented after R-PA a significant decrease of left ear reporting and abnormal lateralization index.

The patients who responded to R-PA versus those who did not differ in terms of the site and extent of their lesion. The nonresponders tended to have larger lesions (range: 135.4–383.0 cm^3; Table 1) than responders (range: 19.7–118.7 cm^3). In nonresponders, but not in responders, the lesions extended over large parts of the temporoparietofrontal cortex and the underlying white matter, including the superior parietal lobule, the intraparietal sulcus, and the posterior part of the temporal lobe. The patients who had normal performance in dichotic listening before R-PA (P7 and P10) had a relatively small lesion (38.1 and 70.6 cm^3), which largely spared the temporoparietal cortex.

In summary, R-PA had a striking effect on left ear extinction in dichotic listening in some but not all patients with initial deficit. In responders, the superior parietal lobule, the intraparietal sulcus, and the posterior part of the temporal lobe tended to be spared, but not in nonresponders.

3.3. Diotic Listening. The effect of R-PA was evaluated at a group level by a repeated measures nonparametric F-test [53]. The number of items reported for either side yielded a significant main effect of side ($F(1, 9) = 9.95$, $p = 0.006$) and a significant main effect of session ($F(1, 9) = 7.93$, $p = 0.014$), but no significant interaction ($F(1, 9) = 0.94$, $p = 0.375$). The lateralization index did not differ significantly between pre- and post-R-PA (Wilcoxon signed-rank test, $Z = -0.652$, $p = 0.515$).

At an individual level, we have identified one patient (P1) who had a significant decrease of reporting for both the right and left spaces prior to R-PA, albeit with a lateralization index within the normal range (Table 2). After R-PA, this patient normalized his reporting for the right space, but remained deficient for the left space; the lateralization index was then outside the normal range, favouring

Table 3: Performance in auditory localization before (pre-R-PA) and after (post-R-PA) exposure to R-PA. Scores outside the normal range are in bold. The global score corresponds to the number of stimuli correctly placed to the left or the right of the previous stimulus. The perceived positions of each of the five stimulus locations are indicated in degrees (positive in the right, negative in the left space). The ability to discriminate between the two positions within either hemispace (LL versus L; R versus RR) was assessed by *t*-tests; positions which failed to be discriminated are highlighted in bold. In the control population, 10% of subjects failed to discriminate the two positions within one hemispace, never within both hemispaces. The number of alloacusis is indicated separately for those where stimuli presented on the left were indicated on the right (L to R) and those where stimuli presented on the right were indicated on the left (R to L). Control subjects never presented alloacusis.

		Pre-R-PA								Post-R-PA						
		Positions (°)					Alloacusis			Positions (°)					Alloacusis	
Patient	Global score	LL	L	CE	R	RR	L to R	R to L	Global score	LL	L	CE	R	RR	L to R	R to L
P1	**51**	**−57.5**	**−53.8**	−2.1	**44.2**	**59.6**	0	0	**47**	**−43.6**	**−35.5**	−3.5	**29.6**	**49.6**	**2**	**2**
P2	55	−82.5	−66.3	**11.9**	55.8	75.0	0	0	57	**−76.3**	**−70.8**	7.5	49.6	70.8	0	0
P3	56	**−30.4**	**−28.3**	**−23.3**	36.7	43.3	0	0	**54**	−32.5	−20.8	**29.6**	**35.0**	**39.6**	0	0
P4	**42**	**−12.1**	**−14.5**	−5.6	**32.2**	**13.0**	**4**	**5**	**42**	**−9.5**	**0.5**	5.0	**28.0**	**27.3**	**7**	**1**
P5	56	**−46.3**	**−41.3**	**−9.2**	**40.0**	**43.8**	0	0	55	−68.3	−52.1	**−26.7**	26.7	47.9	0	0
P6	54	**−40.4**	**−36.7**	**−10.4**	28.3	44.2	0	0	59	**−37.1**	**−36.3**	**−15.4**	22.5	32.9	0	0
P7	54	−59.5	3.5	**41.3**	**58.9**	**68.0**	**4**	0	**46**	**−27.9**	**−28.8**	**17.0**	**29.4**	**60.0**	**3**	0
P8	**52**	−50.8	−37.1	**−24.6**	42.1	57.1	0	0	53	−67.1	−64.2	**−32.1**	**64.2**	**77.9**	0	0
P9	54	**−73.3**	**−68.3**	−0.8	**57.5**	**67.1**	0	0	**44**	**21.7**	**−30.9**	**40.8**	**56.7**	**76.3**	**11**	**1**
P10	**52**	−60.8	−64.2	7.5	**71.3**	**72.3**	0	0	**50**	**−75.0**	**−73.8**	**−48.5**	**82.7**	**80.4**	0	0

the right space. Another patient (P4), who had a normal performance in diotic listening, including a normal lateralization index, prior to R-PA, increased after R-PA reporting for the right but not the left space; his lateralization index was then outside the normal range, favouring the right space. The two patients in whom R-PA induced a rightward spatial bias (P1 and P4) did have rather large lesions (135.4 and 202.6 cm^3; Table 1) which extended over large parts of the temporoparietofrontal cortex and the underlying white matter.

The remaining 8 patients had right and left space reporting as well as lateralization index within the normal range before and after R-PA. Among them, three had pre-R-PA scores for the right and/or left side reporting in the lower range (P5; P8 and P9). After R-PA, two of them (P5 and P8) increased considerably both scores, whereas the third one (P9) did not. The former two (P5 and P8) sustained rather small lesions (19.7 and 44.1 cm^3; Table 1) which spared the superior parietal lobule, the intraparietal sulcus, and basal ganglia. The latter one (P9) sustained a large lesion (382.0 cm^3), which extended over large parts of the hemisphere and included the superior parietal lobule, the intraparietal sulcus, and basal ganglia.

In summary, R-PA induced in specific cases rightward spatial bias in diotic listening by enhancing the reporting within the right but not the left space. This profile was associated with extended lesions which included the superior parietal lobule, the intraparietal sulcus, and basal ganglia. In a few cases, R-PA improved the left side reporting from low to high normal range. The integrity of the superior parietal lobule, the intraparietal sulcus, and basal ganglia appeared to be essential for this to occur.

3.4. Auditory Localization. At a group level, there was no statistically significant difference between pre- and post-R-PA global score measures ($Z = -1.19$, $p = 0.234$) nor for the number of left-to-right ($Z = -1.461$, $p = 0.144$) or right-to-left alloacusis ($Z = 0$, $p = 1$; for all comparisons, Wilcoxon signed-rank test).

Prior to R-PA, all patients were deficient at one or several of the following scores: (i) global score; (ii) the location attributed to the central stimulus; (iii) discriminating L-LL plus R-RR; and (iv) presence of alloacusis (Table 3). After the exposure to R-PA, only one patient (P2) improved his performance and reached normal range. His lesion was rather large (182.5 cm^3; Table 1) and extended over large parts of the temporoparietofrontal cortex and the underlying white matter.

The remaining nine patients worsened their performance. Three (P1, P4, and P9) enhanced their rightward bias by shifting the position attributed to the central stimulus to the right and/or by increasing the number of left-to-right alloacusis, thus aggravating neglect symptoms. Their lesions were rather large (135.4 and 382.0 cm^3) and extended over large parts of the temporoparietofrontal cortex and the underlying white matter. Two patients (P3 and P7) became deficient on their global score, without increasing a rightward bias. Their lesions were relatively small (93.1 and 70.6 cm^3) and extended over the anterior and posterior temporal lobes, frontal convexity, and/or the underlying white matter. One patient (P10) sustained leftward bias by shifting the position attributed to the central stimulus to the left and failed to discriminate the L-LL positions. Her lesion was relatively small (38.1 cm^3) and subcortical.

In summary, the effect of R-PA on auditory localization was varied and in nine of ten cases detrimental. In specific cases, R-PA induced rightward spatial bias in auditory localization. There did not seem to be clear relationship between the site of lesion and the effect of R-PA on auditory localization.

4. Discussion

4.1. Alleviation of Auditory Neglect by Prismatic Adaptation: Ear versus Space. The most striking effect of R-PA which we have observed was the alleviation of left ear extinction on dichotic listening, present in half of the patients. This beneficial effect on ear-related performance contrasted with the modest or even detrimental effects on space-related measures. In diotic listening, we observed an improvement which was limited to reporting the right-space stimuli and created thus rightward spatial bias. In a few cases, R-PA had mostly negative effect on auditory localization, leading to a rightward spatial bias.

The diverging effects of R-PA on different aspects of auditory neglect may be partially explained by the underlying mechanisms. Whereas, the effect on dichotic listening is likely to depend on the same neural mechanisms as the effect on visuospatial attention, the complexity of the encoding of the auditory space at a cortical level may interfere with the effect on auditory localization and possibly on diotic listening.

4.2. Neural Mechanisms Underlying the Effect of Prismatic Adaptation in Auditory Neglect. Visual attention and orienting have been shown to depend on the dorsal and ventral attentional systems. As demonstrated in a series of seminal studies, the dorsal attentional network, which comprises the superior parietal lobule, the intraparietal sulcus, and the superior frontal cortex of both hemispheres, mediates endogenous allocation of visuospatial attention [54]. Its key region, the intraparietal sulcus, encodes predominantly the contralateral visual space [55]. Exogenous attention, that is, the alerting targets that appear at unattended locations, is mediated by the ventral attentional network, which is lateralized to the right hemisphere and includes the temporoparietal junction, IPL, and posterior part of the superior temporal gyrus; this region receives visual information from the whole visual space [54]. The right-dominant ventral and the bilateral dorsal attentional systems are interconnected, so that the alerting input from the ventral system can activate the dorsal system [56]. There is a reciprocal interconnection between the right and left parts of the dorsal attention system [56–58], characterized by an asymmetrical inhibitory effect by which the right posterior parietal cortex inhibits the left homologous region [57, 58].

A brief exposure to R-PA was shown to shift the right-dominant ventral attentional system to the left IPL. The task used in this study was the detection of visual target presented in the left, central, and right spaces, known to activate the ventral attentional system. R-PA leads to a significant increase of the ipsilateral visual field representation in the left IPL and a significant decrease in the right IPL [28]. This same study demonstrated that R-PA did not have the same effect on other types of visuospatial processing, such as visuospatial working memory. In a later study, the shift of the ventral attentional system from the right to the left hemisphere was demonstrated with the same visual detection task in neglect patients [29]. The model derived from these studies, referred to as SHD-VAS (shift in hemispheric dominance within the ventral attentional system), offers a parsimonious explanation for the effects of R-PA on visuospatial attention in normal subjects and neglect patients (for discussion see [37]). This model may be also relevant for auditoryspatial attention, since the dorsal and the ventral attentional systems are involved in auditory attention. Early activation studies reported that auditory alertness involved an extended right hemispheric network, including frontal, cingular, inferior parietal, temporal, and thalamic regions [32] and shared with visual alertness a common region within the ventral attentional system [33].

In view of the above quoted evidence, it is reasonable to assume that the effect of R-PA on auditory neglect relies on the shift of the right-dominant ventral attentional system to the left hemisphere. For the beneficial effect on attentional orienting to the left, the ventral attentional system within the left hemisphere needs to access the dorsal attentional system within the right hemisphere. Thus, a spared dorsal attentional system and intact inputs from the left IPL are necessary for such beneficial effects.

4.3. Effect of Prismatic Adaptation on Dichotic Listening: What Matters? In our population, R-PA alleviated left ear extinction in dichotic listening in four patients, while it failed to do so in four others. The prerequisite for the beneficial effect of R-PA appeared to be intact with the superior parietal lobule, posterior part of the temporal lobe, as well as the periventricular white matter, which convey fibers joining the middle and posterior parts of the corpus callosum (Figure 2). The key role of the superior parietal lobule and of the callosal connections is in agreement with the SHD-VAS model.

Left ear extinction on dichotic listening has been also reported independently of the neglect syndrome, in cases of callosal disconnection and in particular when the splenium and the isthmus of the corpus callosum were damaged [6, 7]. These posterior parts of the corpus callosum are known to convey fibers from the temporal lobe, whereas the parietal callosal pathway tends to involve more anterior parts [59]. In our patient population, we did not have lesions which damaged specifically either the auditory or the parietal callosal pathway. Thus, it remains unclear whether R-PA would alleviate left ear extinction in cases with focal lesions of the splenium and the isthmus, that is, without damage to the dorsal attentional system and the more anterior callosal pathway.

4.4. Worsening Rightward Bias on Diotic Listening. Our results suggest that in specific conditions, R-PA can enhance rightward spatial bias and thus amplify neglect symptoms. When it happened in diotic listening, the initial condition involved scores that were pathologically low or within lower normal range on both sides. R-PA increased the reporting on the right but not on the left side. The beneficial effect on the right side reporting can be explained by the SHD-VAS model and the ensuing activation of the left dorsal attentional system. Both patients who presented this effect (P1 and P4) sustained damage to the right dorsal attentional system, which precluded reorienting attention to the left.

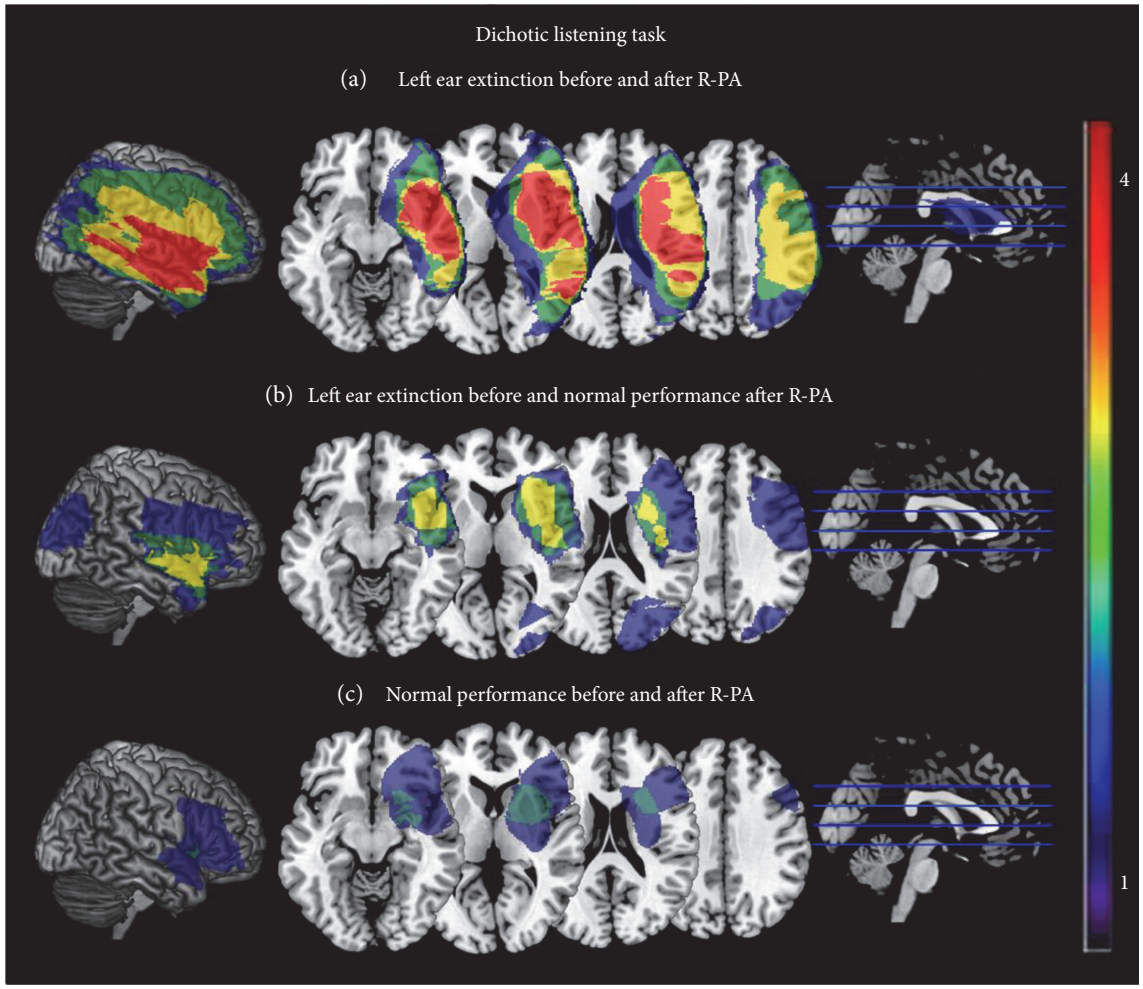

Figure 2: Anatomical correlates of performance in dichotic listening task. Superposition of lesions associated with 3 profiles: (a) Patients with left ear extinction who did not respond to R-PA (P1, P2, P4, and P9). (b) Patients with left ear extinction who responded to R-PA (P3, P5, P6, and P8). (c) Patients without deficits at the dichotic listening task (P7 and P10).

R-PA can enhance the left side reporting in diotic listening, as observed in two patients whose scores were in the lower normal range prior to R-PA and in the upper normal range after it (P5 and P8). Both patients had intact dorsal attentional system on the right side.

4.5. Disturbing Auditory Localization. Our results on auditory localization demonstrate that R-PA can enhance rightward spatial bias and thus aggravate neglect symptoms. Three patients presented this profile (P1, P4, and P9); after prismatic adaptation, they shifted the central position to the right and/or presented more right-to-left alloacusis. All three sustained damage to the right dorsal attentional system, which may explain the paradoxical rightward bias.

Apart from the enhancement of rightward spatial bias, R-PA tended to deteriorate more generally performance in auditory localization and even introduced a pathological leftward spatial bias. The former was observed in two patients whose global score became deficient after R-PA (P3 and P7), the latter in two other patients with a leftward spatial bias for the central position after R-PA (P5 and P10). These varied and rather unfavourable effects of R-PA on auditory localization may be related to the way auditory space is represented at a cortical level. Several lines of evidence indicate that auditory space is not represented in a topographical fashion, but encoded within specific neuronal populations [60–62]. Single neurons in nonhuman primates were reported to have large receptive fields, centered on the contralateral space [62–64]. Human fMRI studies reported a similar organization with preferential responses to contralateral locations and broad spatial tuning [38, 39]. The representation of the auditory space in humans appears to be lateralized, with greater bilaterality in the right and stricter contralaterality in the left hemisphere [40]. This asymmetry is particularly striking within the parietofrontal cortex, as demonstrated in activation [65–68], magnetoencephalography [69], transcranial magnetic stimulation [70, 71], and lesion studies [44]. This frontoparietal asymmetry is further supported by the patterns of structural and functional connectivities [72, 73].

The above quoted evidence suggests that the region invested by the ventral attentional system, and in particular

the IPL, not only supports auditory alertness and attention, but also the representation of auditory space. When shifted to the left hemisphere after R-PA, the ventral attentional system most likely upkeeps its alerting function, and hence the positive effect on dichotic listening, as reported previously [35] and here. The representation of the auditory space, which depends on fine-tuned interactions within neuronal populations, is very likely disturbed by the exposure to R-PA. This may account for the detrimental effect of R-PA on sound localization.

5. Conclusions

The beneficial effect of R-PA on auditory neglect appears to be limited to the alleviation of left ear extinction in dichotic listening. This particular effect can be parsimoniously explained by the SHD-VAS model, that is, shift in hemispheric dominance within the ventral attentional system, induced by R-PA. This model has been initially formulated on the basis of visual activation studies [28, 29], but its predictions appear to be valid for the effect of R-PA on left ear extinction in dichotic listening. In particular, the observation that the right dorsal attentional system needs to be intact to obtain an alleviation of left extinction after R-PA is entirely in adequation with this model. This observation is clinically relevant, since it identifies anatomical profiles of patients for whom R-PA is likely to alleviate ear-related symptoms of auditory neglect.

The effect of R-PA on space-related measures of auditory neglect is varied and mostly detrimental. This is particularly apparent in auditory localization and may be accounted for by the complex way auditory space is represented at a cortical level. Whether the exacerbation of auditory localization deficits after exposure to R-PA has an impact on activities of daily living is currently not known. The effect may be short lived and possibly rapidly corrected as previously described for the realignment of visuo- and auditoryspatial representations in the ventriloquism effect [74–76].

Abbreviations

IPL: Inferior parietal lobule
R-PA: Rightward prismatic adaptation
SHD-VAS: Shift in hemispheric dominance within the ventral attentional system.

Conflicts of Interest

The authors declare that there are no conflicts of interest regarding the publication of this paper.

Acknowledgments

The work was supported by grants from the Swiss National Science Foundation to Sonia Crottaz-Herbette (Marie-Heim-Vögtlin fellowship FNS PMPDP3_129028) and Stephanie Clarke (FNS 320030-159708) and from the Biaggi Foundation to Sonia Crottaz-Herbette. The work was supported by the Centre d'Imagerie BioMédicale (CIBM) of the University of Lausanne (UNIL). The authors thank Jean-Baptiste Ledoux for his help in data acquisition.

References

[1] F. Pavani, M. Husain, E. Ládavas, and J. Driver, "Auditory deficits in visuospatial neglect patients," *Cortex; a Journal Devoted to the Study of the Nervous System and Behavior*, vol. 40, no. 2, pp. 347–365, 2004.

[2] K. M. Heilman and E. Valenstein, "Auditory neglect in man," *Archives of Neurology*, vol. 26, no. 1, pp. 32–35, 1972.

[3] K. Hugdahl, K. Wester, and A. Asbjørnsen, "Auditory neglect after right frontal lobe and right pulvinar thalamic lesions," *Brain and Language*, vol. 41, no. 3, pp. 465–473, 1991.

[4] D. Kimura, "Functional asymmetry of the brain in dichotic listening," *Cortex*, vol. 3, no. 2, pp. 163–178, 1967.

[5] R. Sparks and N. Geschwind, "Dichotic listening in man after section of neocortical commissures," *Cortex*, vol. 4, no. 1, pp. 3–16, 1968.

[6] S. Pollmann, M. Maertens, D. Yves, J. Lepsien, and K. Hugdahl, "Dichotic listening in patients with splenial and nonsplenial callosal lesions," *Neuropsychology*, vol. 16, no. 1, pp. 56–64, 2002.

[7] M. Sugishita, K. Otomo, K. Yamazaki, H. Shimizu, M. Yoshioka, and A. Shinohara, "Dichotic listening in patients with partial section of the corpus callosum," *Brain*, vol. 118, Part 2, pp. 417–427, 1995.

[8] E. D. Renzi, M. Gentilini, and F. Pattacini, "Auditory extinction following hemisphere damage," *Neuropsychologia*, vol. 22, no. 6, pp. 733–744, 1984.

[9] A. Bellmann, R. Meuli, and S. Clarke, "Two types of auditory neglect," *Brain: A Journal of Neurology*, vol. 124, Part 4, pp. 676–687, 2001.

[10] L. Spierer, R. Meuli, and S. Clarke, "Extinction of auditory stimuli in hemineglect: space versus ear," *Neuropsychologia*, vol. 45, no. 3, pp. 540–551, 2007.

[11] A. B. Thiran and S. Clarke, "Preserved use of spatial cues for sound segregation in a case of spatial deafness," *Neuropsychologia*, vol. 41, no. 9, pp. 1254–1261, 2003.

[12] E. Bisiach, L. Cornacchia, R. Sterzi, and G. Vallar, "Disorders of perceived auditory lateralization after lesions of the right hemisphere," *Brain: A Journal of Neurology*, vol. 107, Part 1, pp. 37–52, 1984.

[13] H. Haeske-Dewick, A. G. M. Canavan, and V. Hömberg, "Sound localization in egocentric space following hemispheric lesions," *Neuropsychologia*, vol. 34, no. 9, pp. 937–942, 1996.

[14] N. Soroker, N. Calamaro, J. Glicksohn, and M. S. Myslobodsky, "Auditory inattention in right-hemisphere-damaged patients with and without visual neglect," *Neuropsychologia*, vol. 35, no. 3, pp. 249–256, 1997.

[15] A. Farnè, Y. Rossetti, S. Toniolo, and E. Làdavas, "Ameliorating neglect with prism adaptation: visuo-manual and visuo-verbal measures," *Neuropsychologia*, vol. 40, no. 7, pp. 718–729, 2002.

[16] F. Frassinetti, V. Angeli, F. Meneghello, S. Avanzi, and E. Làdavas, "Long-lasting amelioration of visuospatial neglect by prism adaptation," *Brain*, vol. 125, no. 3, pp. 608–623, 2002.

[17] L. Pisella, G. Rode, A. Farnè, C. Tilikete, and Y. Rossetti, "Prism adaptation in the rehabilitation of patients with visuo-spatial cognitive disorders," *Current Opinion in Neurology*, vol. 19, no. 6, pp. 534–542, 2006.

[18] G. Rode, T. Klos, S. Courtois-Jacquin, Y. Rossetti, and L. Pisella, "Neglect and prism adaptation: a new therapeutic tool for spatial cognition disorders," *Restorative Neurology and Neuroscience*, vol. 24, no. 4–6, pp. 347–356, 2006.

[19] G. Rode, Y. Rossetti, and D. Boisson, "Prism adaptation improves representational neglect," *Neuropsychologia*, vol. 39, no. 11, pp. 1250–1254, 2001.

[20] Y. Rossetti, G. Rode, L. Pisella et al., "Prism adaptation to a rightward optical deviation rehabilitates left hemispatial neglect," *Nature*, vol. 395, no. 6698, pp. 166–169, 1998.

[21] A. Serino, S. Bonifazi, L. Pierfederici, and E. Làdavas, "Neglect treatment by prism adaptation: what recovers and for how long," *Neuropsychological Rehabilitation*, vol. 17, no. 6, pp. 657–687, 2007.

[22] A. Serino, V. Angeli, F. Frassinetti, and E. Làdavas, "Mechanisms underlying neglect recovery after prism adaptation," *Neuropsychologia*, vol. 44, no. 7, pp. 1068–1078, 2006.

[23] H. L. Chapman, R. Eramudugolla, M. Gavrilescu et al., "Neural mechanisms underlying spatial realignment during adaptation to optical wedge prisms," *Neuropsychologia*, vol. 48, no. 9, pp. 2595–2601, 2010.

[24] D. M. Clower, J. M. Hoffman, J. R. Votaw, T. L. Faber, R. P. Woods, and G. E. Alexander, "Role of posterior parietal cortex in the recalibration of visually guided reaching," *Nature*, vol. 383, no. 6601, pp. 618–621, 1996.

[25] J. Danckert, S. Ferber, and M. A. Goodale, "Direct effects of prismatic lenses on visuomotor control: an event-related functional MRI study," *The European Journal of Neuroscience*, vol. 28, no. 8, pp. 1696–1704, 2008.

[26] M. Küper, M. J. S. Wünnemann, M. Thürling et al., "Activation of the cerebellar cortex and the dentate nucleus in a prism adaptation fMRI study," *Human Brain Mapping*, vol. 35, no. 4, pp. 1574–1586, 2014.

[27] J. Luauté, S. Schwartz, Y. Rossetti et al., "Dynamic changes in brain activity during prism adaptation," *The Journal of Neuroscience: The Official Journal of the Society for Neuroscience*, vol. 29, no. 1, pp. 169–178, 2009.

[28] S. Crottaz-Herbette, E. Fornari, and S. Clarke, "Prismatic adaptation changes visuospatial representation in the inferior parietal lobule," *Journal of Neuroscience*, vol. 34, no. 35, pp. 11803–11811, 2014.

[29] S. Crottaz-Herbette, E. Fornari, M. P. Notter, C. Bindschaedler, L. Manzoni, and S. Clarke, "Reshaping the brain after stroke: the effect of prismatic adaptation in patients with right brain damage," *Neuropsychologia*, vol. 104, pp. 54–63, 2017.

[30] E. Salo, T. Rinne, O. Salonen, and K. Alho, "Brain activity during auditory and visual phonological, spatial and simple discrimination tasks," *Brain Research*, vol. 1496, pp. 55–69, 2013.

[31] D. V. Smith, B. Davis, K. Niu et al., "Spatial attention evokes similar activation patterns for visual and auditory stimuli," *Journal of Cognitive Neuroscience*, vol. 22, no. 2, pp. 347–361, 2010.

[32] W. Sturm, F. Longoni, B. Fimm et al., "Network for auditory intrinsic alertness: a PET study," *Neuropsychologia*, vol. 42, no. 5, pp. 563–568, 2004.

[33] C. M. Thiel and G. R. Fink, "Visual and auditory alertness: modality-specific and supramodal neural mechanisms and their modulation by nicotine," *Journal of Neurophysiology*, vol. 97, no. 4, pp. 2758–2768, 2007.

[34] G. Rode, C. Pagliari, L. Huchon, Y. Rossetti, and L. Pisella, "Semiology of neglect: an update," *Annals of Physical and Rehabilitation Medicine*, vol. 60, no. 3, pp. 177–185, 2017.

[35] S. Jacquin-Courtois, G. Rode, F. Pavani et al., "Effect of prism adaptation on left dichotic listening deficit in neglect patients: glasses to hear better?," *Brain*, vol. 133, no. 3, pp. 895–908, 2010.

[36] R. Eramudugolla, A. Boyce, D. R. F. Irvine, and J. B. Mattingley, "Effects of prismatic adaptation on spatial gradients in unilateral neglect: a comparison of visual and auditory target detection with central attentional load," *Neuropsychologia*, vol. 48, no. 9, pp. 2681–2692, 2010.

[37] S. Clarke and S. Crottaz-Herbette, "Modulation of visual attention by prismatic adaptation," *Neuropsychologia*, vol. 92, pp. 31–41, 2016.

[38] K. Derey, G. Valente, B. de Gelder, and E. Formisano, "Opponent coding of sound location (azimuth) in planum temporale is robust to sound-level variations," *Cerebral Cortex (New York, N.Y.: 1991)*, vol. 26, no. 1, pp. 450–464, 2016.

[39] S. A. McLaughlin, N. C. Higgins, and G. C. Stecker, "Tuning to binaural cues in human auditory cortex," *Journal of the Association for Research in Otolaryngology: JARO*, vol. 17, no. 1, pp. 37–53, 2016.

[40] G. C. Stecker, S. A. McLaughlin, and N. C. Higgins, "Monaural and binaural contributions to interaural-level-difference sensitivity in human auditory cortex," *NeuroImage*, vol. 120, pp. 456–466, 2015.

[41] S. Jacquin-Courtois, J. O'Shea, J. Luauté et al., "Rehabilitation of spatial neglect by prism adaptation: a peculiar expansion of sensorimotor after-effects to spatial cognition," *Neuroscience & Biobehavioral Reviews*, vol. 37, no. 4, pp. 594–609, 2013.

[42] G. M. Redding, Y. Rossetti, and B. Wallace, "Applications of prism adaptation: a tutorial in theory and method," *Neuroscience & Biobehavioral Reviews*, vol. 29, no. 3, pp. 431–444, 2005.

[43] J. Fernández-Ruiz and R. Díaz, "Prism adaptation and aftereffect: specifying the properties of a procedural memory system," *Learning & Memory*, vol. 6, no. 1, pp. 47–53, 1999.

[44] L. Spierer, A. Bellmann-Thiran, P. Maeder, M. M. Murray, and S. Clarke, "Hemispheric competence for auditory spatial representation," *Brain*, vol. 132, Part 7, pp. 1953–1966, 2009.

[45] M. Adriani, P. Maeder, R. Meuli et al., "Sound recognition and localization in man: specialized cortical networks and effects of acute circumscribed lesions," *Experimental Brain Research*, vol. 153, no. 4, pp. 591–604, 2003.

[46] S. Clarke, A. B. Thiran, P. Maeder et al., "What and where in human audition: selective deficits following focal hemispheric lesions," *Experimental Brain Research*, vol. 147, no. 1, pp. 8–15, 2002.

[47] S. Clarke, A. Bellmann, R. A. Meuli, G. Assal, and A. J. Steck, "Auditory agnosia and auditory spatial deficits following left hemispheric lesions: evidence for distinct processing pathways," *Neuropsychologia*, vol. 38, no. 6, pp. 797–807, 2000.

[48] M. Cogné, J.-F. Knebel, E. Klinger et al., "The effect of contextual auditory stimuli on virtual spatial navigation in patients with focal hemispheric lesions," *Neuropsychological Rehabilitation*, vol. 6, pp. 1–16, 2016.

[49] C. Y. Ducommun, C. M. Michel, S. Clarke et al., "Cortical motion deafness," *Neuron*, vol. 43, no. 6, pp. 765–777, 2004.

[50] C. Duffour-Nikolov, E. Tardif, P. Maeder et al., "Auditory spatial deficits following hemispheric lesions: dissociation of explicit and implicit processing," *Neuropsychological Rehabilitation*, vol. 22, no. 5, pp. 674–696, 2012.

[51] B. Rey, R. Frischknecht, P. Maeder, and S. Clarke, "Patterns of recovery following focal hemispheric lesions: relationship between lasting deficit and damage to specialized networks," *Restorative Neurology and Neuroscience*, vol. 25, no. 3-4, pp. 285–294, 2007.

[52] P. Azouvi, P. Bartolomeo, J.-M. Beis, D. Perennou, P. Pradat-Diehl, and M. Rousseaux, "A battery of tests for the quantitative assessment of unilateral neglect," *Restorative Neurology and Neuroscience*, vol. 24, no. 4–6, pp. 273–285, 2006.

[53] J.-F. Knebel, D. C. Javitt, and M. M. Murray, "Impaired early visual response modulations to spatial information in chronic schizophrenia," *Psychiatry Research: Neuroimaging*, vol. 193, no. 3, pp. 168–176, 2011.

[54] M. Corbetta, J. M. Kincade, and G. L. Shulman, "Neural systems for visual orienting and their relationships to spatial working memory," *Journal of Cognitive Neuroscience*, vol. 14, no. 3, pp. 508–523, 2002.

[55] M. A. Silver and S. Kastner, "Topographic maps in human frontal and parietal cortex," *Trends in Cognitive Sciences*, vol. 13, no. 11, pp. 488–495, 2009.

[56] M. Corbetta and G. L. Shulman, "Control of goal-directed and stimulus-driven attention in the brain," *Nature Reviews Neuroscience*, vol. 3, no. 3, pp. 201–215, 2002.

[57] G. Koch, M. Cercignani, S. Bonnì et al., "Asymmetry of parietal interhemispheric connections in humans," *Journal of Neuroscience*, vol. 31, no. 24, pp. 8967–8975, 2011.

[58] G. Koch, M. Oliveri, B. Cheeran et al., "Hyperexcitability of parietal-motor functional connections in the intact left-hemisphere of patients with neglect," *Brain*, vol. 131, Part 12, pp. 3147–3155, 2008.

[59] R. Westerhausen, R. Grüner, K. Specht, and K. Hugdahl, "Functional relevance of interindividual differences in temporal lobe callosal pathways: a DTI tractography study," *Cerebral Cortex*, vol. 19, no. 6, pp. 1322–1329, 2009.

[60] I. A. Harrington, G. C. Stecker, E. A. Macpherson, and J. C. Middlebrooks, "Spatial sensitivity of neurons in the anterior, posterior, and primary fields of cat auditory cortex," *Hearing Research*, vol. 240, no. 1-2, pp. 22–41, 2008.

[61] G. C. Stecker, I. A. Harrington, and J. C. Middlebrooks, "Location coding by opponent neural populations in the auditory cortex," *PLoS Biology*, vol. 3, no. 3, article e78, 2005.

[62] G. C. Stecker, B. J. Mickey, E. A. Macpherson, and J. C. Middlebrooks, "Spatial sensitivity in field PAF of cat auditory cortex," *Journal of Neurophysiology*, vol. 89, no. 6, pp. 2889–2903, 2003.

[63] T. M. Woods, S. E. Lopez, J. H. Long, J. E. Rahman, and G. H. Recanzone, "Effects of stimulus azimuth and intensity on the single-neuron activity in the auditory cortex of the alert macaque monkey," *Journal of Neurophysiology*, vol. 96, no. 6, pp. 3323–3337, 2006.

[64] G. H. Recanzone, "Spatial processing in the auditory cortex of the macaque monkey," *Proceedings of the National Academy of Sciences*, vol. 97, no. 22, pp. 11829–11835, 2000.

[65] S. R. Arnott, M. A. Binns, C. L. Grady, and C. Alain, "Assessing the auditory dual-pathway model in humans," *NeuroImage*, vol. 22, no. 1, pp. 401–408, 2004.

[66] K. O. Bushara, R. A. Weeks, K. Ishii et al., "Modality-specific frontal and parietal areas for auditory and visual spatial localization in humans," *Nature Neuroscience*, vol. 2, no. 8, pp. 759–766, 1999.

[67] L. De Santis, S. Clarke, and M. M. Murray, "Automatic and intrinsic auditory "what"and "where"processing in humans revealed by electrical neuroimaging," *Cerebral Cortex (New York, N.Y.: 1991)*, vol. 17, no. 1, pp. 9–17, 2007.

[68] P. P. Maeder, R. A. Meuli, M. Adriani et al., "Distinct pathways involved in sound recognition and localization: a human fMRI study," *NeuroImage*, vol. 14, no. 4, pp. 802–816, 2001.

[69] J. Kaiser, W. Lutzenberger, H. Preissl, H. Ackermann, and N. Birbaumer, "Right-hemisphere dominance for the processing of sound-source lateralization," *The Journal of Neuroscience: The Official Journal of the Society for Neuroscience*, vol. 20, no. 17, pp. 6631–6639, 2000.

[70] A. At, L. Spierer, and S. Clarke, "The role of the right parietal cortex in sound localization: a chronometric single pulse transcranial magnetic stimulation study," *Neuropsychologia*, vol. 49, no. 9, pp. 2794–2797, 2011.

[71] J. Lewald, I. G. Meister, J. Weidemann, and R. Töpper, "Involvement of the superior temporal cortex and the occipital cortex in spatial hearing: evidence from repetitive transcranial magnetic stimulation," *Journal of Cognitive Neuroscience*, vol. 16, no. 5, pp. 828–838, 2004.

[72] L. Cammoun, J. P. Thiran, A. Griffa, R. Meuli, P. Hagmann, and S. Clarke, "Intrahemispheric cortico-cortical connections of the human auditory cortex," *Brain Structure & Function*, vol. 220, no. 6, pp. 3537–3553, 2015.

[73] M. J. Dietz, K. J. Friston, J. B. Mattingley, A. Roepstorff, and M. I. Garrido, "Effective connectivity reveals right-hemisphere dominance in audiospatial perception: implications for models of spatial neglect," *Journal of Neuroscience*, vol. 34, no. 14, pp. 5003–5011, 2014.

[74] G. H. Recanzone, "Rapidly induced auditory plasticity: the ventriloquism aftereffect," *Proceedings of the National Academy of Sciences*, vol. 95, no. 3, pp. 869–875, 1998.

[75] B. Bonath, T. Noesselt, A. Martinez et al., "Neural basis of the ventriloquist illusion," *Current Biology*, vol. 17, no. 19, pp. 1697–1703, 2007.

[76] B. Bonath, T. Noesselt, K. Krauel, S. Tyll, C. Tempelmann, and S. A. Hillyard, "Audio-visual synchrony modulates the ventriloquist illusion and its neural/spatial representation in the auditory cortex," *NeuroImage*, vol. 98, pp. 425–434, 2014.

Hindawi
Neural Plasticity
Volume 2017, Article ID 4050536, 10 pages
https://doi.org/10.1155/2017/4050536

Research Article

White Matter Hyperintensity Load Modulates Brain Morphometry and Brain Connectivity in Healthy Adults: A Neuroplastic Mechanism?

Matteo De Marco,[1] Riccardo Manca,[1] Micaela Mitolo,[2] and Annalena Venneri[1]

[1]*Department of Neuroscience, University of Sheffield, Sheffield, UK*
[2]*Functional MR, S.Orsola-Malpighi Hospital, Department of Biomedical and Neuromotor Science (DIBINEM), Bologna, Italy*

Correspondence should be addressed to Matteo De Marco; m.demarco@sheffield.ac.uk

Received 30 March 2017; Accepted 3 July 2017; Published 3 August 2017

Academic Editor: J. Michael Wyss

White matter hyperintensities (WMHs) are acquired lesions that accumulate and disrupt neuron-to-neuron connectivity. We tested the associations between WMH load and (1) regional grey matter volumes and (2) functional connectivity of resting-state networks, in a sample of 51 healthy adults. Specifically, we focused on the positive associations (more damage, more volume/connectivity) to investigate a potential route of adaptive plasticity. WMHs were quantified with an automated procedure. Voxel-based morphometry was carried out to model grey matter. An independent component analysis was run to extract the anterior and posterior default-mode network, the salience network, the left and right frontoparietal networks, and the visual network. Each model was corrected for age, global levels of atrophy, and indices of brain and cognitive reserve. Positive associations were found with morphometry and functional connectivity of the anterior default-mode network and salience network. Within the anterior default-mode network, an association was found in the left mediotemporal-limbic complex. Within the salience network, an association was found in the right parietal cortex. The findings support the suggestion that, even in the absence of overt disease, the brain actuates a compensatory (neuroplastic) response to the accumulation of WMH, leading to increases in regional grey matter and modified functional connectivity.

1. Introduction

The adult human brain retains the capability for structural and functional modifications. This ability, labelled "neuroplasticity," is the outcome of multiple mechanisms acting at numerous levels, including the cellular and synaptic levels [1], which may result in changes detectable using neuroimaging techniques and data modelling [2]. The study of neuroplasticity has been associated with different types of research. Some studies have explored *induced* neuroplastic changes, through the exploitation of "manoeuvrable" mechanisms in clinical populations (e.g., physical therapy, noninvasive brain stimulation, deep-brain stimulation, neuropharmacology, aerobic exercise, and cognitive rehabilitation). Other studies have investigated the *automatic* processes of neuroplasticity triggered by damage of neural tissue, as is seen after not only acute events (like stroke or traumatic brain injury [3]) but also accompanying chronic neurodegenerative conditions (such as Alzheimer's disease [4]). The mechanisms of plasticity, however, are not unique to clinical populations but are relevant for people who simply undergo the physiological processes of ageing and even young adults. A large number of studies have tested experimental hypotheses based, for instance, on cognitive interventions or motor training in healthy adults, to test for induced neuroplasticity (e.g., [5]). At the same time, some effort has also been made to characterise automatic compensatory instances associated with neural and cognitive ageing. This has been extensively studied in association with task-fMRI paradigms focused on differences in activation between younger and older adults. Although a proportion of older adults maintains levels of behavioural performance indistinguishable from those of young adults, it

Table 1: Demographic, morphometric, and cognitive characterisation of the sample enrolled in this study.

Variable	Mean	SD	Median	Minimum	Maximum
Demographic features					
Age (years)	61.98	16.42	63.00	26.00	100.00
Education (years)	14.88	3.19	15.00	10.00	22.00
Subcortical damage					
WMH load (ml)	3.26	5.83	0.82	0.00	32.58
Global neurostructural indices					
Grey matter volume (ml)	636.28	67.20	633.01	446.74	752.21
White matter volume (ml)	415.07	44.29	408.88	337.43	527.50
Total intracranial volume (ml)	1457.69	157.06	1439.66	1217.24	1855.43
Grey matter fraction	0.44	0.06	0.45	0.33	0.56
White matter fraction	0.29	0.02	0.29	0.22	0.34
Cognitive scores					
WAIS—similarities	24.96	4.17	26.00	15.00	32.00
Prose Memory test—immediate recall	15.98	3.52	16.00	9.00	24.00
Prose Memory test—delayed recall	19.20	2.76	19.00	14.00	25.00
Rey-Osterrieth complex figure—copy	32.23	2.96	33.00	23.00	36.00
Rey-Osterrieth complex figure—recall	15.95	4.83	16.00	7.00	27.00
Letter Fluency test	47.18	13.25	47.00	16.00	75.00
Stroop test—time interference (s)	20.89	14.22	16.50	3.00	84.00
Trail-Making test—part B minus part A (s)	37.75	33.74	30.00	0.00	223.00

One participant did not complete the Stroop test because of colour blindness. One participant, aged 100 years, did not complete the Rey-Osterrieth complex figure, the Stroop test, or the Trail-Making test because of significant macular pathology. SD: standard deviation.

has been noted that this is achieved in association with a tendency to recruit more prefrontal regions during memory and perceptual tasks [6]. Along similar lines, high-performing older adults also tend to show more bilateral patterns of activation, and this has been seen in the prefrontal cortex [7], as well as in the parietal lobes [8]. These compensatory increases in activation to support performance on a task can be considered as due to processes of neuroplasticity [9]. Similar changes have also been seen in paradigms of resting-state functional connectivity, with age-dependent changes (decreases or increases) observed in the posterior and anterior default-mode network [10] and with increased levels of network-to-network interaction [11]. In all likelihood, these changes are compensatory to maintain function in the face of adverse events associated with ageing, such as functional dedifferentiation [12], cerebral atrophy [13], and subcortical white matter damage. Usually of vascular or inflammatory nature [14], the white matter hyperintensities (WMHs) frequently seen in the brain of otherwise healthy adults cause decreases in interneuronal speed of processing and connectivity [15]. As WMHs accumulate, compensatory mechanisms maintain function. When compensation is no longer effective, and reserve is depleted, cognitive function declines. When WMH accumulation generates symptoms, it may put a strain on various cognitive functions [16–18], although mechanisms of reserve may mitigate this trend [19]. A number of studies have shown compensatory task overactivation in the presence of WMHs [20, 21], but no research has yet addressed the association between WMHs and "positive" changes in resting-state functional connectivity, secondary to compensatory plasticity. In addition, there are studies showing positive associations between WMH load and cortical thickness in patients with small-vessel disease and Alzheimer's disease [22, 23], indicating that the neural system reacts to the presence of WMH by inducing a neuroplastic response which may be adaptive or detrimental. Although the presence of WMHs predicts decrements of global grey matter volumes in healthy adults [24], no study has yet focused on regional morphometry.

In this study, we analysed brain images from a sample of neurologically healthy adults who had undergone structural and resting-state fMRI and a comprehensive neuropsychological assessment. We quantified the amount of acquired WMH load using an automated procedure, and we tested the positive association between WMH load and (1) grey matter volume and (2) resting-state network connectivity, with voxel-by-voxel methods.

2. Materials and Methods

2.1. Participants. Fifty-one datasets acquired on healthy volunteers (35 females) were analysed retrospectively to address the research question. Under standard hypothesis-testing conditions (i.e., $\alpha = 0.05$; power = 0.8), this sample size is sufficiently large to detect a significant bivariate correlation associated with a moderate effect size [25].

The demographic characteristics of the participants are illustrated in Table 1. All participants were enrolled in this study as healthy volunteers, at the Royal Hallamshire Hospital, Sheffield (United Kingdom). Neurological screening was carried out at recruitment on each participant aged 48 or

above, to rule out the presence of major neurological symptoms. In addition, each participant completed a comprehensive battery of neuropsychological tests to ascertain the absence of cognitive deficits. Table 1 also reports the descriptive statistics associated with the performance obtained on tests which assess cognitive domains susceptible to ageing and neurodegeneration, namely, abstract-semantic reasoning (the similarities subtest of the WAIS battery), verbal and visuo-spatial memory (the Prose Memory test and the delayed recall of the Rey-Osterrieth complex figure, resp.), visuo-constructional skills (the copy of the Rey-Osterrieth complex figure), inhibition and shifting abilities (the Stroop and the Trail-Making test, resp.), and lexical production (the Letter Fluency test). Since the error interference on the Stroop test was limited (mean = 0.24, standard deviation = 0.90, and 14 errors made in total within the entire sample), the time interference index was the only effect calculated for this test [26].

Ethical approval for the procedures described in this study was obtained from the Yorkshire and Humber Regional Ethics Committee, Reference number: 12/YH/0474. Informed signed consent was obtained from all volunteers. All experimental procedures were strictly in compliance with the Declaration of Helsinki (1964).

2.2. MRI Image Acquisition. An experimental MRI session was completed by each participant. The protocol included anatomical and resting-state functional acquisitions obtained with a Philips Ingenia 3T scanner. Three MRI sequences were used in this study: a three-dimensional T1-weighted image (voxel size: 0.94 mm × 0.94 mm × 1.00 mm; TR: 8.2 s; TE: 3.8 s; FOV: 256 mm; matrix size: 256 × 256 × 170), a three-dimensional T2-weighted fluid-attenuated inversion recovery (FLAIR) magnetic resonance imaging sequence (voxel size: 0.56 mm × 0.56 mm × 0.56 mm; TR: 4.8 s; TE: 0.20 s; matrix size: 448 × 448 × 326), and a resting-state echo planar BOLD scan (voxel size: 1.80 mm × 1.80 mm × 4.00 mm; TR: 2.6 s; TE: 35 s; FOV: 230 mm; number of slices: 35; minimum scan duration: 5 minutes and 25 seconds). Participants were instructed to lay supine and remain as still as possible for the entire duration of the MRI protocol. Dummy scans were acquired prior to the resting-state sequence to obtain electromagnetic equilibrium.

2.3. T1-Weighted Image Processing. The processing and modelling pipeline was run using Matlab R2014a (Mathworks Inc., UK) and Statistical Parametric Mapping (SPM) 12 software (Wellcome Trust Centre for Neuroimaging, London, UK). The T1-weighted images were segmented to compute individual native space maps of grey matter, white matter, and cerebrospinal fluid [27]. Volumetric quantifications of each tissue class were then carried out using the "get_totals" script (http://www0.cs.ucl.ac.uk/staff/g.ridgway/vbm/get_totals.m). The total intracranial volume was calculated by summing up the volumetric quantification of all three tissue classes. Grey matter and white matter fractions were then computed as a ratio between each tissue volume and the total intracranial volume. These anatomical indices are reported in Table 1 for descriptive purposes. In addition, voxel-based morphometry procedures were run [27] for a voxel-by-voxel analysis of the association between WMH load and regional grey matter volumes. Briefly, maps of grey matter were normalised to the SPM 12 T1-weighted template and smoothed with an 8 mm full width at half maximum Gaussian kernel.

2.4. T2-Weighted Image Processing. The Lesion Segmentation Tool was used to segment the WMHs. Originally, this toolbox was developed to segment white matter lesions that are normally found in patients with multiple sclerosis [28]. Subsequent research, however, has reliably utilised it in samples of healthy elderly adults, or adults with cardiovascular risk factors [29–31]. First, this instrument processes the T1-weighted image to create a partial volume estimation image, then coregisters T1-weighted and FLAIR images, and carries out an inverse warping of the white matter tissue map. Subsequently, the FLAIR image intensity distribution is computed for the three tissue classes, and a native space lesion map is created. A threshold of 0.3 was used for this purpose [28]. Importantly, the quantification of WMHs does not differentiate between periventricular and deep WMHs. At the end, the total amount of WMHs (expressed in ml) was divided by the total intracranial volume and was then multiplied by 100 to obtain a ratio expressing WMH load as a percentage of intracranial volume [29].

2.5. Resting-State fMRI Image Processing. Resting-state functional images were preprocessed via a standardised pipeline. This included the following: (1) initial slice timing, conceived to assign homogenous temporal properties to slices within each volume; (2) spatial realignment, devised to "stack up" all volumes within each run and, thus, correct for volume-to-volume spatial displacement; (3) spatial normalisation, designed to register each native space acquisition to the default SPM 12 echo planar template in the Montreal Neurological Institute space; (4) temporal band-pass filtering (0.01 Hz to 0.1 Hz), applied to minimise the impact of nonneurogenic sources of variability on the BOLD signal rhythmicity [32] and achieved using the REST toolbox [33]; and finally (5) spatial smoothing (6 mm) was set up to maximise the signal-to-noise ratio. A quality check was carried out on each image prior to and during the preprocessing steps to rule out the presence of unexpected signal artefacts, excessive in-scanner motion, or normalisation errors.

An independent component analysis was then run on the complete group of 51 smoothed outputs. This type of inferential model assumes that the variability seen in the pattern of observable variables is the result of a linear combination of independent signalling sources [34]. An independent component analysis extrapolates a number of latent and statistically independent variables, which account for the pattern of observable variability with an optimal goodness of fit. The GIFT toolbox was used for this purpose [35], and the Infomax principle was chosen, setting the number of independent components to be estimated at 20.

The maps of six prominent networks were chosen (Figure 1). These were the anterior and posterior default-mode network, the salience network, the left and right

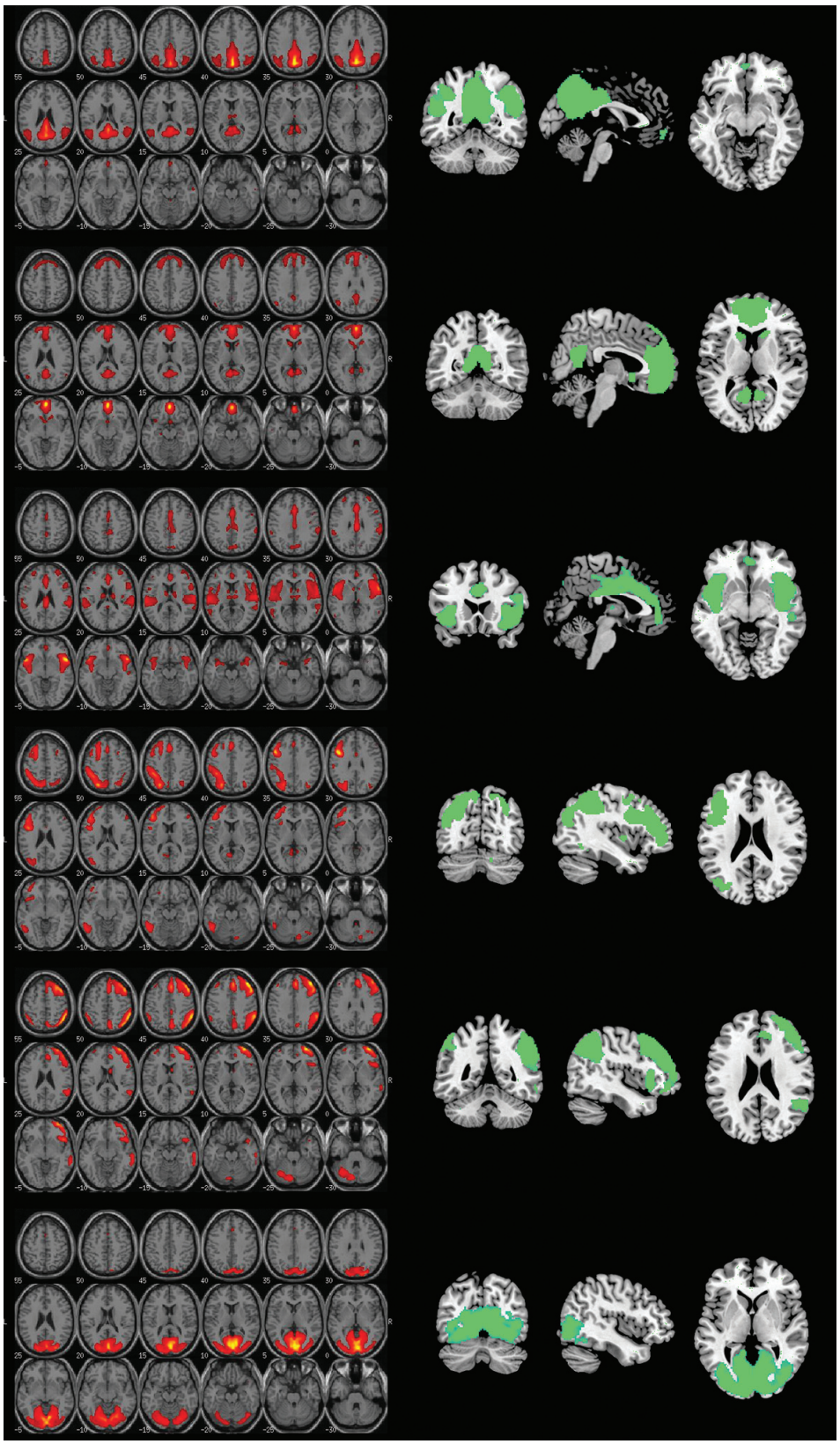

Figure 1: The six haemodynamic networks selected for this study, top to bottom: posterior default-mode network, anterior default-mode network, salience network, left frontoparietal network, right frontoparietal network, and visual network. The output of the independent component analysis is illustrated on the left, with maps expressing the z scores of each component. These same maps are shown on the right side as the output of a one-sample t-test carried out on the entire group.

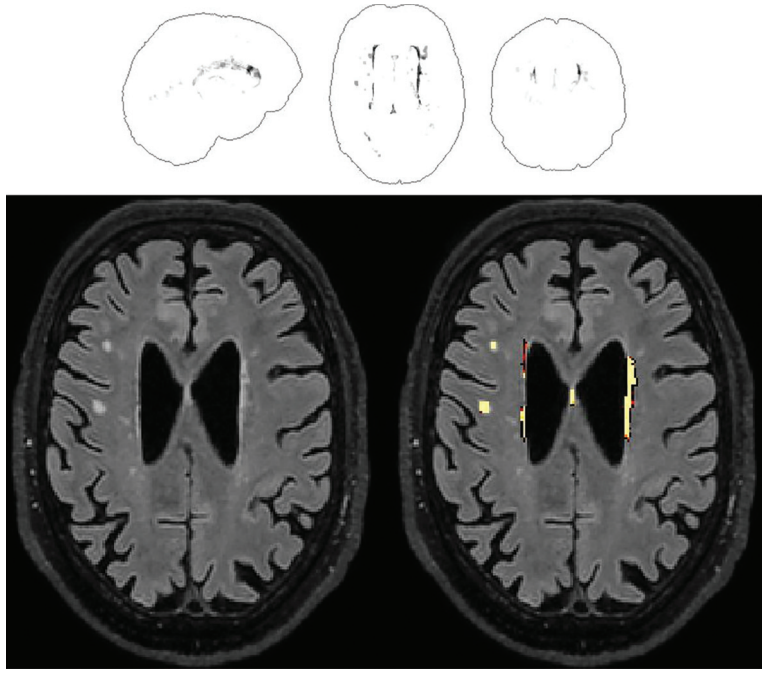

Figure 2: An example of the output from the Lesion Segmentation Tool for the quantification of WMHs. An overview is given in the glass-brain template shown in the upper half. A single slice is instead reproduced in the lower half, showing mainly periventricular, but also some sparse deep WMHs. This specific participant is a 70-year-old man with a raw WMH volume of 3.25 ml, equal to 0.21% of his intracranial volume.

frontoparietal networks, and, as a methodological control, the visual network. Subject-specific networks expressed as three-dimensional maps of z scores represented the dependent variable of the inferential models.

2.6. Statistical Modelling. Nonparametric correlations were run to characterise the association between white matter damage and each of the continuous variables included in Table 1. Linear models were run to test the association between WMH load and grey matter/network connectivity. The multiple-regression option on SPM was used for this purpose. Since the scope of the study was to describe the mechanisms of adaptive plasticity, we focused on the positive association contrasts (i.e., more grey matter, or more connectivity, in association with more subcortical load). Given the strong association found between WMH load on one hand and age and global levels of atrophy estimated by grey matter fraction on the other hand (see Results section), these two variables were included in all models as nuisance regressors. These covariates were also added in order to model the exclusive effects of WMHs independently of the level of atrophy and, importantly, to follow a methodology that would allow us to rule out the possibility that findings may simply be due to general effects of the ageing trajectory. Furthermore, since brain and cognitive reserve can influence the pattern of neural structure and functional connectivity, total grey matter volume and education level were included as additional covariates. For all models, the significance threshold was set at $p < 0.005$ (uncorrected) at the set level and $p < 0.05$ (family-wise error corrected) at the cluster level. Result coordinates were converted into the Talairach space using a nonlinear transformation (http://imaging.mrc-cbu.cam.ac.uk/downloads/MNI2tal/mni2tal-m) and localised using the Talairach Daemon client [36].

3. Results

The raw amount of WMH lesions ranged from 0 to over 32 ml, equivalent to 0% to 2.17% of individual total intracranial volume (see Figure 2 for an illustrative example). Of the entire set of variables included in Table 1, WMH load correlated significantly with age (*Spearman's rho* = 0.848, $p < 0.001$), total grey matter volume (*Spearman's rho* = −0.692, $p < 0.001$), grey matter ratio (*Spearman's rho* = −0.732, $p < 0.001$), immediate recall on the Prose Memory test (*Spearman's rho* = −0.360, $p = 0.009$), delayed recall on the Prose Memory test (*Spearman's rho* = −0.306, $p = 0.029$), and the Stroop time interference index (*Spearman's rho* = 0.532, $p < 0.001$). Since it is well established that age and education levels do influence performance on episodic memory and inhibitory skills, additional partial correlation models were run between WMH load and cognitive performance on these three measures, controlling for age and education. The association with memory scores was no longer significant, but the association with the Stroop time interference index survived. This association was still significant even after further correcting for global levels of atrophy.

Positive associations were found between WMH load and the voxel-based model of grey matter. These were found in the anterior part of the brain, specifically in the right anterior prefrontal cortex and in a large portion of the medial prefrontal cortex and cingulate gyrus (Table 2; Figure 3).

Table 2: Positive association between WMHs and brain structure and functional connectivity.

Cluster-level *p*FWE	Cluster extent (voxels)	*z* score at local maximum	Brodmann area	Side	Brain region	Talairach coordinates		
						x	*y*	*z*
Regional grey matter volume								
0.045	875	4.67	10	R	Superior frontal gyrus	33	51	22
		4.59	10	R	Middle frontal gyrus	45	47	16
		3.69	10	R	Inferior frontal gyrus	46	52	1
		3.64	10	R	Superior frontal gyrus	34	57	16
		3.33	10	R	Superior frontal gyrus	26	56	3
		3.22	10	R	Superior frontal gyrus	30	61	6
<0.001	3149	4.67	8	R	Superior frontal gyrus	10	43	44
		4.54	32	L	Medial frontal gyrus	−6	12	45
		4.50	8	R	Superior frontal gyrus	12	37	46
		3.98	6	R	Superior frontal gyrus	10	23	61
		3.96	8	L	Medial frontal gyrus	−2	25	43
		3.82	9	L	Medial frontal gyrus	−4	50	34
		3.74	6	L	Superior frontal gyrus	−18	22	56
		3.69	32	R	Middle cingulate cortex	3	36	28
		3.59	6	R	Superior frontal gyrus	2	26	56
		3.35	8	L	Superior frontal gyrus	−14	36	53
		3.33	6	L	Superior frontal gyrus	−20	17	62
		3.21	9	L	Superior frontal gyrus	−6	56	27
Anterior default-mode network								
0.046	240	3.77	29	L	Posterior cingulate cortex	−16	−42	8
		3.51		L	Hippocampus	−26	−39	2
		3.40	37	L	Fusiform gyrus	−34	−36	−13
		3.38	36	L	Parahippocampal gyrus	−34	−32	−10
		3.29	19	L	Parahippocampal gyrus	−36	−49	−1
		3.23		L	Hippocampus	−32	−35	−7
		3.11		L	Hippocampus	−24	−37	−3
Salience network								
0.028	267	4.00	3	R	Postcentral gyrus	26	−34	55
		3.56	40	R	Inferior parietal lobule	34	−48	56
		3.31	7	R	Superior parietal lobule	26	−51	63
		3.26	40	R	Inferior parietal lobule	32	−40	52
		3.06	7	R	Superior parietal lobule	32	−51	62
		3.02	3	R	Postcentral gyrus	20	−30	59

L: left; R: right; FWE: family-wise error.

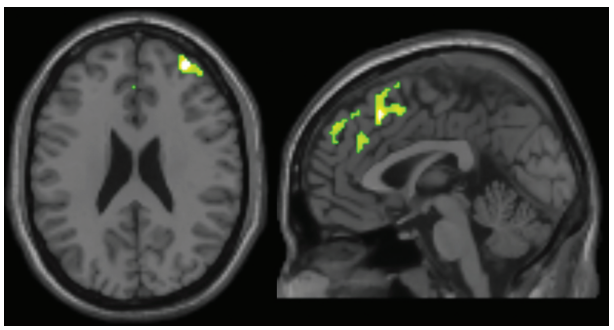

Figure 3: The positive association between WMH load and grey matter volumes.

The only two networks in which positive associations were found were the anterior default-mode network and the salience network (Table 2; Figure 4). Within the anterior default-mode network, increased connectivity correlated with increased WMH load in the left mediotemporal complex, including the posterior cingulate, the parahippocampal gyrus, and the posterior part of the hippocampus. Within the map of the salience network component, a significant association was found in the right parietal lobe, in the primary sensory cortex, and in the superior and inferior parietal lobules.

The average *z* scores for these two clusters were extracted for post hoc correlation models, in an attempt to characterise the results in more detail. In an explorative way, correlation

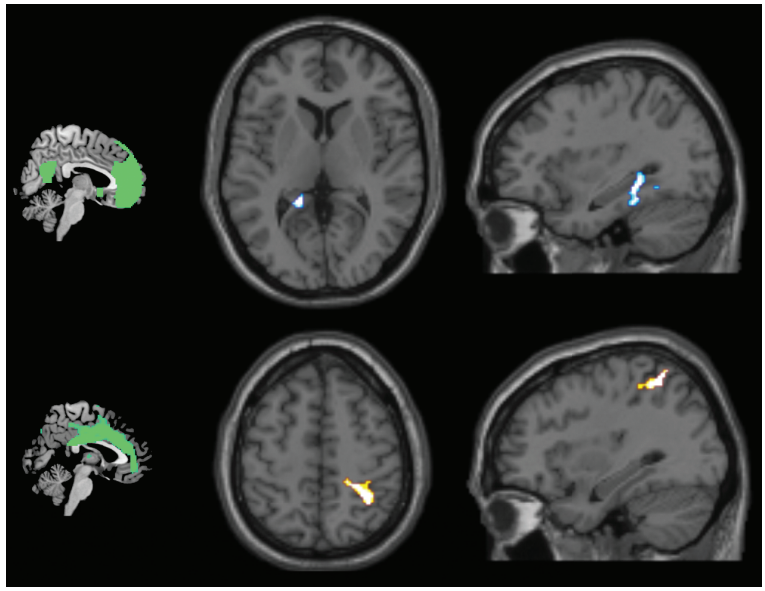

Figure 4: The positive association between WMH load and network connectivity (anterior default-mode network in the upper half and salience network in the lower half). The two networks are illustrated on the left.

models were run between network connectivity of these two clusters and each neurostructural and neuropsychological variable included in Table 1. The sole significant associations were those with white matter volume (anterior default-mode network: $p = 0.010$), white matter ratio (anterior default-mode network: $p < 0.001$; salience network: $p = 0.039$), and with the Stroop time interference index (anterior default-mode network: $p = 0.080$; salience network: $p = 0.028$). These last two p values dropped to 0.008 and 0.010, respectively, after controlling for age and level of education.

Finally, albeit beyond the scope of the study, post hoc models were run to test the presence of negative associations between WMH load and anterior default-mode network and salience network connectivity. No significant results were found.

4. Discussion

WMHs are relatively frequent among healthy adults, and, together with atrophy, they induce a decrease in the healthy neural tissue available for the computations necessary to sustain cognitive functioning. Nonetheless, the brain pursues adaptive plasticity to compensate for the age-associated accumulation of white matter damage. This can take the form of computational "scaffolds" as theorised by the Scaffolding Theory of Ageing and Cognition, indicating that additional neural circuitry is recruited in compensation for brain damage to support cortical functions [37]. On these grounds, in this study, we specifically explored the positive associations between WMHs and functional connectivity of the typical main resting-state networks to clarify which pathways of connectivity are upregulated when lesions accumulate. We constructed an inferential model which could test the "clean" association between WMHs and those neural variables of interest, controlling for both global levels of atrophy (i.e., grey matter fraction) and age. Although a strong negative association was found between WMH load and, both, grey matter volume and grey matter fraction, indicating potential collinearity issues between these aspects, a recent study reported that the statistical association between WMHs and cognition is independent of levels of atrophy [38]. This finding justifies the use of global levels of atrophy as a correction factor, to control for their potential confounding effects. In a similar way, although WMH volume was also profoundly correlated with age, by no means can we limit the entire ageing trajectory to the sole accumulation of WMHs. As a consequence, the possibility that this would result in collinearity issues was ruled out on theoretical grounds.

Out of the six networks analysed, only the anterior default-mode network and salience network showed significant results. The significant cluster within the anterior default-mode network was located in a hub that is normally a key part of the default-mode network [39]. Since increased connectivity of the anterior default-mode network with the posterior cingulate has already been reported in association with ageing [10], it is possible that this increase indicates a preferential avenue of compensation achieved by the system to fight against multiple sources of neural damage. The default-mode network (expressed as a single or double component) has to deactivate when the person engages in a task. It is possible that the changes in connectivity seen in response to ageing, or to specific types of neural insult such as those resulting in WMHs, are necessary to safeguard appropriate and efficient task deactivation. Since our findings simply indicate the presence of a statistical association, any interpretation based on a cause-effect mechanism remains merely speculative.

For the salience network, the cluster was located between regions supporting primary sensory elaboration and regions of high-order perceptual processing, which in part overlap with the parietal portion of the right frontoparietal network. The salience network is usually active in the transitional state

between task deactivation and task activation [40] and is involved in stimulus selection for behaviour guidance. In general terms, the process of ageing causes a general down-regulation of the salience network, with reduced internetwork connectivity between the salience network and the frontoparietal network [41], a finding which goes in the opposite direction of that found in this study. It could be argued, however, that the brain can cope with a limited amount of damage (i.e., that due to mild WMH load) by upregulation of the salience network-frontoparietal network connectivity, but it is not equally successful in limiting all of the detrimental changes induced by the complex process of ageing (e.g., including progressive accumulation of WMH and atrophy).

A positive association was also found in the anatomy of the forebrain. The largest cluster included a portion of the medial prefrontal cortex and the anterior cingulate cortex (Figure 3). This territory is part of the salience network (the posterior part of the cluster) and the anterior default-mode network (the anterior part of the cluster). From an interpretational viewpoint, this is consistent with the findings of the functional connectivity analysis models, as the same cerebral territory appears to be affected by WMH load, structurally and functionally.

Analysis of the effects of WMH load on cognitive performance yielded results consistent with our findings discussed above. The only score that showed a significant association with WMH load was the Stroop time interference index. Evidence has shown that this task is profoundly dependent on the default-mode network and the salience network. As the default-mode network deactivates while the person engages in a Stroop task, hubs of the salience network activate [42]. In our study, this association retained its significance even after correcting for age, education level, and global level of atrophy. This strongly indicates that the executive skills of inhibition and interference resolution are the cognitive domains most susceptible to the presence of WMHs. Interestingly, the regional connectivity expressed at the level of the two clusters emerging from the anterior default-mode network and salience network models was positively correlated with the Stroop time interference index (i.e., more connectivity is needed when interference is overcome in a longer time). On these grounds, we interpret these significant correlations as indicative of an adaptive neuroplastic increase of connectivity in response to the accumulation of WMHs.

Although an anatomical-functional convergence of findings can be extrapolated across modalities, it remains to be clarified why the connectivity of certain networks was not influenced by WMH load. Interestingly, in a previous study carried out on healthy controls and patients suffering from vascular or Alzheimer dementia, WMHs were found to affect the function of the frontal lobe irrespective of their location in the template [43]. Although the authors speculated that this might be due to a prefrontal convergence of white matter tracts, the ultimate reason why this occurs remains unknown. It is interesting to note, however, that we confirmed the preferential influence of WMH load on frontal lobe function and structure.

Despite the neat pattern of findings, which defines a common direction for volumetric, connectivity, and cognitive variables, it is more challenging to delve into the actual mechanisms by which neuroplastic modifications might occur. It was suggested that, aside from reducing the amount of neural tissue, atrophy also acts as an active inductor of plasticity, because age-dependent overactivations are typically seen in those regions which show prominent age-dependent shrinkage [44]. It is possible that the gradual accumulation of WMHs would have a similar active function fostering the stimulation of neuroplastic grey matter adaptations and increases in functional connectivity. Longitudinal studies are needed to address this issue, potentially following up populations of patients who are particularly at risk of developing WMHs (e.g., individuals with one or more cardiovascular risk factors) over time.

Another interpretational point deserves attention. If an authentic causative association existed between WMH load and an increase in prefrontal and antero-limbic grey matter, it would be necessary to clarify its biological correlates. In such case, two major candidate mechanisms might be at play: synaptogenesis and vascular changes [2]. An increase in the number of synapses would be consistent with the evidence of increased functional connectivity, while an increase in regional vasculature would be consistent with the aetiology of the damage, as the vascular system would compensate for the ischaemic blockages that generate WMHs.

This study, however, is not free from limitations. Although previous findings showed that WMHs seem to have a preferential impact on frontal function regardless of their location [43], it would be informative to characterise each single lesion with additional qualitative and topographical details (i.e., whether it was a periventricular or deep WMH and which tracts were affected). This is an important aspect to be considered as part of future studies. A second limitation is that it is not possible to derive a cause-effect link from the pattern of statistical associations. To address this, a prospective longitudinal study might provide the missing interpretational link (i.e., studying the extent to which differences in WMH load from baseline to retest predict any change in brain structure and functional connectivity from baseline to retest).

5. Conclusion

In summary, significant positive associations were found between the brain WMH load and the volume and functional connectivity of the anterior default-mode network and the salience network. The WMH load was also associated with executive function, specifically inhibition skills, measured with the Stroop time interference index. Positive associations were found between these abilities and the connectivity within the significant anterior default-mode network and salience network clusters. This convergence suggests that WMHs may be linked to neuroplastic changes in the frontal and antero-limbic territories in healthy adults. The tendency of prefrontal and antero-limbic regions to be positively responsive to subcortical damage is an aspect that deserves attention. In fact, similar (but, in all likelihood, less effective)

mechanisms may be involved in the structural and functional reorganisation following more serious and extensive brain damage. On this note, rehabilitation programmes might benefit from evidence showing that certain regions of the brain are particularly prone to compensatory changes.

Conflicts of Interest

The authors declare that there is no conflict of interest regarding the publication of this article.

Acknowledgments

This study has been supported by funding from the European Union Seventh Framework Programme (FP7/2007–2013) under Grant Agreement no. 601055, VPH-DARE@IT. The authors would like to thank Sarah Jones for her revision of the manuscript.

References

[1] E. J. Cohen, E. Quarta, R. Bravi, A. Granato, and D. Minciacchi, "Neural plasticity and network remodeling: from concepts to pathology," *Neuroscience*, vol. 344, pp. 326–345, 2017.

[2] R. J. Zatorre, R. D. Fields, and H. Johansen-Berg, "Plasticity in gray and white: neuroimaging changes in brain structure during learning," *Nature Neuroscience*, vol. 15, no. 4, pp. 528–536, 2012.

[3] H. W. Chen, J. Epstein, and E. Stern, "Neural plasticity after acquired brain injury: evidence from functional neuroimaging," *PM & R-The Journal of Injury, Function, and Rehabilitation*, vol. 2, no. 12, pp. S306–S312, 2010.

[4] M. M. Mesulam, "Neuroplasticity failure in Alzheimer's disease: bridging the gap between plaques and tangles," *Neuron*, vol. 24, no. 3, pp. 521–529, 1999.

[5] B. Draganski, C. Gaser, V. Busch, G. Schuierer, U. Bogdahn, and A. May, "Neuroplasticity: changes in grey matter induced by training," *Nature*, vol. 427, no. 6972, pp. 311-312, 2004.

[6] S. W. Davis, N. A. Dennis, S. M. Daselaar, M. S. Fleck, and R. Cabeza, "Que PASA? The posterior-anterior shift in aging," *Cerebral Cortex*, vol. 18, no. 5, pp. 1201–1209, 2008.

[7] R. Cabeza, "Hemispheric asymmetry reduction in older adults: the HAROLD model," *Psychology and Aging*, vol. 17, no. 1, pp. 85–100, 2002.

[8] C. M. Huang, T. A. Polk, J. O. Goh, and D. C. Park, "Both left and right posterior parietal activations contribute to compensatory processes in normal aging," *Neuropsychologia*, vol. 50, no. 1, pp. 55–66, 2012.

[9] S. Heuninckx, N. Wenderoth, and S. P. Swinnen, "Systems neuroplasticity in the aging brain: recruiting additional neural resources for successful motor performance in elderly persons," *Journal of Neuroscience*, vol. 28, no. 1, pp. 91–99, 2008.

[10] D. T. Jones, M. M. Machulda, P. Vemuri et al., "Age-related changes in the default mode network are more advanced in Alzheimer disease," *Neurology*, vol. 77, no. 16, pp. 1524–1531, 2011.

[11] J. A. Archer, A. Lee, A. Qiu, and S. H. Chen, "A comprehensive analysis of connectivity and aging over the adult life span," *Brain Connectivity*, vol. 6, no. 2, pp. 169–185, 2016.

[12] J. O. S. Goh, "Functional dedifferentiation and altered connectivity in older adults: neural accounts of cognitive aging," *Aging and Disease*, vol. 2, no. 1, pp. 30–48, 2011.

[13] G. Ziegler, R. Dahnke, L. Jäncke, R. A. Yotter, A. May, and C. Gaser, "Brain structural trajectories over the adult lifespan," *Human Brain Mapping*, vol. 33, no. 10, pp. 2377–2389, 2012.

[14] N. Raz, Y. Q. Yang, C. L. Dahle, and S. Land, "Volume of white matter hyperintensities in healthy adults: contribution of age, vascular risk factors, and inflammation-related genetic variants," *Biochimica et Biophysica Acta-Molecular Basis of Disease*, vol. 1822, no. 3, pp. 361–369, 2012.

[15] F. M. Gunning-Dixon and N. Raz, "The cognitive correlates of white matter abnormalities in normal aging: a quantitative review," *Neuropsychology*, vol. 14, no. 2, pp. 224–232, 2000.

[16] P. A. Boyle, L. Yu, D. A. Fleischman et al., "White matter hyperintensities, incident mild cognitive impairment, and cognitive decline in old age," *Annals of Clinical and Translational Neurology*, vol. 3, no. 10, pp. 791–800, 2016.

[17] S. N. Lockhart, A. E. Roach, S. J. Luck et al., "White matter hyperintensities are associated with visual search behavior independent of generalized slowing in aging," *Neuropsychologia*, vol. 52, pp. 93–101, 2014.

[18] A. B. V. Mayda, A. Westphal, C. S. Carter, and C. DeCarli, "Late life cognitive control deficits are accentuated by white matter disease burden," *Brain*, vol. 134, Part 6, pp. 1673–1683, 2011.

[19] A. M. Brickman, K. L. Siedlecki, J. Muraskin et al., "White matter hyperintensities and cognition: testing the reserve hypothesis," *Neurobiology of Aging*, vol. 32, no. 9, pp. 1588–1598, 2011.

[20] P. Linortner, F. Fazekas, R. Schmidt et al., "White matter hyperintensities alter functional organization of the motor system," *Neurobiology of Aging*, vol. 33, no. 1, pp. 197.e1–197.e9, 2012.

[21] S. N. Lockhart, S. J. Luck, J. Geng et al., "White matter hyperintensities among older adults are associated with futile increase in frontal activation and functional connectivity during spatial search," *PLoS One*, vol. 10, no. 3, article e0122445, 2015.

[22] H. I. L. Jacobs, L. Clerx, E. H. B. M. Gronenschild, P. Aalten, and F. R. Verhey, "White matter hyperintensities are positively associated with cortical thickness in Alzheimer's disease," *Journal of Alzheimer's Disease*, vol. 39, no. 2, pp. 409–422, 2014.

[23] A. M. Tuladhar, A. T. Reid, E. Shumskaya et al., "Relationship between white matter hyperintensities, cortical thickness, and cognition," *Stroke*, vol. 46, no. 2, pp. 425–432, 2015.

[24] Y. Taki, S. Kinomura, K. Sato et al., "Correlation between degree of white matter hyperintensities and global gray matter volume decline rate," *Neuroradiology*, vol. 53, no. 6, pp. 397–403, 2011.

[25] F. Faul, E. Erdfelder, A. Buchner, and A. G. Lang, "Statistical power analyses using G*Power 3.1: tests for correlation and regression analyses," *Behavior Research Methods*, vol. 41, no. 4, pp. 1149–1160, 2009.

[26] A. Venneri, M. A. Molinari, R. Pentore, B. Cotticelli, P. Nichelli, and P. Caffarra, "Shortened Stroop color-word test—its application in Alzheimer's-disease," *Alzheimers Disease and Related Disorders: Selected Communications*, vol. 87, pp. 81-82, 1993.

[27] J. Ashburner and K. J. Friston, "Voxel-based morphometry—the methods," *NeuroImage*, vol. 11, no. 6, Part 1, pp. 805–821, 2000.

[28] P. Schmidt, C. Gaser, M. Arsic et al., "An automated tool for detection of FLAIR-hyperintense white-matter lesions in multiple sclerosis," *NeuroImage*, vol. 59, no. 4, pp. 3774–3783, 2012.

[29] A. C. Birdsill, R. L. Koscik, E. M. Jonaitis et al., "Regional white matter hyperintensities: aging, Alzheimer's disease risk, and cognitive function," *Neurobiology of Aging*, vol. 35, no. 4, pp. 769–776, 2014.

[30] J. A. Maldjian, C. T. Whitlow, B. N. Saha et al., "Automated white matter total lesion volume segmentation in diabetes," *American Journal of Neuroradiology*, vol. 34, no. 12, pp. 2265–2270, 2013.

[31] R. Wang, L. Fratiglioni, A. Laveskog et al., "Do cardiovascular risk factors explain the link between white matter hyperintensities and brain volumes in old age? A population-based study," *European Journal of Neurology*, vol. 21, no. 8, pp. 1076–1082, 2014.

[32] M. D. Fox and M. E. Raichle, "Spontaneous fluctuations in brain activity observed with functional magnetic resonance imaging," *Nature Reviews Neuroscience*, vol. 8, no. 9, pp. 700–711, 2007.

[33] X. W. Song, Z. Y. Dong, X. Y. Long et al., "REST: a toolkit for resting-state functional magnetic resonance imaging data processing," *PLoS One*, vol. 6, no. 9, article e25031, 2011.

[34] C. Rosazza, L. Minati, F. Ghielmetti, M. L. Mandelli, and M. G. Bruzzone, "Functional connectivity during resting-state functional MR imaging: study of the correspondence between independent component analysis and region-of-interest-based methods," *American Journal of Neuroradiology*, vol. 33, no. 1, pp. 180–187, 2012.

[35] V. D. Calhoun, T. Adali, G. D. Pearlson, and J. J. Pekar, "A method for making group inferences from functional MRI data using independent component analysis," *Human Brain Mapping*, vol. 14, no. 3, pp. 140–151, 2001.

[36] J. L. Lancaster, M. G. Woldorff, L. M. Parsons et al., "Automated Talairach atlas labels for functional brain mapping," *Human Brain Mapping*, vol. 10, no. 3, pp. 120–131, 2000.

[37] P. A. Reuter-Lorenz and D. C. Park, "How does it STAC up? Revisiting the scaffolding theory of aging and cognition," *Neuropsychology Review*, vol. 24, no. 3, pp. 355–370, 2014.

[38] Z. Arvanitakis, D. A. Fleischman, K. Arfanakis, S. E. Leurgans, L. L. Barnes, and D. A. Bennett, "Association of white matter hyperintensities and gray matter volume with cognition in older individuals without cognitive impairment," *Brain Structure & Function*, vol. 221, no. 4, pp. 2135–2146, 2016.

[39] R. L. Buckner, J. R. Andrews-Hanna, and D. L. Schacter, "The brain's default network—anatomy, function, and relevance to disease," *Annals of the New York Academy of Sciences*, vol. 1124, pp. 1–38, 2008.

[40] V. Menon and L. Q. Uddin, "Saliency, switching, attention and control: a network model of insula function," *Brain Structure & Function*, vol. 214, no. 5-6, pp. 655–667, 2010.

[41] X. X. He, W. Qin, Y. Liu et al., "Abnormal salience network in normal aging and in amnestic mild cognitive impairment and Alzheimer's disease," *Human Brain Mapping*, vol. 35, no. 7, pp. 3446–3464, 2014.

[42] S. Zysset, M. L. Schroeter, J. Neumann, and D. Y. von Cramon, "Stroop interference, hemodynamic response and aging: an event-related fMRI study," *Neurobiology of Aging*, vol. 28, no. 6, pp. 937–946, 2007.

[43] M. Tullberg, E. Fletcher, C. DeCarli et al., "White matter lesions impair frontal lobe function regardless of their location," *Neurology*, vol. 63, no. 2, pp. 246–253, 2004.

[44] P. M. Greenwood, "Functional plasticity in cognitive aging: review and hypothesis," *Neuropsychology*, vol. 21, no. 6, pp. 657–673, 2007.

Hindawi
Neural Plasticity
Volume 2017, Article ID 1372946, 7 pages
https://doi.org/10.1155/2017/1372946

Research Article

Anodal Transcranial Direct Current Stimulation Provokes Neuroplasticity in Repetitive Mild Traumatic Brain Injury in Rats

Ho Jeong Kim[1] and Soo Jeong Han[2]

[1]*Department of Rehabilitation Medicine, Seonam Hospital, Ewha Womans University Medical Center, Seoul, Republic of Korea*
[2]*Department of Rehabilitation Medicine, School of Medicine, Ewha Womans University, Seoul, Republic of Korea*

Correspondence should be addressed to Soo Jeong Han; ocrystal@ewha.ac.kr

Received 28 March 2017; Revised 8 June 2017; Accepted 14 June 2017; Published 9 July 2017

Academic Editor: Andrea Turolla

Repetitive mild traumatic brain injury (rmTBI) provokes behavioral and cognitive changes. But the study about electrophysiologic findings and managements of rmTBI is limited. In this study, we investigate the effects of anodal transcranial direct current stimulation (tDCS) on rmTBI. Thirty-one Sprague Dawley rats were divided into the following groups: sham, rmTBI, and rmTBI treated by tDCS. Animals received closed head mTBI three consecutive times a day. Anodal tDCS was applied to the left motor cortex. We evaluated the motor-evoked potential (MEP) and the somatosensory-evoked potential (SEP). T2-weighted magnetic resonance imaging was performed 12 days after rmTBI. After rmTBI, the latency of MEP was prolonged and the amplitude in the right hind limb was reduced in the rmTBI group. The latency of SEP was delayed and the amplitude was decreased after rmTBI in the rmTBI group. In the tDCS group, the amplitude in both hind limbs was increased after tDCS in comparison with the values before rmTBI. Anodal tDCS after rmTBI seems to be a useful tool for promoting transient motor recovery through increasing the synchronicity of cortical firing, and it induces early recovery of consciousness. It can contribute to management of concussion in humans if further study is performed.

1. Introduction

Mild traumatic brain injury (mTBI) or concussion is an acute closed head injury resulting from external physical force applied to the head. According to the operational definition provided by the WHO collaborating task force team, mTBI could lead to confusion or disorientation and it could be symptomized by loss of consciousness for 30 minutes or less or posttraumatic amnesia for less than 24 hours. The Glasgow Coma Scale score is described as 13–15 after 30 minutes postinjury or later upon presentation for health care [1, 2]. In repetitive brain injury, long-term neurological impairment presents as memory disturbance, parkinsonism, behavioral abnormalities, personal changes, speech irregularities, and gait abnormalities [3]. Pathologic changes after repetitive mTBI (rmTBI) have been reported, including brain volume loss, tau-immunoreactive neurofibrillary tangles, the hallmark of chronic traumatic encephalopathy, and amyloid β deposition, the hallmark of Alzheimer's disease [4–6]. In a previous rodent study about rmTBI, not only behavioral changes but also pathologic changes were well proven. Behavioral changes included prolonged duration of righting reflex, decreased balance and motor coordination, and decreased spatial learning and memory. Pathologic changes include chronic gliosis, multifocal axonopathy, neurodegeneration, ventriculomegaly, and cortical thinning [7–10]. However, there is no study assessing the electrophysiological changes after rmTBI, and studies on its management are rather scarce.

Transcranial direct current stimulation (tDCS) is used to polarize local brain regions by the noninvasive application of weak direct current. The mechanism of action is thought to be associated with changes in the resting membrane potential of a neuron led by constant gradient voltage that induces ionic currents. Sodium and calcium channels are modulated by delivering subthreshold electrical currents to the brain. The direction of the current that is applied by tDCS affects the outcome. Cathodal tDCS decreases cortical excitability,

whereas anodal tDCS increases cortical excitability [11, 12]. Previous studies have reported that anodal tDCS provides a therapeutic effect in patients with neurologic disorders, such as stroke, Parkinson's disease, and Alzheimer's disease [13–15]. A recent study showed that anodal tDCS improves spatial memory during the early stage of traumatic brain injury in rats [16]. But, there is still no study assessing the effect of anodal tDCS on rmTBI.

Righting reflex was defined as the animal's ability to right itself from a supine to a prone position. In animals, delayed recovery of the righting reflex indirectly means prolonged loss of consciousness. And previous study showed prolonged righting reflex after repetitive mild traumatic brain injury [8, 10].

The purpose of this study is to investigate the electrophysiological, histologic, and behavioral changes after rmTBI and to reveal the effect of anodal tDCS treatment on rmTBI in a rat model.

2. Materials and Methods

2.1. Experimental Design. A total of thirty-one male Sprague Dawley rats (postnatal day forty-two, 180–240 g) were housed in laboratory cages under a controlled environment (21.0–24.0°C) and maintained in a 12/12 hour light/dark cycle with food and water ad libitum. All experimental protocols were approved by our Institutional Animal Care and Use Committee. Previous study suggested that postnatal day 30 in rat was roughly equivalent to late childhood, 7–11 years of age [17]. Metabolic developmental profiles showed that postnatal day 35 rats reach roughly 90% of adult values and sexual maturity is completed at postnatal day 60 [7]. Based on previous studies, postnatal day 42 meant late juvenile to early adult which is the common age of mild traumatic brain injury (teenagers and young adult) [3]. All procedures and evaluations were carried out under anesthesia. Anesthesia with Zoletil® (tiletamine/zolazepam, 15 mg/kg) was administered via an intramuscular injection. Animals were assigned to the sham group ($n = 10$), the rmTBI group ($n = 11$), and the anodal tDCS group ($n = 10$). The animals in the sham group were given only anesthesia without head impact. In the rmTBI and anodal tDCS groups, closed head traumatic brain injury was repeated three consecutive times in a single day. Then, anodal tDCS was applied in the anodal tDCS group only. The rats in all groups were then placed in a supine position and monitored for the righting reflex time. Motor-evoked potential and sensory-evoked potential tests were performed at baseline and after all procedures in each group such as rmTBI, anodal tDCS treatment, or noninjury. Brain MRI was performed 12 days after rmTBI. Five rats in each group were sacrificed at 12 days after rmTBI or sham injury for immunohistochemical analysis.

2.2. The rmTBI Model. rmTBI was induced in rats using the modified Tang's method [18, 19]. Closed head mild traumatic brain injury was produced using a weight drop device. A 175 g steel weight was dropped on the bregma of rats. The drop height was 30 cm and the weight went through a polyvinyl chloride tube (inner diameter 11 mm) to offer regular drop site. Rats were placed on a wooden plate and fixed by Velcro in a prone position. Rats were subjected to three consecutive injuries in a single day.

2.3. Anodal tDCS. Anodal tDCS was applied using Phoresor II Auto® (IOMED, Salt Lake City, UT, USA) at an intensity of 0.2 mA and a density of 0.255 mA/cm^2 for 30 min. Anodal tDCS was applied in a single session. A cup-shaped active electrode (1.0 cm diameter) was positioned on the scalp (0.785 cm^2 contact area) around the left motor cortex using a high-conductivity fixation cream. A counter electrode (3×3 cm^2-sized rubber pad) was positioned on the ventral thorax and wrapped with a tape [20].

2.4. Motor-Evoked Potential Test. MEP was recorded from the tibialis anterior muscle bilaterally. A monopolar uninsulated stainless steel needle electrode was inserted into the belly of the tibialis anterior muscle as an active electrode and into the tendon of the tibialis anterior muscle as a reference electrode. The ground was positioned at the site of the tail origin. A figure-eight-shaped transcranial magnetic stimulation (TMS) coil, Magstim magnetic stimulator® (Magstim Company Ltd., Whitland, Wales, UK), was positioned within the contralateral motor cortex whose center was anterior and lateral to the bregma. TMS intensity was recorded as percent machine output (MO), with 100% corresponding to the maximal amplitude electrical current conducted through the magnetic coil. We set the stimulation intensity to 100% MO and stimulation at a 7 sec interpulse interval. The most large peak-to-peak amplitude and the earliest latency of MEP among the results of at least 10 trials were assessed [21].

2.5. Somatosensory-Evoked Potential Test. SEP was recorded from the cortex during tail stimulation. The active electrode inserted 2.5 mm posterior to the bregma and the reference electrode inserted in the mid frontal bone. The ground was placed on the sole of the left hind limb. Electrical stimulation was performed via surface electrodes which were positioned at the site of the tail origin and 4 cm distal area. Peak-to-peak amplitude and P1 latency were averaged over 200 stimulations at a 2.0 mV stimulation intensity [22].

2.6. Brain MRI. Rats were anesthetized with an intramuscular injection of Zoletil (tiletamine/zolazepam, 15 mg/kg) and brain MRI was performed at 12 days after rmTBI. MRI scans were performed with a four-element-phased array animal dedicated with a 5 cm inner diameter surface coil (Chenguang Medical Technology Co., Ltd., Shanghai, China). A standard spin echo sequence (TE 22 ms; TR 650 ms; slice thickness 3.00 mm; matrix scan 512; FOV 100.00 mm) was used to acquire the T2-weighted images [19].

2.7. Immunohistochemistry. At 12 days after injury, the animals were deeply anesthetized with Zoletil and euthanized. The brains were extracted and fixed by immersion in 10% buffered formalin solution. Serial coronal sections of the brain were obtained, and 5 μm-thick sections including the motor cortex (primary and secondary motor cortex) and the external capsule were prepared for H-E stain and immunohistochemical study with anti-glial fibrillary acidic protein

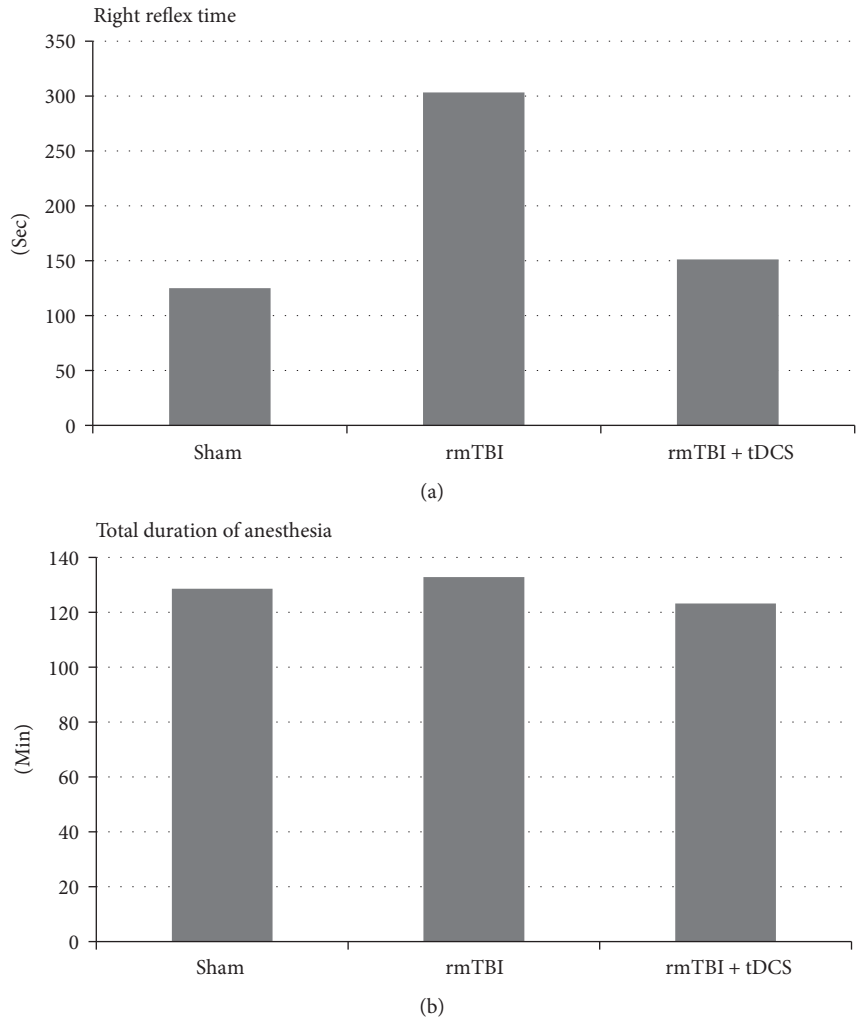

Figure 1: Righting reflex time was increased after repetitive mild traumatic brain injury (rmTBI) compared to that of the sham group, and it was decreased after anodal tDCS therapy (a). Total duration of anesthesia did not change according to brain injury and anodal tDCS therapy (b).

(GFAP) antibody (ab4674, Abcam, Cambridge, MA, 1 : 500 dilution, 30 min) and secondary antibody (ab6877, Abcam, 1 : 200 dilution, 20 min). Immunohistochemical study was performed with Bond Max (Leica Biosystems, Newcastle, UK). Integral intensity of astroglial immunoreactivity in the GFAP staining was measured by computer-assisted image analysis program (AnalySIS, Soft Imaging System, GmbH, Müster, Germany). Images were captured from motor cortex and external capsule. The software automatically changed the color of all immunolabeled elements beyond the threshold range into red pixels and changed the color of the rest of the image into gray pixels. The software then estimated the intensity of pure red pixels [23].

2.8. Statistical Analysis. Wilcoxon signed-rank test was performed to confirm the comparisons of measurements between before and after injuries or anodal tDCS. To analyze the differences among the three groups, Kruskal-Wallis test was used. Statistical analysis was performed using SPSS ver. 20.0 (IBM SPSS, Armonk, NY, USA) and p values under 0.05 were considered statistically significant.

3. Results

There was no serious adverse event after injury and anodal tDCS treatment, and all rats survived the first study day. But, three rats died during anesthesia, which was applied after twelve days for MRI.

3.1. Recovery of the Righting Reflex. Repetitive mild traumatic brain-injured rats had prolonged recovery time of the righting reflex compared to anodal tDCS-treated group (303.46 ± 181.56 sec versus 151.20 ± 131.46 sec, $p = 0.049$) and sham group (125.00 ± 98.93 sec, $p = 0.024$). There was no significant difference in the righting reflex time between the sham and anodal tDCS groups. Total duration of anesthesia was not different among the three groups (Figure 1).

3.2. MEP Findings. Repetitive mild traumatic brain-injured rats had significantly prolonged latency of MEP (6.227 ± 0.233 msec at baseline versus 6.891 ± 0.517 msec after rmTBI, $p = 0.010$) and decreased amplitude of MEP (0.169 ± 0.116 mV at baseline versus 0.076 ± 0.036 mV after rmTBI,

Table 1: The result of motor-evoked potential (MEP) in three groups.

	Rt. MEP latency (msec)	Rt. MEP amplitude (mV)	Lt. MEP latency (msec)	Lt. MEP amplitude (mV)
Sham				
Baseline	6.309 ± 0.358	0.131 ± 0.059	6.472 ± 0.371	0.119 ± 0.075
Postinjury	6.364 ± 0.376	0.122 ± 0.071	6.578 ± 0.292	0.092 ± 0.066
rmTBI				
Baseline	6.227 ± 0.233	0.169 ± 0.116	6.300 ± 0.232	0.132 ± 0.068
Post-rmTBI	6.891 ± 0.517*	0.076 ± 0.036*	7.027 ± 0.648*	0.150 ± 0.229
rmTBI + tDCS				
Baseline	6.550 ± 0.272	0.124 ± 0.066	6.650 ± 0.337	0.151 ± 0.075
Post-tDCS	6.409 ± 0.626	0.460 ± 0.253*	6.584 ± 0.737	0.406 ± 0.259*

Values are expressed as mean ± standard deviation. rmTBI: repetitive mild traumatic brain injury; tDCS: anodal transcranial direct current stimulation. *$p < 0.05$: compared to the result at baseline.

Table 2: The result of sensory-evoked potential (SEP) in three groups.

	SEP latency (msec)	SEP amplitude (mV)
Sham		
Baseline	13.75 ± 1.13	0.84 ± 0.38
Post-injury	13.91 ± 1.30	0.98 ± 0.46
rmTBI		
Baseline	13.85 ± 1.22	1.21 ± 0.34
Post-rmTBI	14.57 ± 1.11*	0.78 ± 0.37*
rmTBI + tDCS		
Baseline	14.50 ± 0.62	1.26 ± 0.47
Post-tDCS	14.18 ± 0.85	1.59 ± 1.23

Values are expressed as mean ± standard deviation. rmTBI: repetitive mild traumatic brain injury; tDCS: anodal transcranial direct current stimulation. *$p < 0.05$: compared to the result at baseline.

$p = 0.016$), which resulted from left motor cortex stimulation. Also, injured rats had significantly prolonged latency of MEP, which resulted from right motor cortex stimulation (6.300 ± 0.232 msec at baseline versus 7.027 ± 0.648 msec after rmTBI, $p = 0.008$). In the anodal tDCS-treated group, MEP amplitude increased from 0.124 ± 0.066 mV to 0.460 ± 0.253 mV ($p = 0.009$) on the left motor cortex stimulation and from 0.151 ± 0.075 mV to 0.406 ± 0.259 mV ($p = 0.005$) on the right motor cortex stimulation. But, the latency after anodal tDCS treatment did not change significantly. The latency and amplitude of MEP in the sham group were not significantly changed on the bilateral motor cortex stimulation. The baseline measurements of MEP were not significantly different among the three groups (Table 1).

3.3. SEP Findings. Repetitive mild traumatic brain-injured rats had significantly prolonged P1 latency of SEP (13.85 ± 1.22 msec at baseline versus 14.57 ± 1.11 msec after rmTBI, $p = 0.022$) and decreased amplitude of SEP (1.21 ± 0.34 mV at baseline versus 0.78 ± 0.37 mV after rmTBI, $p = 0.026$), which resulted from tail stimulation. In the anodal tDCS-treated group, the P1 latency and amplitude of SEP did not change significantly (latency 14.50 ± 0.62 msec at baseline versus 14.18 ± 0.85 msec after anodal tDCS treatment, $p = 0.341$; amplitude 1.26 ± 0.47 mV at baseline versus 1.59 ± 1.23 mV after anodal tDCS treatment, $p = 0.386$). The P1 latency and amplitude of SEP in the sham group were not significantly changed. The baseline measurements of SEP were not significantly different among the three groups (Table 2).

3.4. MRI Findings. To assess any overt structural brain damage, we conducted T2-weighted brain MRI for 30 slices from the frontal tip to the brain stem. Repetitive mild traumatic brain injury did not result in significant volumetric changes such as hydrocephalus and cortical thinning. A similar result was observed in the anodal tDCS group and the sham group (Figure 2). There was no fatal injury finding like hemorrhage, diffuse axonal injury, or skull fracture in all animals.

3.5. Immunohistochemical Findings. Gross examination of 5 brains in each 3 groups, a total of 15 brains, showed no grossly identified abnormal findings. Lateral ventricles were not grossly enlarged. There was no evidence of neuronal degeneration in all 15 cases on H-E stain.

According to immunohistochemical study with GFAP stain, hypertrophy of cell body and minimal extension of cell processes were observed in the rmTBI and anodal tDCS groups compared to those in the sham injury group (Figure 3). The integrated intensity of GFAP was measured and calculated in terms of mean values and standard deviations. The integrated intensities of GFAP in the rmTBI and anodal tDCS groups were increased in comparison with that in the sham group. But, the difference was not statistically significant. The integrated intensity of GFAP in the sham group was 818.50 ± 78.49 μm^2 at the cortex and 1046.94 ± 278.57 μm^2 in the external capsule. In the rmTBI group, the integrated intensity was 989.36 ± 151.48 μm^2 at the cortex and 1236.70 ± 95.93 μm^2 from the external capsule to the caudate putamen. In the anodal tDCS group, the integrated intensity was 859.73 ± 90.94 μm^2 at the cortex and 1203.45 ± 66.04 μm^2 from the external capsule to the caudate putamen (Figure 4).

4. Discussion

This study demonstrated that rmTBI caused loss of consciousness and affected the electrophysiological results. It

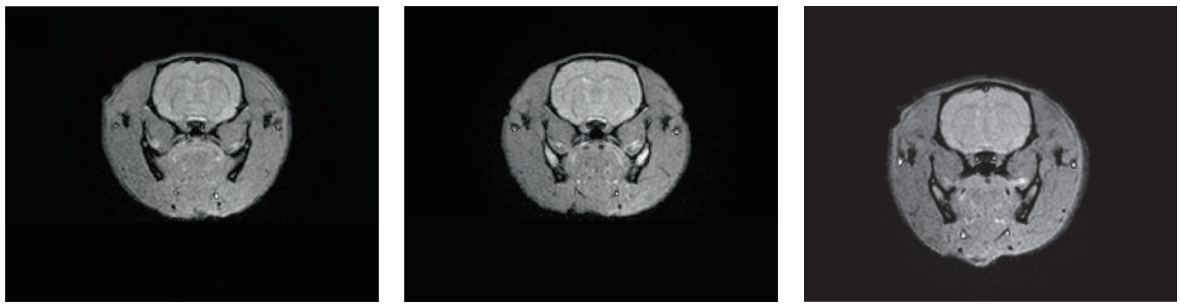

(a) (b) (c)

Figure 2: Magnetic resonance imaging findings among rats with sham (a), repetitive mild traumatic brain injury (b), and anodal tDCS (c) were not significantly different.

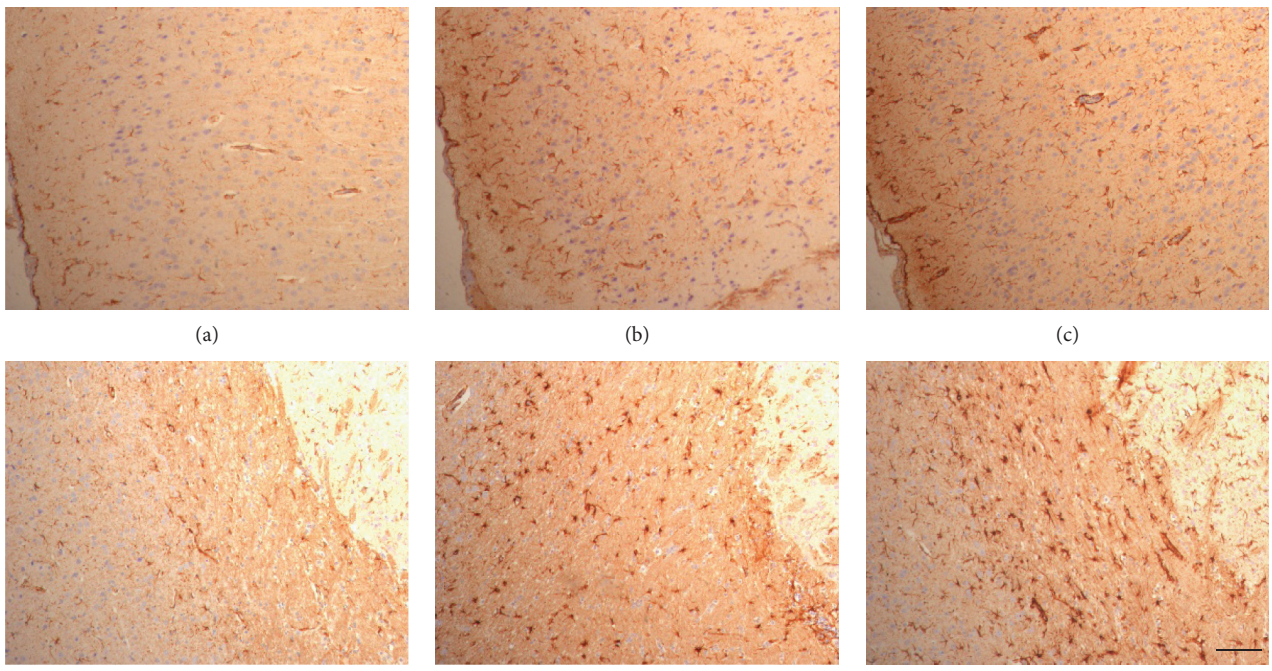

(a) (b) (c)

(d) (e) (f)

Figure 3: Repetitive mild traumatic brain injury led to a slightly increased GFAP expression in the cortex (b) and external capsule (e) compared with that of the sham group (a and d). The result was not significantly different after anodal tDCS (c and f). The calibration bar represents 200 μm scale.

also proved that anodal tDCS, administered immediately after brain injury, yielded therapeutic benefits for loss of consciousness and electrophysiological change. The decreased motor and sensory cortical excitability, which was resulted by repetitive mild traumatic brain injury, was restored by tDCS treatment. It could suppose that neural plasticity was induced by tDCS treatment after repetitive mild traumatic brain injury. And it led to early recovery of loss of consciousness.

In animals, the duration of righting reflex could imply the alertness. In this study, rats had prolonged recovery time of the righting reflex after rmTBI, but application of anodal tDCS to rats after rmTBI resulted in earlier recovery of the righting reflex compared to that of repetitive mild traumatic brain-injured rats. Also, the righting reflex time in the anodal tDCS-treated group was similar to that in the sham group. In other words, anodal tDCS has a positive effect on the recovery from loss of consciousness.

The MEP results showed prolonged onset latency and decreased peak-to-peak amplitude after repetitive mild traumatic brain injury compared to the MEP results before injury. After anodal tDCS treatment, the peak-to-peak amplitude of MEP was increased compared to that before injury. Our findings indicate that rmTBI induces a decrease in cortical excitability of the motor cortex and the decreased cortical excitability recovered after anodal tDCS management. A previous study revealed that rmTBI caused behavioral impairment [3–5]. The accumulation and repetition of decreased cortical excitability would extend the behavioral change, and then, anodal tDCS could be a novel management option for behavioral impairment resulting from rmTBI if

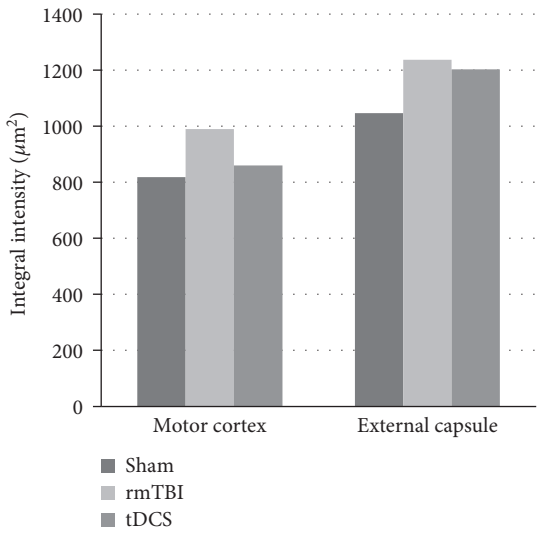

Figure 4: The labeling of GFAP in the motor sensory cortex and external capsule was maximally increased in the repetitive mid traumatic brain injury (rmTBI) group compared to that in the sham and anodal tDCS-treated groups.

further long-term study supports our results. A recent study proved that anodal tDCS applied during the early stage of traumatic brain injury had a beneficial effect on behavioral and spatial memory [16]. Traumatic brain injury is not a common disease that is treated by tDCS because of seizure tendency. However, Yoon et al. applied anodal tDCS in traumatic brain injury and showed a therapeutic effect [16]. Similar to Yoon's study, our study showed the potential of anodal tDCS treatment on rmTBI. Furthermore, our low-intensity stimulation method was safe because there was no adverse event such as seizure during anodal tDCS treatment.

The SEP results showed prolonged P1 latency and peak-to-peak amplitude after rmTBI compared to the findings before injury. This finding indicates that rmTBI also induces a decrease in cortical excitability of the sensory cortex. After anodal tDCS treatment, the latency and amplitude of SEP improved as the values of baseline. It indicates that rmTBI induces a decrease in cortical excitability of the sensory cortex, but the decreased cortical excitability could not recover after anodal tDCS treatment. Monai et al. proposed that tDCS changes the metaplasticity of the cortex through increased astrocytic signaling [24]. In other words, tDCS could induce increased neural plasticity of the nondirectly stimulated site. Therefore, the neural plasticity of the sensory cortex could occur even though anodal tDCS stimulated the motor cortex.

MRI findings showed no significant macroscopic brain change in all animals. Wright et al. reported results similar to those of our study. An advanced MRI technique such as tractography detected abnormalities in mild traumatic brain-injured rats compared to sham-injured rats. However, mild traumatic brain injury did not result in significant volumetric changes in any of the brain lesions, including those in the ipsilateral and contralateral cortex, corpus callosum, hippocampus, and lateral ventricle [25]. On the contrary, Goddeyne et al. reported that mild traumatic brain injury resulted in severe ventriculomegaly and cortical thinning [10]. Judging from the previous studies and our study, if the intensity of the impact caused by rmTBI is strong, it can cause ventriculomegaly and cortical thinning. However, when the intensity is weak, it is difficult to observe the change in gross anatomy. We also think that as the number and intensity of rmTBI increase, it will be easier to observe macroscopic brain damage. Therefore, to diagnose rmTBI, an electrophysiological study could be a diagnostic tool that has higher sensitivity than a radiological study such as MRI.

Reactive astrocytosis is the pathological hallmark of central nervous system lesions and gradated continuum of progressive changes [26]. Although rmTBI did not induce a significant increase in astrocytosis compared to that of the sham group, the mean value of GFAP labeling was increased in the cortex and white matter after brain injury and a minimal decrease was observed after tDCS in this study. Throughout the gray matter and white matter, upregulation of expression of GFAP and hypertrophy of cell body were observed after rmTBI and anodal tDCS. It was mild to moderate reactive astrocytosis. But, the expression of GFAP in the injured brain was more excessive compared to that in the brain treated by anodal tDCS. It means that anodal tDCS has a possibility to reduce the severity of brain damage after rmTBI even though significant changes were not defined in this study. The insignificant change in immunohistochemical study was supposed to be caused by the number of anodal tDCS treatments being limited to only once. The effect of multiple anodal tDCS treatments should be revealed in further studies.

The limitation of this study was that tDCS treatment was just applied in a single session. The multiple times of tDCS attempt could induce critical changes in electrophysiological findings and histologic findings. And a small sample size was the limitation to reveal the pathologic change from anodal tDCS. However, this single tDCS treatment for repetitive mild traumatic brain injury and small sample-sized study can provide preliminary data for further studies.

In conclusion, a single anodal tDCS can have a positive effect on repetitive concussion in terms of loss of consciousness and modulation of cortical excitability. Anodal tDCS after rmTBI seems to be a useful tool for promoting transient motor recovery through increasing the synchronicity of cortical firing, and it induces early recovery of consciousness. In the future, the effect of numerous sessions of anodal tDCS therapy on repetitive mild traumatic brain injury could reveal whether it can protect the brain against a delayed unpleasant degenerative change in the brain and functional impairment.

Disclosure

The funders had no role in study design, data collection and analysis, decision to publish, or preparation of the manuscript.

Conflicts of Interest

No competing financial interests exist.

Acknowledgments

This research was supported by the Basic Science Research Program through the National Research Foundation of Korea (NRF) funded by the Ministry of Education (NRF 2013R1A1A2059711) and Research Grant of the Alumni Chapters of the Medical College of Ewha Womans University in 2015. The authors would like to acknowledge Professor Dr. Hae Soo Koo for her expert work on pathology. Also, the authors are grateful for her advices on pathology.

References

[1] L. J. Carroll, J. D. Cassidy, P. M. Peloso, C. Garritty, and L. Giles-Smith, "Systematic search and review procedures: results of the WHO collaborating centre task force on mild traumatic brain injury," *Journal of Rehabilitation Medicine*, vol. 43, pp. 11–14, 2004.

[2] L. J. Carroll, J. D. Cassidy, P. M. Peloso et al., "Prognosis for mild traumatic brain injury: results of the WHO collaborating centre force on mild traumatic brain injury," *Journal of Rehabilitation Medicine*, vol. 43, pp. 84–105, 2004.

[3] L. Holm, J. D. Cassidy, L. J. Carroll, and J. Borg, "Summary of the WHO collaborating centre for neurotrauma task force on mild traumatic brain injury," *Journal of Rehabilitation Medicine*, vol. 37, pp. 137–141, 2005.

[4] A. C. McKee, R. C. Cantu, C. J. Nowinski et al., "Chronic traumatic encephalopathy in athletes: progressive tauopathy after repetitive head injury," *Journal of Neuropathology and Experimental Neurology*, vol. 68, pp. 706–735, 2009.

[5] H. Grahmann and G. Ule, "Diagnosis of chronic cerebral symptoms in boxers (dementia pugilistica and traumatic encephalopathy of boxers)," *Psychiatria et Neurologia*, vol. 134, pp. 261–283, 1957.

[6] K. Uryu, H. Laurer, T. McIntosh et al., "Repetitive mild brain trauma accelerates Aβ deposition, lipid peroxidation, and cognitive impairment in a transgenic mouse model of Alzheimer amyloidosis," *The Journal of Neuroscience*, vol. 22, pp. 446–454, 2002.

[7] M. L. Prins, A. Hales, M. Reger, C. C. Giza, and D. A. Hovda, "Repetitive mild traumatic brain injury in the juvenile rat in associated with increased axonal injury and cognitive impairments," *Developmental Neuroscience*, vol. 32, pp. 510–518, 2010.

[8] M. J. Kane, M. A. Pérez, D. I. Briggs, D. C. Viano, C. W. Kreipke, and D. M. Kuhn, "A mouse model of human repetitive mild traumatic brain injury," *Journal of Neuroscience Methods*, vol. 203, pp. 41–49, 2012.

[9] R. Mannix, J. Berglass, J. Berkner et al., "Chronic gliosis and behavioral deficits in mice following repetitive mild traumatic brain injury," *Journal of Neurosurgery*, vol. 121, pp. 1342–1350, 2014.

[10] C. Goddeyne, J. Nichols, C. Wu, and T. Anderson, "Repetitive mild traumatic brain injury induces ventriculomegaly and cortical thinning in juvenile rats," *Journal of Neurophysiology*, vol. 113, pp. 3268–3280, 2015.

[11] M. A. Nitsche and W. Paulus, "Excitability changes induced in the human motor cortex by weak transcranial direct current stimulation," *The Journal of Physiology*, vol. 527, pp. 633–639, 2000.

[12] Q. M. Wang, H. Cui, S. J. Han et al., "Combination of transcranial direct current stimulation and methylphenidate in subacute stroke," *Neuroscience Letters*, vol. 569, pp. 6–11, 2014.

[13] F. Hummel, P. Celnik, P. Giraux et al., "Effects of non-invasive cortical stimulation on skilled motor function in chronic stroke," *Brain*, vol. 128, pp. 490–499, 2005.

[14] F. Fregni, P. S. Boggio, M. C. Santos et al., "Noninvasive cortical stimulation with transcranial direct current stimulation in Parkinson's disease," *Movement Disorders*, vol. 21, pp. 1693–1702, 2006.

[15] R. Ferrucci, F. Mameli, I. Guidi et al., "Transcranial direct current stimulation improves recognition memory in Alzheimer disease," *Neurology*, vol. 71, pp. 493–498, 2008.

[16] K. J. Yoon, Y. T. Lee, S. W. Chae, C. R. Park, and D. Y. Kim, "Effects of anodal transcranial direct current stimulation (tDCS) on behavioral and spatial memory during the early stage of traumatic brain injury in the rats," *Journal of the Neurological Sciences*, vol. 362, pp. 314–320, 2016.

[17] R. Mychasiuk, H. Hehar, and M. J. Esser, "A mild traumatic brain injury (mTBI) induces secondary attention-deficit hyperactivity disorder-like symptomology in young rats," *Behavioural Brain Research*, vol. 286, pp. 285–292, 2015.

[18] Y. P. Tang, Y. Noda, T. Hasegawa, and T. Nabeshima, "A concussive-like brain injury model in mice (I): impairment in learning and memory," *Journal of Neurotrauma*, vol. 14, pp. 851–862, 1997.

[19] H. J. Kim and S. J. Han, "A simple rat model of mild traumatic brain injury: a device to reproduce anatomical and neurological changes of mild traumatic brain injury," *PeerJ*, vol. 5, article e2818, 2017.

[20] S. J. Kim, B. K. Kim, Y. J. Ko, M. S. Bang, M. H. Kim, and T. R. Han, "Functional and histologic changes after repeated transcranial direct current stimulation in rat stroke model," *Journal of Korean Medical Science*, vol. 25, pp. 1499–1505, 2010.

[21] A. Rotenberg, P. A. Muller, A. M. Vahabzadeh-Hagh et al., "Lateralization of forelimb motor evoked potentials by transcranial magnetic stimulation in rats," *Clinical Neurophysiology*, vol. 121, pp. 104–108, 2010.

[22] K. H. Han, S. H. Kim, I. C. Jeong et al., "Electrophysiological and behavioral changes by phosphodiesterase 4 inhibitor in a rat model of alcoholic neuropathy," *Journal of Korean Neurosurgical Association*, vol. 52, pp. 32–36, 2012.

[23] E. Limoa, S. Hashioka, T. Miyaoka et al., "Electroconvulsive shock attenuated microgliosis and astrogliosis in the hippocampus and ameliorated schizophrenia-like behavior of Gunn rat," *Journal of Neuroinflammation*, vol. 13, p. 230, 2016.

[24] H. Monai, M. Ohkura, M. Tanaka et al., "Calcium imaging reveals glial involvement in transcranial direct current stimulation-induced plasticity in mouse brain," *Nature Communications*, vol. 7, article 11100, 2016.

[25] D. K. Wright, J. Trezise, A. Kamnaksh et al., "Behavioral, blood, and magnetic resonance imaging biomarkers of experimental mild traumatic brain injury," *Scientific Reports*, vol. 6, article 28713, 2016.

[26] M. V. Sofroniew and H. V. Vinters, "Astrocytes: biology and pathology," *Acta Neuropathologica*, vol. 119, pp. 7–35, 2010.

Hindawi
Neural Plasticity
Volume 2017, Article ID 7125057, 12 pages
https://doi.org/10.1155/2017/7125057

Review Article

Understanding the Mechanisms of Recovery and/or Compensation following Injury

Michael J. Hylin,[1] Abigail L. Kerr,[2] and Ryan Holden[1]

[1]*Neurotrauma and Rehabilitation Laboratory, Department of Psychology, Southern Illinois University, Carbondale, IL, USA*
[2]*Department of Psychology, Illinois Wesleyan University, Bloomington, IL, USA*

Correspondence should be addressed to Michael J. Hylin; mhylin@siu.edu

Received 19 December 2016; Revised 24 February 2017; Accepted 26 March 2017; Published 20 April 2017

Academic Editor: Andrea Turolla

Injury due to stroke and traumatic brain injury result in significant long-term effects upon behavioral functioning. One central question to rehabilitation research is whether the nature of behavioral improvement observed is due to recovery or the development of compensatory mechanisms. The nature of functional improvement can be viewed from the perspective of behavioral changes or changes in neuroanatomical plasticity that follows. Research suggests that these changes correspond to each other in a bidirectional manner. Mechanisms surrounding phenomena like neural plasticity may offer an opportunity to explain how variables such as experience can impact improvement and influence the definition of recovery. What is more, the intensity of the rehabilitative experiences may influence the ability to recover function and support functional improvement of behavior. All of this impacts how researchers, clinicians, and medical professionals utilize rehabilitation.

1. Recovery or Compensation

One important question in the study of adult brain injury and repair is whether behavioral improvement reflects true behavioral recovery or whether the behavioral changes are simply due to the use of compensatory strategies in reaction to a disrupted nervous system. Part of the difficulty with recovery, from a clinical perspective, is in how it is defined. To a clinician, recovery may be generally defined in terms of improved behavior following an injury. Good recovery is defined by the Glasgow Outcome Scale as a "resumption of normal activities even though there may be minor neurological and psychophysical deficits" [1, 2]. Therefore, from the clinical perspective, an individual is "recovered" if they are able to show some improvement in functioning independently [3, 4]. Still, defining recovery as simply returning to normal life is a fairly limited concept in that it does not take into account whether the individual is simply compensating for their lost behaviors. Foroud and Whishaw [5] analyzed the kinematic profiles of two stroke patients during a reaching task and found that while the patients were able to perform the task, they demonstrated kinematic abnormalities during reaching. Though in only two patients, this evidence of compensatory limb use suggests a qualitatively different functional outcome than true behavioral recovery. These qualitative differences are likely reflected in central nervous system structure and function, the effects of which may have long-term impacts on behavioral outcome.

Typically, the focus of rehabilitative treatments following stroke or traumatic brain injury is often upon encouraging the development of compensatory strategies in order to resume independent daily living [6–8]. For instance, individuals that are hemiplegic have difficulty using their impaired limbs and rehabilitative therapy may encourage the use of their unimpaired side. Patients may also use compensatory strategies to cope with cognitive impairments. For example, if an individual is impaired in their ability to remember, a clinician may encourage the use of a journal or diary to help them remember daily events [9–12]. However, in both of these examples, even though the individual may be equipped to return to daily independent living, their impairments are still present and may interfere with long-term functional outcome instead of focusing on encouraging the lost behavior to return; the focus is upon compensating for their loss.

Essentially, the goal of rehabilitation is often focused on independence as opposed to the impairment, which may lead to improved behavioral function but prevent true behavioral recovery.

Up to this point, it could be argued that the scenarios discussed illustrate how individuals are able to compensate for the lost behavior. In fact, it is important to point out that sometimes even when an individual appears to have "recovered" and is able to function independently, they may continue to show "silent" cognitive and motor deficits in areas such as emotion, attention, or fine motor control [13–19]. These deficits are important to take into consideration in discussing whether an individual has recovered as they may otherwise go ignored. Usually, depending upon the severity of the injury, deficits will abate over time, although some residual deficits may remain [20–22]. In fact, some authors have questioned whether it is possible to observe true recovery [23–25]. If we hope to improve the efficacy of rehabilitative strategies following brain injury, it is important to distinguish between true recovery and compensation and to understand the consequences of each for long-term neural and behavioral function. This review focuses on the anatomical and behavioral mechanisms surrounding the distinction between recovery and compensation in the adult with the aim of using this distinction to guide strategies for successful rehabilitation. As the majority of human strokes are ischemic in nature, we focus specifically on ischemic insult in the adult (human, nonhuman primate, and rodent models) [26]. Traumatic brain injuries (TBI) have a fairly distinct pathological response that is separate from stroke [27, 28]. While within TBI characterization, focal and diffuse injuries have distinct pathologies; most TBIs have elements of both types of injury and are heterogeneous in nature making the distinction difficult from the perspective of recovery and treatment [29–31]. In addition, traumatic axonal injury has been shown to lead to selective atrophy in a regional manner similar to what is observed following focal injury [32]. This review considers how the cognitive reserve applies to functional improvement following injury and how the intensity of rehabilitation plays a role in recovery and compensation.

2. Neuroanatomical Effects of Damage upon Recovery/Compensation

In understanding how compensatory strategies are developed, one must consider the anatomical and cellular events that are associated with injury. Following unilateral brain injury, there is a sequence of events that have devastating effects upon the primary site of damage. Regardless of how the damage occurs (e.g., ischemic stroke or TBI), this usually begins with the interruption of the blood supply to the brain, which causes cells to die through over excitation due to excess glutamate release [33–38]. Following the initial damage, tissues become swollen and inflamed, compromising the integrity of areas that are distant from the primary site of damage [37, 39–42]. This swelling and inflammation may cause deficits that will abate over time [43, 44]. There is also a decrease in the metabolic activity in the ipsilesional hemisphere suggesting that the damage can impact areas distal to the injury, a phenomenon known as diaschisis [45–47].

While injury results in devastating events, it also induces a cascade of growth-related events that enable remaining neurons near and distant to the lesion locus to survive, repair, and form new connections [48–53]. Some researchers have even proposed that some of the events that occur following damage are similar to what is observed during normal development, possibly suggesting that the brain has an intrinsic ability to react to change [54–59]. Changes in perilesion cortex (i.e., the area of vulnerable but surviving tissue immediately around the lesion core), including cortical reorganization, neurogenesis, axonal sprouting, dendritic plasticity, and angiogenesis, have been linked to spontaneous recovery of behavioral deficits following the resolution of diaschisis as described above [60–65]. Within the perilesion area, there is also an increase in the expression of growth-promoting genes which begins to be seen shortly after injury [66, 67]. This altered environment is arguably becoming growth permissive, as increased axonal sprouting will occur in this region [53, 68]. Increased levels of GAP-43, a marker for the presence of growth cones, have been observed shortly after injury [69, 70]. Carmichael and Chesselet [71] found that the increased axonal sprouting correlates with an altered physiological response in the perilesion area. This increase in synchronous activity is followed by activity in other cortical regions associated with the damaged area including the contralesional homotopic cortex. Further, it is likely that the axonal sprouting and altered activity in this region is what underlies reorganization of the remaining cortical representations in the perilesion area [42, 68, 71–75].

The perilesion area is not the only location that is altered in response to injury. Frost et al. [21] found that following lesions of the hand area of the primary motor cortex in primates, there is an expansion of the hand area of the ventral premotor cortex (PMv) in the same hemisphere [76]. This increased expansion is associated with altered axonal sprouting from the PMv [72, 77]. Both of these changes are correlated with improved motor behavior. Following injury, the contralesional hemisphere also exhibits an increase in dendritic growth [78–80] as well as increased sprouting of corticostriatal axons [78, 81]. Further, reorganization of contralesional hemisphere usually corresponds to increased synapse number [82, 83]. Some authors have suggested that this growth is the result of a compensatory behavioral response (e.g., [80, 84]).

Compensatory sprouting has also been looked at in models of TBI, as diffuse axonal injury is frequently observed following injury. The temporal lobes and hippocampus are one of the most vulnerable areas after a TBI [85, 86]. Injury results in robust neural plastic changes in the hippocampus, which include increased synaptogenesis, increased expression plasticity-related proteins such as extracellular signal-regulated kinase, and altered expression of genes associated with structural changes [87–93]. However, it remains to be determined if these changes reflect a positive impact following injury and if methods inducing recovery could employ them to support improved outcome. Utilizing a model of combined TBI with entorhinal cortex deafferentation,

Philips et al. (1994) observed cognitive deficits (impairments in the water maze) that were associated with aberrant neural sprouting and synapse formation. Damage to the entorhinal cortex has been shown to produce reactive synaptogenesis and collateral sprouting and result in the formation of novel synapses in the dentate gyrus [94–96]. In patients following TBI, compensatory neural tracts extending from the contralesional fornix have been observed and may underlie recovery of memory impairments [97].

It appears that the brain is able to undergo neuroanatomical changes that lead to the reorganization of remaining tissue following damage. However, this reorganization has behavioral consequences that need to be considered when determining whether recovery or compensation has occurred.

3. Behavioral Effects of Recovery/Compensation

Instead of regarding recovery as a "general" improvement in behavioral functioning, researchers have a more varied and sometimes less well-defined criterion. One view of behavioral recovery is whether an end point has been achieved that is similar to the preoperative performance of the animal or to the performance of a nonlesioned animal [22, 98–100]. For instance, if an animal is able to learn to navigate a maze successfully, even if it takes more trials to learn than an intact control, one could argue that the animal has demonstrated functional recovery [101–104]. A similar result is seen with animals that have received motor cortex lesions. Initially animals are impaired in their ability to reach for food, but they will eventually be able to successfully improve their reaching behavior following weeks of testing [105]. However, it is important to point out that while they are able to become more successful over time they are still impaired relative to even their own preoperative baseline [24]. Depending upon the task, animals usually show some improvement in behavior over time, possibly suggesting that some form of "recovery" may be possible [106, 107]. It should be noted that with focused training of the impaired limb, animals often reach preoperative performance levels [108–111], suggesting that behavior can interact with naturally occurring plastic changes following stroke to drive functional outcome.

Often, behavioral changes are associated with the presence of neuroanatomical changes in areas functionally related to the damage. Following a unilateral lesion of the sensorimotor cortex, there is an increased reliance upon the unimpaired limb for movement and postural support which coincides with increased dendritic growth in the contralesional hemisphere [46, 47, 79]. The increased growth peaks at three weeks following injury, and pruning of this over growth begins to occur over the next few weeks. The overreliance on the unimpaired limb will also begin to decrease shortly after the dendritic pruning begins, possibly suggesting that the behavior of the animal over time following injury influences the ability for plasticity to occur [103, 112]. Jones and Schallert [80] tested this by restricting the movement of the unimpaired limb and forcing the animal to use their impaired limb. By restricting the unimpaired limb, the increased growth was blocked suggesting that the plasticity that occurs due to injury interacts with the behavioral deficit [80, 113]. Similar results have been found in rodent models of TBI, although the mechanistic differences remain to be elucidated [114–117]. Although it is tempting to suggest that the increased neuronal growth that is observed following damage is beneficial as it is seen following improvements in behavior, it is possible that the growth is promoting compensatory behaviors rather than true recovery [24, 118, 119], which may be interfering with or even preventing true recovery [84, 109, 120–122].

Forced use of the unimpaired limb following stroke, mimicking compensatory use following injury, is associated with decreased neuronal activation [123, 124] and further reduction of forelimb movement representations in the perilesion cortex [84]. Kim and colleagues report not only decreased forelimb representation area in perilesion motor cortex but also an increase in axodendritic synapses and multiple synaptic boutons following forced use of the unimpaired limb (i.e., compensatory limb training) [84]. This synaptic density negatively correlated with functional outcome of the impaired limb, suggesting that aberrant synaptogenesis, potentially of transcallosal projections, may contribute to the poor functional outcome associated with compensatory limb use following injury. Interestingly, animals that have had callosal transections do not exhibit the compensatory limb effect, with forced use of the unimpaired limb having no impact on bad limb recovery [122].

Another way experimental researchers define recovery is by whether the means (i.e., methods) to achieve a particular end point following injury is similar to how it would be performed in the intact animal [104]. Following injury, there is an emergence of what has been regarded as "self-taught" behaviors that develop spontaneously as behavioral deficits begin to subside. These behaviors may develop as a response to compensate for those behaviors lost as a result of injury [125, 126]. For instance, following an ischemic injury to the motor cortex, squirrel monkeys are unable to use their affected hand in reaching for a pellet of food [64]. Over time, there is a gradual return in the ability to use the limb, and this improvement corresponds to reorganization of the motor map [21, 72, 77, 127]. However, recovery of limb movement is due to the use of compensatory behavioral strategies that are fundamentally different from preinjury strategies [128–130]. Even more careful analysis has demonstrated that although the ability to grasp has returned, there are residual fine motor deficits that lead to the development of compensatory movement of individual digits despite further training [73, 131, 132].

In a similar vein, injury to the motor cortex in rats results in an inability to successfully reach for a food pellet that abates over time. Rats with motor cortex lesions are unable to make rotational movements and demonstrate impaired digit use [24]. A more detailed analysis of the reaching behavior in rodents also suggests that even though lesioned animals may regain use of the impaired limb, many qualitative aspects of the behavior are different [133]. Further, a return of the reaching ability in the rat occurs in distinct stages [134].

In the acute stage following ischemic injury, lesioned animals are unsuccessful at their reaching attempts.

Erickson et al. [135] suggested that animals are in a sense "learning" that they are likely to be unsuccessful in reaching for the pellet as there is a decline in the number of reaching attempts during this period. This "learned nonuse" occurs only in the acute stages following damage; 8 days post damage, rats increase their number of reach attempts [135]. As animals show an increase in their number of reach attempts, there is a corresponding increase in the number of individually repeated gestures. An animal may advance its limb and withdraw several times without ever grasping the food. Even though there is an increase in the number of attempts, if there is a reduction in the number of successful reaches due to the additional gestures, this behavior could be characterized as "learned bad-use" [136, 137]. Encouraging the unimpaired limb to be used can interfere with later training of the impaired limb [109, 111, 120, 123, 138]. It is possible that remaining motor systems take advantage of the beneficial growth that occurs following ischemic injury, which leads to increased use of the unimpaired limb. Interestingly, bilateral limb use (via either focused, skilled training or home-cage enrichment that encourages dexterous use of both limbs) ameliorates this effect, resulting in a restoration of rehabilitative potential of the impaired limb [109, 123].

It may also be possible for behavioral substitution to take place following injury-induced loss of behavior. Rauschecker [139] found that cats that were deprived of vision early in life can solve a visual maze using tactile sensation that is complimented by expanded cortical representation of their facial vibrissae. Therefore, in the absence of one means for solving a task, it appears that another can substitute and allow for the goal to be accomplished via sensory substitution or a different behavioral strategy. Whishaw et al. [140] demonstrated that hemidecorticate rats are able to learn to successfully navigate a maze, which may suggest that different strategies, possibly mediated by subcortical areas, can be substituted in order for them to successfully navigate. This result is not to be unexpected considering rats are able to substitute one spatial strategy in the absence of another in order to successfully navigate an environment [141].

Part of the difficulty of determining whether true recovery has occurred in the experimental setting has been in the analysis of the behavior. Some authors have even stated that using just a few (often only one) behavioral measures may lead to biased estimates of behavior and that a better assessment of behavior comes from using a "battery" of species-typical and learned behaviors [105]. The use of simple "end point" measures also limits the interpretation of whether a motor behavior has returned [134, 136, 142]. Further, the fractionation of more complex behaviors (e.g., reaching) enables researchers to determine what is possible with regard to recovery and whether animals are using compensatory behaviors [134, 143].

As mentioned previously, most rehabilitative treatments encourage the use of compensatory strategies following injury. However, there are clinical studies of rehabilitative therapies for motor deficits that have focused on training the impaired limb following stroke [144–147]. Some researchers have suggested that what is observed during natural recovery is the development of compensatory behaviors and that "true" recovery is possible following specific rehabilitative training focused on the impairment rather than behavioral outcome [148, 149]. Still, other researchers have taken an extreme stance on the issue suggesting that when recovery is observed, it is due to the reorganization of remaining areas that lead to the development of compensatory behaviors [24]. Even if the behavior is similar to preinjury conditions, the argument is that the remaining functional areas now have to compensate for the loss. Therefore, this argument posits that in order for true recovery to occur, the neurons and their corresponding neural connections that were lost during injury need to be replaced rather than substituted [24, 150].

4. The Role of Reserve after Brain Injury

In the field of brain injury, there remains a clear disconnect between brain trauma severity and clinical emergence [151, 152]. A similar brain injury among two, separate individuals may not result in the same degree of behavioral impairments. It has been proposed that this observation could be a result of individual differences in a concept known as cognitive reserve. Cognitive reserve (CR) is considered to be an accumulation of complex neural networks that allows for unique task processing in the brain [153]. CR can be increased through a variety of mental activities that keep the brain active. In other words, "exercising" or strengthening the brain's neuronal connections leads to a large CR. This "exercise" works to provide the brain with a more plastic and varied neural circuitry. CR has been associated with characteristics such as a balanced diet, occupational complexity [154], IQ [152], and participation in various lifestyle activities [155]. According to Murray et al. [156], level of education can also be used as a marker for cognitive reserve. As such, studies have shown that those with high levels of educational attainment have been associated with greater short- and long-term functional recovery after brain injury, in cases of both ischemic stroke [157] and moderate/severe traumatic brain injuries [158, 159].

Another hypothesis that has been put forth is that cognitive reserve is based upon one's entire lifetime. If this is the case, then older individuals should, in theory, have more cognitive reserve capacity than younger individuals since they have had longer to fully develop their more elaborate and intricate communicative system. Although, it must be pointed out that the brain processing in those with high CR is the same for all individuals [153]. The capacity of CR may vary, but its way of action does not change. A larger CR would give an individual a higher threshold for injury and would require an injury of greater severity for clinical symptoms to show [152]. However, research has shown that CR positively influences functional recovery not only in adults but also in children and adolescents [158]. It would seem that a larger CR, at any age or time point during development, could help the brain to better sustain injuries [160]. Although, the literature also suggests that a CR of lower capacity can exacerbate the secondary effects of brain injuries, particularly in instances of TBIs [158]. Therefore, CR may serve as a preventative compensatory mechanism in

order to keep the injury from producing further and unnecessary damage after brain injury.

There is the possibility that cognitive reserve may be acting as the nervous system's natural means of compensation after brain injury. Specifically, a large cognitive reserve could provide a more convenient outlet for plasticity to occur, allowing for the more efficient and established neural connections to help the brain better sustain injuries because of its higher level of threshold [159, 161]. In addition to compensatory action through an emphasis on well-established connections, individuals that accumulate a strong CR throughout their lifetime may have a brain that is unique in neural organization in another way, such that the brain communicates in a more holistic manner through a more varied neural network rather than through a limited number of possible neuronal pathways [154]. Since the level of redundancy is high in those with a large CR, it is unlikely that a brain injury will disrupt all communicative routes, thereby fostering a quicker, less intrusive cognitive recovery through the utilization of alternative neural circuitry [162]. It remains to be shown if cognitive reserve is a form of preventive compensation (i.e., the brain is compensating for natural loss because there is synaptic loss as we age and neurons compensate for the loss by increasing synaptic number) [163]. But if there is an injury, this compensation from natural aging gets used up.

5. The Impact of Timing and Intensity on Rehabilitation Efficacy

Following CNS injury, experience-induced plasticity (e.g., changes induced via rehabilitation) interacts with the natural richly plastic environment described above. The ultimate efficacy of rehabilitative training depends on how well coordinated those plastic events are. There are a number of factors that may drive more functionally beneficial effects of rehabilitative training, including the timing and intensity of training.

As we have discussed, the injured brain can both promote and inhibit neural plasticity. In order to maximize the functional benefit of rehabilitative training, the timing of training onset must coincide with a naturally more growth permissive environment following injury. Identifying the ideal "window of recovery" following injury is difficult, though research in rodents suggests that there is an early vulnerable period following injury during which training can have negative effects on recovery and exacerbate neural damage. For instance, forced use of the impaired forelimb during the first seven days following stroke results in poor functional outcome and larger lesion size compared to rats permitted to engage either forelimb [164–166]. Similar results are found with exercise as a rehabilitative strategy, with early exercise reducing neuroplasticity-related molecules in the hippocampus following traumatic brain injury in rats. More favorable outcomes are reported if the exercise is initiated two weeks following TBI, with the same molecules being upregulated and spatial memory improving [167, 168]. Early exercise can also be problematic following ischemic stroke causing increased apoptosis and impaired learning performance [169, 170].

When is the best time to introduce rehabilitative training—the question is somewhat difficult. Biernaskie and colleagues found that rehabilitative training was more effective in improving behavioral outcome when initiated five days rather than 30 days following stroke [171]. Similar results were reported by Norrie et al. [172], who found that though stepping function in rats improved after motor rehabilitative training initiated both immediately after spinal cord injury and after a three-month delay, the immediate rehabilitation was much more efficacious. Early onset training is also more beneficial to structural plasticity; motor maps in monkeys exhibit decreased sparing of movement representation areas in the motor cortex when training is initiated one month after ischemic cortical infarct rather than one week [173]. Together, these findings suggest that the ideal time to introduce symptom-specific, skilled rehabilitative training is early, but not immediately, after insult. However, the exact time window for beneficial structural and functional outcomes is still unclear. It is important that we continue to explore the regenerative and degenerative responses of the brain to injury and how these responses interact with behaviorally induced experience-dependent plasticity to drive functional outcome.

Another factor that affects behavioral outcome following injury is the intensity of rehabilitative training. In the intact brain, training intensity impacts both the rate of behavioral change as well as the neural consequences associated with new learning. For instance, mice that receive twice daily motor skill training sessions exhibit a faster acquisition of the skill [174]. MacLellan and colleagues (2011) found that enriched rehabilitation (skilled reaching combined with enriched housing) was only effective in improving functional recovery when enrichment was provided during the more active dark cycle, when rats are more likely to engage with enrichment options at higher intensity [175]. The researchers suggest that there may be a threshold of rehabilitation that is necessary to provide functional benefits. Similarly, Bell et al. [108] found that twice-daily training on the Pasta Matrix Reaching Task (i.e., skilled rehabilitative training) was more beneficial for functional outcome than once-daily training sessions. Specifically, high-intensity training resulted in a faster return to preoperative performance levels [108]. Results from these studies suggest that high-intensity rehabilitative training, initiated early after insult, would be the most effective strategy to employ in humans. It should be noted that current rehabilitative regimens in humans are considerably less intense than those practiced in animal models [22].

6. Conclusions

Although the proceeding discussion has focused on compensation/recovery following injury, it is likely that these mechanisms reflect a natural phenomenon that allows an organism to constantly adapt to an ever-changing environment rather than exclusively occurring following injury. While this is a novel consideration in understanding compensation, it has its basis in the observation of what occurs

during learning and may reflect the nervous system's ability to adapt to an ever-changing environment (i.e., experience-dependent plasticity). In most normal situations for solving a task, there is a hierarchy of behaviors in order to successfully complete it. If, for instance, an individual is blindfolded, they may still be able to complete a maze through the use of tactile or auditory cues [98]. Also, if a "normal" individual is blindfolded and taught to tacitly discriminate for a prolonged period, there is a temporary increase in activity present in the occipital cortex when tactile stimulation is given [176].

The plastic changes that occur following injury are strikingly similar to those that are observed in normal brains following learning or other experiences [105, 177]. For instance, training of a particular motor sequence induces an altered representation in a normally functioning nervous system that is similar to what occurs following damage [178, 179]. One explanation for this may be that the nervous system is able to change in response to behavioral demand. In many instances, plastic changes occur in at all levels of organization from gene expression to neural systems following injury or during "normal" training [180]. This may suggest that there is a common thread between what occurs following damage and what occurs in situations where plasticity normally occurs. Therefore, one possible method to understand the changes associated with recovery/compensation is observing situations where plasticity normally occurs. However, future work needs to focus on determining and defining what entails complete recovery and whether it is possible for it to occur naturally or through the use of therapeutic intervention or if compensation is the only possibility.

Conflicts of Interest

The authors declare that they have no conflicts of interest.

References

[1] B. Jennett and M. Bond, "Assessment of outcome after severe brain damage," *Lancet*, vol. 1, no. 7905, pp. 480–484, 1975.

[2] T. McMillan, L. Wilson, J. Ponsford, H. Levin, G. Teasdale, and M. Bond, "The Glasgow Outcome Scale-40 years of application and refinement," *Nature Reviews Neurology*, vol. 12, no. 8, pp. 477–485, 2016.

[3] R. Nakase-Richardson, J. Whyte, J. T. Giacino et al., "Longitudinal outcome of patients with disordered consciousness in the NIDRR TBI Model Systems programs," *Journal of Neurotrauma*, vol. 29, no. 1, pp. 59–65, 2012.

[4] D. G. Stein and M. M. Glasier, "An overview of developments in research on recovery from brain injury," in *Recovery from Brain Damage: Reflections and Directions*, F. D. Rose and D. A. Johnson, Eds., pp. 1–22, Plenum Press, New York, NY, 1992.

[5] A. Foroud and I. Q. Whishaw, "Changes in the kinematic structure and non-kinematic features of movements during skilled reaching after stroke: a Laban Movement Analysis in two case studies," *Journal of Neuroscience Methods*, vol. 158, no. 1, pp. 137–149, 2006.

[6] E. W. Twamley, K. R. Thomas, A. M. Gregory et al., "CogSMART compensatory cognitive training for traumatic brain injury: effects over 1 year," *The Journal of Head Trauma Rehabilitation*, vol. 30, no. 6, pp. 391–401, 2015.

[7] E. W. Twamley, A. J. Jak, D. C. Delis, M. W. Bondi, and J. B. Lohr, "Cognitive Symptom Management and Rehabilitation Therapy (CogSMART) for veterans with traumatic brain injury: pilot randomized controlled trial," *Journal of Rehabilitation Research and Development*, vol. 51, no. 1, pp. 59–70, 2014.

[8] S. E. Nadeau, B. Dobkin, S. S. Wu, Q. Pei, P. W. Duncan, and LEAPS Investigative Team, "The effects of stroke type, locus, and extent on long-term outcome of gait rehabilitation: the LEAPS experience," *Neurorehabilitation and Neural Repair*, vol. 30, no. 7, pp. 615–625, 2016.

[9] M. M. Sohlberg and C. A. Mateer, "Training use of compensatory memory books: a three stage behavioral approach," *Journal of Clinical and Experimental Neuropsychology*, vol. 11, no. 6, pp. 871–891, 1989.

[10] D. Shum, J. Fleming, H. Gill, M. J. Gullo, and J. Strong, "A randomized controlled trial of prospective memory rehabilitation in adults with traumatic brain injury," *Journal of Rehabilitation Medicine*, vol. 43, no. 3, pp. 216–223, 2011.

[11] A. McDonald, C. Haslam, P. Yates, B. Gurr, G. Leeder, and A. Sayers, "Google calendar: a new memory aid to compensate for prospective memory deficits following acquired brain injury," *Neuropsychological Rehabilitation*, vol. 21, no. 6, pp. 784–807, 2011.

[12] T. Bergquist, C. Gehl, J. Mandrekar et al., "The effect of internet-based cognitive rehabilitation in persons with memory impairments after severe traumatic brain injury," *Brain Injury*, vol. 23, no. 10, pp. 790–799, 2009.

[13] S. T. Pendlebury, F. C. Cuthbertson, S. J. Welch, Z. Mehta, and P. M. Rothwell, "Underestimation of cognitive impairment by mini-mental state examination versus the Montreal cognitive assessment in patients with transient ischemic attack and stroke: a population-based study," *Stroke*, vol. 41, no. 6, pp. 1290–1293, 2010.

[14] S. Weintraub, "Neuropsychological assessment of mental state," in *Principles of Behavioral and Cognitive Neurology*, M. M. Mesulam, Ed., pp. 121–173, Oxford University Press, New York, NY, 2000.

[15] S. Lai, A. Panarese, C. Spalletti et al., "Quantitative kinematic characterization of reaching impairments in mice after a stroke," *Neurorehabilitation and Neural Repair*, vol. 29, no. 4, pp. 382–392, 2015.

[16] S. K. Moon, M. Alaverdashvili, A. R. Cross, and I. Q. Whishaw, "Both compensation and recovery of skilled reaching following small photothrombotic stroke to motor cortex in the rat," *Experimental Neurology*, vol. 218, no. 1, pp. 145–153, 2009.

[17] G. A. Metz, I. Antonow-Schlorke, and O. W. Witte, "Motor improvements after focal cortical ischemia in adult rats are mediated by compensatory mechanisms," *Behavioural Brain Research*, vol. 162, no. 1, pp. 71–82, 2005.

[18] J. M. Smith, P. Lunga, D. Story et al., "Inosine promotes recovery of skilled motor function in a model of focal brain injury," *Brain*, vol. 130, part 4, pp. 915–925, 2007.

[19] M. Wang, H. Pu, Y. Liu, Z. Wang, B. Wang, and W. Xu, "A comparison of different models with motor dysfunction after traumatic brain injury in adult rats," *Journal of Integrative Neuroscience*, vol. 13, no. 4, pp. 579–593, 2014.

[20] S. C. Cramer, R. R. Benson, V. C. Burra et al., "Mapping individual brains to guide restorative therapy after stroke: rationale and pilot studies," *Neurological Research*, vol. 25, no. 8, pp. 811–814, 2003.

[21] S. B. Frost, S. Barbay, K. M. Friel, E. J. Plautz, and R. J. Nudo, "Reorganization of remote cortical regions after ischemic brain injury: a potential substrate for stroke recovery," *Journal of Neurophysiology*, vol. 89, no. 6, pp. 3205–3214, 2003.

[22] J. W. Krakauer, S. T. Carmichael, D. Corbett, and G. F. Wittenberg, "Getting neurorehabilitation right: what can be learned from animal models?" *Neurorehabilitation and Neural Repair*, vol. 26, no. 8, pp. 923–931, 2012.

[23] P. Langhorne, J. Bernhardt, and G. Kwakkel, "Stroke rehabilitation," *Lancet*, vol. 377, no. 9778, pp. 1693–1702, 2011.

[24] I. Q. Whishaw, "Loss of the innate cortical engram for action patterns used in skilled reaching and the development of behavioral compensation following motor cortex lesions in the rat," *Neuropharmacology*, vol. 39, no. 5, pp. 788–805, 2000.

[25] F. E. Buma, M. Raemaekers, G. Kwakkel, and N. F. Ramsey, "Brain function and upper limb outcome in stroke: a cross-sectional fMRI study," *PLoS One*, vol. 10, no. 10, article e0139746, 2015.

[26] Writing Group Members, D. Mozaffarian, E. J. Benjamin et al., "Heart disease and stroke statistics-2016 update: a report from the American Heart Association," *Circulation*, vol. 133, no. 4, pp. e38–e360, 2016.

[27] H. W. Phipps, "Systematic review of traumatic brain injury animal models," *Methods in Molecular Biology*, vol. 1462, pp. 61–88, 2016.

[28] S. T. Carmichael, "Rodent models of focal stroke: size, mechanism, and purpose," *NeuroRx*, vol. 2, no. 3, pp. 396–409, 2005.

[29] T. Skandsen, K. A. Kvistad, O. Solheim, I. H. Strand, M. Folvik, and A. Vik, "Prevalence and impact of diffuse axonal injury in patients with moderate and severe head injury: a cohort study of early magnetic resonance imaging findings and 1-year outcome," *Journal of Neurosurgery*, vol. 113, no. 3, pp. 556–563, 2010.

[30] P. E. Vos, "Biomarkers of focal and diffuse traumatic brain injury," *Critical Care*, vol. 15, no. 4, p. 183, 2011.

[31] T. M. Andriessen, B. Jacobs, and P. E. Vos, "Clinical characteristics and pathophysiological mechanisms of focal and diffuse traumatic brain injury," *Journal of Cellular and Molecular Medicine*, vol. 14, no. 10, pp. 2381–2392, 2010.

[32] M. A. Warner, T. S. Youn, T. Davis et al., "Regionally selective atrophy after traumatic axonal injury," *Archives of Neurology*, vol. 67, no. 11, pp. 1336–1344, 2010.

[33] A. Chodobski, B. J. Zink, and J. Szmydynger-Chodobska, "Blood-brain barrier pathophysiology in traumatic brain injury," *Translational Stroke Research*, vol. 2, no. 4, pp. 492–516, 2011.

[34] X. Wang, X. Bao, R. Pal, A. Agbas, and E. K. Michaelis, "Transcriptomic responses in mouse brain exposed to chronic excess of the neurotransmitter glutamate," *BMC Genomics*, vol. 11, no. 1, p. 360, 2010.

[35] L. P. Vera-Portocarrero, C. D. Mills, Z. Ye et al., "Rapid changes in expression of glutamate transporters after spinal cord injury," *Brain Research*, vol. 927, no. 1, pp. 104–110, 2002.

[36] U. Dirnagl, C. Iadecola, and M. A. Moskowitz, "Pathobiology of ischaemic stroke: an integrated view," *Trends in Neurosciences*, vol. 22, no. 9, pp. 391–397, 1999.

[37] E. H. Lo, T. Dalkara, and M. A. Moskowitz, "Mechanisms, challenges and opportunities in stroke," *Nature Reviews Neuroscience*, vol. 4, no. 5, pp. 399–415, 2003.

[38] D. W. Choi and S. M. Rothman, "The role of glutamate neurotoxicity in hypoxic-ischemic neuronal death," *Annual Review of Neuroscience*, vol. 13, pp. 171–182, 1990.

[39] V. E. Johnson, J. E. Stewart, F. D. Begbie, J. Q. Trojanowski, D. H. Smith, and W. Stewart, "Inflammation and white matter degeneration persist for years after a single traumatic brain injury," *Brain*, vol. 136, part 1, pp. 28–42, 2013.

[40] F. Gomez-Pinilla, H. Tram, C. W. Cotman, and M. Nieto-Sampedro, "Neuroprotective effect of MK-801 and U-50488H after contusive spinal cord injury," *Experimental Neurology*, vol. 104, no. 2, pp. 118–124, 1989.

[41] M. A. Moskowitz, E. H. Lo, and C. Iadecola, "The science of stroke: mechanisms in search of treatments," *Neuron*, vol. 67, no. 2, pp. 181–198, 2010.

[42] S. T. Carmichael, "The 3 Rs of stroke biology: radial, relayed, and regenerative," *Neurotherapeutics*, vol. 13, no. 2, pp. 348–359, 2016.

[43] D. M. Feeney and J. C. Baron, "Diaschisis," *Stroke*, vol. 17, no. 5, pp. 817–830, 1986.

[44] A. Lipsanen and J. Jolkkonen, "Experimental approaches to study functional recovery following cerebral ischemia," *Cellular and Molecular Life Sciences*, vol. 68, no. 18, pp. 3007–3017, 2011.

[45] S. C. Cramer and E. P. Bastings, "Mapping clinically relevant plasticity after stroke," *Neuropharmacology*, vol. 39, no. 5, pp. 842–851, 2000.

[46] M. P. van Meer, K. van der Marel, K. Wang et al., "Recovery of sensorimotor function after experimental stroke correlates with restoration of resting-state interhemispheric functional connectivity," *The Journal of Neuroscience*, vol. 30, no. 11, pp. 3964–3972, 2010.

[47] M. P. van Meer, K. van der Marel, W. M. Otte, B. van der Sprenkel JW, and R. M. Dijkhuizen, "Correspondence between altered functional and structural connectivity in the contralesional sensorimotor cortex after unilateral stroke in rats: a combined resting-state functional MRI and manganese-enhanced MRI study," *Journal of Cerebral Blood Flow and Metabolism*, vol. 30, no. 10, pp. 1707–1711, 2010.

[48] J. J. Ohab, S. Fleming, A. Blesch, and S. T. Carmichael, "A neurovascular niche for neurogenesis after stroke," *The Journal of Neuroscience*, vol. 26, no. 50, pp. 13007–13016, 2006.

[49] S. Li and S. T. Carmichael, "Growth-associated gene and protein expression in the region of axonal sprouting in the aged brain after stroke," *Neurobiology of Disease*, vol. 23, no. 2, pp. 362–373, 2006.

[50] L. Wang, C. Yu, H. Chen et al., "Dynamic functional reorganization of the motor execution network after stroke," *Brain*, vol. 133, part 4, pp. 1224–1238, 2010.

[51] K. M. Schoch, S. K. Madathil, and K. E. Saatman, "Genetic manipulation of cell death and neuroplasticity pathways in traumatic brain injury," *Neurotherapeutics*, vol. 9, no. 2, pp. 323–337, 2012.

[52] C. C. Giza, M. L. Prins, D. A. Hovda, H. R. Herschman, and J. D. Feldman, "Genes preferentially induced by depolarization after concussive brain injury: effects of age and injury severity," *Journal of Neurotrauma*, vol. 19, no. 4, pp. 387–402, 2002.

[53] N. Kobori, G. L. Clifton, and P. Dash, "Altered expression of novel genes in the cerebral cortex following experimental brain injury," *Brain Research. Molecular Brain Research*, vol. 104, no. 2, pp. 148–158, 2002.

[54] S. C. Cramer and M. Chopp, "Recovery recapitulates ontogeny," *Trends in Neurosciences*, vol. 23, no. 6, pp. 265–271, 2000.

[55] S. R. Zeiler, R. Hubbard, E. M. Gibson et al., "Paradoxical motor recovery from a first stroke after induction of a second stroke: reopening a postischemic sensitive period," *Neurorehabilitation and Neural Repair*, vol. 30, no. 8, pp. 794–800, 2016.

[56] A. Shehadah, J. Chen, A. Pal et al., "Human placenta-derived adherent cell treatment of experimental stroke promotes functional recovery after stroke in young adult and older rats," *PLoS One*, vol. 9, no. 1, article e86621, 2014.

[57] A. W. Dromerick, M. A. Edwardson, D. F. Edwards et al., "Critical periods after stroke study: translating animal stroke recovery experiments into a clinical trial," *Frontiers in Human Neuroscience*, vol. 9, no. 231, 2015.

[58] A. Pollock, G. Baer, V. Pomeroy, and P. Langhorne, "Physiotherapy treatment approaches for the recovery of postural control and lower limb function following stroke," *Cochrane Database of Systematic Reviews*, no. 1, p. CD001920, 2007.

[59] B. J. Kollen, S. Lennon, B. Lyons et al., "The effectiveness of the Bobath concept in stroke rehabilitation: what is the evidence?" *Stroke*, vol. 40, no. 4, pp. e89–e97, 2009.

[60] J. Biernaskie and D. Corbett, "Enriched rehabilitative training promotes improved forelimb motor function and enhanced dendritic growth after focal ischemic injury," *The Journal of Neuroscience*, vol. 21, no. 14, pp. 5272–5280, 2001.

[61] M. A. Castro-Alamancos and J. Borrel, "Functional recovery of forelimb response capacity after forelimb primary motor cortex damage in the rat is due to the reorganization of adjacent areas of cortex," *Neuroscience*, vol. 68, no. 3, pp. 793–805, 1995.

[62] J. M. Conner, A. A. Chiba, and M. H. Tuszynski, "The basal forebrain cholinergic system is essential for cortical plasticity and functional recovery following brain injury," *Neuron*, vol. 46, no. 2, pp. 173–179, 2005.

[63] R. J. Nudo, "Postinfarct cortical plasticity and behavioral recovery," *Stroke*, vol. 38, Supplement 2, pp. 840–845, 2007.

[64] R. J. Nudo and G. W. Milliken, "Reorganization of movement representations in primary motor cortex following focal ischemic infarcts in adult squirrel monkeys," *Journal of Neurophysiology*, vol. 75, no. 5, pp. 2144–2149, 1996.

[65] D. Ramanathan, J. M. Conner, and M. H. Tuszynski, "A form of motor cortical plasticity that correlates with recovery of function after brain injury," *Proceedings of the National Academy of Sciences of the United States of America*, vol. 103, no. 30, pp. 11370–11375, 2006.

[66] S. T. Carmichael, I. Archibeque, L. Luke, T. Nolan, J. Momiy, and S. Li, "Growth-associated gene expression after stroke: evidence for a growth-promoting region in peri-infarct cortex," *Experimental Neurology*, vol. 193, no. 2, pp. 291–311, 2005.

[67] N. G. Harris, Y. A. Mironova, D. A. Hovda, and R. L. Sutton, "Pericontusion axon sprouting is spatially and temporally consistent with a growth-permissive environment after traumatic brain injury," *Journal of Neuropathology and Experimental Neurology*, vol. 69, no. 2, pp. 139–154, 2010.

[68] L. I. Benowitz and S. T. Carmichael, "Promoting axonal rewiring to improve outcome after stroke," *Neurobiology of Disease*, vol. 37, no. 2, pp. 259–266, 2010.

[69] B. Sist, K. Fouad, and I. R. Winship, "Plasticity beyond peri-infarct cortex: spinal up regulation of structural plasticity, neurotrophins, and inflammatory cytokines during recovery from cortical stroke," *Experimental Neurology*, vol. 252, pp. 47–56, 2014.

[70] R. P. Stroemer, T. A. Kent, and C. E. Hulsebosch, "Neocortical neural sprouting, synaptogenesis, and behavioral recovery after neocortical infarction in rats," *Stroke*, vol. 26, no. 11, pp. 2135–2144, 1995.

[71] S. T. Carmichael and M. F. Chesselet, "Synchronous neuronal activity is a signal for axonal sprouting after cortical lesions in the adult," *The Journal of Neuroscience*, vol. 22, no. 14, pp. 6062–6070, 2002.

[72] N. Dancause, S. Barbay, S. B. Frost et al., "Extensive cortical rewiring after brain injury," *The Journal of Neuroscience*, vol. 25, no. 44, pp. 10167–10179, 2005.

[73] K. M. Friel and R. J. Nudo, "Recovery of motor function after focal cortical injury in primates: compensatory movement patterns used during rehabilitative training," *Somatosensory & Motor Research*, vol. 15, no. 3, pp. 173–189, 1998.

[74] S. T. Carmichael, "Emergent properties of neural repair: elemental biology to therapeutic concepts," *Annals of Neurology*, vol. 79, no. 6, pp. 895–906, 2016.

[75] T. A. Jones and D. L. Adkins, "Motor system reorganization after stroke: stimulating and training toward perfection," *Physiology (Bethesda)*, vol. 30, no. 5, pp. 358–370, 2015.

[76] E. J. Plautz, S. Barbay, S. B. Frost et al., "Post-infarct cortical plasticity and behavioral recovery using concurrent cortical stimulation and rehabilitative training: a feasibility study in primates," *Neurological Research*, vol. 25, no. 8, pp. 801–810, 2003.

[77] N. Dancause, S. Barbay, S. B. Frost et al., "Topographically divergent and convergent connectivity between premotor and primary motor cortex," *Cerebral Cortex*, vol. 16, no. 8, pp. 1057–1068, 2006.

[78] R. H. Andres, N. Horie, W. Slikker et al., "Human neural stem cells enhance structural plasticity and axonal transport in the ischaemic brain," *Brain*, vol. 134, part 6, pp. 1777–1789, 2011.

[79] T. A. Jones and T. Schallert, "Overgrowth and pruning of dendrites in adult rats recovering from neocortical damage," *Brain Research*, vol. 581, no. 1, pp. 156–160, 1992.

[80] T. A. Jones and T. Schallert, "Use-dependent growth of pyramidal neurons after neocortical damage," *The Journal of Neuroscience*, vol. 14, no. 4, pp. 2140–2152, 1994.

[81] H. W. Cheng, J. Tong, and T. H. McNeill, "Lesion-induced axon sprouting in the deafferented striatum of adult rat," *Neuroscience Letters*, vol. 242, no. 2, pp. 69–72, 1998.

[82] T. A. Jones, "Multiple synapse formation in the motor cortex opposite unilateral sensorimotor cortex lesions in adult rats," *Journal of Comparative Neurology*, vol. 414, no. 1, pp. 57–66, 1999.

[83] B. Kolb, G. C. Teskey, and R. Gibb, "Factors influencing cerebral plasticity in the normal and injured brain," *Frontiers in Human Neuroscience*, vol. 4, no. 204, 2010.

[84] S. Y. Kim, R. P. Allred, D. L. Adkins et al., "Experience with the "good" limb induces aberrant synaptic plasticity in the perilesion cortex after stroke," *The Journal of Neuroscience*, vol. 35, no. 22, pp. 8604–8610, 2015.

[85] M. Ariza, J. M. Serra-Grabulosa, C. Junqué et al., "Hippocampal head atrophy after traumatic brain injury," *Neuropsychologia*, vol. 44, no. 10, pp. 1956–1961, 2006.

[86] W. L. Maxwell, K. Dhillon, L. Harper et al., "There is differential loss of pyramidal cells from the human hippocampus with survival after blunt head injury," *Journal of Neuropathology and Experimental Neurology*, vol. 62, no. 3, pp. 272–279, 2003.

[87] N. M. Wilson, D. J. Titus, A. A. Oliva Jr, C. Furones, and C. M. Atkins, "Traumatic brain injury upregulates phosphodiesterase expression in the hippocampus," *Frontiers in Systems Neuroscience*, vol. 10, no. 5, 2016.

[88] A. Sierra, T. Laitinen, O. Gröhn, and A. Pitkänen, "Diffusion tensor imaging of hippocampal network plasticity," *Brain Structure & Function*, vol. 220, no. 2, pp. 781–801, 2015.

[89] J. N. Campbell, B. Low, J. E. Kurz, S. S. Patel, M. T. Young, and S. B. Churn, "Mechanisms of dendritic spine remodeling in a rat model of traumatic brain injury," *Journal of Neurotrauma*, vol. 29, no. 2, pp. 218–234, 2012.

[90] G. S. Griesbach, F. Gomez-Pinilla, and D. A. Hovda, "Time window for voluntary exercise-induced increases in hippocampal neuroplasticity molecules after traumatic brain injury is severity dependent," *Journal of Neurotrauma*, vol. 24, no. 7, pp. 1161–1171, 2007.

[91] S. W. Scheff, D. A. Price, R. R. Hicks, S. A. Baldwin, S. Robinson, and C. Brackney, "Synaptogenesis in the hippocampal CA1 field following traumatic brain injury," *Journal of Neurotrauma*, vol. 22, no. 7, pp. 719–732, 2005.

[92] P. K. Dash, S. A. Mach, and A. N. Moore, "The role of extracellular signal-regulated kinase in cognitive and motor deficits following experimental traumatic brain injury," *Neuroscience*, vol. 114, no. 3, pp. 755–767, 2002.

[93] D. A. Matzilevich, J. M. Rall, A. N. Moore, R. J. Grill, and P. K. Dash, "High-density microarray analysis of hippocampal gene expression following experimental brain injury," *Journal of Neuroscience Research*, vol. 67, no. 5, pp. 646–663, 2002.

[94] O. Steward, S. L. Vinsant, and L. Davis, "The process of reinnervation in the dentate gyrus of adult rats: an ultrastructural study of changes in presynaptic terminals as a result of sprouting," *Journal of Comparative Neurology*, vol. 267, no. 2, pp. 203–210, 1988.

[95] T. M. Reeves and O. Steward, "Changes in the firing properties of neurons in the dentate gyrus with denervation and reinnervation: implications for behavioral recovery," *Experimental Neurology*, vol. 102, no. 1, pp. 37–49, 1988.

[96] O. Steward, "Reorganization of neuronal connections following CNS trauma: principles and experimental paradigms," *Journal of Neurotrauma*, vol. 6, no. 2, pp. 99–152, 1989.

[97] S. H. Jang and H. D. Lee, "Compensatory neural tract from contralesional fornical body to ipsilesional medial temporal lobe in a patient with mild traumatic brain injury: a case report," *American Journal of Physical Medicine & Rehabilitation*, vol. 95, no. 2, pp. e14–e17, 2016.

[98] C. R. Almli and S. Finger, "Toward a definition of recovery of function," in *Brain Injury and Recovery: Theoretical and Controversial Issues*, C. R. Almli, S. Finger, T. E. LeVere and D. Stein, Eds., pp. 1–14, Springer-Verlag, New York, NY, 1988.

[99] J. A. Long, L. T. Watts, J. Chemello, S. Huang, Q. Shen, and T. Q. Duong, "Multiparametric and longitudinal MRI characterization of mild traumatic brain injury in rats," *Journal of Neurotrauma*, vol. 32, no. 8, pp. 598–607, 2015.

[100] A. Encarnacion, N. Horie, H. Keren-Gill, T. M. Bliss, G. K. Steinberg, and M. Shamloo, "Long-term behavioral assessment of function in an experimental model for ischemic stroke," *Journal of Neuroscience Methods*, vol. 196, no. 2, pp. 247–257, 2011.

[101] W. Almaguer-Melian, D. Mercerón-Martínez, N. Pavón-Fuentes et al., "Erythropoietin promotes neural plasticity and spatial memory recovery in fimbria-fornix-lesioned rats," *Neurorehabilitation and Neural Repair*, vol. 29, no. 10, pp. 979–988, 2015.

[102] J. Jacqmain, E. T. Nudi, S. Fluharty, and J. S. Smith, "Pre and post-injury environmental enrichment effects functional recovery following medial frontal cortical contusion injury in rats," *Behavioural Brain Research*, vol. 275, pp. 201–211, 2014.

[103] T. Schallert and T. A. Jones, ""Exuberant" neuronal growth after brain damage in adult rats: the essential role of behavioral experience," *Journal of Neural Transplantation & Plasticity*, vol. 4, no. 3, pp. 193–198, 1993.

[104] S. Laurence and D. G. Stein, "Recovery after brain damage and the concept of localization of function," in *Recovery from Brain Damage: Research and Theory*, S. Finger, Ed., pp. 369–409, Plenum Press, New York, NY, 1978.

[105] B. Kolb, *Brain, Plasticity, and Behavior*, Lawrence Erlbaum Associates, Mahwah, NJ, USA, 1995.

[106] T. A. Jones, R. P. Allred, S. C. Jefferson et al., "Motor system plasticity in stroke models: intrinsically use-dependent, unreliably useful," *Stroke*, vol. 44, 6 Supplement 1, pp. S104–S106, 2013.

[107] A. L. Kerr, S. Y. Cheng, and T. A. Jones, "Experience-dependent neural plasticity in the adult damaged brain," *Journal of Communication Disorders*, vol. 44, no. 5, pp. 538–548, 2011.

[108] J. A. Bell, M. L. Wolke, R. C. Ortez, T. A. Jones, and A. L. Kerr, "Training intensity affects motor rehabilitation efficacy following unilateral ischemic insult of the sensorimotor cortex in C57BL/6 mice," *Neurorehabilitation and Neural Repair*, vol. 29, no. 6, pp. 590–598, 2015.

[109] A. L. Kerr, M. L. Wolke, J. A. Bell, and T. A. Jones, "Post-stroke protection from maladaptive effects of learning with the non-paretic forelimb by bimanual home cage experience in C57BL/6 mice," *Behavioural Brain Research*, vol. 252, pp. 180–187, 2013.

[110] L. M. Luke, R. P. Allred, and T. A. Jones, "Unilateral ischemic sensorimotor cortical damage induces contralesional synaptogenesis and enhances skilled reaching with the ipsilateral forelimb in adult male rats," *Synapse*, vol. 54, no. 4, pp. 187–199, 2004.

[111] J. E. Hsu and T. A. Jones, "Time-sensitive enhancement of motor learning with the less-affected forelimb after unilateral sensorimotor cortex lesions in rats," *The European Journal of Neuroscience*, vol. 22, no. 8, pp. 2069–2080, 2005.

[112] D. A. Kozlowski, J. L. Leasure, and T. Schallert, "The control of movement following traumatic brain injury," *Comprehensive Physiology*, vol. 3, no. 1, pp. 121–139, 2013.

[113] B. Zhang, Q. He, Y. Y. Li et al., "Constraint-induced movement therapy promotes motor function recovery and downregulates phosphorylated extracellular regulated protein kinase expression in ischemic brain tissue of rats," *Neural Regeneration Research*, vol. 10, no. 12, pp. 2004–2010, 2015.

[114] T. A. Jones, D. J. Liput, E. L. Maresh et al., "Use-dependent dendritic regrowth is limited after unilateral controlled cortical impact to the forelimb sensorimotor cortex," *Journal of Neurotrauma*, vol. 29, no. 7, pp. 1455–1468, 2012.

[115] D. L. Adkins, L. Ferguson, S. Lance et al., "Combining multiple types of motor rehabilitation enhances skilled forelimb use following experimental traumatic brain injury in rats," *Neurorehabilitation and Neural Repair*, vol. 29, no. 10, pp. 989–1000, 2015.

[116] S. C. Jefferson, E. R. Clayton, N. A. Donlan, D. A. Kozlowski, T. A. Jones, and D. L. Adkins, "Cortical stimulation concurrent with skilled motor training improves forelimb function and enhances motor cortical reorganization following controlled cortical impact," *Neurorehabilitation and Neural Repair*, vol. 30, no. 2, pp. 155–158, 2016.

[117] H. L. Combs, T. A. Jones, D. A. Kozlowski, and D. L. Adkins, "Combinatorial motor training results in functional reorganization of remaining motor cortex after controlled cortical impact in rats," *Journal of Neurotrauma*, vol. 33, no. 8, pp. 741–747, 2016.

[118] J. Z. Guo, A. R. Graves, W. W. Guo et al., "Cortex commands the performance of skilled movement," *eLife*, vol. 4,, no. e10774, 2015.

[119] E. V. Shanina, T. Schallert, O. W. Witte, and C. Redecker, "Behavioral recovery from unilateral photothrombotic infarcts of the forelimb sensorimotor cortex in rats: role of the contralateral cortex," *Neuroscience*, vol. 139, no. 4, pp. 1495–1506, 2006.

[120] R. P. Allred, M. A. Maldonado, J. E. Hsu And, and T. A. Jones, "Training the "less-affected" forelimb after unilateral cortical infarcts interferes with functional recovery of the impaired forelimb in rats," *Restorative Neurology and Neuroscience*, vol. 23, no. 5-6, pp. 297–302, 2005.

[121] R. P. Allred, D. L. Adkins, M. T. Woodlee et al., "The vermicelli handling test: a simple quantitative measure of dexterous forepaw function in rats," *Journal of Neuroscience Methods*, vol. 170, no. 2, pp. 229–244, 2008.

[122] R. P. Allred, C. H. Cappellini, and T. A. Jones, "The "good" limb makes the "bad" limb worse: experience-dependent interhemispheric disruption of functional outcome after cortical infarcts in rats," *Behavioral Neuroscience*, vol. 124, no. 1, pp. 124–132, 2010.

[123] R. P. Allred and T. A. Jones, "Maladaptive effects of learning with the less-affected forelimb after focal cortical infarcts in rats," *Experimental Neurology*, vol. 210, no. 1, pp. 172–181, 2008.

[124] J. Clarke, K. D. Langdon, and D. Corbett, "Early poststroke experience differentially alters periinfarct layer II and III cortex," *Journal of Cerebral Blood Flow and Metabolism*, vol. 34, no. 4, pp. 630–637, 2014.

[125] R. P. Allred and T. A. Jones, "Experience–a double edged sword for restorative neural plasticity after brain damage," *Future Neurology*, vol. 3, no. 2, pp. 189–198, 2008.

[126] T. A. Jones, R. P. Allred, D. L. Adkins, J. E. Hsu, A. O'Bryant, and M. A. Maldonado, "Remodeling the brain with behavioral experience after stroke," *Stroke*, vol. 40, Supplement 3, pp. S136–S138, 2009.

[127] E. J. Plautz, S. Barbay, S. B. Frost et al., "Effects of subdural monopolar cortical stimulation paired with rehabilitative training on behavioral and neurophysiological recovery after cortical ischemic stroke in adult squirrel monkeys," *Neurorehabilitation and Neural Repair*, vol. 30, no. 2, pp. 159–172, 2016.

[128] F. Buma, G. Kwakkel, and N. Ramsey, "Understanding upper limb recovery after stroke," *Restorative Neurology and Neuroscience*, vol. 31, no. 6, pp. 707–722, 2013.

[129] M. Murray and M. E. Goldberger, "Restitution of function and collateral sprouting in the cat spinal cord: the partially hemisected animal," *Journal of Comparative Neurology*, vol. 158, no. 1, pp. 19–36, 1974.

[130] M. E. Goldberger and M. Murray, "Restitution of function and collateral sprouting in the cat spinal cord: the deafferented animal," *Journal of Comparative Neurology*, vol. 158, no. 1, pp. 37–53, 1974.

[131] K. H. Lee, "The role of compensatory movements patterns in spontaneous recovery after stroke," *Journal of Physical Therapy Science*, vol. 27, no. 9, pp. 2671–2673, 2015.

[132] Y. Murata, N. Higo, T. Hayashi et al., "Temporal plasticity involved in recovery from manual dexterity deficit after motor cortex lesion in macaque monkeys," *The Journal of Neuroscience*, vol. 35, no. 1, pp. 84–95, 2015.

[133] I. Q. Whishaw, S. M. Pellis, B. P. Gorny, and V. C. Pellis, "The impairments in reaching and the movements of compensation in rats with motor cortex lesions: an endpoint, videorecording, and movement notation analysis," *Behavioural Brain Research*, vol. 42, no. 1, pp. 77–91, 1991.

[134] I. Q. Whishaw, M. Alaverdashvili, and B. Kolb, "The problem of relating plasticity and skilled reaching after motor cortex stroke in the rat," *Behavioural Brain Research*, vol. 192, no. 1, pp. 124–136, 2008.

[135] C. A. Erickson, O. A. Gharbawie, and I. Q. Whishaw, "Attempt-dependent decrease in skilled reaching characterizes the acute postsurgical period following a forelimb motor cortex lesion: an experimental demonstration of learned nonuse in the rat," *Behavioural Brain Research*, vol. 179, no. 2, pp. 208–218, 2007.

[136] M. Alaverdashvili, A. Foroud, D. H. Lim, and I. Q. Whishaw, ""Learned baduse" limits recovery of skilled reaching for food after forelimb motor cortex stroke in rats: a new analysis of the effect of gestures on success," *Behavioural Brain Research*, vol. 188, no. 2, pp. 281–290, 2008.

[137] P. Raghavan, "Upper limb motor impairment after stroke," *Physical Medicine and Rehabilitation Clinics of North America*, vol. 26, no. 4, pp. 599–610, 2015.

[138] A. L. Kerr, K. A. Cheffer, M. C. Curtis, and A. Rodriguez, "Long-term deficits of the paretic limb follow post-stroke compensatory limb use in C57BL/6 mice," *Behavioural Brain Research*, vol. 303, pp. 103–108, 2016.

[139] J. P. Rauschecker, "Compensatory plasticity and sensory substitution in the cerebral cortex," *Trends in Neurosciences*, vol. 18, no. 1, pp. 36–43, 1995.

[140] I. Q. Whishaw, J. A. Zaborowski, and B. Kolb, "Postsurgical enrichment aids adult hemidecorticate rats on a spatial navigation task," *Behavioral and Neural Biology*, vol. 42, no. 2, pp. 183–190, 1984.

[141] B. J. Clark, J. P. Rice, K. G. Akers, F. T. Candelaria-Cook, J. S. Taube, and D. A. Hamilton, "Lesions of the dorsal tegmental nuclei disrupt control of navigation by distal landmarks in cued, directional, and place variants of the Morris water task," *Behavioral Neuroscience*, vol. 127, no. 4, pp. 566–581, 2013.

[142] M. Alaverdashvili, D. H. Lim, and I. Q. Whishaw, "No improvement by amphetamine on learned non-use, attempts,

success or movement in skilled reaching by the rat after motor cortex stroke," *The European Journal of Neuroscience*, vol. 25, no. 11, pp. 3442–3452, 2007.

[143] M. S. Yong and K. Hwangbo, "Skilled reach training influences brain recovery following intracerebral hemorrhage in rats," *Journal of Physical Therapy Science*, vol. 26, no. 3, pp. 405–407, 2014.

[144] E. Taub, "Harnessing brain plasticity through behavioral techniques to produce new treatments in neurorehabilitation," *The American Psychologist*, vol. 59, no. 8, pp. 692–704, 2004.

[145] V. W. Mark and E. Taub, "Constraint-induced movement therapy for chronic stroke hemiparesis and other disabilities," *Restorative Neurology and Neuroscience*, vol. 22, no. 3–5, pp. 317–336, 2004.

[146] S. Zhao, M. Zhao, T. Xiao, J. Jolkkonen, and C. Zhao, "Constraint-induced movement therapy overcomes the intrinsic axonal growth-inhibitory signals in stroke rats," *Stroke*, vol. 44, no. 6, pp. 1698–1705, 2013.

[147] S. S. Zhao, Y. Zhao, T. Xiao, M. Zhao, J. Jolkkonen, and C. S. Zhao, "Increased neurogenesis contributes to the promoted behavioral recovery by constraint-induced movement therapy after stroke in adult rats," *CNS Neuroscience & Therapeutics*, vol. 19, no. 3, pp. 194–196, 2013.

[148] M. Nishibe, E. T. Urban 3rd, S. Barbay, and R. J. Nudo, "Rehabilitative training promotes rapid motor recovery but delayed motor map reorganization in a rat cortical ischemic infarct model," *Neurorehabilitation and Neural Repair*, vol. 29, no. 5, pp. 472–482, 2015.

[149] J. J. Braun, "Time and recovery from brain damage," in *Recovery from Brain Damage: Research and Theory*, S. Finger, Ed., pp. 369–409, Plenum Press, New York, NY, 1978.

[150] P. Ramos-Cabrer, C. Justicia, D. Wiedermann, and M. Hoehn, "Stem cell mediation of functional recovery after stroke in the rat," *PLoS One*, vol. 5, no. 9, article e12779, 2010.

[151] D. Nunnari, P. Bramanti, and S. Marino, "Cognitive reserve in stroke and traumatic brain injury patients," *Neurological Sciences*, vol. 35, no. 10, pp. 1513–1518, 2014.

[152] Y. Stern, "Cognitive reserve," *Neuropsychologia*, vol. 47, no. 10, pp. 2015–2028, 2009.

[153] Y. Stern, C. Habeck, J. Moeller et al., "Brain networks associated with cognitive reserve in healthy young and old adults," *Cerebral Cortex*, vol. 15, no. 4, pp. 394–402, 2005.

[154] L. J. Whalley, I. J. Deary, C. L. Appleton, and J. M. Starr, "Cognitive reserve and the neurobiology of cognitive aging," *Ageing Research Reviews*, vol. 3, no. 4, pp. 369–382, 2004.

[155] N. Scarmeas and Y. Stern, "Cognitive reserve and lifestyle," *Journal of Clinical and Experimental Neuropsychology*, vol. 25, no. 5, pp. 625–633, 2003.

[156] A. D. Murray, R. T. Staff, C. J. McNeil et al., "The balance between cognitive reserve and brain imaging biomarkers of cerebrovascular and Alzheimer's diseases," *Brain*, vol. 134, part 12, pp. 3687–3696, 2011.

[157] J. S. Elkins, W. T. Longstreth Jr, T. A. Manolio, A. B. Newman, R. A. Bhadelia, and S. C. Johnston, "Education and the cognitive decline associated with MRI-defined brain infarct," *Neurology*, vol. 67, no. 3, pp. 435–440, 2006.

[158] T. B. Fay, K. O. Yeates, H. G. Taylor et al., "Cognitive reserve as a moderator of postconcussive symptoms in children with complicated and uncomplicated mild traumatic brain injury," *Journal of the International Neuropsychological Society*, vol. 16, no. 1, pp. 94–105, 2010.

[159] E. B. Schneider, S. Sur, V. Raymont et al., "Functional recovery after moderate/severe traumatic brain injury: a role for cognitive reserve?" *Neurology*, vol. 82, no. 18, pp. 1636–1642, 2014.

[160] J. E. Farmer, S. M. Kanne, J. S. Haut, J. Williams, B. Johnstone, and K. Kirk, "Memory functioning following traumatic brain injury in children with premorbid learning problems," *Developmental Neuropsychology*, vol. 22, no. 2, pp. 455–469, 2002.

[161] P. Satz, "Brain reserve capacity on symptom onset after brain injury: a formulation and review of evidence for threshold theory," *Neuropsychology*, vol. 7, no. 3, pp. 273–295, 1993.

[162] M. Dennis, K. O. Yeates, H. G. Taylor, and J. M. Fletcher, "Brain reserve capacity, cognitive reserve capacity, and age-based functional plasticity after congenital and acquired brain injury in children," in *Cognitive Reserve: Theory and Applications*, Y. Stern, Ed., pp. 53–83, Taylor & Francis, Philadelphia, PA, 2007.

[163] D. G. Flood and P. D. Coleman, "Neuron numbers and sizes in aging brain: comparisons of human, monkey, and rodent data," *Neurobiology of Aging*, vol. 9, no. 5-6, pp. 453–463, 1988.

[164] J. L. Humm, D. A. Kozlowski, D. C. James, J. E. Gotts, and T. Schallert, "Use-dependent exacerbation of brain damage occurs during an early post-lesion vulnerable period," *Brain Research*, vol. 783, no. 2, pp. 286–292, 1998.

[165] D. A. Kozlowski, D. C. James, and T. Schallert, "Use-dependent exaggeration of neuronal injury after unilateral sensorimotor cortex lesions," *The Journal of Neuroscience*, vol. 16, no. 15, pp. 4776–4786, 1996.

[166] M. T. Woodlee and T. Schallert, "The interplay between behavior and neurodegeneration in rat models of Parkinson's disease and stroke," *Restorative Neurology and Neuroscience*, vol. 22, no. 3–5, pp. 153–161, 2004.

[167] G. S. Griesbach, F. Gomez-Pinilla, and D. A. Hovda, "The upregulation of plasticity-related proteins following TBI is disrupted with acute voluntary exercise," *Brain Research*, vol. 1016, no. 2, pp. 154–162, 2004.

[168] G. S. Griesbach, D. A. Hovda, R. Molteni, A. Wu, and F. Gomez-Pinilla, "Voluntary exercise following traumatic brain injury: brain-derived neurotrophic factor upregulation and recovery of function," *Neuroscience*, vol. 125, no. 1, pp. 129–139, 2004.

[169] Y. J. Sim, S. S. Kim, J. Y. Kim, M. S. Shin, and C. J. Kim, "Treadmill exercise improves short-term memory by suppressing ischemia-induced apoptosis of neuronal cells in gerbils," *Neuroscience Letters*, vol. 372, no. 3, pp. 256–261, 2004.

[170] Y. J. Sim, H. Kim, J. Y. Kim et al., "Long-term treadmill exercise overcomes ischemia-induced apoptotic neuronal cell death in gerbils," *Physiology & Behavior*, vol. 84, no. 5, pp. 733–738, 2005.

[171] J. Biernaskie, G. Chernenko, and D. Corbett, "Efficacy of rehabilitative experience declines with time after focal ischemic brain injury," *The Journal of Neuroscience*, vol. 24, no. 5, pp. 1245–1254, 2004.

[172] B. A. Norrie, J. M. Nevett-Duchcherer, and M. A. Gorassini, "Reduced functional recovery by delaying motor training after spinal cord injury," *Journal of Neurophysiology*, vol. 94, no. 1, pp. 255–264, 2005.

[173] S. Barbay, E. J. Plautz, K. M. Friel et al., "Behavioral and neurophysiological effects of delayed training following a small ischemic infarct in primary motor cortex of squirrel monkeys," *Experimental Brain Research*, vol. 169, no. 1, pp. 106–116, 2006.

[174] K. A. Tennant, D. L. Adkins, M. D. Scalco, N. A. Donlan, A. L. Asay, and N. Thomas, "The effects of duration and intensity of motor skill training on plasticity of the forelimb representation in the motor cortex of C57BL/6 mice," in *Society for Neuroscience*, San Diego, CA, 2010.

[175] C. L. MacLellan, M. B. Keough, S. Granter-Button, G. A. Chernenko, S. Butt, and D. Corbett, "A critical threshold of rehabilitation involving brain-derived neurotrophic factor is required for poststroke recovery," *Neurorehabilitation and Neural Repair*, vol. 25, no. 8, pp. 740–748, 2011.

[176] L. B. Merabet, R. Hamilton, G. Schlaug et al., "Rapid and reversible recruitment of early visual cortex for touch," *PLoS One*, vol. 3, no. 8, article e3046, 2008.

[177] B. Kolb, R. Brown, A. Witt-Lajeunesse, and R. Gibb, "Neural compensations after lesion of the cerebral cortex," *Neural Plasticity*, vol. 8, no. 1-2, pp. 1–16, 2001.

[178] R. J. Nudo, "Mechanisms for recovery of motor function following cortical damage," *Current Opinion in Neurobiology*, vol. 16, no. 6, pp. 638–644, 2006.

[179] R. J. Nudo, G. W. Milliken, W. M. Jenkins, and M. M. Merzenich, "Use-dependent alterations of movement representations in primary motor cortex of adult squirrel monkeys," *The Journal of Neuroscience*, vol. 16, no. 2, pp. 785–807, 1996.

[180] B. Kolb, "Overview of cortical plasticity and recovery from brain injury," *Physical Medicine and Rehabilitation Clinics of North America*, vol. 14, Supplement 1, pp. S7–S25, 2003.

Hindawi
Neural Plasticity
Volume 2017, Article ID 1389475, 15 pages
https://doi.org/10.1155/2017/1389475

Review Article

Assessed and Emerging Biomarkers in Stroke and Training-Mediated Stroke Recovery: State of the Art

Marialuisa Gandolfi,[1,2] Nicola Smania,[1,2] Antonio Vella,[3] Alessandro Picelli,[1,2] and Salvatore Chirumbolo[1]

[1]*Department of Neurosciences, Biomedicine and Movement Sciences, University of Verona, Verona, Italy*
[2]*UOC Neurorehabilitation, AOUI Verona, Verona, Italy*
[3]*Immunology Unit, Azienda Ospedaliera Universitaria Integrata, Verona, Italy*

Correspondence should be addressed to Marialuisa Gandolfi; marialuisa.gandolfi@univr.it

Received 9 November 2016; Accepted 11 January 2017; Published 8 March 2017

Academic Editor: Annalena Venneri

Since the increasing update of the biomolecular scientific literature, biomarkers in stroke have reached an outstanding and remarkable revision in the very recent years. Besides the diagnostic and prognostic role of some inflammatory markers, many further molecules and biological factors have been added to the list, including tissue derived cytokines, growth factor-like molecules, hormones, and microRNAs. The literatures on brain derived growth factor and other neuroimmune mediators, bone-skeletal muscle biomarkers, cellular and immunity biomarkers, and the role of microRNAs in stroke recovery were reviewed. To date, biomarkers represent a possible challenge in the diagnostic and prognostic evaluation of stroke onset, pathogenesis, and recovery. Many molecules are still under investigation and may become promising and encouraging biomarkers. Experimental and clinical research should increase this list and promote new discoveries in this field, to improve stroke diagnosis and treatment.

1. Introduction

Biomarkers in stroke have reached an outstanding and remarkable revision in the very recent years, since the increasing update of the biomolecular scientific literature in the field. Besides the diagnostic and prognostic role of some inflammatory markers, such as CRP, IL-6, TNF-α, or IL-1β, many further molecules and biological factors in the serum or plasma compartment have been added to the list, including tissue derived cytokines (myokines, adipokines), growth factor-like molecules, hormones, and microRNAs [1]. The latter ones have become important markers in many neurodegenerative and neuroimmune disorders, such as multiple sclerosis, Alzheimer disease, or Parkinson disease [2–5]. Neuroinflammation represents the main mechanism underlying the onset and development of stroke and the peripheral level of soluble immune factors and immune cells should give insights either on the onset and pathogenesis of stroke or on its recovery [6–8]. Poststroke rehabilitation, particularly following physical exercise and training, generates a crowded mass of mediators, more than 90, called myokines, which plays an emerging role in the biomarker field, which should update the role of plasma or circulating markers in stroke [9, 10] (see Figure 1).

Stroke risk and even poststroke recovery are strictly related to endothelial function. A correlation exists between arterial stiffness index and endothelia function in patients with acute ischemic stroke [11], while the association of stroke with hypertension should be better outlined. A recent paper reported that prestroke use of beta-blockers in hypertensive subjects did not affect neither stroke severity nor functional outcome [12]. The relationship between stroke and the cardiovascular system is particularly complex, as a huge panoply of different humoral and cellular participants make it highly complex to comprehend how stroke occurs and how to manage its recovery. Some recent papers revealed that the short-term management of hypertension in hypertensive patients has a positive effect on the long-term risk reduction of stroke [13]. Elevated arterial pressure remains a fundamental risk

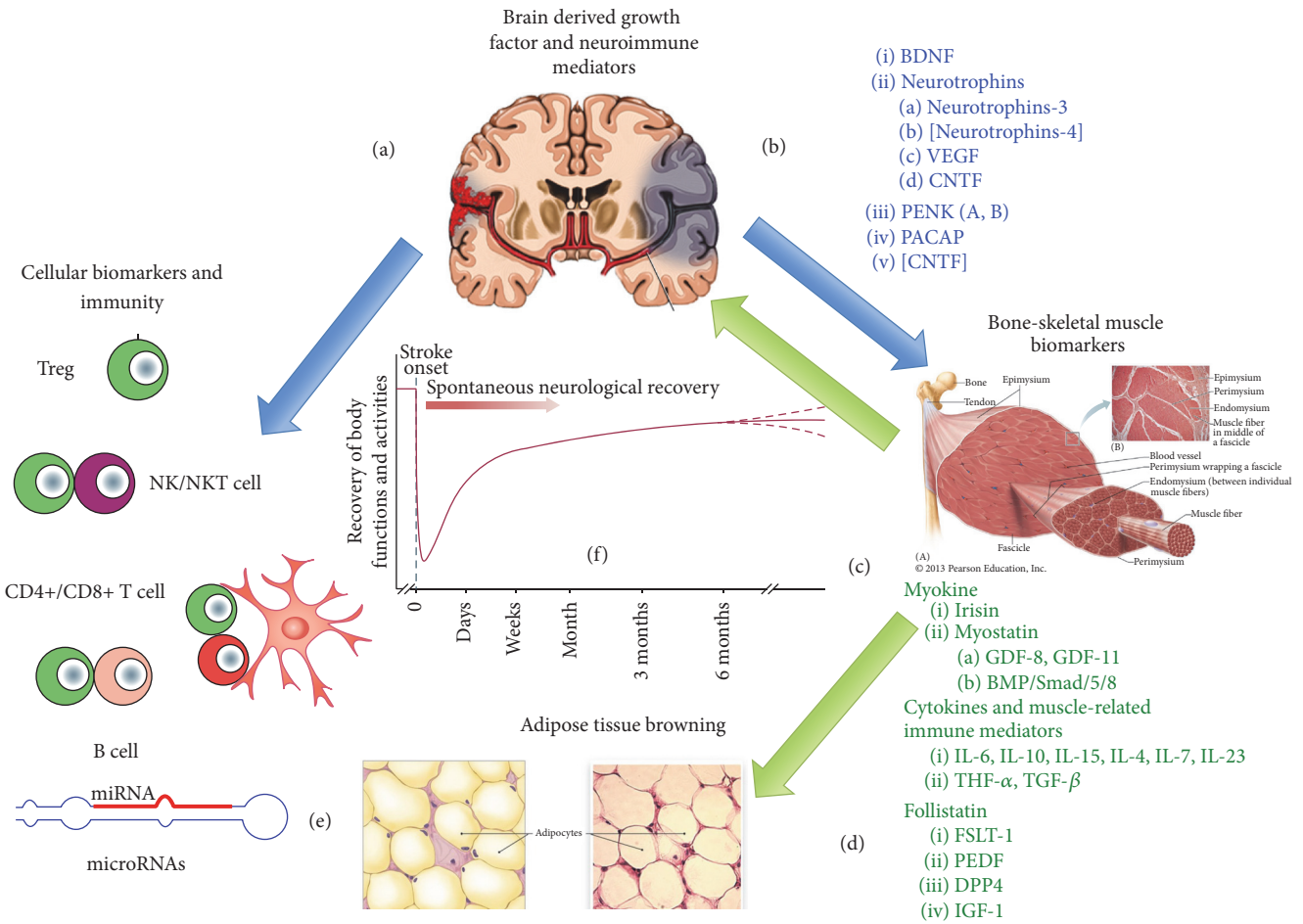

Figure 1: Cartoon showing the relationship between brain, muscle, and the immune system during stroke onset and stroke recovery, in order to highlight possible biomarkers of these events, as described in the text. Damaged brain, either following ischemic or hemorrhagic stroke, produces a panoply of different biomolecules, mainly BDNF or other neuromodulators, which link brain function with the immune system (a) and skeletal muscle (b). The first releases cytokines and cellular markers and the second one myokines, many of which interact with BDNF (c). Many of these myokines modulate the activity of other tissues such as vascular tissue (endothelia), bone, and adipose tissue. Irisin is a known "browning stimulator" (d). Downstream regulators of these mechanisms are represented by newly discovered miRNAs (e). The relationship between the activity of a defined biomarker (dose/time in plasma) and stroke recovery can be plotted in a time course curve as exemplified in (f).

factor also for the pediatric population, in elderly subjects [14]. This would mean that a major concern for rehabilitation medicine and neurology is the search for the best circulating markers of this relationship. Many of these markers, actually, pertain to the ability of the immune system to counteract with the oxidative and mechanical stress associated with the cardiovascular function.

The most recent literature on the field stresses on the role of inflammatory molecules as biomarkers in stroke. Stroke, which can be simply considered as an injury occurring in brain when blood flow is cut off, may be of ischemic or hemorrhagic nature and each year about 800,000 people experience a new or recurrent stroke, being the fifth leading cause of death in the United States and about a third in Italy [15–18]. This circumstance suggests that searching for new emerging biomarkers for either stroke predictivity, diagnosis, or prognosis has come in the spotlight and is asking for new insights and data from experimental research [19, 20]. Emerging new biomarkers should come from the many novelties in the scientific field of stroke, which should help clinicians to improve addressing this pathology and its dramatic consequences also on the social life and habits. This review tries to give a state of the art of the topic.

2. Brain Derived Growth Factor (BDNF) and Other Neuroimmune Mediators in Stroke

The involvement in stroke of BDNF, a 13 kDa protein that belongs to the neurotrophin family, emerged some years ago. In particular low serum concentration of BDNF, particularly in the acute phase of ischemic stroke, is considered a factor of poor prognosis for the functional status of patients [57]. Physical exercise should ameliorate this circumstance, even by increasing the hippocampal level of BDNF in the early

stages of a stroke (cerebral embolism) [58]. The enhancement of BDNF seems to be related to improvements in stroke recovery, even in animal models [59, 60], which show how social interactions are fundamental in the poststroke recovery [61]. BDNF increase in the hippocampus may improve also poststroke depression following estrogen-based therapy [37], a role that is also reached by physical exercise and muscular training [62]. Therefore, BDNF may be a good candidate to follow stroke development, even in chronic poststroke subjects, where circulating BDNF is very low with respect to controls [47, 48]. Besides BDNF further neurotrophins were recently involved in stroke and may fulfil the list of potential biomarkers.

Neurotrophin-3 has a major role in both traumatic and ischemic injury of the brain, such as in stroke. It is produced by neuroglia as an adaptation factor to hypoxic conditions and, together with proinflammatory cytokines such as IL-6 and TNF-α, it participates in the brain response to ischemic injury [49]. In mouse models, an upregulation of the neurotrophic receptor p75 (NTR) in striatal neurons during an ischemic damage was reported [40]. Neurotrophins should act with biochemical factors the ability of which is to regulated endothelial and vascular function. Actually, vascular endothelial growth factor (VEGF) has been recently associated with BDNF as a biomarker in stroke [63, 64], though with some criticism [39]. In animal models, the neurotrophin ciliary neurotrophic factor (CNTF), which is endogenously upregulated in a stroke onset, mediates the neurogenesis and an anti-inflammatory process [41]. The correct neuron-astrocyte interaction dampens CNTF release, which is upregulated by astrocytes therefore during a traumatic or ischemic damage to this integrin-mediated linkage [42]. To date there are no evidence reporting the role of plasmatic CNTF in stroke, though the circulating levels of this neurotrophin have gained much more importance in the study of patients with amyotrophic lateral sclerosis [43]. Still, in rat models, neurotrophin-4 increases its serum levels after a stroke event and exhibits the same properties of BDNF, as it is likewise a ligand of trkB [65]. Neuropeptide biology is moreover very rich of suggestions in order to retrieve emerging biomarkers for stroke. Yet, genetics should be involved in these issues, as genetic polymorphism highly influences the analytical performance of whatever would be introduced as a biomarker, particularly for neuropeptides. For example, neuropeptide Y may be a good prognostic biomarker in subjects with certain gene promoter polymorphisms [45]. Proenkephalin (PENK), or proenkephalin A, as proenkephalin B is known as prodynorphin, is a neuropeptide of recent introduction in the biomarker list. Its plasma level may be used as an indicator of prognostic outcome of stroke, as elevated concentrations in the bloodstream correlate with exacerbation of the cerebral injury [66, 67]. The neuropeptide pituitary adenylate-cyclase activation protein (PACAP) is involved, as many other factors here described, in the poststroke neurogenesis [68]. Also PACAP increase in plasma may be used as a prognostic marker of stroke, as an increase has been associated with severity of intracranial hemorrhage [69]. Neuromediators in stroke, detectable in the bloodstream and being considered as emerging biomarkers, should suggest that the ability to set a panoply of biomarkers for diagnosis and prognosis of stroke is a fundamental point at issue in the clinical research of this pathology.

3. Bone-Skeletal Muscle Biomarkers in Stroke

The involvement of the skeletal and muscular function, and its relationship, in stroke prevention and management, should be taken into account when addressing the issue of stroke biomarkers, as skeletal muscle undergoes deep changes in poststroke events [70]. Furthermore, myokines play a major role in the cross-talk bone-muscle [27, 71]. The role of skeletal muscle in stroke is of major interest. Markers of inflammation increase both systematically and locally in the skeletal muscle during stroke, while the anti-inflammatory feedback mechanism involves both myokines and the cholinergic anti-inflammatory pathway, which should be activated by physical exercise [9]. Myokines are muscle derived factors, with a role similar either to cytokines or growth factors, which modulate the complex relationship between skeletal muscle and other fundamental compartments, such as bone or adipose tissue, and whose upregulation is dependent on subject's physical exercise [21, 22, 27, 72]. Their activity in stroke should suggest a possible role as biomarkers of stroke pathogenesis and/or recovery [73].

3.1. Irisin. Irisin, otherwise known with its precursor name, that is, fibronectin type III domain-containing protein 5 (FNDC5), is a muscular trans-membrane protein, with a fibronectin type III-like ectodomain that can be cleaved giving the soluble molecule known as irisin [74]. This myokine fundamentally regulates the cross-talk skeletal muscle-adipose tissue [71]. Serum levels of irisin increase with training and physical exercise [75, 76]; therefore it may appear intriguing to ascertain if irisin may be involved as a possible and promising serum marker in poststroke training and stroke recovery or neuromuscular rehabilitation. To the best of our knowledge, there are no or very few reports showing or suggesting a relationship between irisin and stroke. During heart failure (HF), the expression FNDC5 was related to an improvement in the aerobic performance in HF patients, therefore suggesting that FNDC5 may work as a hormone counteracting stress coming from injury, tissue damage, hypoxia, and inflammation [77]. Its association with training is yet much more encouraging. Together with other myokines and neuromodulators, irisin should participate in the regulation of resistance training periodization, particularly in subjects with sedentary or rarely active life [78]. Furthermore, physical exercise induces the hippocampal expression of the brain derived neurotropic factor (BDNF), through a PGC-1α/FNDC5 pathway, that is, PGC-1α (which is a marker of mitochondrial function and biogenesis), during endurance exercise in mice, which elicits the expression of the neuronal gene for FNDC5, which in turn induces BDNF expression [79]. This relationship irisin precursor, namely, FNDC5, and BDNF may be of fundamental importance in the comprehension of the role of training in stroke [80], particularly because physical exercise induces BDNF but also synapsin I in the hippocampal trisynaptic circuit [81]. BDNF

induces local synaptic plasticity [82] and more interestingly cyclin-dependent kinase 5 (Cdk5), a serine/threonine kinase involved in the rescue of synaptic plasticity [83], is involved in the BDNF-stimulated dendritic growth in hippocampus [84]. In poststroke patients, the role of Cdk5 has been associated with the long-term postischemic neurodegeneration and Cdk5 might be a pharmacological target; its inhibition or gene silencing increases the expression of BDNF in the hippocampal neurons [85]. The loss of this serine/threonine kinase in the nucleus accumbens reduces the ability to sustain a muscular physical exercise [85]. The relationship between the different degrees of the muscular activity (training, sustained and endurance physical exercise, moderate aerobic exercise, etc.) and the newly incoming biomarkers is still puzzling, particularly if related to poststroke rehabilitation. The role of irisin and its precursor FNDC5 in stroke recovery with training is quite far to be fully elucidated. As far as irisin is concerned, both muscle and brain express this hormone, which even participates in neurological and neuropsychiatric function such as regulation of behaviour and the mechanism of boosting reward-related learning and motivation [86] and is considered as one of the major linkers between muscular activity and brain [23]. Both irisin and BDNF are possible candidates as markers of sarcopenia [24], together with the transforming growth factor-β (TGF-β), follistatin, insulin-like growth factor-I (IGF-1), fibroblast growth factor-2 (FGF-2), osteoglycin, FAM5C, interleukin (IL-6), leukemia inhibitory factor (LIF), IL-7, IL-15, monocyte chemoattractant protein-1 (MCP-1), ciliary neurotrophic factor (CNTF), osteonectin, and matrix metalloproteinase 2 (MMP2), which affect also bone cells [27]. It is tempting to speculate that serum irisin would be an emerging biomarker in the relationship muscular activity/brain function and possibly an emerging biomarker also for stroke recovery.

3.2. Myostatin. This myokine, known also as growth differentiation factor 8 (GDF-8), is a member of the TGF-β protein family [25, 27] and has been recently related to the role and activity of GDF-11, with which it shares some similarities [25]. Myostatin is associated with muscle catabolism and actually antibodies against myostatin were considered to prevent sarcopenia, cancer cachexia, and muscle wasting disorders [26, 87]. People who survive stroke experience a disproportionate atrophy of their muscle mass or other detrimental tissue changes in the composition on the paretic side. Recent evidence supports the suggestion for a fundamental role of myostatin in these subjects, as an increase in myostatin mRNA was reported in the paretic thigh, while a reduction was observed following resistive training [88]. The serum level of myostatin, which is a negative regulator of muscle growth, has been associated with muscle function in a maintenance grip strength; that is, higher serum myostatin has been related to lower muscle function [89] and is a marker of muscle wasting [90]. Myostatin shares with irisin or FNDC5 a role in the browning phenomenon of the adipose tissue; therefore this myokine, as well as irisin, has a role in glucose and fat metabolism, besides muscle function [91]. This would suggest a possible relationship between stroke and nutrition in the myokine activity [92, 93]. Serum myostatin, as a possible biomarker in stroke-related disorders, has been reported for myocardial ischemia-related injury, as a cardiac myostatin upregulation immediately occurs after myocardial ischemia and participates in the ubiquitin-proteasome degradation of proteins, via the atrogin and MuRF1 involvement, in the skeletal muscle [94]. To the best of our knowledge, there are very few reports about the association of myostatin with poststroke neurorehabilitation, but evidence should suggest that this myokine may be upregulated following stroke and downregulated with muscular training. Animal models support this hypothesis. Muscle is involved in maintaining the bone mineral content and in electrical muscle stimulation following sciatic neurectomy in rats; muscle fibers downregulated myostatin gene expression, a model that should suggest the downregulation of this myokine in stroke-derived paretic limbs [95]. Cerebral ischemia causes also the activation of the bone morphogenetic protein (BMP)/Smad/5/8 signaling in muscle atrophy occurring following stroke. The ubiquitin-proteasome degradation of muscle proteins in paretic limbs following the severe sensorimotor deficits after cerebral ischemia involves a biomolecular mechanism in muscle fibers that inhibits the Akt/mTOR pathway and increases, besides myostatin, many actors of the ubiquitin-proteasome degradation such as muscle RING finger-1 or MuRF1, muscle atrophy F-box (MAFbx), and muscle ubiquitin ligase of SCF complex in atrophy-1 or Musa1 [96]. This evidence may suggest even a role of myostatin as a prognostic marker for stroke.

3.3. Cytokines and Muscle-Related Immune Mediators. Skeletal muscle is one of the major producers of interleukin-6 (IL-6), which contributes with other factors such as irisin to the fine regulation of bone metabolism and adipose tissue homeostasis after physical exercise [10, 97, 98]. The relationship between IL-6 and stroke is established principally by neuroinflammatory mechanisms in the CNS, where the expression of genes such as IL-6, besides myeloperoxidase (MPO), IL-1β, and TNF-α, is fundamental for stroke susceptibility [99] but also myocardial stroke generates a peripheral proinflammatory response in skeletal muscle [100]. In chronic heart failure training muscular exercise reduces muscle production of IL-6, TNF-α, IL-1β, and iNOS [101] although those markers involved in muscle atrophy, that is, atrogin and MuRF1, do not change their expression pattern in skeletal muscle [102], assessing that this model is not fully comparable to stroke-related muscle disorders. Following stroke huge panoply of proinflammatory cytokines that are released in the bloodstream and detectable in the serum, besides IL-6 and TNF-α, also IL-10, IL-4, IL-17, IL-23, and TGF-β increase [103]. Low frequency electrical stimulation together with acupuncture in denervation muscle induced atrophy in mice, reduced the expression of myostatin, and transiently increased the level of inflammation by enhancing the expression of IL-5, TNF-α, arginase-1 expressing macrophages (M1-type), and muscle specific microRNA, that is, miRNA-1 and miRNA-206, but also upregulated IGF-1 expression [104, 105]. This should suggest that inflammation in muscle is initially triggered to attenuate muscle degeneration and atrophy, by activating, for example, mitochondria-biogenesis markers,

such as PGC-1α and autophagy [106–108]. Factors inhibiting autophagy in muscle fibers and the intracellular accretion of unfolded, damaged proteins may lead to apoptosis and muscle atrophy [109]. The intriguing relationship between muscle inflammation and PGC-1α is finely modulated. At least, as emerging from in vitro heart models, PGC-1α is upregulated following short-term exercise and interestingly an anti-inflammatory stimulus may reduce the activity of PGC-1α by attenuating its downstream effectors, such as NRF-1 and several respiratory genes, as most probably oxidative stress generated by either inflammation or muscular exercise is a main trigger of PGC-1α [110]. Mediators of this muscle response include several immune mediators besides IL-6. Interleukin 15 (IL-15) induces mitochondrial activity, via a PPAR-δ signaling during physical exercise [111]. Although there seems to be lack of evidence reporting a role of IL-15 in muscle atrophy following stroke, the most recent reports about this cytokine in this field suggest a possible involvement in this mechanism. At least, in diabetic rats, resistance training increasing both muscle and serum levels of IL-15 [112] and IL-15 is one of the main protective factors in sepsis-induced muscular wasting and proteolysis in mice [113]. In this sense, IL-15 should play a protective role against stroke or its dependent effects, as likely as further cytokines such as IL-19 [114] or IL-33 [115]. Despite its well-known anti-inflammatory role, IL-10 has been recently associated with worsening of muscle atrophy. Even a short bed rest in aged patients with leg lean mass or muscle wasting associated symptoms increases some proinflammatory cytokines and also IL-10 [116]. Furthermore, an excessive IL-10 response may even worsen stroke recovery, depending on genetics and sex [117, 118]. Actually, the inflammatory participation in stroke recovery should be profoundly revised. Interleukin 6 is still associated with worsening in muscle activity [119, 120], assessing the detrimental role of inflammatory cytokines in stroke-dependent muscle damage. But, as an example, anti-inflammatory drugs should act as a double-edged sword, both exacerbating brain injury and helping the pathway to poststroke recovery, suggesting the existence of more complex machinery in the neuromuscular rehabilitation [121]. For example, interleukin 17A (IL-17A), produced by $\gamma\delta$T, cells was initially thought to have detrimental action in the pathogenesis of acute ischemic stroke but a deeper focusing onto its activity showed that IL-17A participates in neuronal differentiation, synaptogenesis, and spontaneous recovery following ischemic stroke [122]. Both IL-17A and IL-23 failed in being associated with biomarkers in muscle damage, following physical exercise [123]. Fundamentally, muscle produces cytokines that are widely expressed in the innate and adaptive immune system, such as IL-6, IL-8, IL-10, IL-1ra, TNF-α, MCP-1, IL-1β, IL-12p35/p40, and IL-15 [124]. Particularly for IL-1 receptor antagonist (IL-1ra) it is well-known that this cytokine reverses immune suppression associated with stroke, generating concerns about the effect of immunosuppression during the acute phase of stroke [28]. Yet, there are controversial opinions about the therapeutic effect of this anti-inflammatory cytokine in stroke [29, 30]; probably one must distinguish the effect of systemic IL-1ra from local (e.g., skeletal muscle, myocardium). However, a lot of molecules with a growth factor-like activity have come in the spotlight as potential biomarkers in stroke.

3.4. Follistatin-Like 1, Insulin Growth Factors, and Other Myokines. Follistatin, known also as activin-binding protein (ABP), is considered as an antagonist of myostatin. Recent reports showed that the ratio myostatin to follistatin is a good marker of the denervated muscular atrophy and its recovery [125]. Circulating follistatin levels are correlated with muscular mass in healthy individuals [126]; therefore its presence in the peripheral blood should be interpreted as a positive prognostic marker of the recovery of muscle damage and atrophy following stroke, a hallmark of several myokines [73, 127, 128]. Follistatin-like 1 is a myokine which promotes revascularization and endothelial cell function following an ischemic injury [129]. Follistatin-like 1 (FSTL1) is a protein very similar to follistatin, which does not bind to activin A, but rather BMP4 and TGF-β [130, 131]. The neuroprotective role of FSTL1 has been reported in rats, where the glycoprotein is able to repair and improve neuron deficits inducing Akt phosphorylation and hence its receptor disco-interacting protein 2 homolog A (DIP2A) activation [132, 133]. FSTL1 is a marker of remodelling also in cardiac function, where in subjects with heart failure an increase in the serum FSTL1 was observed [31]. Actually, FSTL1 has been recently considered an independent circulating biomarker of inflammation and oxidative stress and likewise hsCRP, associated with markers predictive of stroke [32]. Despite its proinflammatory-like nature [130], FSTL1 is a cardioprotective molecule, which is upregulated following exercise training, particularly after myocardial infarction [134] and which modulates vascular remodelling [33].

Serum level of FSTL1 may give fundamental insights on the individual's response to ischemic stress. Pigment epithelium derived factor (PEDF) known as serpin F1, is a myokine with neurotropic activity, which has been recently associated, as a neuroprotective and antiangiogenic agent in animal models, with ischemic stroke [34, 135]. However, to the best of our knowledge, there are yet no data about the association between serum PEDF and stroke-related disorders, particularly for muscle. Rat models showed that PEDF induces the production of inflammatory chemokines such as MIP-2 and MIP-3α in microglia [136]. The myokine dipeptidyl-peptidase 4 (DPP4) has recently come in the spotlight because its inhibition, as well as the use of glucagon-like receptor 1 (GLP-1) agonists, leads to an antistroke effect [137, 138] and a cardioprotective role [139]. During physical exercise, DPP4 inhibitors improve mitochondrial biogenesis and muscle activity through the activation of GLP-1 signaling [140]. Yet, this myokine should act at a more systemic level, in the energetic balance of the organism, as their inhibitors are able to act in a similar way to sulfonylureas or pioglitazone for diabetes [141]. Insulin-like growth factors (IGFs), particularly with the involvement of CXCR4, are fundamental molecules in remodelling, even after stroke [50, 142, 143]. The serum level of IGF-1 in elderly men with muscle frailty has been considered as positive prognostic marker, also for bone mineral density [51]. IGF-I and IGF-II are important myokines recently related to stroke [52]. The relationship between IGF-1

and physical training is particularly intriguing, as serum total IGF-1 in response to a resistance exercise is highly variable and depends on the subject's body mass [144]. However, recent reports indicate that IGF-1 has a major role, together with BDNF, in neuroplasticity and in the recovery of the neuromuscular function following stroke by active muscle exercise [145–147], although an excess in IGF-1 production can induce neuroinflammation and exacerbation of stroke effects, as occurring following treatment with apolipoprotein A-1 mimetic peptide, which reduces white matter damage from stroke [148]. Therefore, besides the complexity of events related to IGF-1 activity, even when associated with BDNF, for many emerging myokines a possible role as biomarkers in stroke yet needs confirmation in clinical studies, despite the encouraging evidence coming from in vitro or animal studies. Usually, the serum level of IGF-1 in patients with stroke-derived intracerebral hemorrhage during admission (hospitalization) is lower than healthy controls, while VEGF and hepatocyte growth factor (HGF) are higher [149]. Further factors related to IGFs have been recently associated with stroke and may suggest emerging biomarkers in this pathology. A recent study showed that not only low levels of IGF-1 were associated with an unfavourable functional outcome of stroke but also the level of insulin-like growth factor binding protein-3 (IGFBP-3) [35]. More favourable outcomes should be yet associated with the evaluation of the decrease in the IGF-1 ratio and with IGFBP-3, rather than with serum levels of IGF-1 [150]. Actually, a more complex relationship between IGF-1, IGF-II, IGFBP-1, and IGFBP3 should give important insights on the risk of ischemic stroke [151, 152]. This complex pattern is a hallmark of many myokines involved in stroke. Myokines includes cytokines, hormone-like molecules, and growth factors. Fibroblast growth factor 21 (FGF21) is a myokine, which may be important in detecting subclinical atherosclerosis, which may be a pathogenetic cause of stroke [153]. FGF21 is related to metabolism, stress response, mitochondria function, and insulin resistance, as serum levels of FGF21 are elevated in certain types of mitochondria dysfunction, particularly in the muscle [154, 155]. Some reports have investigated also its relationship with bone physiology but the topic asks for further insights [156, 157]. It would be interesting to ascertain if serum level of FGF21 may be associated with positive outcome given by physical exercise. This has been reported for metabolic syndrome [158], yet not for poststroke training; then FGF21 may be suggested as an indirect biomarker.

Table 1 summarizes most of the assessed and emerging biomarkers in stroke onset and recovery.

4. Cellular Biomarkers and Immunity of Stroke

The role of the immune system in stroke and in its recovery-rehabilitation process, using physical training or others, includes both soluble factors (cytokines, chemokines, myokines, adipokines, and neuroimmunokines) and immune cells. Immune cells may be investigated mainly using flow cytometry and can give fundamental insights on the role and activity of innate immunity in the remodelling process following stroke [55, 56, 103, 159–161]. Some circulating cytokines and reactive molecules, such as interleukin 11 (IL-11), are considered important markers of ischemic stroke [162, 163], though some consideration should be taken into account about the role of the different subtypes of stroke [164]. Cellular signals, such as the immunoproteasome, are correlated with ischemic stroke with intracranial hemorrhage [165]. The phenotypic subsetting of the different lymphocyte populations would be an interesting biomarker of stroke and stroke recovery. For example, a peripheral persistence of $CD4^+CD28^-$ T cells (CD28 *null* cells) has been reported in acute ischemic stroke [166], assessing previously reported evidence [167]. Fox $P3^+CD25^+CD4^+$ regulatory T cells (Tregs) are presumably involved in stroke-related events [168]. In this regard, the program death 1 ligand (PF-L1) on Tregs should have a major role in neuroprotection against cerebral ischemia, as it mediated the suppressive action exerted by Tregs on metalloproteinase 9 (MMP9), which is released by inflamed neutrophils [169]. Innate immunity plays a fundamental role in stroke. It has been recently reported that nucleotide binding oligomerization domain- (NOD-) like receptors (NLRs), which are a class of cytoplasmic pattern-recognition receptors, are upregulated and highly expressed in a mouse model of ischemic stroke [170]. Recent pharmacological strategies have taken into consideration the innate immune hallmark of inflammation in stroke. This allowed researchers to realize that the anti-inflammatory mechanism induced by the damaged brain may be a good target for therapy. The cholinergic anti-inflammatory pathway, when modulated by α7-nicotinic acetylcholine receptor (α7-nAChR) ligands, may facilitate stroke recovery. By using a polychromatic flow cytometry approach, it is possible to investigate how circulating leukocytes change their surface phenotypes and subtypes and/or their amount in relation to stroke-associated-events. Invariant natural killer T cells (iNKT) infiltrate mouse ischemic hemisphere in animals undergoing an ischemic stroke [171, 172]. Alpha-galactosyl ceramide (αGC), which specifically activates iNKT, is requested to promote the protective role of iNKT in myocardial stroke [173], a circumstance that would be suggested also for brain stroke [172]. A high number of circulating NK cells within the first hours of an ischemic stroke, particularly if followed by a rapid falling down of other lymphocyte subsets, may indicate a possible risk of pejorative inflammatory disorders in stroke patients [174]. Infiltrations of NK cells in brain occur also in human during ischemic stroke, where cells are probably activated by IP-10 [175]. This evidence assesses the role of innate immune cells infiltration in the development of stroke-related damage. Stroke-induced lymphopenia is related to a reduction of circulating high mobility group protein B1 (HMGPB1) and by the activity of T cells [176]. $CD4^+$ T cells, together with $CD8^+$, $\gamma\delta$-T cells, and Tregs, change their peripheral pattern following stroke [177]. Very recently, Klehmet et al. reported that stroke induces defined alterations in the memory T cell compartment [178]. Gamma-delta T cells, which are with Th17 the main producers of IL-17A, increase dramatically during ischemic stroke [179]. Leukocyte subtypes that dynamically should change with

Table 1: List of the main assessed and emerging circulating biomarkers in stroke.

Biomarker group	Molecule	Diagnostic or prognostic value[(1)]				References
Myokines	Irisin			↑	Good prognostic marker of stroke recovery with training	[21, 22]
	Myostatin (GDF-8)	↑	Muscular biomarker of stroke Muscle wasting			[23–26]
	Follistatin			↑	Good prognostic marker of stroke (muscular level)	[27–30]
	PEDF			↑	Good prognostic marker of stroke (angiogenic level)	[31, 32]
	DPP4			↓	Ameliorating stroke recovery	[33, 34]
	Osteonectin (SPARC)			↑	Neural repair following stroke	
	FGF-21	↑	Negatively associated with stroke			[35]
Neurotropic factors	Brain derived neurotropic factor (BDNF)	↑	Improvement in stroke recovery Biomarker of stroke onset	↓	Bad prognosis stroke recovery	[17, 19, 20, 36]
	Neurotrophin-3	↑	Biomarkers of stroke onset	↑	Stroke recovery	[37, 38]
	Neurotrophin-4	↑	Biomarkers of stroke onset			[39]
	CNTF	↑	Biomarkers of stroke onset			[40]
Neuropeptides	Neuropeptide Y			↑	Good prognostic biomarker in certain SNP patterns	[41]
	Proenkephalin A			↑	Bad prognosis in stroke progression	[42–44]
	PACAP			↑	Bad prognosis in hemorrhagic stroke progression	[45]
	Substance P			↑	Very bad prognosis in ischemic stroke progression	[46]
Growth factors and GF-like molecules	VEGF	↑	Biomarkers of stroke onset			[47–49]
	IGF-1, IGF-II			↑	Good prognosis in ischemic stroke progression (remodelling)	[50–52]
Cytokines	Interleukin 6 (IL-6)	↑	Stroke onset and progression	↑	Prognostic value to be reviewed	[1, 15, 16]
	Interleukin-33 (IL-33)	↑	Biomarkers of stroke onset	↓	Bad prognosis in ischemic stroke progression	[53]
	Interleukin 15 (IL-15)	↑	Biomarkers of stroke onset	↑	Brain injury	[54]
	Interleukin-11 (IL-11)	↑	Biomarkers of stroke onset			[55, 56]

[(1)] Arrows show the plasma and/or serum level or the level in peripheral blood.

stroke and change their surface markers are very different depending on the time of stroke onset and its subtype. Therefore, this evidence should render particularly complex any interpretation of the flow cytometry panel used to highlight the percentage and nature of the various lymphocyte subsets in the bloodstream. B cell compartment is also involved in stroke biology. Particularly, for pre-B cells, the released factor nicotinamide phosphoribosyltransferase (NAMPT), more simply known as pre-B-cell colony-enhancing factor (PBEF), plays a fundamental role in the mitochondrial survival and biogenesis after ischemic damage, protecting neurons from apoptosis [180]. B cells in stroke showed heterogeneity in their function and subtypes and participate in prestroke neuroprotective mechanisms [181]. Regulatory B cells contribute to limiting the inflammatory events occurring in CNS following stroke and IL-10 secreting B cells appear to have the major role in this mechanism [182]. Regulatory T cells have also a fundamental function in addressing stroke-related damage, particularly in poststroke recovery [183]. Actually, their role in this recovery process has suggested Tregs as a cellular therapy in stroke [170].

Much lesser importance has been given to circulating granulocytes in their possible relationship with stroke. Peripheral eosinophils have been associated with stroke, as the eosinophil count appears to have a fundamental impact on the outcome of stroke [184]. Blood neutrophil counts appeared to be associated with intracranial hemorrhage following stroke but this association was recently criticized [185, 186]. A role for basophils in stroke was reported several years ago but there is no further association to date, although mast cells are probably the early responders in the regulation, following ischemic stroke, of the blood-brain barrier [187, 188]. At least in mouse models, the CD36+ monocyte/macrophage system is involved in the poststroke recovery phase, leading to a correct phagocytosis [189]. In these models, monocyte-derived macrophages exhibit a repair function in the poststroke event [190]. Very recently, the role of monocytes in ischemic stroke has been thoroughly reviewed [191]. Interestingly, monocytes recruited to the ischemic site in mouse differentiate to an alternative activated macrophage (AAM) or M2-macrophage [56].

Particular interest has been recently devoted to brain dendritic cells in stroke events [192]. However, also antigen-presenting cells (APCs) in peripheral blood should give important insight on immune response to stroke and the mechanism of tolerance [193]. During cerebral focal ischemia a reduced peripheral costimulatory activity has been observed [194]. Stroke generates imbalance in the acquired immune response and a decrease in circulating dendritic cells [195].

5. MicroRNAs as Biomarkers in Stroke

MicroRNAs are the latest novelty in the emerging role of biomarkers in stroke [196]. These short modulatory RNA fragments play a fundamental role in the management of stroke, as much as that polymorphism in the microRNAs miRNA-130b, miRNA-200b, and miRNA-495 affects stroke susceptibility and the level of poststroke outcome [197]. MicroRNAs participate in the regulation of blood-brain barrier and in the function of microglia and astrocytes [198, 199]. Peripheral microRNAs are promising and emergent biomarkers for stroke [200]. Some miRNAs play prognostic or high diagnostic value to evaluate or predict stroke onset and development.

For example, low level of serum miRNA-320b is a high-risk factor for carotid atherosclerosis, a prodromic event possibly leading to cerebral ischemia and stroke [201], while miRNA-146a correlates with neuroprotection from cerebral ischemia [202]. The downregulation of miRNA-30a reduces ischemic injury via the enhancement of the beclin-1 mediated autophagy [203]. This neuroprotection role is exerted also by the downregulation of miRNA-181b, at least in the mouse model, via the involvement of the heat shock protein 45 and the ubiquitin carboxyl-terminal hydrolase isozyme L1, a role shared also by miRNA-30a [204, 205]. A neuroprotective role is exerted by miRNA-134 by targeting another heat shock protein, namely, HSPA12B [36]. Mesenchymal stem cells (MSC) may be primed by serum from stroke patients and this priming upregulates the expression of miRNA-20a, which in turn promotes MSC proliferation by regulating cell cycle and p21 CDKN1A [38]. This should suggest that miRNA-20a participates in the remodelling of damaged tissue after stroke. MicroRNAs as a biomarker for stroke may use either cerebrospinal fluid (CSF) or peripheral blood. After stroke some miRNAs, such as let-7c an miRNA-221-3p, are upregulated in CSF, while, in whole blood, where more than 250 different miRNAs were detected, miRNA-151a-3p and miRNA-140-5p were upregulated while miRA-18b-5p was downregulated [44, 46, 53, 54, 206–210].

6. Conclusions

Biomarkers in stroke represent a possible challenge in the diagnostic and prognostic evaluation of stroke onset and pathogenesis and in poststroke recovery. Many of the molecules described in the text are still under investigation and may become promising and encouraging biomarkers, either diagnostic or prognostic emerging biomarkers. In this perspective, research is actually asking for further insights, particularly about newly incoming myokines (for stroke recovery following muscular training) but also for those neuropeptidergic and neurotropic molecules, which should be better suited to fit as circulating biomarker in stroke rehabilitation due to nonmuscle exercise. Experimental and clinical research should increase this list and promote new discoveries in this field, in order to improve stroke diagnosis and treatment.

Competing Interests

The authors declare that they have no competing interests.

Acknowledgments

The authors acknowledge support from the James S. McDonnell Foundation 21st Century Science Initiative in Cognitive Rehabilitation-Collaborative Award (#220020413).

References

[1] Q. Ji, Y. Ji, J. Peng et al., "Increased brain-specific MiR-9 and MiR-124 in the serum exosomes of acute ischemic stroke patients," *PLoS ONE*, vol. 11, no. 9, Article ID e0163645, 2016.

[2] M. Kacperska, J. Walenczak, and B. Tomasik, "Plasmatic microRNA as potential biomarkers of multiple sclerosis: literature review," *Advances in Clinical and Experimental Medicine*, vol. 25, no. 4, pp. 775–779, 2016.

[3] P. H. Reddy, S. Tonk, S. Kumar et al., "A critical evaluation of neuroprotective and neurodegenerative MicroRNAs in Alzheimer's disease," *Biochemical and Biophysical Research Communications*, 2016.

[4] L. Qiu, E. K. I. Tan, and L. Zeng, "microRNAs and neurodegenerative diseases," *Advances in Experimental Medicine and Biology*, vol. 888, pp. 85–105, 2015.

[5] Y. Xie and Y. Chen, "microRNAs: emerging targets regulating oxidative stress in the models of Parkinson's disease," *Frontiers in Neuroscience*, vol. 10, article no. 298, 2016.

[6] N. Quillinan, P. S. Herson, and R. J. Traystman, "Neuropathophysiology of brain injury," *Anesthesiology Clinics*, vol. 34, no. 3, pp. 453–464, 2016.

[7] M. S. V. Elkind, "Inflammatory markers and stroke," *Current Cardiology Reports*, vol. 11, no. 1, pp. 12–20, 2009.

[8] R. B. Schnabel and S. Blankenberg, "Commentary: Circulating cytokines and risk stratification of stroke incidence—will we do better in future?" *International Journal of Epidemiology*, vol. 38, no. 1, pp. 261–262, 2009.

[9] H. J. Coelho Junior, B. B. Gambassi, T. A. Diniz et al., "Inflammatory mechanisms associated with skeletal muscle sequelae after stroke: role of physical exercise," *Mediators of Inflammation*, vol. 2016, Article ID 3957958, 19 pages, 2016.

[10] A. P. Lightfoot and R. G. Cooper, "The role of myokines in muscle health and disease," *Current Opinion in Rheumatology*, vol. 28, no. 6, pp. 661–666, 2016.

[11] A. Tuttolomondo, A. Casuccio, V. Della Corte et al., "Endothelial function and arterial stiffness indexes in subjects with acute ischemic stroke: relationship with TOAST subtype," *Atherosclerosis*, vol. 256, pp. 94–99, 2017.

[12] S. Koton, D. Tanne, and E. Grossman, "Prestroke treatment with beta-blockers for hypertension is not associated with severity and poor outcome in patients with ischemic stroke," *Journal of Hypertension*, 2016.

[13] Z. Wang, G. Hao, X. Wang et al., "Short-term hypertension management in community is associated with long-term risk of stroke and total death in China: a community controlled trial," *Medicine*, vol. 95, no. 48, p. e5245, 2016.

[14] J. C. Kupferman, D. I. Zafeiriou, M. B. Lande, F. J. Kirkham, and S. G. Pavlakis, "Stroke and hypertension in children and adolescents," *Journal of Child Neurology*, vol. 32, no. 4, pp. 408–417, 2017.

[15] R. Chen, B. Ovbiagele, and W. Feng, "Diabetes and stroke: epidemiology, pathophysiology, pharmaceuticals and outcomes," *The American Journal of the Medical Sciences*, vol. 351, no. 4, pp. 380–386, 2016.

[16] S. Sacco, F. Stracci, D. Cerone, S. Ricci, and A. Carolei, "Epidemiology of stroke in Italy," *International Journal of Stroke*, vol. 6, no. 3, pp. 219–227, 2011.

[17] V. Arnao, M. Acciarresi, E. Cittadini, and V. Caso, "Stroke incidence, prevalence and mortality in women worldwide," *International Journal of Stroke*, vol. 11, no. 3, pp. 287–301, 2016.

[18] T. Truelsen, B. Piechowski-Jóźwiak, R. Bonita, C. Mathers, J. Bogousslavsky, and G. Boysen, "Stroke incidence and prevalence in Europe: a review of available data," *European Journal of Neurology*, vol. 13, no. 6, pp. 581–598, 2006.

[19] A. Shoamanesh, S. R. Preis, A. S. Beiser et al., "Circulating biomarkers and incident ischemic stroke in the Framingham Offspring Study," *Neurology*, vol. 87, no. 12, pp. 1206–1211, 2016.

[20] O. S. Mattila, H. Harve, S. Pihlasviita et al., "Ultra-acute diagnostics for stroke: large-scale implementation of prehospital biomarker sampling," *Acta Neurologica Scandinavica*, 2016.

[21] B. K. Pedersen, "Exercise-induced myokines and their role in chronic diseases," *Brain, Behavior, and Immunity*, vol. 25, no. 5, pp. 811–816, 2011.

[22] J. Dong, Y. Dong, Y. Dong, F. Chen, W. E. Mitch, and L. Zhang, "Inhibition of myostatin in mice improves insulin sensitivity via irisin-mediated cross talk between muscle and adipose tissues," *International Journal of Obesity*, vol. 40, no. 3, pp. 434–442, 2016.

[23] J. Zhang and W. Zhang, "Can irisin be a linker between physical activity and brain function?" *Biomolecular Concepts*, vol. 7, no. 4, pp. 253–258, 2016.

[24] A. Kalinkovich and G. Livshits, "Sarcopenia—the search for emerging biomarkers," *Ageing Research Reviews*, vol. 22, pp. 58–71, 2015.

[25] R. G. Walker, T. Poggioli, L. Katsimpardi et al., "Biochemistry and biology of GDF11 and myostatin: similarities, differences, and questions for future investigation," *Circulation Research*, vol. 118, no. 7, pp. 1125–1142, 2016.

[26] M. R. Laurent, V. Dubois, F. Claessens et al., "Muscle-bone interactions: from experimental models to the clinic? A critical update," *Molecular and Cellular Endocrinology*, vol. 432, pp. 14–36, 2016.

[27] H. Kaji, "Effects of myokines on bone," *BoneKEy Reports*, vol. 5, article 826, 2016.

[28] C. J. Smith, H. C. Emsley, C. T. Udeh et al., "Interleukin-1 receptor antagonist reverses stroke-associated peripheral immune suppression," *Cytokine*, vol. 58, no. 3, pp. 384–389, 2012.

[29] S. K. McCann, F. Cramond, M. R. Macleod, and E. S. Sena, "Systematic review and meta-analysis of the efficacy of interleukin-1 receptor antagonist in animal models of stroke: an update," *Translational Stroke Research*, vol. 7, no. 5, pp. 395–406, 2016.

[30] V. Banwell, E. S. Sena, and M. R. Macleod, "Systematic review and stratified meta-analysis of the efficacy of interleukin-1 receptor antagonist in animal models of stroke," *Journal of Stroke and Cerebrovascular Diseases*, vol. 18, no. 4, pp. 269–276, 2009.

[31] A. El-Armouche, N. Ouchi, K. Tanaka et al., "Follistatin-like 1 in chronic systolic heart failure a marker of left ventricular remodeling," *Circulation: Heart Failure*, vol. 4, no. 5, pp. 621–627, 2011.

[32] S. Hayakawa, K. Ohashi, R. Shibata et al., "Association of circulating follistatin-like 1 levels with inflammatory and oxidative stress markers in healthy men," *PLoS ONE*, vol. 11, no. 5, Article ID e0153619, 2016.

[33] M. Miyabe, K. Ohashi, R. Shibata et al., "Muscle-derived follistatin-like 1 functions to reduce neointimal formation after vascular injury," *Cardiovascular Research*, vol. 103, no. 1, pp. 111–120, 2014.

[34] E. J. Duh, H. S. Yang, I. Suzuma et al., "Pigment epithelium-derived factor suppresses ischemia-induced retinal neovascularization and VEGF-induced migration and growth," *Investigative Ophthalmology and Visual Science*, vol. 43, no. 3, pp. 821–829, 2002.

[35] M. Ebinger, N. Ipsen, C. O. Leonards et al., "Circulating insulin-like growth factor binding protein-3 predicts one-year outcome after ischemic stroke," *Experimental and Clinical Endocrinology and Diabetes*, vol. 123, no. 8, pp. 461–465, 2015.

[36] W. Chi, F. Meng, Y. Li et al., "Downregulation of miRNA-134 protects neural cells against ischemic injury in N2A cells and mouse brain with ischemic stroke by targeting HSPA12B," *Neuroscience*, vol. 277, pp. 111–122, 2014.

[37] Q. Su, Y. Cheng, K. Jin et al., "Estrogen therapy increases BDNF expression and improves post-stroke depression in ovariectomy-treated rats," *Experimental and Therapeutic Medicine*, vol. 12, no. 3, pp. 1843–1848, 2016.

[38] E. H. Kim, D. H. Kim, H. R. Kim, S. Y. Kim, H. H. Kim, and O. Y. Bang, "Stroke serum priming modulates characteristics of mesenchymal stromal cells by controlling the expression miRNA-20a," *Cell Transplantation*, vol. 25, no. 8, pp. 1489–1499, 2016.

[39] M. B. Jensen, M. R. Chacon, J. A. Sattin, A. Aleu, and P. D. Lyden, "The promise and potential pitfalls of serum biomarkers for ischemic stroke and transient ischemic attack," *Neurologist*, vol. 14, no. 4, pp. 243–246, 2008.

[40] G. Andsberg, Z. Kokaia, and O. Lindvall, "Upregulation of p75 neurotrophin receptor after stroke in mice does not contribute to differential vulnerability of striatal neurons," *Experimental Neurology*, vol. 169, no. 2, pp. 351–363, 2001.

[41] S. S. Kang, M. P. Keasey, S. A. Arnold, R. Reid, J. Geralds, and T. Hagg, "Endogenous CNTF mediates stroke-induced adult CNS neurogenesis in mice," *Neurobiology of Disease*, vol. 49, no. 1, pp. 68–78, 2013.

[42] S. S. Kang, M. P. Keasey, J. Cai, and T. Hagg, "Loss of neuron-astroglial interaction rapidly induces protective CNTF expression after stroke in mice," *Journal of Neuroscience*, vol. 32, no. 27, pp. 9277–9287, 2012.

[43] H. Laaksovirta, S. Soinila, V. Hukkanen, M. Röyttä, and M. Soilu-Hänninen, "Serum level of CNTF is elevated in patients with amyotrophic lateral sclerosis and correlates with site of disease onset," *European Journal of Neurology*, vol. 15, no. 4, pp. 355–359, 2008.

[44] S. S. Sørensen, A.-B. Nygaard, M.-Y. Nielsen, K. Jensen, and T. Christensen, "miRNA expression profiles in cerebrospinal fluid and blood of patients with acute ischemic stroke," *Translational Stroke Research*, vol. 5, no. 6, pp. 711–718, 2014.

[45] X.-F. Fu, X. Zhang, D.-J. Wang, B. Zhao, and Y.-R. Li, "Neuropeptide Y gene promoter -399T/C polymorphism increases risk of ischemic stroke," *Balkan Medical Journal*, vol. 30, no. 2, pp. 147–150, 2013.

[46] C. Rink and S. Khanna, "MicroRNA in ischemic stroke etiology and pathology," *Physiological Genomics*, vol. 43, no. 10, pp. 521–528, 2011.

[47] G. L. Santos, C. C. Alcântara, M. A. Silva-Couto, L. F. García-Salazar, and T. L. Russo, "Decreased brain-derived neurotrophic factor serum concentrations in chronic post-stroke subjects," *Journal of Stroke and Cerebrovascular Diseases*, vol. 25, no. 12, pp. 2968–2974, 2016.

[48] A. Alhusban, A. Y. Fouda, and S. C. Fagan, "ARBs improve stroke outcome through an AT2-dependent, BDNF-induced proangiogenic and pro-recovery response," *Neural Regeneration Research*, vol. 11, no. 6, pp. 912–913, 2016.

[49] D. Pasarica, M. Gheorghiu, F. Topârceanu, C. Bleotu, L. Ichim, and T. Trandafir, "Neurotrophin-3, TNF-alpha and IL-6 relations in serum and cerebrospinal fluid of ischemic stroke patients," *Roumanian Archives of Microbiology and Immunology*, vol. 64, no. 1–4, pp. 27–33, 2005.

[50] J. Ren and P. Anversa, "The insulin-like growth factor I system: physiological and pathophysiological implication in cardiovascular diseases associated with metabolic syndrome," *Biochemical Pharmacology*, vol. 93, no. 4, pp. 409–417, 2015.

[51] M. I. Mohamad and M. S. Khater, "Evaluation of insulin like growth factor-1 (IGF-1) level and its impact on muscle and bone mineral density in frail elderly male," *Archives of Gerontology and Geriatrics*, vol. 60, no. 1, pp. 124–127, 2015.

[52] R. Kooijman, S. Sarre, Y. Michotte, and J. D. Keyser, "Insulin-like growth factor I: a potential neuroprotective compound for the treatment of acute ischemic stroke?" *Stroke*, vol. 40, no. 4, pp. e83–e88, 2009.

[53] M. Niimi, K. Hashimoto, W. Kakuda et al., "Role of brain-derived neurotrophic factor in beneficial effects of repetitive transcranial magnetic stimulation for upper limb hemiparesis after stroke," *PLoS ONE*, vol. 11, no. 3, Article ID e0152241, 2016.

[54] X.-L. Chen, B.-J. Yu, and M.-H. Chen, "Circulating levels of neuropeptide proenkephalin A predict outcome in patients with aneurysmal subarachnoid hemorrhage," *Peptides*, vol. 56, pp. 111–115, 2014.

[55] C. Iadecola and J. Anrather, "The immunology of stroke: from mechanisms to translation," *Nature Medicine*, vol. 17, no. 7, pp. 796–808, 2011.

[56] F. Miró-Mur, X. Urra, M. Gallizioli, A. Chamorro, and A. M. Planas, "Antigen presentation after stroke," *Neurotherapeutics*, vol. 13, no. 4, pp. 719–728, 2016.

[57] A. Lasek-Bal, H. Jędrzejowska-Szypułka, J. Różycka et al., "Low concentration of BDNF in the acute phase of ischemic stroke as a factor in poor prognosis in terms of functional status of patients," *Medical Science Monitor*, vol. 21, pp. 3900–3905, 2015.

[58] N. Himi, H. Takahashi, N. Okabe et al., "Exercise in the early stage after stroke enhances hippocampal brain-derived neurotrophic factor expression and memory function recovery," *Journal of Stroke and Cerebrovascular Diseases*, vol. 25, no. 12, pp. 2987–2994, 2016.

[59] X. Li, W. Zheng, H. Bai et al., "Intravenous administration of adipose tissue-derived stem cells enhances nerve healing and promotes BDNF expression via the TrkB signaling in a rat stroke model," *Neuropsychiatric Disease and Treatment*, vol. 12, pp. 1287–1293, 2016.

[60] R. Verma, N. M. Harris, B. D. Friedler et al., "Reversal of the detrimental effects of post-stroke social isolation by pair-housing is mediated by activation of BDNF-MAPK/ERK in aged mice," *Scientific Reports*, vol. 6, Article ID 25176, 2016.

[61] V. R. Venna and L. D. McCullough, "Role of social factors on cell death, cerebral plasticity and recovery after stroke," *Metabolic Brain Disease*, vol. 30, no. 2, pp. 497–506, 2015.

[62] J. Lu, Y. Xu, W. Hu et al., "Exercise ameliorates depression-like behavior and increases hippocampal BDNF level in ovariectomized rats," *Neuroscience Letters*, vol. 573, pp. 13–18, 2014.

[63] A. Pikula, A. S. Beiser, T. C. Chen et al., "Serum brain-derived neurotrophic factor and vascular endothelial growth factor levels are associated with risk of stroke and vascular brain injury framingham study," *Stroke*, vol. 44, no. 10, pp. 2768–2775, 2013.

[64] A. Pikula, A. S. Beiser, C. Decarli et al., "Multiple biomarkers and risk of clinical and subclinical vascular brain injury: the framingham offspring study," *Circulation*, vol. 125, no. 17, pp. 2100–2107, 2012.

[65] J.-Y. Chung, M.-W. Kim, M.-S. Bang, and M. Kim, "Increased expression of neurotrophin 4 following focal cerebral ischemia in adult rat brain with treadmill exercise," *PLOS ONE*, vol. 8, no. 3, Article ID e52461, 2013.

[66] W. Doehner, S. Von Haehling, J. Suhr et al., "Elevated plasma levels of neuropeptide proenkephalin a predict mortality and functional outcome in ischemic stroke," *Journal of the American College of Cardiology*, vol. 60, no. 4, pp. 346–354, 2012.

[67] W. Whiteley, W. L. Chong, A. Sengupta, and P. Sandercock, "Blood markers for the prognosis of ischemic stroke: a systematic review," *Stroke*, vol. 40, no. 5, pp. e380–e389, 2009.

[68] M. Matsumoto, T. Nakamachi, J. Watanabe et al., "Pituitary Adenylate Cyclase-Activating Polypeptide (PACAP) is involved in adult mouse hippocampal neurogenesis after stroke," *Journal of Molecular Neuroscience*, vol. 59, no. 2, pp. 270–279, 2016.

[69] B.-Q. Ma, M. Zhang, and L. Ba, "Plasma pituitary adenylate cyclase-activating polypeptide concentrations and mortality after acute spontaneous basal ganglia hemorrhage," *Clinica Chimica Acta*, vol. 439, pp. 102–106, 2015.

[70] O. Aze, É. Odjardias, X. Devillard, B. Akplogan, P. Calmels, and P. Giraux, "Structural and physiological muscle changes after post-stroke hemiplegia: a systematic review," *Annals of Physical and Rehabilitation Medicine*, vol. 59, article e79, 2016.

[71] G. Colaianni, T. Mongelli, S. Colucci, S. Cinti, and M. Grano, "Crosstalk between muscle and bone via the muscle-myokine irisin," *Current Osteoporosis Reports*, vol. 14, no. 4, pp. 132–137, 2016.

[72] B. K. Pedersen and C. Brandt, "The role of exercise-induced myokines in muscle homeostasis and the defense against chronic diseases," *Journal of Biomedicine and Biotechnology*, vol. 2010, Article ID 520258, 6 pages, 2010.

[73] D. Di Raimondo, A. Tuttolomondo, G. Musiari, C. Schimmenti, A. D'Angelo, and A. Pinto, "Are the myokines the mediators of physical activity-induced health benefits?" *Current Pharmaceutical Design*, vol. 22, no. 24, pp. 3622–3647, 2016.

[74] P. Boström, J. Wu, M. P. Jedrychowski et al., "A PGC1-α-dependent myokine that drives brown-fat-like development of white fat and thermogenesis," *Nature*, vol. 481, no. 7382, pp. 463–468, 2012.

[75] Y. Tsuchiya, T. Ijichi, and K. Goto, "Effect of sprint training on resting serum irisin concentration—sprint training once daily vs. twice every other day," *Metabolism: Clinical and Experimental*, vol. 65, no. 4, pp. 492–495, 2016.

[76] Y. Lu, H. Li, S. Shen et al., "Swimming exercise increases serum irisin level and reduces body fat mass in high-fat-diet fed Wistar rats," *Lipids in Health and Disease*, vol. 15, no. 1, article no. 93, 2016.

[77] S. H. Lecker, A. Zavin, P. Cao et al., "Expression of the irisin precursor FNDC5 in skeletal muscle correlates with aerobic exercise performance in patients with heart failure," *Circulation: Heart Failure*, vol. 5, no. 6, pp. 812–818, 2012.

[78] J. Prestes, D. da Cunha Nascimento, R. A. Tibana et al., "Understanding the individual responsiveness to resistance training periodization," *Age*, vol. 37, no. 3, article no. 55, 2015.

[79] C. D. Wrann, J. P. White, J. Salogiannnis et al., "Exercise induces hippocampal BDNF through a PGC-1α/FNDC5 pathway," *Cell Metabolism*, vol. 18, no. 5, pp. 649–659, 2013.

[80] B. Xu, "BDNF (I)rising from exercise," *Cell Metabolism*, vol. 18, no. 5, pp. 612–614, 2013.

[81] S. Vaynman, Z. Ying, and F. Gómez-Pinilla, "Exercise induces BDNF and synapsin I to specific hippocampal subfields," *Journal of Neuroscience Research*, vol. 76, no. 3, pp. 356–362, 2004.

[82] G. Leal, D. Comprido, and C. B. Duarte, "BDNF-induced local protein synthesis and synaptic plasticity," *Neuropharmacology*, vol. 76, pp. 639–656, 2014.

[83] C. Jiang, W. Kong, Y. Wang et al., "Changes in the cellular immune system and circulating inflammatory markers of stroke patients," *Oncotarget*, vol. 8, no. 2, pp. 3553–3567, 2017.

[84] Z. H. Cheung, W. H. Chin, Y. Chen, Y. P. Ng, and N. Y. Ip, "Cdk5 is involved in BDNF-stimulated dendritic growth in hippocampal neurons," *PLoS Biology*, vol. 5, no. 4, article e63, 2007.

[85] G. N. Ruegsegger, R. G. Toedebusch, T. E. Childs, K. B. Grigsby, and F. W. Booth, "Loss of Cdk5 function in the nucleus accumbens decreases wheel running and may mediate age-related declines in voluntary physical activity," *The Journal of Physiology*, vol. 595, no. 1, pp. 363–384, 2017.

[86] J. Zsuga, G. Tajti, C. Papp, B. Juhasz, and R. Gesztelyi, "FNDC5/irisin, a molecular target for boosting reward-related learning and motivation," *Medical Hypotheses*, vol. 90, pp. 23–28, 2016.

[87] A. Maddahi and L. Edvinsson, "Cerebral ischemia induces microvascular pro-inflammatory cytokine expression via the MEK/ERK pathway," *Journal of Neuroinflammation*, vol. 7, article 14, 2010.

[88] A. S. Ryan, F. M. Ivey, S. Prior, G. Li, and C. Hafer-Macko, "Skeletal muscle hypertrophy and muscle myostatin reduction after resistive training in stroke survivors," *Stroke*, vol. 42, no. 2, pp. 416–420, 2011.

[89] D.-S. Han, Y.-M. Chen, S.-Y. Lin et al., "Serum myostatin levels and grip strength in normal subjects and patients on maintenance haemodialysis," *Clinical Endocrinology*, vol. 75, no. 6, pp. 857–863, 2011.

[90] C.-R. Ju and R.-C. Chen, "Serum myostatin levels and skeletal muscle wasting in chronic obstructive pulmonary disease," *Respiratory Medicine*, vol. 106, no. 1, pp. 102–108, 2012.

[91] X. Ge, D. Sathiakumar, B. J. G. Lua, H. Kukreti, M. Lee, and C. McFarlane, "Myostatin signals through miR-34a to regulate Fndc5 expression and browning of white adipocytes," *International Journal of Obesity*, vol. 41, pp. 137–148, 2017.

[92] J. Y. Huh, F. Dincer, E. Mesfum, and C. S. Mantzoros, "Irisin stimulates muscle growth-related genes and regulates adipocyte differentiation and metabolism in humans," *International Journal of Obesity*, vol. 38, no. 12, pp. 1538–1544, 2014.

[93] M. Foroughi, M. Akhavanzanjani, Z. Maghsoudi, R. Ghiasvand, F. Khorvash, and G. Askari, "Stroke and nutrition: a review of studies," *International Journal of Preventive Medicine*, vol. 4, pp. S165–S179, 2013.

[94] E. Castillero, H. Akashi, C. Wang et al., "Cardiac myostatin upregulation occurs immediately after myocardial ischemia and is involved in skeletal muscle activation of atrophy," *Biochemical and Biophysical Research Communications*, vol. 457, no. 1, pp. 106–111, 2015.

[95] B. Feng, W. Wu, H. Wang, J. Wang, D. Huang, and L. Cheng, "Interaction between muscle and bone, and improving the effects of electrical muscle stimulation on amyotrophy and bone loss in a denervation rat model via sciatic neurectomy," *Biomedical Reports*, vol. 4, no. 5, pp. 589–594, 2016.

[96] M. M. Desgeorges, X. Devillard, J. Toutain et al., "Molecular mechanisms of skeletal muscle atrophy in a mouse model of cerebral ischemia," *Stroke*, vol. 46, no. 6, pp. 1673–1680, 2015.

[97] G. Lombardi, F. Sanchis-Gomar, S. Perego, V. Sansoni, and G. Banfi, "Implications of exercise-induced adipo-myokines in bone metabolism," *Endocrine*, vol. 54, no. 2, pp. 284–305, 2016.

[98] G. Morris, M. Berk, P. Galecki, K. Walder, and M. Maes, "The neuro-immune pathophysiology of central and peripheral fatigue in systemic immune-inflammatory and neuro-immune diseases," *Molecular Neurobiology*, vol. 53, no. 2, pp. 1195–1219, 2016.

[99] H. Manso, T. Krug, J. Sobral et al., "Variants in the inflammatory IL6 and MPO genes modulate stroke susceptibility through main effects and gene-gene interactions," *Journal of Cerebral Blood Flow and Metabolism*, vol. 31, no. 8, pp. 1751–1759, 2011.

[100] S. S. Welc, T. L. Clanton, S. M. Dineen, and L. R. Leon, "Heat stroke activates a stress-induced cytokine response in skeletal muscle," *Journal of Applied Physiology*, vol. 115, no. 8, pp. 1126–1137, 2013.

[101] S. Gielen, V. Adams, S. Möbius-Winkler et al., "Anti-inflammatory effects of exercise training in the skeletal muscle of patients with chronic heart failure," *Journal of the American College of Cardiology*, vol. 42, no. 5, pp. 861–868, 2003.

[102] D. E. Forman, K. M. Daniels, L. P. Cahalin et al., "Analysis of skeletal muscle gene expression patterns and the impact of functional capacity in patients with systolic heart failure," *Journal of Cardiac Failure*, vol. 20, no. 6, pp. 422–430, 2014.

[103] C. Jiang, W. Kong, Y. Wang et al., "Changes in the cellular immune system and circulating inflammatory markers of stroke patients," *Oncotarget*, 2016.

[104] Z. Su, L. Hu, J. Cheng et al., "Acupuncture plus low-frequency electrical stimulation (Acu-LFES) attenuates denervation-induced muscle atrophy," *Journal of Applied Physiology*, vol. 120, no. 4, pp. 426–436, 2016.

[105] Z. Su, A. Robinson, L. Hu et al., "Acupuncture plus low-frequency electrical stimulation (Acu-LFES) attenuates diabetic myopathy by enhancing muscle regeneration," *PLOS ONE*, vol. 10, no. 7, Article ID e0134511, 2015.

[106] C. Kang and L. Li Ji, "Role of PGC-1α signaling in skeletal muscle health and disease," *Annals of the New York Academy of Sciences*, vol. 1271, no. 1, pp. 110–117, 2012.

[107] A. Vainshtein and D. A. Hood, "The regulation of autophagy during exercise in skeletal muscle," *Journal of Applied Physiology*, vol. 120, no. 6, pp. 664–673, 2016.

[108] P. A. Grimaldi, "Roles of PPARδ in the control of muscle development and metabolism," *Biochemical Society Transactions*, vol. 31, no. 6, pp. 1130–1132, 2003.

[109] W. J. Smiles, E. B. Parr, V. G. Coffey, O. Lacham-Kaplan, J. A. Hawley, and D. M. Camera, "Protein coingestion with alcohol following strenuous exercise attenuates alcohol-induced intramyocellular apoptosis and inhibition of autophagy," *American Journal of Physiology—Endocrinology And Metabolism*, vol. 311, no. 5, pp. E836–E849, 2016.

[110] A. Botta, I. Laher, J. Beam et al., "Short term exercise induces PGC-1α, ameliorates inflammation and increases mitochondrial membrane proteins but fails to increase respiratory enzymes in aging diabetic hearts," *PLoS ONE*, vol. 8, no. 8, Article ID e70248, 2013.

[111] M. J. Abbott, J. E. Krolopp, S. M. Thornton, and A. Kawata, "PPARδ is required For IL-15-induced mitochondrial activity in C2C12 skeletal muscle cells," *Medicine & Science in Sports & Exercise*, vol. 48, no. 5, supplement 1, p. 544, 2016.

[112] M. Molanouri Shamsi, Z. H. Hassan, R. Gharakhanlou et al., "Expression of interleukin-15 and inflammatory cytokines in skeletal muscles of STZ-induced diabetic rats: effect of resistance exercise training," *Endocrine*, vol. 46, no. 1, pp. 60–69, 2014.

[113] H. C. Kim, H.-Y. Cho, and Y.-S. Hah, "Role of IL-15 in sepsis-induced skeletal muscle atrophy and proteolysis," *Tuberculosis and Respiratory Diseases*, vol. 73, no. 6, pp. 312–319, 2012.

[114] W. Xie, L. Fang, S. Gan, and H. Xuan, "Interleukin-19 alleviates brain injury by anti-inflammatory effects in a mice model of focal cerebral ischemia," *Brain Research*, vol. 1650, pp. 172–177, 2016.

[115] P. Korhonen, K. M. Kanninen, Š. Lehtonen et al., "Immunomodulation by interleukin-33 is protective in stroke through modulation of inflammation," *Brain, Behavior, and Immunity*, vol. 49, pp. 322–336, 2015.

[116] M. J. Drummond, K. L. Timmerman, M. M. Markofski et al., "Short-term bed rest increases TLR4 and IL-6 expression in skeletal muscle of older adults," *American Journal of Physiology—Regulatory Integrative and Comparative Physiology*, vol. 305, no. 3, pp. R216–R223, 2013.

[117] S. E. Conway, M. Roy-O'Reilly, B. Friedler, I. Staff, G. Fortunato, and L. D. McCullough, "Sex differences and the role of IL-10 in ischemic stroke recovery," *Biology of Sex Differences*, vol. 6, article 17, 2015.

[118] W. He, H. Song, L. Ding, C. Li, L. Dai, and S. Gao, "Association between IL-10 gene polymorphisms and the risk of ischemic stroke in a Chinese population," *International Journal of Clinical and Experimental Pathology*, vol. 8, no. 10, pp. 13489–13494, 2015.

[119] S. P. M. Janssen, G. Gayan-Ramirez, A. Van Den Bergh et al., "Interleukin-6 causes myocardial failure and skeletal muscle atrophy in rats," *Circulation*, vol. 111, no. 8, pp. 996–1005, 2005.

[120] L. Pelosi, M. G. Berardinelli, L. De Pasquale et al., "Functional and morphological improvement of dystrophic muscle by interleukin 6 receptor blockade," *EBioMedicine*, vol. 2, no. 4, pp. 285–293, 2015.

[121] M. A. Alam, V. P. Subramanyam Rallabandi, and P. K. Roy, "Systems biology of immunomodulation for post-stroke neuroplasticity: multimodal implications of pharmacotherapy and neurorehabilitation," *Frontiers in Neurology*, vol. 7, article 94, 2016.

[122] Y. Lin, J. C. Zhang, C. Y. Yao et al., "Critical role of astrocytic interleukin-17 A in post-stroke survival and neuronal differentiation of neural precursor cells in adult mice," *Cell Death and Disease*, vol. 7, no. 6, Article ID e2273, 2016.

[123] K. Kanda, K. Sugama, J. Sakuma, Y. Kawakami, and K. Suzuki, "Evaluation of serum leaking enzymes and investigation into new biomarkers for exerciseinduced muscle damage," *Exercise Immunology Review*, vol. 20, pp. 39–54, 2014.

[124] J. M. Peake, P. D. Gatta, K. Suzuki, and D. C. Nieman, "Cytokine expression and secretion by skeletal muscle cells: regulatory mechanisms and exercise effects," *Exercise Immunology Review*, vol. 21, pp. 8–25, 2015.

[125] R. H. Wu, P. Wang, L. Yang, Y. Li, Y. Liu, and M. Liu, "A potential indicator of denervated muscle atrophy: the ratio of myostatin to follistatin in peripheral blood," *Genetics and Molecular Research*, vol. 10, no. 4, pp. 3914–3923, 2011.

[126] A. D. Anastasilakis, S. A. Polyzos, E. C. Skouvaklidou et al., "Circulating follistatin displays a day-night rhythm and is associated with muscle mass and circulating leptin levels in healthy, young humans," *Metabolism*, vol. 65, no. 10, pp. 1459–1465, 2016.

[127] S. Raschke, K. Eckardt, K. Bjørklund Holven, J. Jensen, and J. Eckel, "Identification and validation of novel contraction-regulated myokines released from primary human skeletal muscle cells," *PLoS ONE*, vol. 8, no. 4, Article ID e62008, 2013.

[128] M. Catoire, M. Mensink, E. Kalkhoven, P. Schrauwen, and S. Kersten, "Identification of human exercise-induced myokines using secretome analysis," *Physiological Genomics*, vol. 46, no. 7, pp. 256–267, 2014.

[129] N. Ouchi, Y. Oshima, K. Ohashi et al., "Follistatin-like 1, a secreted muscle protein, promotes endothelial cell function and revascularization in ischemic tissue through a nitric-oxide synthase-dependent mechanism," *Journal of Biological Chemistry*, vol. 283, no. 47, pp. 32802–32811, 2008.

[130] Y. Chaly, B. Hostager, S. Smith, and R. Hirsch, "Follistatin-like protein 1 and its role in inflammation and inflammatory diseases," *Immunologic Research*, vol. 59, no. 1–3, pp. 266–272, 2014.

[131] S. Raschke and J. Eckel, "Adipo-myokines: two sides of the same coin—mediators of inflammation and mediators of exercise," *Mediators of Inflammation*, vol. 2013, Article ID 320724, 16 pages, 2013.

[132] X. Liang, Q. Hu, B. Li et al., "Follistatin-like 1 attenuates apoptosis via disco-interacting protein 2 homolog A/Akt pathway after middle cerebral artery occlusion in rats," *Stroke*, vol. 45, no. 10, pp. 3048–3054, 2014.

[133] N. Ouchi, Y. Asaumi, K. Ohashi et al., "DIP2A functions as a FSTL1 receptor," *Journal of Biological Chemistry*, vol. 285, no. 10, pp. 7127–7134, 2010.

[134] Y. Xi, D.-W. Gong, and Z. Tian, "FSTL1 as a potential mediator of exercise-induced cardioprotection in post-myocardial infarction rats," *Scientific Reports*, vol. 6, Article ID 32424, 2016.

[135] M. Zille, A. Riabinska, M. Y. Terzi et al., "Influence of pigment epithelium-derived factor on outcome after striatal cerebral ischemia in the mouse," *PLoS ONE*, vol. 9, no. 12, Article ID e114595, 2014.

[136] A. Takanohashi, T. Yabe, and J. P. Schwartz, "Pigment epithelium-derived factor induces the production of chemokines by rat microglia," *GLIA*, vol. 51, no. 4, pp. 266–278, 2005.

[137] V. Darsalia, M. Larsson, D. Nathanson, T. Klein, T. Nyström, and C. Patrone, "Glucagon-like receptor 1 agonists and DPP-4 inhibitors: potential therapies for the treatment of stroke," *Journal of Cerebral Blood Flow and Metabolism*, vol. 35, no. 5, pp. 718–723, 2015.

[138] K. Tziomalos, S. D. Bouziana, M. Spanou et al., "Prior treatment with dipeptidyl peptidase 4 inhibitors is associated with better functional outcome and lower in-hospital mortality in patients with type 2 diabetes mellitus admitted with acute ischaemic stroke," *Diabetes and Vascular Disease Research*, vol. 12, no. 6, pp. 463–466, 2015.

[139] M. DeNicola, J. Du, Z. Wang et al., "Stimulation of glucagon-like peptide-1 receptor through exendin-4 preserves myocardial performance and prevents cardiac remodeling in infarcted myocardium," *American Journal of Physiology—Endocrinology and Metabolism*, vol. 307, no. 8, pp. E630–E643, 2014.

[140] S. Takada, Y. Masaki, S. Kinugawa et al., "Dipeptidyl peptidase-4 inhibitor improved exercise capacity and mitochondrial biogenesis in mice with heart failure via activation of glucagon-like peptide-1 receptor signalling," *Cardiovascular Research*, vol. 111, no. 4, pp. 338–347, 2016.

[141] T. Karagiannis, P. Paschos, K. Paletas, D. R. Matthews, and A. Tsapas, "Dipeptidyl peptidase-4 inhibitors for treatment of type 2 diabetes mellitus in the clinical setting: systematic review and meta-analysis," *BMJ*, vol. 344, no. 7850, Article ID e1369, 2012.

[142] H. Lee, H. Chang, S. Lee et al., "Role of IGF1R$^+$ MSCs in modulating neuroplasticity via CXCR4 cross-interaction," *Scientific Reports*, vol. 6, Article ID 32595, 2016.

[143] H. K. Haider, S. Jiang, N. M. Idris, and M. Ashraf, "IGF-1—overexpressing mesenchymal stem cells accelerate bone marrow stem cell mobilization via paracrine activation of SDF-1α/CXCR4 signaling to promote myocardial repair," *Circulation Research*, vol. 103, no. 11, pp. 1300–1308, 2008.

[144] A. Arnarson, O. G. Geirsdottir, A. Ramel, P. V. Jonsson, and I. Thorsdottir, "Insulin-like growth factor-1 and resistance exercise in community dwelling old adults," *Journal of Nutrition, Health and Aging*, vol. 19, no. 8, pp. 856–860, 2015.

[145] M. Ploughman, M. W. Austin, L. Glynn, and D. Corbett, "The effects of poststroke aerobic exercise on neuroplasticity: a systematic review of animal and clinical studies," *Translational Stroke Research*, vol. 6, no. 1, pp. 13–28, 2015.

[146] C. S. Mang, K. L. Campbell, C. J. D. Ross, and L. A. Boyd, "Promoting neuroplasticity for motor rehabilitation after stroke: considering the effects of aerobic exercise and genetic variation on brain-derived neurotrophic factor," *Physical Therapy*, vol. 93, no. 12, pp. 1707–1716, 2013.

[147] J. Li, Y. Tang, Y. Wang et al., "Neurovascular recovery via cotransplanted neural and vascular progenitors leads to improved functional restoration after ischemic stroke in rats," *Stem Cell Reports*, vol. 3, no. 1, pp. 101–114, 2014.

[148] X. Cui, M. Chopp, A. Zacharek et al., "D-4F decreases white matter damage after stroke in mice," *Stroke*, vol. 47, no. 1, pp. 214–220, 2016.

[149] H. Okazaki, H. Beppu, K. Mizutani, S. Okamoto, and S. Sonoda, "Changes in serum growth factors in stroke rehabilitation patients and their relation to hemiparesis improvement," *Journal of Stroke and Cerebrovascular Diseases*, vol. 23, no. 6, pp. 1703–1708, 2014.

[150] A. E. Mattlage, M. A. Rippee, J. Sandt, and S. A. Billinger, "Decrease in insulin-like growth factor-1 and insulin-like growth factor-1 ratio in the first week of stroke is related to positive outcomes," *Journal of Stroke and Cerebrovascular Diseases*, vol. 25, no. 7, pp. 1800–1806, 2016.

[151] S. P. Johnsen, H. H. Hundborg, H. T. Sørensen et al., "Insulin-like growth factor (IGF) I, -II, and IGF binding protein-3 and risk of ischemic stroke," *Journal of Clinical Endocrinology and Metabolism*, vol. 90, no. 11, pp. 5937–5941, 2005.

[152] R. C. Kaplan, A. P. McGinn, M. N. Pollak et al., "Association of total insulin-like growth factor-I, insulin-like growth factor binding protein-1 (IGFBP-1), and IGFBP-3 levels with incident coronary events and ischemic stroke," *Journal of Clinical Endocrinology and Metabolism*, vol. 92, no. 4, pp. 1319–1325, 2007.

[153] Y. Xiao, L. Liu, A. Xu et al., "Serum fibroblast growth factor 21 levels are related to subclinical atherosclerosis in patients with type 2 diabetes," *Cardiovascular Diabetology*, vol. 14, article 72, 2015.

[154] E. Lovadi, M. Csereklyei, H. Merkli et al., "Elevated FGF 21 in myotonic dystrophy type 1 and mitochondrial diseases," *Muscle & Nerve*, 2016.

[155] X. Wang, H. Xiao, L. Liu, D. Cheng, X. Li, and L. Si, "FGF21 represses cerebrovascular aging via improving mitochondrial biogenesis and inhibiting p53 signaling pathway in an AMPK-dependent manner," *Experimental Cell Research*, vol. 346, no. 2, pp. 147–156, 2016.

[156] P. Lee, J. Linderman, S. Smith et al., "Fibroblast growth factor 21 (FGF21) and bone: is there a relationship in humans?" *Osteoporosis International*, vol. 24, no. 12, pp. 3053–3057, 2013.

[157] X. Li, S. Stanislaus, F. Asuncion et al., "FGF21 is not a major mediator for bone homeostasis or metabolic actions of PPARα

and PPARγ agonists," *Journal of Bone and Mineral Research*, 2016.

[158] C. Loyd, I. J. Magrisso, M. Haas et al., "Fibroblast growth factor 21 is required for beneficial effects of exercise during chronic high-fat feeding," *Journal of Applied Physiology*, vol. 121, no. 3, pp. 687–698, 2016.

[159] X. Xu and Y. Jiang, "The yin and yang of innate immunity in stroke," *BioMed Research International*, vol. 2014, Article ID 807978, 8 pages, 2014.

[160] D. Petrovic-Djergovic, S. N. Goonewardena, and D. J. Pinsky, "Inflammatory disequilibrium in stroke," *Circulation Research*, vol. 119, no. 1, pp. 142–158, 2016.

[161] J. H. Tapia-Pérez, D. Karagianis, R. Zilke, V. Koufuglou, I. Bondar, and T. Schneider, "Assessment of systemic cellular inflammatory response after spontaneous intracerebral hemorrhage," *Clinical Neurology and Neurosurgery*, vol. 150, pp. 72–79, 2016.

[162] H.-Y. Fang, W.-J. Ko, and C.-Y. Lin, "Plasma interleukin 11 levels correlate with outcome of spontaneous intracerebral hemorrhage," *Surgical Neurology*, vol. 64, no. 6, pp. 511–517, 2005.

[163] A. Tuttolomondo, D. Di Raimondo, R. di Sciacca, A. Pinto, and G. Licata, "Inflammatory cytokines in acute ischemic stroke," *Current Pharmaceutical Design*, vol. 14, no. 33, pp. 3574–3589, 2008.

[164] A. Tuttolomondo, D. Di Raimondo, R. Pecoraro, V. Arnao, A. Pinto, and G. Licata, "Inflammation in ischemic stroke subtypes," *Current Pharmaceutical Design*, vol. 18, no. 28, pp. 4289–4310, 2012.

[165] X. Chen, Y. Wang, M. Fu, H. Lei, Q. Cheng, and X. Zhang, "Plasma immunoproteasome predicts early hemorrhagic transformation in acute ischemic stroke patients," *Journal of Stroke and Cerebrovascular Diseases*, vol. 26, no. 1, pp. 49–56, 2017.

[166] A. Tuttolomondo, R. Pecoraro, A. Casuccio et al., "Peripheral frequency of CD4+ CD28-cells in acute ischemic stroke relationship with stroke subtype and severity markers," *Medicine (Baltimore)*, vol. 94, no. 20, article no. e813, 2015.

[167] Z. G. Nadareishvili, H. Li, V. Wright et al., "Elevated proinflammatory CD4+CD28- lymphocytes and stroke recurrence and death," *Neurology*, vol. 63, no. 8, pp. 1446–1451, 2004.

[168] S. Chen, H. Wu, D. Klebe, Y. Hong, J. Zhang, and J. Tang, "Regulatory T cell in stroke: a new paradigm for immune regulation," *Clinical and Developmental Immunology*, vol. 2013, Article ID 689827, 9 pages, 2013.

[169] P. Li, L. Mao, X. Liu et al., "Essential role of program death 1-ligand 1 in regulatory T-cell–afforded protection against blood–brain barrier damage after stroke," *Stroke*, vol. 45, no. 3, pp. 857–864, 2014.

[170] Y. Xia, W. Cai, A. W. Thomson, and X. Hu, "Regulatory T cell therapy for ischemic stroke: how far from clinical translation?" *Translational Stroke Research*, vol. 7, no. 5, pp. 415–419, 2016.

[171] S. Neumann, N. J. Shields, T. Balle, M. Chebib, and A. N. Clarkson, "Innate immunity and inflammation post-stroke: an α7-nicotinic agonist perspective," *International Journal of Molecular Sciences*, vol. 16, no. 12, pp. 29029–29046, 2015.

[172] Z. Wang, L. Xue, T. Wang, X. Wang, and Z. Su, "Infiltration of invariant natural killer T cells occur and accelerate brain infarction in permanent ischemic stroke in mice," *Neuroscience Letters*, vol. 633, pp. 62–68, 2016.

[173] T. Homma, S. Kinugawa, M. Takahashi et al., "Activation of invariant natural killer T cells by α-galactosylceramide ameliorates myocardial ischemia/reperfusion injury in mice," *Journal of Molecular and Cellular Cardiology*, vol. 62, pp. 179–188, 2013.

[174] S. De Raedt, A. De Vos, A. Van Binst et al., "High natural killer cell number might identify stroke patients at risk of developing infections," *Neurology—Neuroimmunology Neuroinflammation*, vol. 2, no. 2, article no. e71, 2015.

[175] Y. Zhang, Z. Gao, D. Wang et al., "Accumulation of natural killer cells in ischemic brain tissues and the chemotactic effect of IP-10," *Journal of Neuroinflammation*, vol. 11, article no. 79, 2014.

[176] L. Gu, X. Xiong, D. Wei, X. Gao, S. Krams, and H. Zhao, "T cells contribute to stroke-induced lymphopenia in rats," *PLOS ONE*, vol. 8, no. 3, Article ID e59602, 2013.

[177] D. Gill and R. Veltkamp, "Dynamics of T cell responses after stroke," *Current Opinion in Pharmacology*, vol. 26, pp. 26–32, 2016.

[178] J. Klehmet, S. Hoffmann, G. Walter, C. Meisel, and A. Meisel, "Stroke induces specific alteration of T memory compartment controlling auto-reactive CNS antigen-specific T cell responses," *Journal of the Neurological Sciences*, vol. 368, pp. 77–83, 2016.

[179] Y. Hu, Y. Zheng, Y. Wu, B. Ni, and S. Shi, "Imbalance between IL-17A-producing cells and regulatory T cells during ischemic stroke," *Mediators of Inflammation*, vol. 2014, Article ID 813045, 8 pages, 2014.

[180] X. Wang, H. Li, and S. Ding, "Pre-B-cell colony-enhancing factor protects against apoptotic neuronal death and mitochondrial damage in ischemia," *Scientific Reports*, vol. 6, article 32416, 2016.

[181] U. M. Selvaraj, K. Poinsatte, V. Torres, S. B. Ortega, and A. M. Stowe, "Heterogeneity of B cell functions in stroke-related risk, prevention, injury, and repair," *Neurotherapeutics*, vol. 13, no. 4, pp. 729–747, 2016.

[182] X. Ren, K. Akiyoshi, S. Dziennis et al., "Regulatory B cells limit CNS inflammation and neurologic deficits in murine experimental stroke," *Journal of Neuroscience*, vol. 31, no. 23, pp. 8556–8563, 2011.

[183] A. Liesz and C. Kleinschnitz, "Regulatory T cells in post-stroke immune homeostasis," *Translational Stroke Research*, vol. 7, no. 4, pp. 313–321, 2016.

[184] L.-B. Guo, S. Liu, F. Zhang, G.-S. Mao, L.-Z. Sun, and Y. Liu, "The role of eosinophils in stroke: A Pilot Study," *European Review for Medical and Pharmacological Sciences*, vol. 19, no. 19, pp. 3643–3648, 2015.

[185] I. Maestrini, D. Strbian, S. Gautier et al., "Higher neutrophil counts before thrombolysis for cerebral ischemia predict worse outcomes," *Neurology*, vol. 85, no. 16, pp. 1408–1416, 2015.

[186] L. Roever and S. R. Levine, "Cerebral hemorrhage following thrombolytic therapy for stroke: are neutrophils really neutral?" *Neurology*, vol. 85, no. 16, pp. 1360–1361, 2015.

[187] E. Thonnard-Neumann, "Monocytes and basophilic granulocytes in the cranial circulation of patients with organic brain disorders," *Stroke*, vol. 3, no. 3, pp. 286–299, 1972.

[188] P. J. Lindsberg, D. Strbian, and M.-L. Karjalainen-Lindsberg, "Mast cells as early responders in the regulation of acute blood-brain barrier changes after cerebral ischemia and hemorrhage," *Journal of Cerebral Blood Flow and Metabolism*, vol. 30, no. 4, pp. 689–702, 2010.

[189] M. S. Woo, J. Yang, C. Beltran, and S. Cho, "Cell surface CD36 protein in monocyte/macrophage contributes to phagocytosis

during the resolution phase of ischemic stroke in mice," *The Journal of Biological Chemistry*, vol. 291, no. 45, pp. 23654–23661, 2016.

[190] S. Wattananit, D. Tornero, N. Graubardt et al., "Monocyte-derived macrophages contribute to spontaneous long-term functional recovery after stroke in mice," *Journal of Neuroscience*, vol. 36, no. 15, pp. 4182–4195, 2016.

[191] A. ElAli and N. J. LeBlanc, "The role of monocytes in ischemic stroke pathobiology: new avenues to explore," *Frontiers in Aging Neuroscience*, vol. 8, article no. 29, 2016.

[192] J. C. Felger, T. Abe, U. W. Kaunzner et al., "Brain dendritic cells in ischemic stroke: time course, activation state, and origin," *Brain, Behavior, and Immunity*, vol. 24, no. 5, pp. 724–737, 2010.

[193] X. Urra, F. Miró, A. Chamorro, and A. M. Planas, "Antigen-specific immune reactions to ischemic stroke," *Frontiers in Cellular Neuroscience*, vol. 8, article 278, 2014.

[194] A. Hug, A. Liesz, B. Muerle et al., "Reduced efficacy of circulating costimulatory cells after focal cerebral ischemia," *Stroke*, vol. 42, no. 12, pp. 3580–3586, 2011.

[195] A. Yilmaz, T. Fuchs, B. Dietel et al., "Transient decrease in circulating dendritic cell precursors after acute stroke: potential recruitment into the brain," *Clinical Science*, vol. 118, no. 2, pp. 147–157, 2010.

[196] K. Duris and J. Lipkova, "The role of microRNA in ischemic and hemorrhagic stroke," *Current Drug Delivery*, vol. 14, no. 8, 2017.

[197] J. Kim, G. H. Choi, K. H. Ko et al., "Association of the single nucleotide polymorphisms in microRNAs 130b, 200b, and 495 with ischemic stroke susceptibility and post-stroke mortality," *PLoS ONE*, vol. 11, no. 9, Article ID e0162519, 2016.

[198] K. Toyama, J. Spin, and P. Tsao, "Role of microRNAs on blood brain barrier dysfunction in vascular cognitive impairment," *Current Drug Delivery*, vol. 13, pp. 1–14, 2016.

[199] A. Karthikeyan, R. Patnala, S. Jadhav, L. Eng-Ang, and S. Dheen, "MicroRNAs: key players in microglia and astrocyte mediated inflammation in CNS pathologies," *Current Medicinal Chemistry*, vol. 23, no. 30, pp. 3528–3546, 2016.

[200] M. Vijayan and P. H. Reddy, "Peripheral biomarkers of stroke: focus on circulatory microRNAs," *Biochimica et Biophysica Acta*, vol. 1862, no. 10, pp. 1984–1993, 2016.

[201] R. Zhang, Y. Qin, G. Zhu, Y. Li, and J. Xue, "Low serum miR-320b expression as a novel indicator of carotid atherosclerosis," *Journal of Clinical Neuroscience*, vol. 33, pp. 252–258, 2016.

[202] X. Zhou, S. Su, S. Li et al., "MicroRNA-146a down-regulation correlates with neuroprotection and targets pro-apoptotic genes in cerebral ischemic injury in vitro," *Brain Research*, vol. 1648, pp. 136–143, 2016.

[203] P. Wang, J. Liang, Y. Li et al., "Down-regulation of miRNA-30a alleviates cerebral ischemic injury through enhancing Beclin 1-mediated autophagy," *Neurochemical Research*, vol. 39, no. 7, pp. 1279–1291, 2014.

[204] Z. Peng, J. Li, Y. Li et al., "Downregulation of miR-181b in mouse brain following ischemic stroke induces neuroprotection against ischemic injury through targeting heat shock protein A5 and ubiquitin carboxyl-terminal hydrolase isozyme L1," *Journal of Neuroscience Research*, vol. 91, no. 10, pp. 1349–1362, 2013.

[205] P. Wang, N. Zhang, J. Liang, J. Li, S. Han, and J. Li, "MicroRNA-30a regulates ischemia-induced cell death by targeting heat shock protein HSPA5 in primary cultured cortical neurons and mouse brain after stroke," *Journal of Neuroscience Research*, vol. 93, no. 11, pp. 1756–1768, 2015.

[206] D. A. Duricki, T. H. Hutson, C. Kathe et al., "Delayed intramuscular human neurotrophin-3 improves recovery in adult and elderly rats after stroke," *Brain*, vol. 139, no. 1, pp. 259–275, 2016.

[207] L. Lorente, M. M. Martín, T. Almeida et al., "Serum levels of substance P and mortality in patients with a severe acute ischemic stroke," *International Journal of Molecular Sciences*, vol. 17, no. 6, article no. 991, 2016.

[208] Q. Li, Y. Lin, W. Huang et al., "Serum IL-33 is a novel diagnostic and prognostic biomarker in acute ischemic stroke," *Aging and Disease*, vol. 7, no. 5, pp. 614–622, 2016.

[209] S. M. Lloyd-Burton, E. M. York, M. A. Anwar, A. J. Vincent, and A. J. Roskams, "SPARC regulates microgliosis and functional recovery following cortical ischemia," *Journal of Neuroscience*, vol. 33, no. 10, pp. 4468–4481, 2013.

[210] L. Minshu, L. Zhiguo, W. Kristofer, J. Weina, S. Fu-Dong, and L. Qiang, "Abstract 144: astrocyte-derived interleukin-15 accelarates Ischemic Brain Injury Int Stroke Conference," *Stroke*, vol. 47, article A144, 2016.